Pacific Northwest
NATIONAL LABORATORY

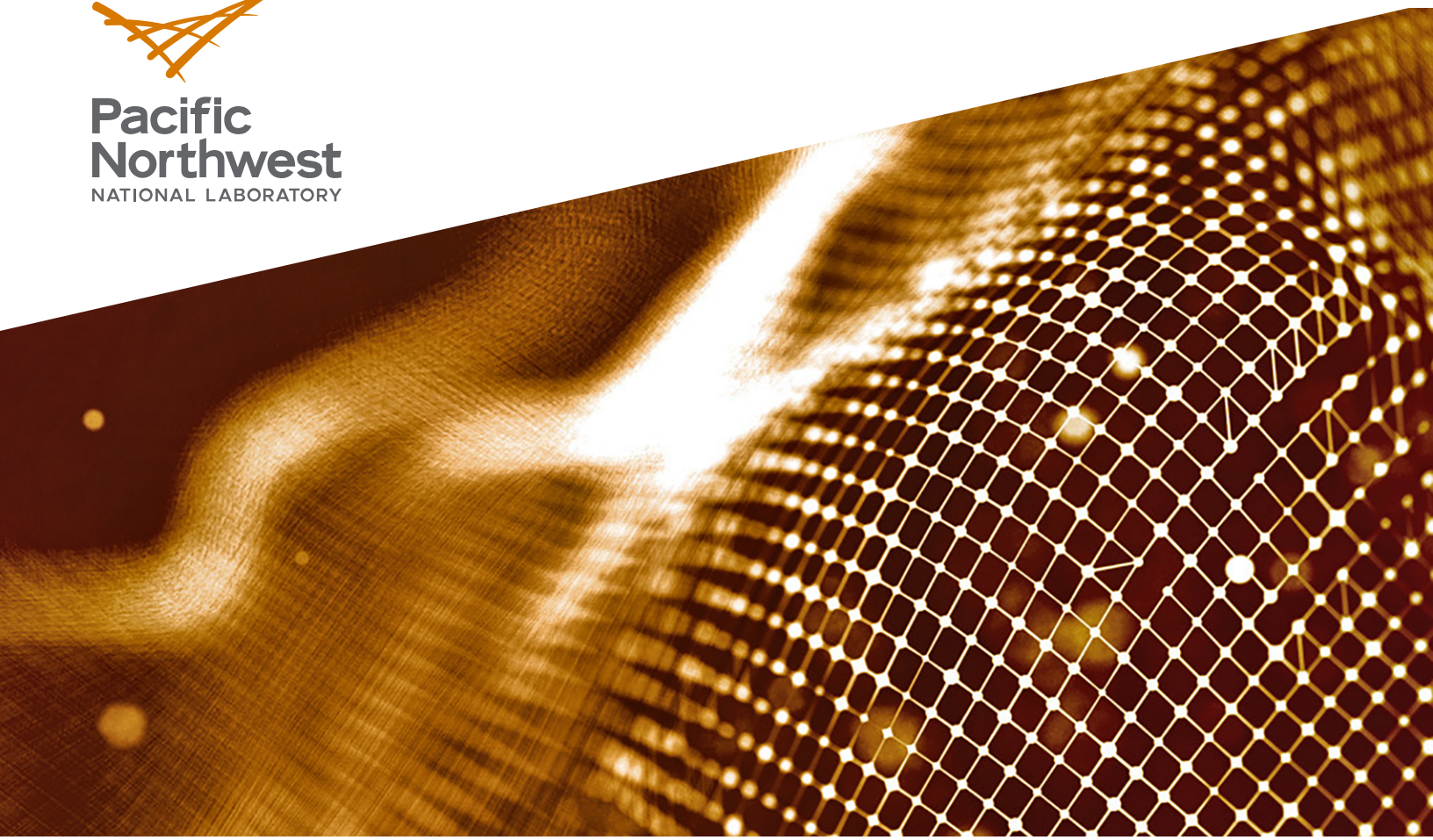

PNNL-XXXXX

2018 Annual Report

Laboratory Directed Research & Development at Pacific Northwest National Laboratory

March 2019

U.S. DEPARTMENT OF ENERGY

Prepared for the U.S. Department of Energy
under Contract DE-AC05-76RL01830

PACIFIC NORTHWEST NATIONAL LABORATORY
operated by
BATTELLE
for the
UNITED STATES DEPARTMENT OF ENERGY
under Contract DE-AC05-76RL01830

PNNL-XXXXX

2018 Annual Report

Laboratory Directed Research & Development at Pacific Northwest National Laboratory

March 2019

Prepared for
the U.S. Department of Energy
under Contract DE-AC05-76RL01830

Pacific Northwest National Laboratory
Richland, Washington 99354

Contents


Advanced Sensors and
Instrumentation

A Probe-based Microtiter Plate Assay for Characterization of Protein Binding Partners of Small Molecules

Aaron T. Wright
PN17055/2945

We are developing a novel method for rapidly characterizing small molecule-protein interactions. solid support surfaces derivatized with chemical probes enable the rapid identification of protein-small molecules binding partners.

Small molecule-protein interactions are critical to cell communication, nutrient scavenging, inhibition or activation of metabolic pathways as enzyme cofactors, and numerous other processes. Small molecules also are used to control protein functions relevant to energy and human health, for instance to trigger a biosynthetic pathway that produces hydrocarbons or to inhibit a bacterial pathogen. However, discovery of the interactions occurring between small molecules and proteins in diverse biological systems is not simple. *In silico* predictions are limited to proteins for which we have quality structural information (e.g., crystal structures), which are primarily limited to mammalian systems. Thereby, a novel method for rapidly characterizing small molecule-protein interactions has significant potential to transform our understanding of biological functions.

The current state of the art in the development of new drug compounds centers around *in silico* docking studies of a target protein with theoretical compound libraries. These screens result in high-priority drug compound leads that are then synthesized in the laboratory and tested in binding assays to the target protein. If all is successful up to this point, they will start cell line and animal studies to see if the drug binds to the target protein and reverses whatever the negative cell phenotype is (e.g., cancer). The next step is a long and arduous process in animal studies to determine side effects, often without having any idea of the mechanism for observed side effects.

Within microbes and microbiomes, it is difficult 1) to predict microbes with the potential to salvage small molecules, particularly nutrients such as B vitamins, and 2) to identify small molecule regulatory functions that impact cell physiology and functions. Instead of laborious chemical and computational screens, we present an alternative in which a chemical is derivatized to contain a reactive group that enables attachment between the chemical and a strong interacting protein. The chemical molecule is on a resin, which enables its easy placement in an array format. Analysis of small molecule-protein interactions is performed by mass spectrometry.

We synthesized a chemical mimic of the antifungal agent, ketoconazole. This drug has recently been suggested as a therapy for tuberculosis treatment. We demonstrated our ketoconazole-ABP (activity-based probe) had the same impacts on *Mycobacterium tuberculosis (Mtb) H37Rv* cell viability, while retaining a similar minimum inhibitory concentration. We then determined how best to append the drug probe to glass and magnetic resins.

Prior to developing an assay (solid-support), ketoconazole-ABP has identified a number of protein targets based on the drug's presumed interactions *in vivo* by proteomic analysis. There were several unanticipated targets that required more stringent processing of protein bound to probe. To first approach attachment of the probe to varying surface types, we focused our efforts with commercially prepared magnetic bead resins (DynaBeads). By synthesizing a cleavable linker bound to the magnetic bead surface, we were able to attach our probe using click chemistry. This revealed the feasibility of attaching a probe to a surface, probing in lysate (or purified protein), and using mass spectrometry to identify proteins. The assay using ketoconazole-ABP was treated with Mtb, and multiple anticipated protein targets were identified. We discovered that the standard washing treatments typically used with solution-based proteomics was not effective at completely removing non-specific proteins. Improving upon prior methods, washing

treatments were extended and less unexpected targets were identified.

Moving closer to developing a microtiter assay, we investigated optimal concentrations of ketoconazole-ABP bound to the prepared surface. Competition with the known drug compound and proteomics determined that this solid-support approach decreased the number of unanticipated targets while still maintaining a high number of authentic targets. The findings provided by these exploratory studies have now guided towards glass microspheres, a more amenable surface for use in plate assays. These high-throughput assays can be translated to improved understanding of drug candidates with selectivity profiles with proteomics. We are now translating the ketoconazole-ABP approach with other types of probes, using findings from the microtiter assay to improve our understanding of microbial communities.

An Autonomous Acoustic Receiver for Monitoring Real-time Fish Survival

Jayson J. Martinez
PN18023/3022

This project has developed a cloud-based, real-time underwater acoustic receiver that advances the state of the art in underwater acoustic telemetry technology in several ways such as estimating in near real-time (less than 1 hour) fish behavior or survival, monitoring the health of the acoustic receiver, and incorporating off-the-shelf electronic sensors for environmental monitoring. This work opens up new design opportunities for future real-time and multifunctional underwater acoustic systems.

Underwater acoustic receivers have been widely used for studying the behavior of aquatic animals and assessing the environmental impact of structures such as hydroelectric power plants. However, the current implementation of acoustic receivers requires manual recovery of the data stored from each of the deployed acoustic receivers at remote underwater locations after multiple weeks of deployment, which inevitably leads to a large delay of data availability. Furthermore, after the receivers are deployed, there is no way to identify whether they are continuing to operate properly or not until they are recovered for data download. Therefore, we developed a novel underwater acoustic receiver system that would allow detection information to be broadcast from underwater acoustic receivers to a cloud-based server for estimating fish behavior or survival and monitoring environmental parameters in near real-time (less than 1 hour).

The overall system consists of a commercially available acoustic receiver, a microcontroller board that intercepts the raw detection data from the receiver and applies filtering and compression to the data, an underwater acoustic telemetry modem for long-distance underwater wireless communication in an aquatic environment, a radio frequency (RF) module for wireless communication between the microcontroller and the cloud-based server, and a web-based Graphical User Interface (GUI) for data post-processing and visualization.

The hardware design included developing two systems. The first system includes the underwater components that are located offshore. This system intercepts the detection data from a commercially available acoustic receiver. For this system, we used a small, low-power, single-board computer (Arduino Zero). As the data is intercepted from the acoustic receiver, it is filtered to remove likely false-positives that don't match the expected transmission pattern, using embedded multipath and pulse repetitive interval filtering algorithms. Given the low baud rate of acoustic modems (max transmission speed of 15,360 bits/sec), it is not feasible to transmit all the raw detection information even after filtering. To overcome this limitation, the detection information was compressed before being transmitted. In addition to the detection data, environmental data from the acoustic receiver (temperature) and from additional sensors integrated into the system (dissolved oxygen, pH, and conductivity) are transmitted.

The second system we developed is the surface-based receiver, located on the shore, which collects the detection summary and environmental data from each acoustic receiver and communicates it to a cloud-based server. For this system, we also used the same single-board computer as the first system (Arduino Zero), running a custom-made, real-time operating system. The board is connected to an acoustic modem through an RS232 serial interface. Once the surface-based receiver has obtained data from each acoustic receiver in the array, the information is broadcast to a cloud-server using a standalone cellular modem. The cellular modem interfaces to the host microcontroller board through a serial port for serial communication and passes the received data packet from the host to the cloud with a preset IP address and port using transmission control protocol. The full hardware implementations were validated in a laboratory

environment. Field testing was performed to investigate the performance of the acoustic modems used for transmitting the data packets.

The data from multiple receivers in the study area are combined and inputted into a web-based GUI to calculate different metrics including survival, residency time, and travel time. The cloud-based system is available anytime, anywhere. RESTful APIs (application program interfaces) and web services are applicable to any other monitoring applications.

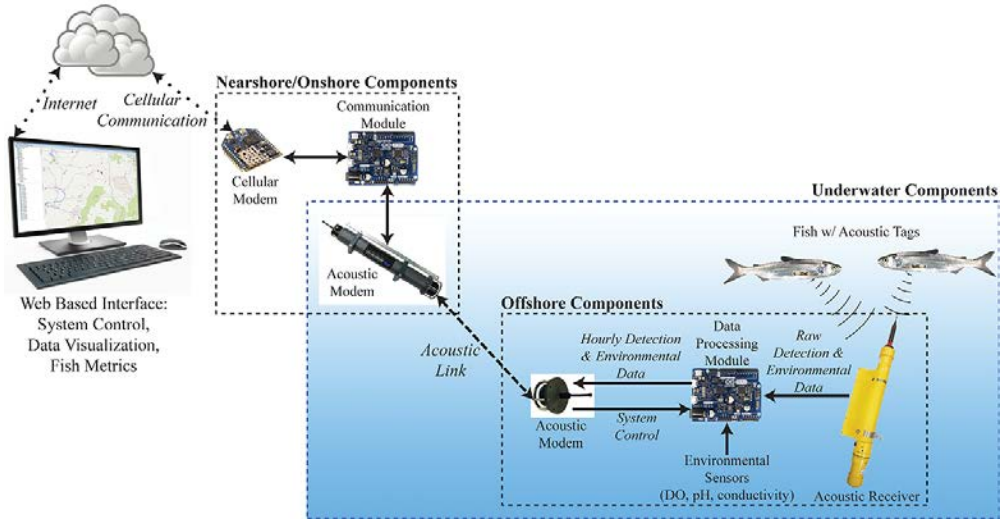

System overview of the real-time autonomous acoustic receiver.

Development of Translational Assays Prognostic of Poor Disease Outcomes in Deadly Infections

Thomas O. Metz
PN18077/3076

Various studies have been performed to identify molecules and pathways that characterize the human response to infectious disease. In this project, we will leverage and exploit this existing knowledge and work to develop field-deployable devices for characterizing infectious disease severity.

The pathogenesis of infectious diseases in humans is complex. In this context, our group has been studying viral mechanisms of pathogenesis. To better understand the contribution of host responses to infection pathophysiology, we performed a comprehensive molecular characterization of blood plasma from patients infected with the Ebola virus. Our preliminary results indicate that the Ebola virus disease has overlapping molecular signatures with those of sepsis and other severe infections. However, there remains a significant gap between biomarker identification and development of field-deployable devices for routine use in clinical or field settings that have limited infrastructure support. Here, we propose to begin development toward deployable diagnostic devices that can be used to predict the severity of deadly infections, allowing medical professionals to administrate adequate treatment for patients.

Our experimental approach is two-fold: 1) we are investigating subsets of the initial biomarkers identified in our previous studies using advanced informatics approaches to determine their performance in distinguishing between infections with fatal and survivable outcomes, and 2) we are assessing potential analytical approaches for selective laboratory-based detection of the best distinguishing markers, with a focus on readily available reagents that are amenable to incorporation into a deployable kit.

To determine the set of markers that best distinguish between Ebola infections with fatal and survivable outcomes, we used a two-pronged informatics approach, with both methods using our previous data from analyses of blood from infected individuals as input. We employed a nested, leave-one-out cross-validation design for biomarker discovery and assessment. This was performed on multiple data sources separately (e.g., protein, metabolite, lipid) and for all combined into one. We also included controls for overfitting in this approach.

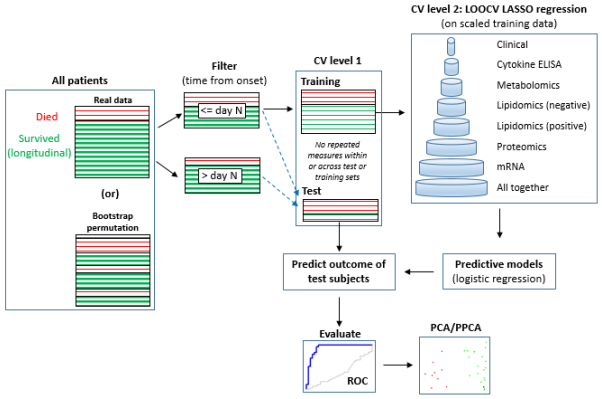

Nested cross-validation pipeline for biomarker discovery.

As a second, independent step to ensure that the most distinguishing molecules were selected in the final target set, we employed a machine learning approach with recursive feature elimination with 100 random samplings of the source data. The results of both informatics approaches returned a list of about 20 high-confidence markers, which formed the basis for the assessment of potential analytical approaches for selective detection.

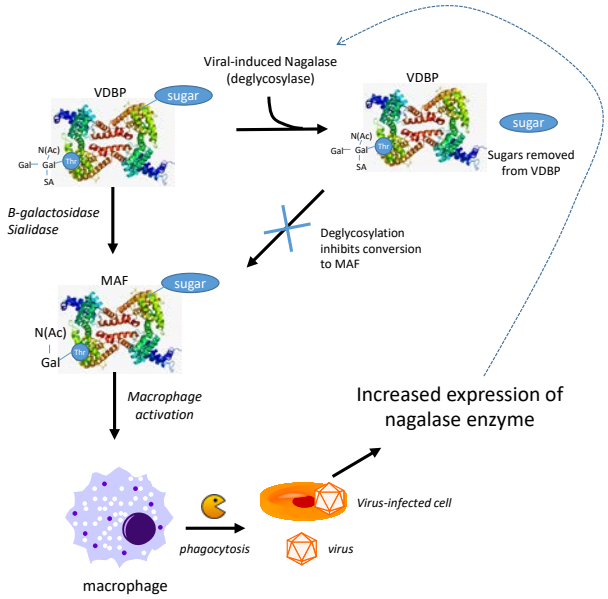

Conversion of Vitamin D Binding Protein (VDBP) to Macrophage Activation Factor (MAF).

In addition to the informatics-based selection of the most promising set of markers for distinguishing fatal from survivable infections, we performed an enrichment analysis to determine those metabolic and signaling pathways most closely associated with pathogenic viral infection. Based on our source data, vitamin D binding protein activation of macrophages was identified as a key host response mechanism that may differentiate between individuals that survive versus succumb to highly pathogenic infections.

To determine possible analytical approaches for laboratory-based selective detection of the best distinguishing markers of fatal versus survivable viral infection, we emphasized those assays that could be multiplexed and that might be more universal in assessing outcomes of highly pathogenic viral infection (e.g., as opposed to specificity towards only a single pathogen). We also considered a variety of analytical technology platforms for the assays; their amenability for use as a kit that could be implemented at point-of-care facilities, either nationally or internationally; and the current availability of reagents. Currently, the best assay candidates are those based on affinity interactions (e.g., antibodies) and those based on enzymatic reactions.

Flow-through Pressurized Magic Angle Spinning (PMAS) Nuclear Magnetic Resonance (NMR) Rotors for Multimodal Analysis

John S. Loring

PN18072/3071

This project advanced high-pressure (HP) solid-state NMR technology by developing a flow-through version of PNNL's R&D-100-award-winning PMAS-NMR rotors, thereby dramatically expanding the conditions and systems to which the molecular-scale PMAS-NMR technique can be applied.

Unraveling complex, molecular-level processes at material interfaces with high-pressure fluids is an important but challenging problem across scientific foci such as catalysis, subsurface energy production, biogeochemical element cycling, and energy waste disposal. PMAS-NMR rotors were developed at PNNL to help address this research need. The original PMAS-NMR rotors, however, were sometimes limited, because they serve as poor reaction vessels for certain systems. This is because they contain relatively large masses of reactive solid but small volumes of reactive fluid, which can result in incompletely reacted solids and/or unknown fluid compositions after reaction.

This project addressed these limitations by developing new PMAS-NMR rotors that allow, for the first time, fluid flow to completely react and equilibrate solid samples at known fluid humidities and volatile compositions. The flow-through design allows exposure to enough fluid reactant for solids to fully react. The rotors can be incorporated in a flow loop that includes other successful PNNL HP capabilities, including HP-infrared (-IR) spectroscopy and HP X-ray powder diffraction (XRD). Flow-through PMAS-NMR technology will revolutionize the field by allowing measurements of fluid humidity (or other volatile concentration) by IR and structural parameters by XRD, prior to transfer into NMR systems for PMAS analysis.

In FY 2018, this project supported labor to design, machine, and test flow-through PMAS-NMR rotors and a rotor loader, as well a purchase required materials. The rotors use two types of valves: a one-way check valve that allows fluid into the rotor but not out, and a two-way screw valve. The rotor loader provides a means to pressurize the rotors, and it allows fluid flow into the rotor through the one-way valve, over a solid-phase sample inside the rotor, and out the rotor through the screw valve. After reaction, the screw valve is closed, and the rotor removed from the rotor loader so that reacted samples can be analyzed in an NMR spectrometer by the PMAS technique. A total of five rotors were machined and assembled. Successful testing included confirming that the rotors could spin as required for the PMAS-NMR measurement, and validating fluid flow by testing in a high-pressure flow system that included IR spectroscopy.

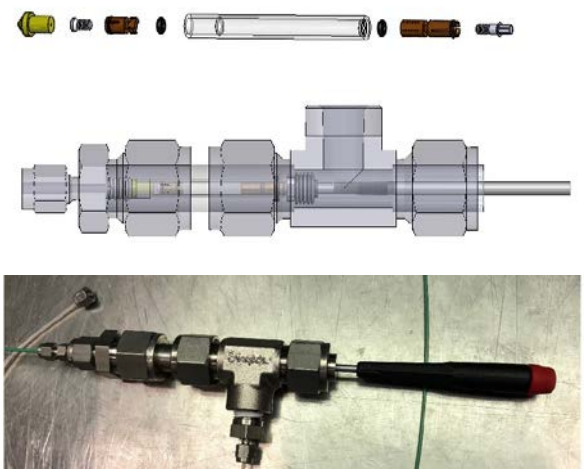

Top: Exploded-view of the new flow-through PMAS-NMR rotor, showing a one-way check valve on the left side and a two-way screw valve on the right. Middle: Semi-transparent schematic of the rotor loader housing a flow-through PMAS-NMR rotor. Bottom: Photo of the rotor loader; the screwdriver on the right is for opening/closing the screw valve while maintaining pressure.

In Situ Battery Degradation Mechanism Study Using Solid-State Nuclear Magnetic Resonance (NMR) Characterization

Daiwon Choi
PN18030/3029

The overarching goal of this project is to improve our understanding of battery chemistry in terms of reliability and cycle life, leading to more cost-effective energy storage systems. To achieve this goal, we propose to develop an* in situ *magic angle spinning (MAS) NMR cell for fundamental degradation study of full cell batteries, such as the Li-ion battery. This* in situ *MAS-NMR cell makes it possible to analyze chemical species that belong to the electrolyte, the solid electrolyte interface formed on both anode and cathode during operation, as well as at rest, detecting multiple NMR sensitive nuclei (^{1}H, ^{6,7}Li, ^{13}C, ^{31}P, ^{19}F, ^{27}Al, etc.).

In situ NMR has been used in battery research for several decades, but all research has been done at static state (i.e., without sample spinning). It is hard to discriminate chemical species from *in situ* static NMR spectroscopy due to signal overlapping resulting from chemical shift anisotropy (CSA) and/or dipolar broadening, etc. When *in situ* MAS-NMR can suppress the line broadening due to CSA and dipolar interaction, it can reduce the ambiguity in specifying chemical species from the working battery cells. In this project, we are working to develop an *in situ* battery MAS-NMR rotor to suppress CSA and dipolar broadening for verifying chemical species in the working battery cells.

We have successfully developed an *in situ* battery MAS-NMR rotor with 7.5 mm OD, which can be electrochemically cycled with a different cathode, anode, and electrolyte. From the *in situ* MAS-NMR cell fabricated, we obtained ^{7}Li and ^{31}P MAS-NMR spectra from $LiFePO_4$ (LFP) / $Li_4Ti_5O_{12}$ (LTO) battery cells in fully charged and discharged states, which clearly shows Li (de)intercalation on the LFP site by changing the charge state of the battery.

So far, we have accomplished making flexible electrodes suitable for the *in situ* MAS-NMR cells, using a thin film deposition technique (Au coating) to increase the conductivity of the graphite rod current collector without heating the MAS-NMR cell during MAS, and making an electrolyte leak-proof cell design. The *in situ* cell made can withstand the centrifugal force generated by high rotation speeds that potentially distort the electrodes and cause electrolyte leaks. The LFP/LTO full cell was fabricated and electrochemically cycled without any problems, the ^{7}Li and ^{31}P signal was successfully obtained from the LFP/LTO cell after it cycled multiple times, and the LFP/LTO cell cycled well even after MAS-NMR measurement. The sample must be axially symmetric to spin stably.

For validating the performance of the *in situ* MAS-NMR cell, a very stable LFP cathode/LTO anode combination was used, which can be cycled more than 5,000 cycles without degradation. Further study is required with different cathode/anode combinations and to verify the NMR signals obtained. However, our concept has proven that it is possible to make an *in situ* MAS-NMR cell that works as a battery cell.

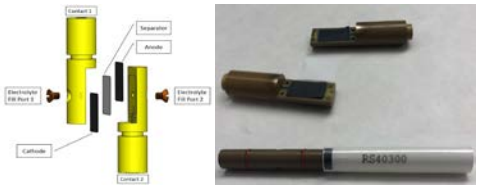

In situ MAS-NMR rotor cell design (left) and an actual cell photo (right).

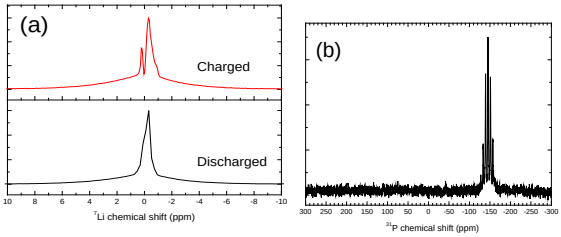

(a) ^{7}Li MAS-NMR spectra obtained from *in situ* battery MAS-NMR rotor fabricated with LFP/LTO and LiPF6/EC/DMC electrolyte in charged and discharged states. (b) ^{31}P MAS-NMR spectra obtained from LFP/LTO battery cells, which show strong PF_6- signal from electrolyte.

Ion Manipulation at Atmospheric Pressure

Yehia M. Ibrahim
PN17089/2979

This project aims to advance our ability to detect and characterize various molecular species relevant to the environment, health, security, and new materials. When successful, this project will result in development of a sensitive and highly selective device and do so with reduced cost.

Portable ion mobility spectrometers have limited performance due to the constraints of size and operating parameters. These constraints stem from the inherit nature of the constant electric field used in such devices and its inability to provide confinement of ions at atmospheric pressure.

This work uses a different approach to confine ions at atmospheric pressure. Using traveling wave (TW) direct current profiles with appropriate device geometry and TW parameters, ions can be efficiently confined and transmitted through the device. TW can also be used to affect ion mobility separation (IMS). Unlike constant field IMS, TW is a fixed amplitude revolving voltage profile enabling a significant increase in the resolution by increasing the path length. Since the ions can be confined efficiently at atmospheric pressure, one can achieve high IMS resolution without compromising sensitivity. This project is focused on optimizing the geometry of the device and its operating parameters using ion trajectory simulation to show the proof-of-concept ion transmission through the device.

Different geometries of the electrode patterns were investigated using ion trajectory simulations, which provided insights on the optimum geometry and operation of the device. Results indicated the importance of electric field strength and its frequency to provide efficient operation of the device. Ion simulations also produced snapshots of ion velocity vectors, ion plume, and voltage at an instant of time, which helped understand the ion confinement.

We designed and fabricated the lenses of the ion confinement at atmospheric pressure (APIC device) using printed circuit board (PCB) technology. The PCB fabrication method provided a flexible, fast, and affordable means to build the device. A TW was applied to the eight electrodes to confine ions. The lenses were assembled into a 10-cm-long device. APIC was integrated with electrospray ionization source to provide ions from a standard mixture of compounds. Ion current was measured at different points throughout the device using a miniature probe. An ion current of about 50 pA was measured at the exit of the device using a Faraday plate. These results indicate the success of the device to confine and transport ions at atmospheric pressure. The experimental results also confirm the predictions provided by the ion trajectory simulations.

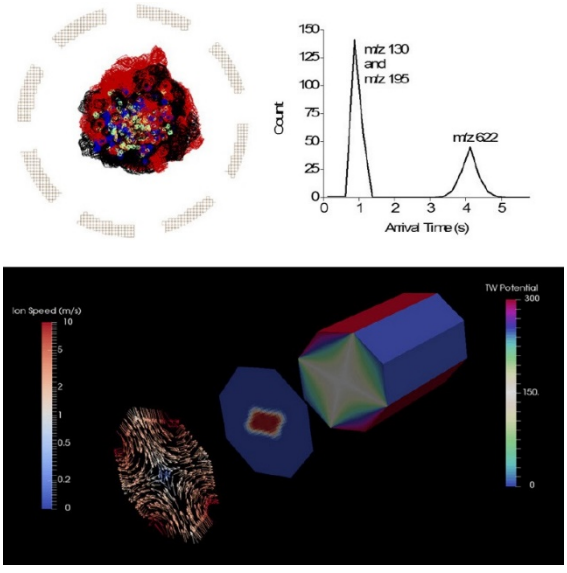

(Top left) SIMION trajectory simulation showing ions confined within APIC device. (Top right) IMS separations simulated in SIMION. (Bottom left) Velocity vectors of ion. (Bottom center) Ion plume distribution. (Bottom right) Voltage profile at an instant of time.

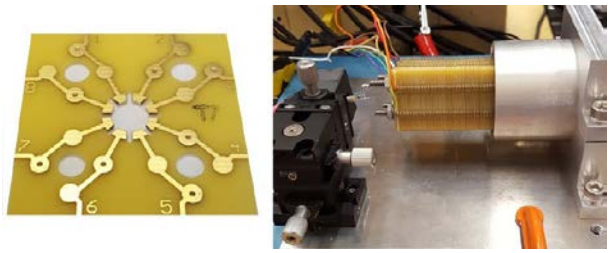

(Left) Photo of individual lens showing eight electrodes forming a central confinement region. (Right) Photo of the assembled device integrated with an electrospray ion source.

Since the stackable APIC can provide extended path length in a straight fashion, we further explored alternative geometries that can extended the path length without increasing the footprint of the device. Using extensive ion trajectory simulations, we successfully were able to design a planar geometry of the device using two parallel surfaces. Electrodes patterned on each surface were supplied with appropriate electric field. We were able to move and separate ions around corners, a tee-junction, and eventually, a serpentine path, which translates to longer path length (i.e., high-resolution) in a small footprint.

Learning Control for Building Systems

Dustin L. Arendt
PN17025/2915

Reinforcement learning is a promising approach for learning a control system through the process of trial and error. This work developed advanced visualization techniques to support data scientists training reinforcement learning models for control systems, like the ones found in buildings.

Reinforcement learning is a rapidly evolving branch of machine learning, where models use trial and error to learn an optimal policy (i.e., the best action at a particular state). The appeal of reinforcement learning for control systems is that it can potentially reduce or eliminate the requirement of needing an expert to fine tune control systems for each application (e.g., every building); ideally, the algorithm learns how to tune the control system on its own.

Unlike "traditional machine learning" (e.g., supervised classification), reinforcement learning does not rely on a pre-defined collection of training data. Instead, the model explores an environment by taking actions and receiving a reward for some good actions. We refer to a model exploring its environment for a short period as an "episode." The agent learns how to better accomplish a goal by repeating episodes within a run. A data scientist also will perform multiple runs while tuning model hyper-parameters, such as noise learning rate, to optimize the effectiveness of the learning.

This history of the model's process of trial and error is a very large and complex dataset, making it challenging to understand what's going on. Questions like, "What did the model learn to do," "What are good versus bad behaviors," and "What models/parameters were the best," are challenging to answer but important during the normal development and debugging process of designing and tuning a model architecture.

Current approaches to understand the training of a reinforcement learning model are not very sophisticated, often simply being graphs showing reward over time. However, these visualizations fail to help the data scientist better answer the above questions without significant *ad hoc* data analysis. Data scientists training reinforcement learning models can become easily overwhelmed and not know what steps to try next.

We developed a visual analytics system that supports a data scientist in building and evaluating reinforcement learning models, specifically tailored toward control systems. We address the above challenges with a visual analytics tool that allows the data scientist to understand the relationship between hyperparameters and model performance, understand patterns of behavior within and between runs, and explore the relationship between state, action, and reward.

At the heart of our approach is the use of "squiggles" to represent single episodes. A squiggle is a representation of a complex timeseries as a simple, tiny thumbnail. These are crucial to understanding not only single behaviors, but many behaviors in overview visualizations. We leverage squiggles to help summarize behavior within a run, as a model learns, as well as behavior across runs/models.

Our interface has several views that help the data scientist answer important questions about how their reinforcement learning model is learning to control a complex system. The first view allows the user to overview and organize runs, and to understand the relationship between model hyper-parameters, reward, and behaviors within episodes. Additional views allow the user to understand behaviors in more detail.

A screenshot of our user interface. The view helps the user understand the relationship between episodes, runs, reward, and model hyper-parameters.

We leveraged state-of-the-art manifold learning techniques to show what types of behaviors are common across episodes. We also implemented a heatmap view that is effective in showing how these model behaviors emerge over time during the learning process; some behaviors only appear late in the process, as it takes time for the model to learn sophisticated strategies.

Another view that embeds episodes in a plot of reward versus time is effective to let the user understand how quickly the model is learning and what behaviors lead to higher or lower reward. We have demonstrated our tool with several control problems of varying difficulty from the OpenAI Gym (e.g., inverted pendulum, double pendulum, lunar lander, cartpole, mountain car, and walker). Our tool made the selection of model parameters and understanding model behavior straightforward. It was also effective for debugging and explaining undesirable model behavior. In future work, the tools and techniques we developed for reinforcement learning data can be extended to other application domains involving large collections of timeseries and provide similar benefit to the analyst.

Three-dimensional Millimeter-wave Motion Tracking

Trevor Clark
PN18067/3066

This project simulated millimeter-wave (MMW) imaging technology to evaluate its potential for tracking human body position and motion in real time. MMW imaging is well-suited for tracking body surface, as it "sees through" optically opaque clothing. For this study, high-performance computers simulated radar scanning of free-breathing humans. Body surface features were identified in the scan data for motion tracking, and the tracking results were compared with the surface models. We demonstrate the plausibility for using this technology to validate patient positioning and to compensate for respiratory motion during external beam radiation therapy.

MMW imaging at PNNL has been developed for applications such as security screening and body measurements. This project looks to use real-time MMW imaging to confirm body position and track body motion over time. Currently, during radiation therapy, optical techniques are used to track motion, but unlike MMW, they cannot see through clothing. For radiation oncology, accurate tracking of respiratory motion is particularly important, as tumors in the lower chest and upper abdomen move as the patient breathes. This technology could increase the efficacy of radiation therapy, reduce ionizing radiation exposure to healthy tissue, improve patient comfort, and lead to reduced imaging artifacts in security screening and other applications.

We animated digital human models with varying ratios of "chest breathing" to "belly breathing." Each sequence generated 150 surface models representing one breath over 5 seconds. These surface model sequences were fed into a physical optics simulation (developed at PNNL) to generate synthetic MMW data as imaged with a specific antenna configuration. The synthesized MMW data was reconstructed as a series of three-dimensional (3D) data volumes.

A body surface estimate was extracted from each 3D volume, and we used OpenPose software to label anatomic orientation and limb position. Surface locations were identified on the chest and abdomen on the first frame of each sequence and then tracked across subsequent animation frames using normalized cross correlation. The location of these surface points across the animation is then compared with the location and motion of the corresponding point on the original surface model.

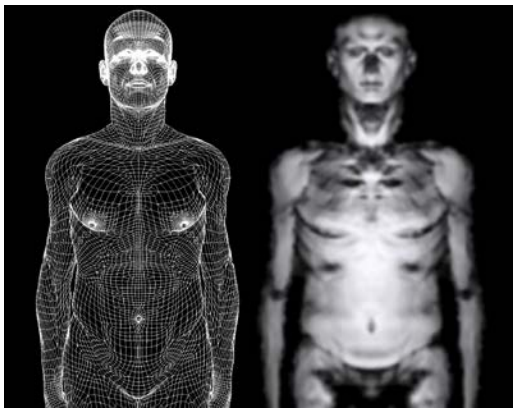

On the left is a faceted surface model used in the physical optics simulation to generate synthetic radar data. On the right is the resulting radar image after reconstruction.

Motion derived from the MMW data follows the original surface model closely. Error between the true model position and the position derived from the MMW data averages less than 5 mm. This suggests that MMW imaging may be useful for motion tracking applications requiring high accuracy such as radiation oncology.

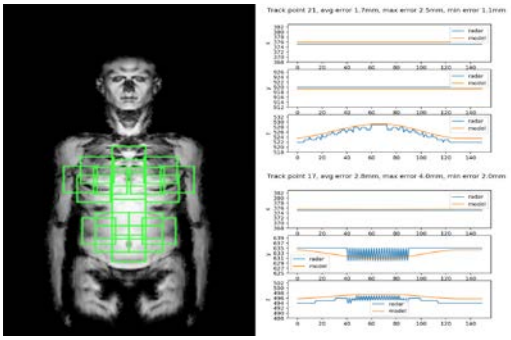

On the left is the radar image with square patches that are to be tracked throughout the animation. On the right are the tracking results for two selected patches. Error is less than 5 mm and can likely be improved with more work on smoothing and interpolation.

Untethered – Coherent Millimeter-wave Sensing Using Drones with Visual Motion Capture

Jonathan R. Tedeschi
PN17002/2892

This project has developed next-generation millimeter-wave (MMW) imaging techniques for national security and commercial applications with the use of drones and advanced MMW RADARs. Our work enables autonomous, through-barrier, high-resolution, close-range imaging.

Previously developed imaging systems for use on low-altitude flying drones perform two-dimensional (2D) synthetic aperture radar with resolution on the order of 3 meters from distances of kilometers. While this may be sufficient for air-to-air recon and terrain mapping, this does not achieve substantial resolution to detect personnel-born explosives, improvised explosive devices/explosively formed penetrators, or infrastructure inspection. These technologies are inherently limited, as they must operate at high frequencies to achieve any lateral resolution, which limits penetration through barriers.

Through-barrier MMW imaging technologies have achieved resolution better than 1 mm for security screening, with standoff ranges of less than 1 meter to several meters. The limitation of conventional MMW imaging is the requirement for a controlled antenna aperture to be scanned in order to mathematically focus the image. Unpredicted motion of either the object being scanned or the antenna array creates image distortion. This project aims to remove the barrier of rigidly controlled scan requirements and achieve high-resolution imaging at the centimeter level by fusing additional sensors with the MMW system in advanced focusing algorithms. The sensor fusion enables MMW systems to operate at close ranges with uncontrolled motion.

PNNL has developed an indoor operating environment for drone-based MMW data collection. The prototype configuration utilizes a drone with a max payload of 24 pounds, allowing for antennas, RADARs, and additional control hardware to be installed locally on the drone.

The Untethered project demonstrated the ability of the fused sensors and an unmanned aerial vehicle platform to form 2D MMW images in 2017. In 2018, a high-frequency MMW imaging system with an integrated antenna array was demonstrated with motion-induced hand-scanning to create 3D through barrier imaging with lateral resolution of 1 cm and downrange resolution of 3 cm.

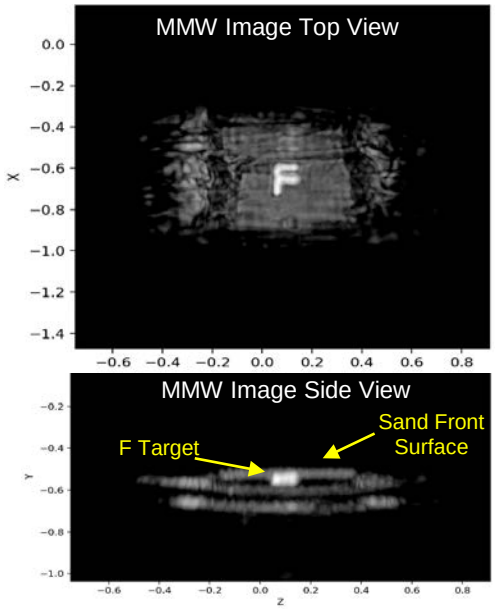

A 3D MMW image of a concealed 6-inch metal F target buried in sand, which successfully demonstrates the system's ability to image through barriers and resolve surface/sub-surface features.

Utilizing High Resolution Ion Mobility Separations in Multi-omic Analyses of Biologically Important Isomers

Erin M. Baker

PN17047/2937

The objective of this research was to study small molecule isomers that have been implicated in phenomics but are known to be difficult to detect or separate with currently available technology. Initially, we analyzed chemical standards with the drift tube ion mobility separations (DTIMS) system, and then we utilized DTIMS with rapid solid-phase extraction (SPE) capabilities to increase the speed of measurement throughput.

Small molecules have very similar elemental and structural makeups; therefore, new technologies with high resolution, sensitivity, and throughput are needed for better separations to occur. The overall objective of this study was to perform better structural separations of small molecules with currently available DTIMS and then compare these to our high-resolution on mobility spectrometry (IMS) separations in structures for lossless ion manipulations (SLIM) devices. We expected that the SLIM IMS analyses would unveil structures that were hidden from our currently available IMS systems.

To accomplish the aims of this project, we first optimized the speed, sensitivity, and dynamic range of the ion mobility spectrometry–mass spectrometry (IMS-MS) platform. To allow the use of the IMS-MS platform in small molecule measurements, first we created a collision cross-section (CCS) database of more than 600 small molecules with the DTIMS instrument. To date, IMS small molecule studies have been limited by an inadequate number of accurate CCS values for small molecules, causing features to be detected but not confidently identified. To perform this study, we utilized DTIMS to directly measure CCS values for over 600 small molecules, including primary metabolites, secondary metabolites, and xenobiotics. Since DTIMS measurements do not need calibration like some other IMS techniques, they avoid the calibration errors that can cause problems for distinguishing structurally similar molecules. All measurements were performed in triplicate, in both positive and negative polarities, with nitrogen gas and seven different electric fields, so that relative standard deviations could be assessed for each molecule and structural differences studied. The primary metabolites analyzed to date have come from key metabolism pathways, such as glycolysis, pentose phosphate pathway, and tricarboxylic acid (TCA) cycle, while the secondary metabolites consisted of classes such as terpenes and flavonoids, and the xenobiotics represented a range of molecules from antibiotics to polycyclic aromatic hydrocarbons. Different CCS trends were observed for several of the diverse small molecule classes, and when urine features were matched to the database, the addition of the IMS dimension greatly reduced the possible number of candidate molecules.

To perform our next aim of adding speed to the analysis, we worked on combining the automated RapidFire 365 SPE system with the DTIMS-MS. Since many isomers coelute in the SPE-MS systems, there is great benefit for adding an IMS separation stage. The RapidFire system is a high-throughput instrument from Agilent that has up to twelve different SPE cartridges (e.g., HILIC, C4, C18, graphitic carbon, etc.) to quickly prepare samples for IMS-MS analysis. In RapidFire, samples of interest are injected into a specific cartridge and then washed with solvent to remove salts and other contaminants that might cause ionization suppression. The flow is then reversed, and only molecules bound to the cartridge media are injected into the MS for 10-second analyses. This quick analysis time allows multiple cartridges to be used in under 1 minute, so that polar and nonpolar metabolites from the same sample can be studied in about 20 seconds. The increase in DTIMS-MS sensitivity obtained from the SPE front-end separation was quantitatively evaluated by comparing the limits of detection (LODs) and calibration curves for twenty environmental chemicals spiked into blood and

urine, with and without the front-end separation. The twenty exogenous metabolites were detected with LODs ≤ 10 nM in 1 µL of raw urine and plasma (which was extracted and diluted), and six metabolites were detected at ≤ 500 pM. Sensitivity was increased by a factor of about threefold compared to analyses without the SPE upfront separation and the r^2 values for the standard curves were greater than 98% for most chemicals, evidence of consistent linear responses. Instrument reproducibility was tested using triplicate analyses and an average coefficient of variance (CV) of less than 3% was detected for all concentrations except at the LOD for each chemical, which had CVs of ≤ 8% due to the lower signals. Additionally, the C18 and graphitic carbon cartridges were sufficient for the analysis of the twenty test compounds, resulting in a total sample analysis time of 20 seconds. Thus, the SPE-DTIMS-MS analyses provided extremely high throughput measurements with low intensity variability and a linear concentration response.

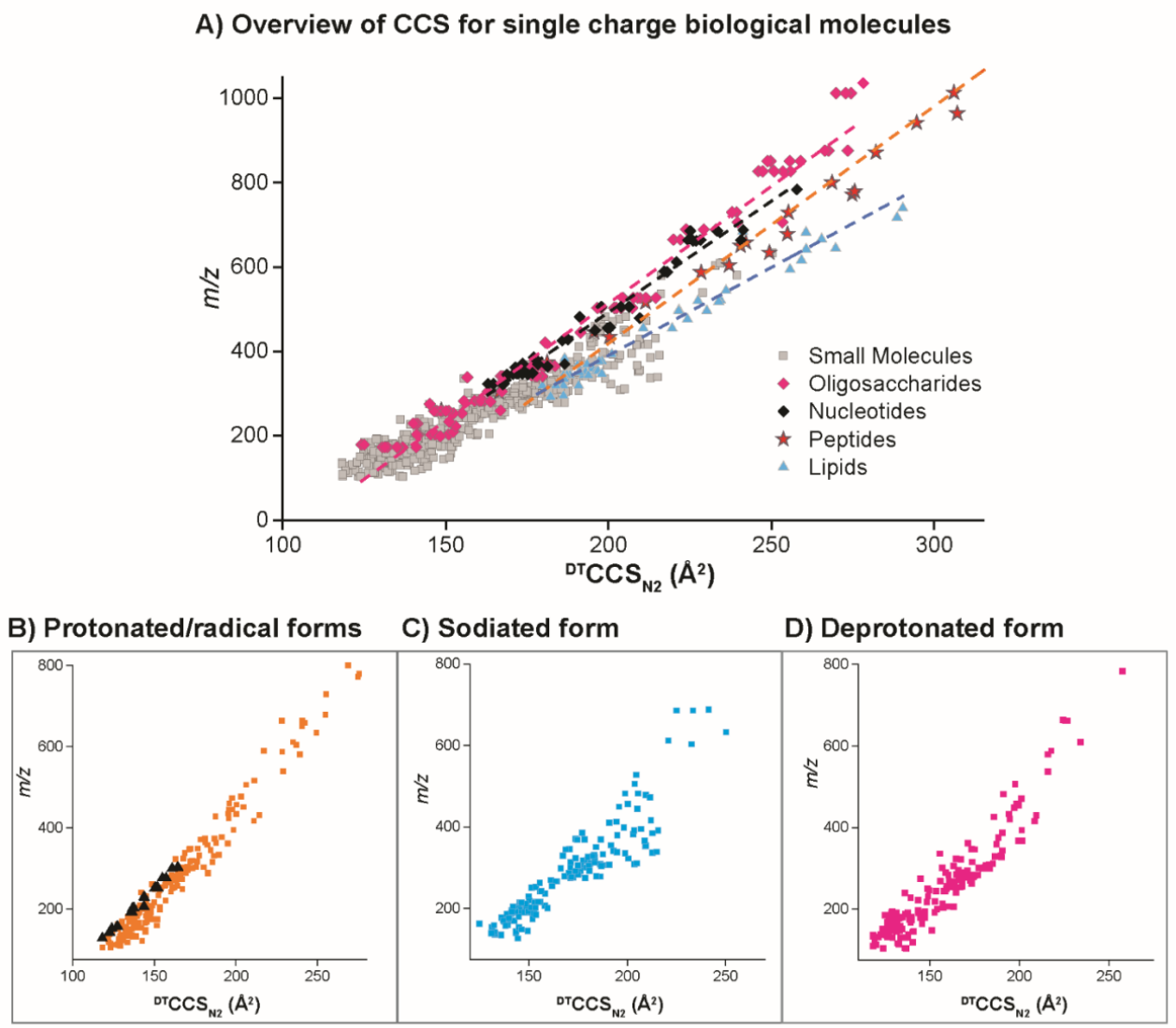

$^{DT}CCS_{N2}$ values for the small molecules in the database plotted with larger nucleotides, oligosaccharides, lipids, and peptides to observe trends. A) Illustrates an overview of all molecules measured in this work. The different ionization groups are broken out as B) protonated/radical forms (radicals are shown in black), C) sodiated forms, and D) deprotonated forms.


Biological Sciences

Advancing Ecosystem Understanding of Carbon Turnover and Storage through Molecular Characterization

Kirsten S. Hofmockel
PN16073/2850

We are developing a mechanistic understanding of carbon and nitrogen cycling coupling through biotic and abiotic interactions in order to improve community-based land models. These models play an important role in helping to understand feedbacks between terrestrial carbon cycling and climate change.

The main goal of this project is to evaluate the extent to which nitrogen (N) inputs into the terrestrial environment alter the composition and availability of carbon (C) residues for mineralization. The concurrently changing C and N cycles remain a key uncertainty in understanding feedbacks between the terrestrial C cycle and climate change, despite decades of research on decomposition responses to elevated rates of human-caused atmospheric N deposition. The coupling of C and N in Earth system models fundamentally alters critical feedbacks between the land biosphere and the global climate system, greatly attenuating ecosystem response to rising atmospheric CO_2 concentrations compared to carbon-only models. Yet, existing coupled models do not consider the full suite of linked C-N processes, particularly belowground. For example, the investigation of mineral and C interactions is not well understood. Here, it is generally accepted that nutrient additions increase belowground net primary productivity that should enhance physical protection of organic matter, especially in clay-rich soils, where acidification can increase the solubility and abundance of trivalent hydrolyzing cations (Fe^{+3}, Al^{+3}) that are particularly effective at stabilizing organic matter onto clays via cation bridging.

In order to complete the stated project goal, we have partnered with the Nutrient Network (an ecosystem scale nutrient addition field experiment) in obtaining grassland soils from six field sites. Research plots at each of these grassland field sites have received N amendments over several years. We are currently extending molecular knowledge about these sites to include the characterization and comparison of soil organic matter (SOM), mineralogy, metagenomics, and microbial community profiles between amended and control plots within each site. Further, to address our hypothesis that “N addition combined with microbial activity will alter the sorption of SOM onto mineral surfaces,” we conducted soil studies and incubations under controlled moisture and temperature conditions, importantly in the absence of new C inputs. Our experiments began during FY 2016 and were completed during FY 2017. The generation of different molecular datatypes and the reporting of findings from our research was carried out during FY 2018.

Two major analyses were conducted on data obtained: 1) from initial samples collected from each grassland site, and 2) from an 8-month incubation experiment using these collected samples. Analysis of molecular data associated with the initial grassland samples led to significant findings pertaining to different components making up SOM (e.g., proteins, lignin, lipid-like molecules) and their relation to iron minerals measured within these grassland field sites. Notwithstanding the diverse vegetation, microorganisms, and soil properties at each site, lignin-like compounds generally considered to be biochemically stable actually accumulate in the soluble phase of soil as residual C, making them more available for loss through leaching. Microbially derived, lipid-like compounds and proteins preferentially accumulate on iron (oxyhydr)oxide surfaces where they are less available for further microbial decomposition. In addition, our results show that the magnitude of accumulated SOM constituents is a function of the amount of poorly crystalline iron minerals in soils. For example, the more poorly crystalline iron minerals in the grassland soil, the lower the relative abundance of molecules similar to lignin. However, there is an increase in abundance of lipid-like compounds with increasing iron minerals. This indicates that in a predictive manner, different

classes of SOM are protected from microbial degradation because of their interactions with minerals found within prairie soils.

Nitrogen addition to prairie soils resulted in less significant correlations between iron bearing mineral phases and SOM classes, compared to unamended soil. This phenomenon has not been previously recognized in mechanistic models and soil C management practices and may strongly influence biogeochemical and microbial dynamics in grassland and arable ecosystems with implications for long-term SOM storage.

Data analysis from grassland samples collected as part of the 8-month incubation study revealed how the turnover of carbon in soils responds to elevated N. High-resolution mass spectrometry (FTICR-MS) data revealed that a variety of carbon-based organic chemicals within SOM decreased, yet the variety of microorganisms remained relatively constant over the course of the incubation. Such dynamics in compound-specific C chemistry suggest that diverse forms originally utilized by microorganisms are being converted to forms of C that are less favorable for microbial mineralization. This suggests that without the new addition of C, carbon respired as CO_2 is obtained from a larger residual carbon pool as time progresses. Here we revealed why specific classes of molecules (lignins, tanins) persist in the soluble phase in a gradient of soil environments.

Metagenomics results indicate that habitat associated with the different grassland ecosystems is the largest factor in determining microbial composition. For example, the influence of N addition on altering community composition was not apparent from our grassland samples, which contrasts research done by others, but could be explained by the longevity of our incubation and the possibility of convergence through acclimation; yet, we know that N addition has an impact on SOM composition. This suggests that understanding the dynamics of C within grassland soils cannot be determined solely by DNA-based measurements, but requires additional sophisticated phenotypic measurements, like those obtained as part of this project (i.e., using world-class FTICR-MS capabilities available at the Environmental Molecular Sciences Laboratory). Ultimately, the findings from our analyses of molecular data will be important drivers for future studies on grassland ecosystems.

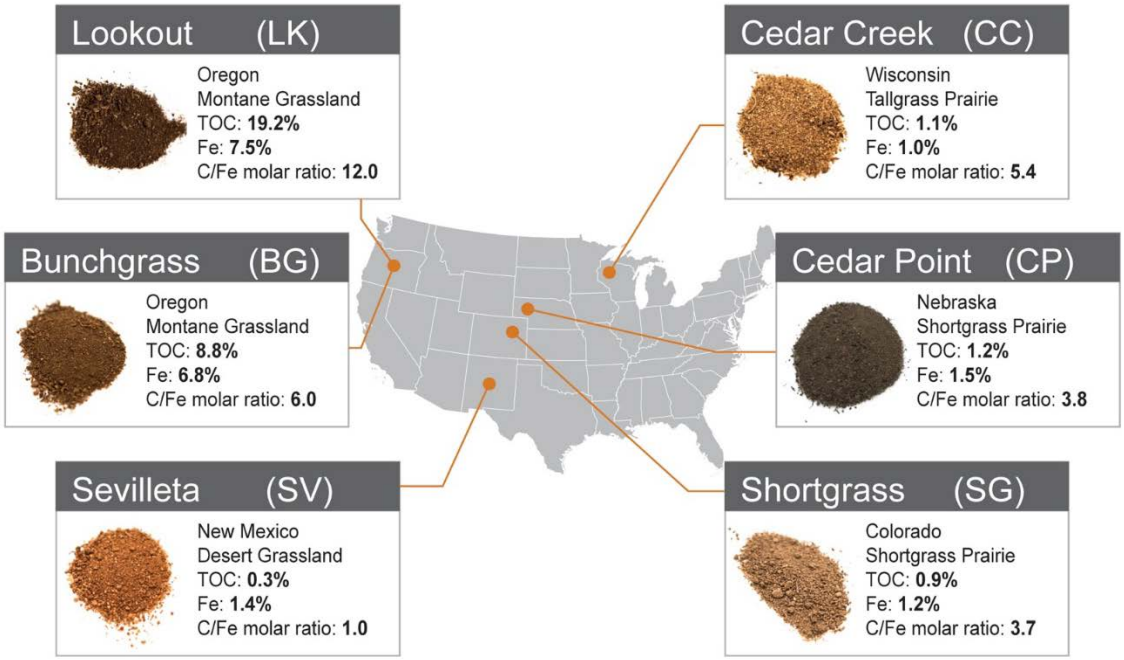

Soil analysis results from locations across the United States.

At the Fringe of a Shifting Carbon Paradigm with Climate Change: Unlocking the Organo-mineral Controls on the Bioavailability of Carbon at the Terrestrial-aquatic Interface

Ryan S. Renslow
PN16075/2852

Through our creative, experimental approach of simulated pedogenesis and unique combination of technologies that span across fields and disciplines, this work will advance our understanding of the mineralogical and biological mechanisms that regulate carbon cycling along the terrestrial-aquatic continuum in soils and sediments.

Recent evidence highlights the importance of organo-mineral interactions in regulating the source or sink capacity of soil. High surface area soils, such as allophane-rich or clay-rich soils, retain organic matter (OM) via sorption to mineral surfaces, which can also contribute physical isolation in interlayer spaces. In addition to the mineralogical influence, stabilization of OM can be influenced by development of reduced conditions (high water content and solubility and transport limitations on oxygen availability) that inhibit decomposition. Though recent literature for soils suggests that mineral interactions are important in governing the fate of OM, the capillary fringe can be permanently or seasonally inundated with water, making it hydrologically similar to marine sediments, where mineral adsorption is considered the governing process for persistence of OM. Since near-surface capillary fringe sediments would be subject to pedogenic processes, it is unclear what the contribution of surface area and adsorption is to stabilization of OM in these sediments. Most of the work to date, which relates surface area to stabilization of OM, has focused on investigations of natural soils, where OM has been incorporated onto mineral surfaces before sampling, and details on the mechanisms for this dynamic system can only be inferred, limiting our ability to properly predict the source sink capacity of soil. This research is taking methodical steps toward elucidating these mechanisms.

To test the mechanisms of mineral surface area protection of OM, we are facilitating secondary precipitation of alumino-silicates in the presence of OM held at two different temperatures in natural Nisqually River sediments (located at Mt. Rainier). A 3-month reaction was completed, which is intended to simulate early pedogenesis.

We coupled high-resolution carbon classification with microbiome characterization and CO_2 emissions in a short-term laboratory incubation to test the combined effects of temperature (4° versus 20°C) and moisture (50% versus 100% water-saturated) in capillary fringe-sediments maintained under different mineralogical conditions (mineral-amended versus non-amended). Our results show that less CO_2 was produced in mineral-amended sediments compared to non-amended sediments at 20°C and only in water-saturated sediments at 4°C. The abundance of condensed hydrocarbons, and compounds less thermodynamically favorable to microorganisms, were also relatively depleted in mineral-amended sediments compared to non-amended sediments. In these mineral-amended sediments, the reduction in thermodynamic favorability was especially enhanced in water-saturated versus non-saturated sediments. Shifts in the microbiome were most pronounced between water-saturated and non-saturated samples from mineral-amended sediments (with little effect of moisture content in non-amended sediments). Our results show that increased mineral content accentuated the effect of moisture on CO_2 production, carbon composition, and on the microbiome, suggesting that microbial access to carbon is governed by both mineral sorption and moisture content.

Furthermore, we found that increase in temperature showed a net increase in iron coatings, mineral surface area, and formation of colloids less than 200 nm in diameter. The result was a leaching rate of the higher-temperature-conditions soils that was two to three times higher than the lower temperature. This information helps fill knowledge gaps on mechanisms for carbon release from soil at the terrestrial-aquatic interface, thus improving our understanding of carbon cycling in general.

Deciphering Microbial Communication through Metabolites

Thomas O. Metz

PN16019/2796

This project will develop the advanced measurement capabilities necessary to define the metabolic processes of microbiomes and determine how these processes change due to perturbation.

Scientific questions to be addressed include 1) what are the impacts of perturbations on microbial community metabolic processes, 2) what are the impacts of changes in microbial community metabolic processes on ecosystem function and health, 3) can a systems-level understanding of microbial community interactions and metabolic processes be developed, and 4) can improved models be developed to better predict the impact of perturbations on microbial community metabolic processes.

With these questions in mind, understanding microbial metabolism in a community context is essential. Metabolomics measurements will play a key role in defining the metabolic processes of microbial communities and in determining how these processes change due to perturbations. Examples of microbiome perturbations include transitions of the human microbiome due to industrial processes associated with energy extraction and production (e.g., exposures to radiation, oil spills, pesticides, and fertilizers for biofuel feedstocks) and transitions of environmental microbiomes due to climate change.

A related aspect of microbial metabolism is communication via metabolites and other small molecules. These molecules are used by microbes to communicate with each other, their environments, and their hosts. However, the majority of microbial metabolites have not yet been identified, nor have their roles in interactions between community members been characterized.

The objectives of this work are to 1) determine the relative influence of direct (e.g., via secondary metabolites) versus indirect (e.g., via changes in microbial community metabolite pools) microbial communication and interaction through metabolites and other small molecules; 2) increase the identification coverage of the metabolomes of microbial communities, their hosts, and their environments; and 3) identify the mechanisms by which metabolites involved in communication and interaction are generated, transported, and sequestered within microbial communities.

In FY 2018, this project had the goal of developing a pipeline for structural elucidation of important, novel, or unidentifiable molecules detected in soil and gut microbiomes. Work toward this goal involved attempts to identify unknown metabolites in complex soil and mouse gut microbiome samples.

The samples were first analyzed using in-house Fourier transform ion cyclotron resonance mass spectrometry or gas chromatography-mass spectrometry capabilities in order to identify or annotate as many molecules as possible. Next, those compounds that could not be matched to relevant metabolite reference libraries or databases were isolated and enriched using offline liquid chromatographic separations. The enriched compounds were then subjected to nuclear magnetic resonance analysis in order to achieve confident chemical structure characterization. Analysis of the soil samples led to several interesting candidate unknowns for further study.

Determining Mechanisms of Microbial Metal Mobilization in Coastal Wetland Environments

Rene M. Boiteau
PN16106/2883

Environmental and land use change is expected to significantly alter patterns of terrestrial temperature and hydrology, which affect the availability of micronutrient metals. The purpose of this project is to understand feedbacks between hydrologic and climatic factors and metal availability that impact the rates at which organisms produce and break down organic carbon in soils and sediments.

Many biologically essential trace metals, such as iron, cobalt, nickel, copper, and zinc, are scarcely soluble in aquatic environments. Previous studies have demonstrated that organisms regulate the solubility and bioavailability of these metals through the production of organic metal chelating agents with a range of metal binding strengths and specificities. Determining what compounds are produced where and when is central to understanding how microbial communities adapt to changes in metal supply that result from external environmental factors such as hydrology or pH. The goal of this project is to characterize metal active compounds directly from soil environments using hyphenated liquid chromatography mass spectrometry, and determine which organisms are utilizing them by identifying the microbes that possess the biosynthetic pathways for these compounds in order to address the following questions:
1) What metabolites bind and solubilize metals in soil/waters across environmental gradients, and how do they impact metal bioavailability? 2) What organisms produce and take up these metal species in the environment? 3) What chemical or environmental triggers activate specific metal acquisition strategies? 4) What metabolic pathways are co-regulated with metal metabolism, and what is the potential impact of these changes on rates of organism growth and carbon cycling?

During the current year of this project, several new approaches for the confident identification of metal-binding species were studied using ultra-high mass resolution (21 Tesla) Fourier transform ion cyclotron resonance mass spectrometry (FTICR-MS). We investigate the molecular speciation of organic molecules that solubilize trace metals in calcareous soils from Eastern Washington. FTICR-MS enables the confident detection and identification of metal chelators that are produced by microbes that inhabit these soils based on screening for features that match diagnostic metal isotope patterns. We compared two approaches, one based on direct infusion using the incorporation of a rare isotope to validate true iron-binding features, and another based on liquid chromatographic coherence of isotopologues. While the isotopic exchange method requires significantly shorter analysis time, nearly twice as many features were observed with liquid chromatography mass spectrometry (LCMS), mostly due to the reduction in ion suppression where major features limit the sensitivity of minor features. In addition, LCMS enabled the collection of higher quality fragmentation spectra and facilitated feature identification. Siderophores belonging to four major classes were identified, including ferrioxamines, pseudobactins, enterobactins, and arthrobactins. Each of these siderophores likely derives from a unique member of the microbial community, and each possesses different chemical characteristics and uptake pathways, likely contributing to fierce competition for iron within these soils. Our results provide insight into the metabolic pathways by which microbes that co-inhabit calcareous soils compete for this essential micronutrient.

During the current year of this project, the capability of analyzing trace metal speciation at PNNL using trace metal clean chromatography hyphenated with inductively coupled plasma mass spectrometry have been established to achieve sufficient detection limits to detect metal complexes at naturally occurring concentrations.

This analytical tool was used to detect metal binding species (Fe, Cu, Ni, Zn) in environmental samples, which were then identified by coupling the same chromatography to high-resolution electrospray ionization mass spectrometry (Orbitrap or FTICR) to obtain parent ion and fragmentation information, and by capturing the fractions and analyzing the isolated compounds by direct infusion with FT-ICRMS to obtain molecular formula based on accurate mass.

Numerous compounds bound to these elements were detected and identified in grassland soils. These compounds included plant siderophores involved in iron acquisition by grass species, and siderophores that are commonly produced by Basidiomycota and Ascomycota fungi, which dominated the fungal taxa at this site based on ITS sequencing. In addition, several compounds were metal complexes that have not previously been observed but appear to be analogues of plant metabolites. Many of these compounds were complexed to metals other than iron, suggesting alternative roles for these compounds in acquisition of other micronutrient metals. The affinity for different metals was compound specific. This further implies that suites of molecules that compete for metal binding are used in metal regulation and highlights previously unrecognized interdependences of metal acquisition pathways.

In addition, microbial metagenome mining was used to investigate which organisms produce these compounds. Metagenomes from Kansas Native Prairie soils were screened for the presence of genes involved in metal metabolite production. An entire assembled cluster containing multiple pyoverdine biosynthesis genes was found. This gene cluster closely matches those of *Pseudomonas*, an abundant taxa within these soils, suggesting that pyoverdines may potentially be important for iron acquisition in these environments. Follow up chemical characterization experiments revealed that sorption of pyoverdines to soil particles reduces their solubility in bulk soils—a characteristic that is not true of plant or fungal analogues that appear in the same soils. This result raises new questions about the microenvironments that *Pseudomonas* species actively secrete these metal chelators compared to the plant and fungal species.

During FY 2018, additional experiments were conducted using a model strain of *Pseudomonas* to understand which conditions promote pyoverdine production, which members of the rhizosphere community of Kansas soil are capable of utilizing pyoverdine bound iron, and whether pyoverdine biosynthesis aids the growth of grass species in calcareous soils.

In order to evaluate the effect of these metal chelating metabolisms on growth rates, energy expenditure, and interactions between organisms, models of metal uptake must be constructed. Metal addition experiments with the compounds isolated from Kansas soil suggested that the kinetics of metal exchange are likely slow (hours to days), and thus, metal speciation is likely controlled not by equilibrium binding processes, as is typically assumed in environmental systems, but by kinetic association and dissociation processes. A platform for generating kinetic models of metal speciation with multiple ligands and metals has been generated in R and was expanded during FY 2018 to include multiple plant and microbial chelators and multiple metals.

Compound turnover rates are important parameters that determine the efficiency of chelation strategies but are currently unknown in environmental systems. These were determined by ^{13}C incorporation into chelate pools in laboratory experiments. To achieve this goal, a novel computational algorithm was developed to identify compound labelling rates from chromatographically resolved ultra-high-resolution mass spectrometry (21 Tesla FTICR) data in an untargeted fashion. As a model system to develop this approach, switchgrass was grown in calcareous soils and incubated with isotopically labelled carbon dioxide for two days. These tools simultaneously determine the turnover rate of other major metabolite groups within the rhizosphere.

Development of an *In Vitro* Platform for Inhalation Toxicology

Thomas J. Weber
PN18032/3031

With the national science agenda placing increased weight on* in vitro *toxicology to predict human and environmental health outcomes, a need for comprehensive species and organ-specific testing platforms has risen. This project seeks to develop the methods needed to immortalize lung epithelial cells to build comprehensive species-specific* in vitro *testing platforms to support inhalation toxicology.

A variety of methods have been developed to immortalize mammalian cells, producing cellular phenotypes ranging from normal to cancer-like. For toxicological analysis, the normal cellular phenotype is desired. For pulmonary toxicology, there is a need to assess the toxicity of environmental and man-made toxicants on a variety of cell types from different regions of the lung. Parallelogram approaches are then used to extrapolate results of toxicological analyses from animal models to humans through the integration of *in vitro/in vivo* data.

There is currently no platform that provides comprehensive coverage of the major lung cell types from humans and the major animal models used for inhalation toxicology. Immortalization of lung epithelial cells with telomerase reverse transcriptase (hTERT) and either overexpression of cyclin dependent kinase 4 (CDK4) or retinoblastoma protein (Rb) knockout has been reported to produce immortalized lung epithelial cells with a normal phenotype. If true, this approach could be used to immortalize the major lung epithelial cell types from humans and experimental animal models to build a comprehensive toxicology testing platform. This project seeks to compare these two immortalization methods and prioritize the best method for platform development.

Using lentivirus technology, hTERT was successfully expressed in primary normal human bronchial epithelial cells (NHBEC) in association with either overexpression of CDK4 or Rb knockout.

High viral transduction efficiency was observed when virus was added to cells in suspension prior to seeding them in culture plates. High viral transduction efficiency is desired to maximize heterogeneity in the immortalized cell population and mimic the heterogeneity occurring in normal lung tissue.

The combination of hTERT + CDK4 or hTERT + Rb knockout successfully immortalized human lung epithelial cells; hTERT + CDK4 produces a lung epithelial phenotype that produces surfactant proteins known to be synthesized by the primary lung epithelial cell, and the hTERT + Rb knockout cells are currently being characterized.

NHBECs immortalized with hTERT + CDK4 retain expression of lung surfactant proteins (SFPA2, SFPB, SFPD) and E-cadherin.

Development of High-throughput Metabolomics Technologies: Application to Studying the Flowering Time in *Arabidopsis thaliana*

David W. Hoyt
PN17011/2901

In this project, we are developing novel approaches for rapid identification and quantitation of unknown and known metabolites in complex metabolite mixtures. We apply these new methods to understanding developmental timing of plants in response to atmospheric CO_2 rise, which is elucidating our understanding of how elevated CO_2 can impact and potentially disrupt carbon cycling within ecosystems.

The total number of different metabolites in our universe could range up to 200,000 or more. Currently, we are limited to routine analysis of only less than 1% of them; the remaining 99% have unknown structures. Mass spectrometry (MS) and nuclear magnetic resonance (NMR) spectroscopy are the two major experimental analysis techniques in the analysis of metabolites. The future trajectory of metabolomics and its applications largely depend on the analytical capabilities of NMR and MS and their combination. Although the use of both NMR and MS methods is increasing, in the majority of these studies, the two methods are essentially implemented independently from each other. This approach does not fully capitalize on the complementary strengths of these two analytical techniques.

Our goal has been to develop advanced sample preparation, hyphenation (e.g., liquid chromatography [LC]-MS) and computational approaches with enhanced integration of NMR and MS. We will use these capabilities for accurate and high-throughput identification and quantitation of unknown and known metabolites in the model plant organism, *Arabidopsis* (*A.*) *thaliana*. Previous studies have shown that sugars act as signaling molecules that can influence the downstream expression of flowering genes. Elevated CO_2 generally increases the sugar profile of plants. This may be the fundamental mechanism for how elevated CO_2 influences flowering time. In order to fully test this hypothesis, comprehensive profiling of all carbohydrates and metabolites is needed, which is only possible by identification and quantitation of all unknown and known biomarker metabolites in *A. thaliana*.

In this project, we have made significant efforts to identify new biomarker metabolites and metabolic pathways regulating the flowering time of *A. thaliana*. In FY 2017, our first task was to develop an optimized sample preparation protocol for comprehensive study of plant metabolome. The next step was to develop a combined LC-MS and NMR protocol for characterization of plant metabolites. Moreover, we further integrated this with a new cheminformatics approach, named as ISEL NMR/MS^2. ISEL NMR/MS^2 allows rapid identification of unknown metabolites in metabolomics samples by combining MS/MS and NMR predictions. We tested the ISEL NMR/MS^2 approach in *A. thaliana*. This led our ability to identify a new secondary metabolite (glucoraphanin) enrolled in plant signaling.

During FY 2018, our focus on developing advanced quantitation techniques for combined NMR/MS analysis and its application was successful. Although combined use of NMR and MS is becoming popular, the majority of these studies perform separate multivariate analyses of their respective NMR and MS data sets. Only at the end are the results combined in an attempt to enhance the total information content. Such analyses completely ignore the highly informative correlations between NMR and MS data sets and, therefore, are not ideal to handle data analysis of combined NMR/MS studies.

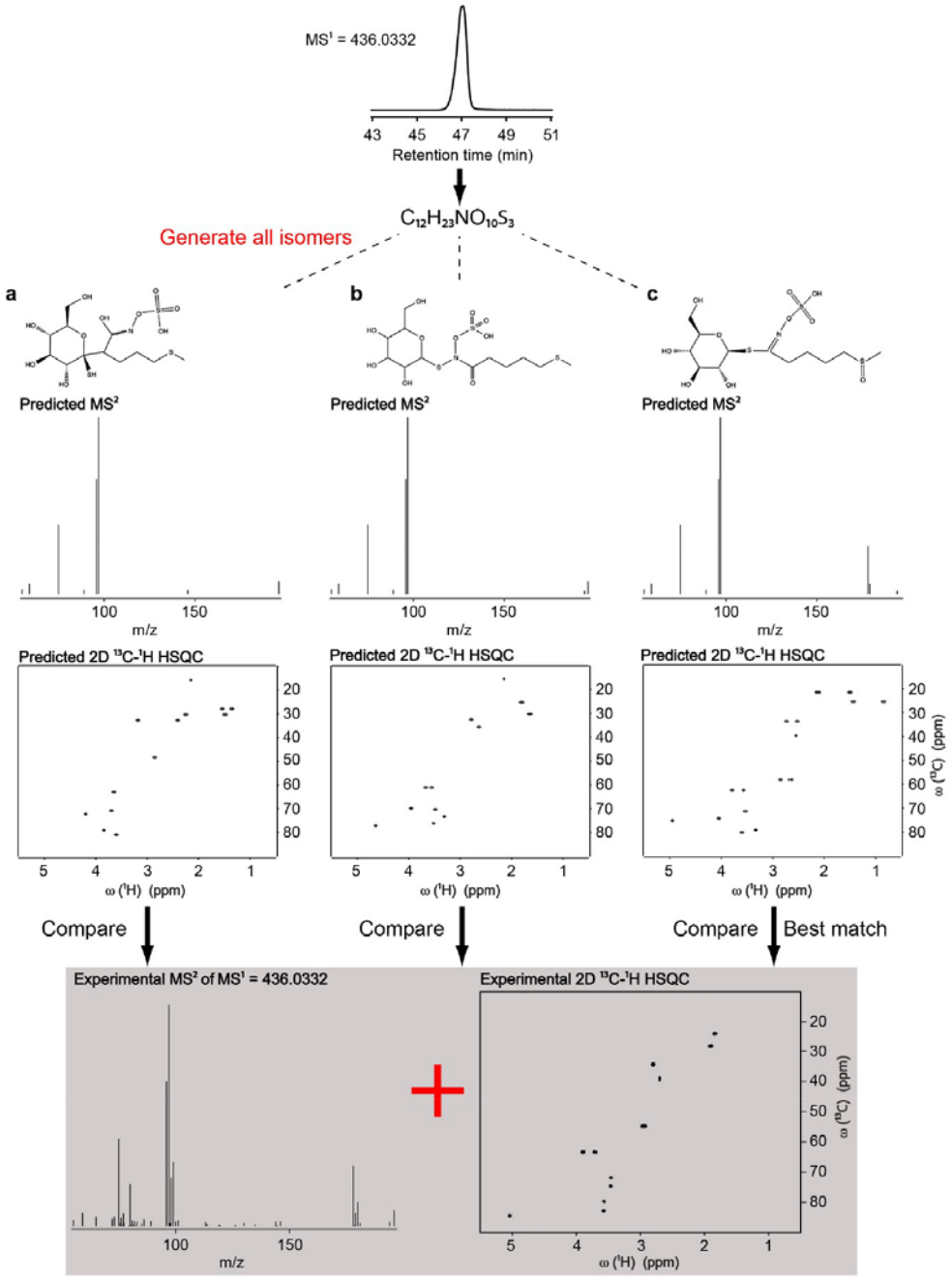

Application of ISEL NMR/MS^2 on *A. thaliana* metabolite extract having a single unknown metabolite in the NMR spectrum. The approach starts with an unknown LC-MS feature and then combines the experimental MS/MS and NMR information of the unknown to effectively filter the false positive candidate structures based on their predicted MS/MS and NMR spectra. This allowed identification of glucoraphanin, which was not present in the experimental metabolomics databases (i.e., unknown/uncatalogued metabolite). ISEL NMR/MS^2 is the first metabolomics approach that combines MS/MS and NMR predictions for unknown metabolite identification.

Development of Metabolite Sensors for Directed Strain Evolution

Alexander S. Beliaev
PN18018/3017

The overarching aim of the proposed technology is to dramatically accelerate engineering of high-productivity strains for conversion of renewable feedstocks into fuels and chemicals using novel metabolite sensors devices. A successful outcome will lead to the development of foundational capabilities and poise the laboratory to take leadership positions in innovative science and transformational solutions for a wide range of energy, environmental, and national security needs through advanced metabolic engineering and synthetic biology.

Current metabolic engineering strategies emphasize targeted and extensive genetic modifications intended to significantly improve product yields and strain productivity. This approach requires clear understanding of the organism's metabolic and regulatory makeup to predict consequences arising from genetic manipulations. Often, success via this direct approach is confounded if there are unanticipated regulatory features, feedbacks, or interactions between various pathways. Alternatively, strain engineering can be achieved through natural selection by carrying out iterative rounds of random mutagenesis and selection to identify desirable traits. To accomplish this, we will develop directed evolution technology for accelerated strain engineering using riboswitch-based metabolite-sensing circuits. Our concept is based on a previously developed method for *in vivo* selection and combinatorial design of functional riboswitches that drive expression of selection markers in response to specific target molecules in a dose-dependent manner. The key innovation features continuous sensor-driven strain evolution to dramatically improve product yields via redirection of metabolite flux.

This work was focused on creating lysine responsive riboswitches in *E. coli*. To perform this work, we collected a lysine responsive aptamer (region of RNA binding lysine) that is naturally occurring in *E. coli* and cloned it upstream of a sequence of random nucleotides (termed a switch sequence). We generated a library of switch sequences, each containing the lysine aptamer and a different specific switch sequence. Downstream of each aptamer/switch sequence pair, we cloned a tetracycline resistance gene.

This library of cassettes was then transformed into *E. coli*, and the resistance of *E. coli* cells to tetracycline in the presence of lysine was evaluated. We cultured two collections of *E. coli*, each containing the library of aptamer/switch pairs. One collection was cultured without lysine and one with lysine, and both were cultured with tetracycline. An *E. coli* cell containing a functional aptamer/switch pair will be resistant to tetracycline in the presence of lysine. This *E. coli* cell will, therefore, grow and divide more (creating more copies of the aptamer/switch pair) in the presence of lysine. Following this growth, we collected DNA from samples with and without lysine at various timepoints and carried out deep sequencing to identify the number of copies of aptamer/switch pairs with and without lysine; those higher with lysine represent functional riboswitches.

Deep sequencing of DNA isolated from *E. coli* grown with and without lysine was carried out to identify certain random regions representing switch sequences. Alignment of reads from both conditions showed a clear region of variability at the same position in several reads. This region represents the variable sequence, and we have identified several variable regions that show much higher abundance when lysine is present in the system versus when it is absent. Interestingly, many of these variable regions show only small differences, suggesting that a consensus sequence is emerging that we can focus on.

The higher abundance of these variable regions with lysine reflects the increased growth and replication of the *E. coli* cells harboring these variable regions, likely because the regions form the switch sequence portion of a lysine responsive riboswitch that confers resistance to

tetracycline. When lysine is absent from the system, the same riboswitch is no longer active in an *E. coli* cell, and the bacterium is not resistant to tetracycline, slowing their growth and leading to reduced replication of the variable region. These results have provided us with, not only a list of candidate lysine responsive riboswitches for downstream experiments, but also a general methodology for developing new riboswitches in the future.

Dynamic Multiscale Modeling of Complex Biosystems (DMMCB): A Framework for Multiscale Metabolic Modeling

Garrett B. Goh
PN16003/2780

This project envisions creating an interpretable deep learning framework for computational chemistry applications, working toward a data-driven research paradigm that uses artificial intelligence to accelerate conventional research and development.

The rise and fall of artificial neural networks are well documented in the scientific literature of both computer science and computational chemistry. Yet almost two decades later, we are now seeing a resurgence of interest in deep learning (DL), a machine learning (ML) algorithm based on multilayer neural networks. Within the last few years, we have seen the transformative impact of deep learning in many domains, particularly in speech recognition and computer vision, to the extent that most expert practitioners in those fields are now regularly eschewing prior established models in favor of deep learning models. Unlike traditional machine learning, deep learning distinguishes itself in its use of a hierarchical cascade of non-linear functions. This allows it to learn representations and extract out the necessary features from raw unprocessed data needed to make the necessary predictions, all without needing expert knowledge.

Since the start of this project, deep learning for computational chemistry has grown from a non-existent field into an emerging and rapidly developing research topic. However, to date, much of the ongoing literature still focuses on using DL models from a tool perspective instead of fully utilizing the “artificial intelligence” aspect of these algorithms (e.g., representation learning, transfer learning, etc.).

In FY 2016 to 2017, we laid the groundwork for intelligent DL models. Our first model was Chemception, a deep convolutional neural network that uses simple, two-dimensional molecular drawings for predicting a broad range of chemical properties. Despite being trained on unsophisticated raw data, we demonstrate how even with minimal expert knowledge, it can consistently outperform more established models that rely on sophisticated engineered features such as molecular fingerprints and descriptors.

In parallel, we also explored using chemical text data (SMILES) to predict chemical properties. The resulting model, SMILES2prop, was shown to perform at a level similar to Chemception. In addition, we developed interpretability features that suggested the network identifies chemically relevant functional groups when making predictions, thus indicating that DL models are capable of learning technically accurate scientific concepts without specific supervision.

A key shortcoming when working with chemical data is the lack of labeled data, which is a pre-requisite for DL models to work effectively. To overcome this, in FY18, we developed a novel weak supervised transfer learning approach to train “domain-expert” neural networks, using rule-based labels, cumulating in development of the ChemNet.

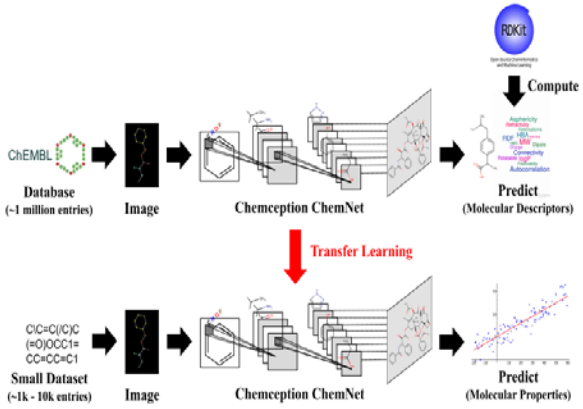

Diagram showing how the DL model uses ChemNet to make predictions.

Other efforts in FY 2018 include collaborations with the chemical engineering department at the University of Washington exploring multimodal learning for DL models and using expert knowledge to design furcated network architectures. Such approaches ultimately resulted in increased model accuracy without using more data.

Lastly, we also explored using generative DL models for inverse design, a paradigm where instead of predicting the properties of a list of candidate chemicals, we would utilize the DL model to generate or suggest chemicals that possess the properties specified. This was achieved using a generative recurrent neural network model with reinforcement learning, and we demonstrated how to simultaneously optimize the designed chemical against more than twenty different properties. This was achieved by developing a curriculum learning heuristic.

Dynamic, Multimodal, Molecular Imaging of Live Biological Systems

Venky Prabhakaran
PN17004/2894

This project has developed a multimodal platform for quantitative, dynamic imaging of metabolic pathways in living cells and tissues with exceptional molecular sensitivity and selectivity.

Molecular-level understanding of complex dynamics of biological systems, such as signaling or metabolic pathways over lengths and time scales, is a grand challenge in biology. Many existing individual imaging modalities are typically limited to specific molecular properties and biological processes. Therefore, multimodal imaging is necessary for predictive understanding of complex and adaptive living biological systems. In this project, we aim to develop a unique platform that combines electrochemical microscopy (ECM), nano-DESI mass spectrometry imaging (nano-DESI MSI), hyperspectral optical microscopy (HOM), and super resolution fluorescence microscopy (SRF), thereby providing an unprecedented depth of information about molecules involved in communication within and between living cells in their native environment.

Nano-DESI enables minimally invasive quantitative MSI of hundreds of endogenous molecules in biological samples using localized liquid extraction. ECM is an emerging technique for imaging biological systems that provides several powerful modalities for contact-free mapping of the cell topography, studying protein dynamics at the nanoscale, and quantitative imaging of selected redox-active species in complex biological systems.

Coupling with highly complementary SRF and HOM techniques will enable quantitative imaging of endogenous chromophores using spectrally (377-1051 nm, $\Delta\lambda < 5$ nm) and spatially (sampled at 50 nm^2/pixel) resolved optical absorption microscopy.

In FY 2017, we have successfully combined the ECM and HOM modalities. This was achieved using a finely pulled, precisely positioned nanopipette containing an optical that facilitates surface topography mapping along with optical and electrochemical measurements. This system allowed us to obtain high-resolution images of stomata in the epidermal layer of *Portulacaria afra*. A substantial change in absorbance in and around stomata indicates the presence of different chromophores in these regions of the plant tissue. The metabolites around stomata also exhibit natural fluorescence.

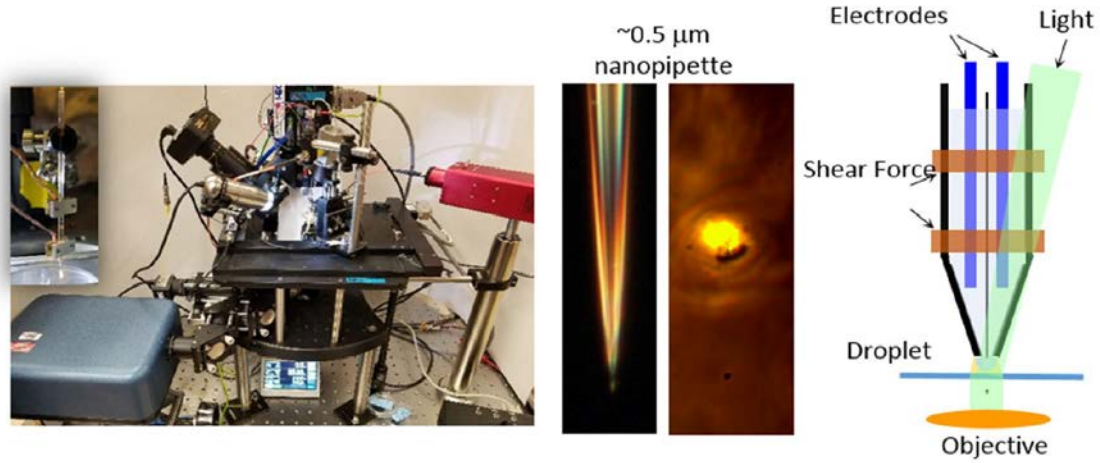

Prototype of optical/electrochemical/shear force imaging platform.

In FY 2018, we demonstrated the working principle of ECM and HOM modalities and developed a platform to combine with nano-DESI modality in the future. We have identified that stomata in the epidermal layer of *Portulacaria afra* showed many metabolites-related species in nano-DESI, ECM, and HOM modalities. This work provided initial insights on molecules involved in microbe-plant interactions.

Proof-of-principle experiments performed on model plant systems have demonstrated the working principle of individual capabilities of the multi-modal system. Numerous metabolites were spatially mapped using nano-DESI MSI. Meanwhile, ECM provided information on the topographic changes in the regions of interest in the samples and inform on the dynamics of protein complexes.

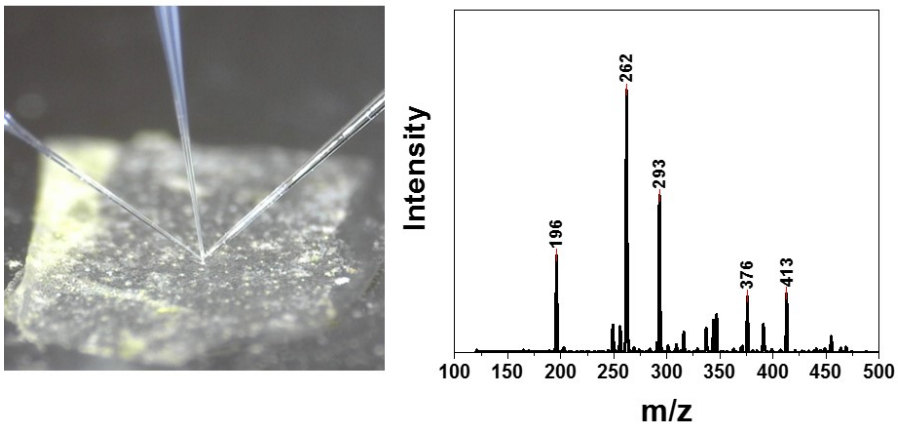

Prototype of Nano-DESI/shear-force imaging platform used to obtain the metabolic information on stomata in the epidermal layer of *Portulacaria afra.*

Enabling Prescriptive “Treatments” for Precision Soil Microbiomes by Activity-based Profiling

Aaron T. Wright

PN18016/3015

This project addresses the lack of understanding concerning the functional role of microbes in complex soil samples, with an aim to enhance agricultural- and biofuel-related productivity.

Plant health and productivity is largely defined by access to water and requisite nutrients, including macronutrients such as carbon, nitrogen, phosphorous, and sulfur. Nutrient availability to the plant is promoted by the soil microbiome surrounding the plant roots (i.e., rhizosphere) and microbes that grow directly on the plant roots (i.e., endophytes). Enzymes within the soil microbiota play several critical nutrient processing roles, such as phosphatases and sulfatases that deposit phosphate and sulfate into the soil near the roots for subsequent uptake by the plant, or serine proteases, which contribute to nitrogen acquisition. Predicting the activities present in a soil microbiome is greatly limited due to access to metagenomes and poor correlations between metagenomes and actual activities. Numerous reports ranging from human cells to complex microbiomes have shown inferences made from genomic sequence are deficient in describing enzymatic activity, resulting in a lack of understanding concerning phenotypic response to environmental perturbations.

In order to enable predictive functional measurements within the soil that can facilitate precision soil amendments that improve desirable microbial activities, and thereby plant growth and productivity, new technologies are needed. These novel technologies should enable the facile characterization of functional soil microbiome activities at native physiological conditions, which will be groundbreaking for predicting plant growth and response to change/stress. To deal with the complexity of field sites, functional measurement technologies should also be field deployable and sufficiently straightforward enough to enable the procurement of many samples. Such measurements will enable prediction of plant health and growth by determining the activity levels of microbiome functions that provide nutrients to plants. Our work this year aimed to enable the characterization of enzymatic activity in complex samples via the functionalization of glass surfaces with activity-based probes. These functionalized glass surfaces can be applied to complex microbiomes to measure enzymatic activity in their native physiological state. In total, this work is developing novel technology that can identify target enzymatic activity in soil using activity-based protein profiling.

Due to the large effect proteases have on nutrient acquisition, we began functionalization of glass surfaces with a serine hydrolase targeting activity-based probe, termed FP2-ABP. To do this, we performed a sequence of chemical steps to clean and subsequently functionalize the surface with a polyethylene glycol (PEG) linker bound to a click-chemistry compatible azide on the terminal end of the PEG chain. This enables the use of click chemistry to covalently bind the alkyne handle of small molecules, such as activity-based probes, to the glass surface. Probe-functionalized surfaces may then be applied to soil samples to identify enzymes responsible for nutrient acquisition and measure their activity.

We initially tested this methodology using a fluorescent reporter with an alkyne handle. We found that the fluorescent reporter was successful in covalently binding to the surface through the click chemistry reaction. We followed this by functionalizing a glass surface with our serine hydrolase targeting FP2-ABP. A second click chemistry step on the probe-functionalized surface using a fluorescent reporter yielded no fluorescence, indicating that the FP2-ABP covalently bound to the surface. Thus, using click chemistry, we were able to react the azide on the surface with the alkyne handle present on both a fluorescent reporter and the FP2-ABP. We are currently analyzing the surface using analytical techniques such as X-ray photoelectron spectroscopy.

Additionally, we are optimizing application of the FP2-ABP functionalized glass surface to biological samples by comparing data obtained from solution-phase probing to surface-based probing. Preliminary results reveal a highly selective surface for a specific serine protease, and we are optimizing conditions to expand the range of targeted serine proteases to closely resemble that of solution-phase probing. Optimization of our current protocol and application to complex soil samples are the immediate next steps we are performing. Additionally, since enzymes that impact plant health in complex samples, such as soil, are diverse, predicting microbiome activity will require a variety of activity-based probes to detect specific macronutrient acquisition mechanisms. The application of different probes we have developed to the glass slides using a similar protocol to that of the FP2-ABP will allow for these measurements to be made, providing a novel, robust method for measuring enzymatic activity in complex soil samples.

Fungal Solid State Fermentation for Citric Acid and Enzyme Co-products that Derive Value from Agricultural Waste

Jon K. Magnuson

PN17082/2972

Aspergillus niger is a fungus that readily converts sugars from corn or sugar cane to citric acid to supply the large existing global citric acid market. We are developing a low-cost, solid-state fermentation capability using advanced strains of A. niger to produce citric acid and valuable enzymes from residual sugars in agricultural (food processing) waste found in hundreds of locations across the United States.

Aspergillus niger is a fungus that has been utilized for over 100 years to convert sugars, such as glucose and sucrose, to a valuable product found in soft drinks and other products: citric acid. This fungus is also used by industry to produce other valuable products such as enzymes that can break down non-food plant biomass into sugars. This project developed high-performance strains of *A. niger* for use in a solid-state bioprocess. In solid-state processing, the fungus grows on top of the solid plant residues (food waste) instead of in large vigorously stirred and aerated tanks of sugars found in typical liquid bioprocesses. The advantages of the solid-state method are that equipment and energy costs are lower, and it can be established at sites where relatively small amounts of plant waste are generated, like food processors. This translates to economic and environmental benefits by using these waste streams, which would have had a disposal cost, to instead generate valuable products. Our advanced strains of *A. niger* produce higher levels of citric acid on these food processing waste substrates and do not require addition of valuable sugars or other nutrients.

We have obtained agricultural residues from the local fruit juice and wine-making industry, namely apple pomace. This is a solid, fiber-rich residue (basically, pulp) remaining after the juice has been extracted from the fruit. These residues have low to no value in their current state, so they represent an inexpensive substrate (e.g., source of carbon, nitrogen, and other nutrients) for a bioprocess such as the citric acid process we have proposed.

We have tested three *A. niger* strains for growth and production of citric acid on apple pomace hydrated with varying amounts of water, citric acid production medium or only the salts (nitrogen and trace elements) found in citric acid production media. The three strains of *A. niger* that have been tested include two proprietary PNNL strains, one of which has a specific gene deleted and the other a specific gene inserted. The isogenic control for the study (i.e., the parental strain) is *A. niger*: Δ*kusA*, which has the *kusA* gene deleted, thus allowing targeted gene integration or deletion. This is a necessary precursor strain in order to create the other engineered strains.

We have made three exciting and practical discoveries. The first discovery is that our gene over-expression strain performs better than the control strain with respect to citric acid production under these solid-state fermentation conditions, so we have a high-performance practical strain. The second discovery is that the pomace and water cultures performed just as well as those with added nutrients. This means that no expensive nutrients need to be added, thus making the process more economical. The fact that we only needed one gram of water per gram of substrate (pomace) is also important, since water usage is an economically and environmentally expensive part of such processes, which makes our minimal water usage very encouraging. Third, we detected substantial amounts of polygalacturonase (pectinase) enzyme activity in the liquid. These enzymes are used to digest the pectin in the pulp of the fruit; breaking down the pulp increases the yield of juice.

The research in this project has shown that we can utilize a low-value agricultural waste or residue, apple pomace, as a substrate for producing two valuable products. These products, citric acid and pectinase, are both used in the juice industry. Thus, we can potentially create an efficient closed cycle where a waste is used to generate valuable products and simultaneously reduce waste.

Gut-on-a-Chip for Multi-omic Studies of the Gut Microbiome

Joshua N. Adkins
PN16108/2885

There is a need for reproducible, comprehensive characterization of biomolecules from small complex microbiomes. One of the main challenges in the field is to understand the interactions between micro-organisms and their hosts* in situ *at the small spatial scales of these interactions to avoid artifacts, averaging, and blending effects from the surrounding tissues. Current mass-spectrometry-based omics technologies do not enable this type of analysis, as the amount of biomaterial that can be analyzed is very small. We have worked to overcome this major obstacle in small-scale.

Alteration of the human gut microbiota composition and function has been associated with many human diseases. The impacts of perturbation resulting from pathogens, antibiotics, or toxins on the microbiome, despite great interest, remain largely unknown because of the difficulty accessing molecular information on the direct interactions between hosts and microbes and on the microbes living in small, localized communities inside the body of their host.

A critical challenge to effectively study perturbations on microbiota is the lack of methods to perform small-scale global measurement in specific microenvironments throughout the body of hosts. If obtaining the small amount of spatially localized biomaterial to access this molecular information is achievable using specific isolation methods, such as laser micro-dissection, the size of the samples generated in order to get relevant information on these molecular details must be small, and the number of microbes that can typically be harvested using these strategies is below 10,000 microbial cells.

As proteomics does not benefit from amplification technologies, such as nucleic acid studies, sample losses on the surfaces during sample preparation is a major bottleneck, impairing the analysis of small samples. For this reason, in NanoPOTS, all the steps of samples preparation and handling are realized by a robot in a nanoliter-sized droplet placed on a hydrophobic pedestal. This methodology recently achieved proteomics on only few cells and even allowed to us to distinguish individual mammalian cells based on their proteomics profile.

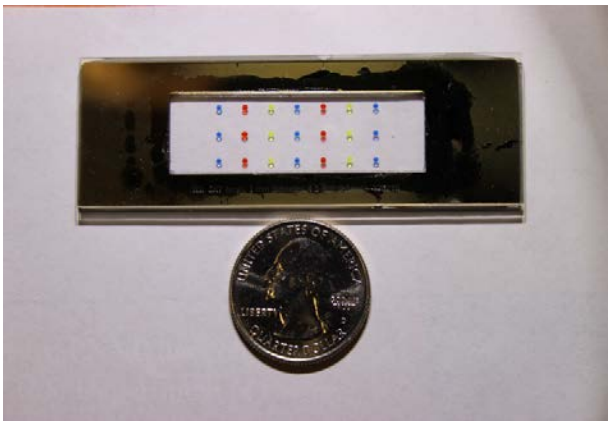

Picture of a NanoPOT chip with artificially colored droplets, in which all the sample preparation steps can be carried out.

However, if the methodology is nearly ideal for mammalian cells, it suffers a main drawback for the analysis of bacteria. All the steps of the sample preparation need to be carried out inside a nanodroplet, including the cell lysis; therefore, mechanical methods of lysis (including bead-beating, sonication, and any pressure-based lysis) are unfeasible in this platform. Unfortunately, the bacterial cell envelope is usually stiffer and harder to break than mammalian cells due to the presence of peptidoglycan, a polymer consisting of sugars and amino acids, which forms a mesh-like layer outside the plasma membrane of most bacteria, forming the cell wall. The thickness of the peptidoglycan is variable between the two main classes of bacteria found in nature. Typically, the peptidoglycan of the Gram-positive bacteria is thicker than the one of Gram-negative. If enzymes, such as Lysozyme, can break peptidoglycan, their utilization in NanoPOTS is

not an option, as it would constitute a high source of protein contamination hindering peptides from the small sample analyzed.

Consequently, the first step we took to enable the utilization of NanoPOTS was to evaluate an array of chemically based methods (in addition, with heating, which is possible in the NanoPOTS pipeline) to disrupt the bacterial cell-wall and lipids. This evaluation was carried on both Gram-positive and -negative bacteria in order to estimate if they were presenting a bias toward one or the other type of peptidoglycan. After successfully identifying various methods that enable the extraction of the proteins at equivalent or better yield than mechanical lysis, we have evaluated their applicability onto a NanoPOT chip.

Subsequently, using serial dilutions, we have generated samples of *B. subtilis* containing 30,000, 7,000, and 1,500 cells and analyzed those by down-scaling the best chemical lysis working extraction method onto chips.

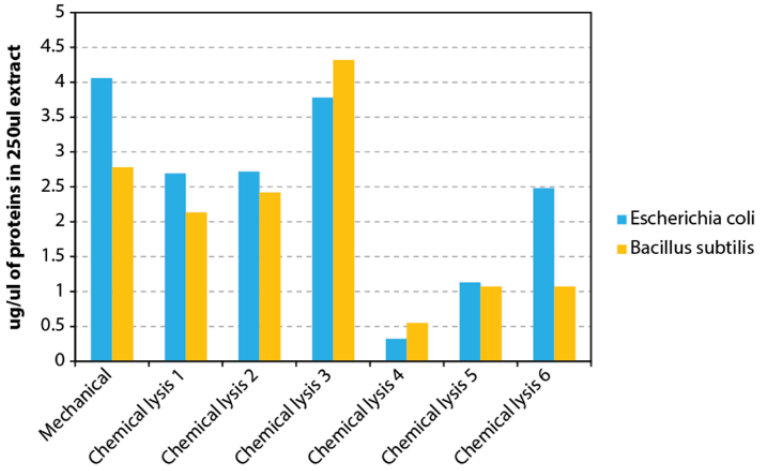

An array of fully chemical extraction methods was tested to extract proteins from 250 µl of 1 × 10^9 Gram-positive and Gram-negative bacterium. The graph presented shows average of triplicates for each method on each type of bacteria.

Metabolic Responses of Eelgrass to Environmental Stressors

Nicholas D. Ward
PN18021/3020

This project developed a new, molecular-level approach for evaluating how eelgrass, a critical coastal habitat, responds to environmental conditions. This approach has the potential to greatly improve the success of restoration efforts and our understanding of the role of eelgrass in global biogeochemical cycles in a changing world.

The Environmental Protection Agency and the Washington State Department of Ecology have made large investments for restoration of eelgrass, a keystone species in Puget Sound, but the success rate of restoration is limited by a lack of fundamental knowledge of how eelgrass responds or adapts to changing ocean conditions. The seagrass community is in the early stages of linking ecophysiology with phenotypic responses based on cutting edge "omics" analyses, with recent publication of the *Zostera marina* genome enabling annotation of genes and associated metabolites. This project focused on developing a suite of biomarker proxies for eelgrass health based on cellular metabolite abundance, which was applied to samples collected from controlled experiments testing the effects of ocean acidification on eelgrass productivity. From these new metabolomic analyses, we hope to ultimately develop a tool for rapidly screening eelgrass fitness in a given environment.

This project consisted of multiple main applications of our metabolomics-based toolset that we developed for eelgrass during the first quarter of FY 2018.

Evaluation of CO_2 enrichment effects on metabolism. Samples were obtained from Old Dominion University collaborators from a 19-month CO_2 enrichment experiment. We have analyzed a subset of these samples via gas chromatography-mass spectrometry and liquid chromatography-mass spectrometry for metabolomic fingerprints and metabolite identification. We found not only that metabolomic fingerprints responded significantly to CO_2 abundance, but that there are also significant strain-specific responses, suggesting that different strains have varying capacities to respond to environmental stressors. We identified a handful of specific metabolites that will prove useful for evaluating responses to specific stress factors.

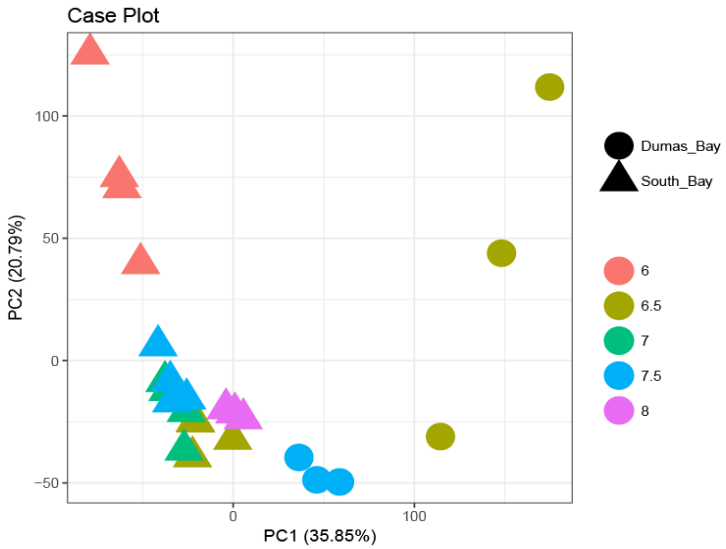

Principal Component Analysis comparing metabolomic fingerprints of *Z. marina* leaves from two strains under pH conditions ranging from 6 (enriched pCO_2) to 8 (ambient pCO_2). Both pH and strain had a large influence on the metabolome.

Regional survey of Puget Sound eelgrass. We worked with the Marine Science Laboratory eelgrass restoration team to collect samples of opportunity around the Puget Sound region during summer FY 2018. Samples have been processed and archived for analysis. Our goal is to evaluate the metabolic fitness of these different strains for the wide range of environmental conditions in Puget Sound, specifically during the growth season.

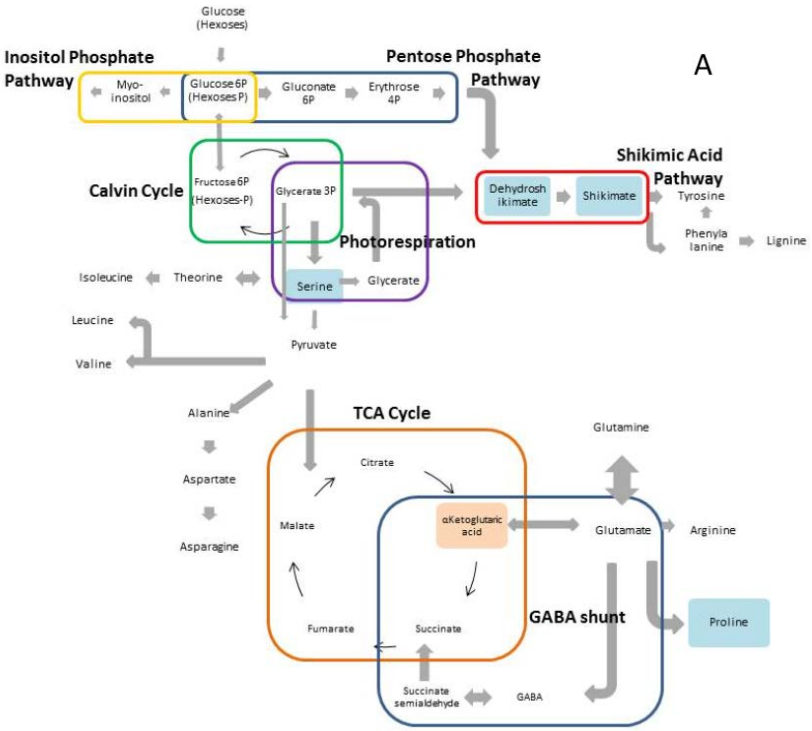

Schematic representation of individual metabolite responses in metabolic pathways of *Z. marina* exposed to high (pH 6) and low (pH 8) CO_2 conditions. Major influenced pathways include TCA cycle, Calvin cycle, and other linked associated pathways such as the pentose phosphate pathway (PPP), the Shikimate pathway, and amino acids synthesized from various metabolites of Calvin and TCA cycle.

Metabolomics of Programmed Cell Death

Jennifer E. Kyle
PN18078/3077

The objective of this project is to provide the first comprehensive multi-omic analysis of PI3K-AKT-mTOR inhibition in cancer cells and detail the alterations in lipid metabolism to lay the groundwork for newer treatment modalities that will override the complexities of drug resistance. Extrapolating the concept of targeted intervention to other systems may enhance our ability to manipulate biological systems for human benefit.

Targeted therapeutics directed at specific biological processes, such as lipid metabolism, are emerging as the treatment of choice for many diseases. Lipidomics is the study of cellular lipids to understand the function and structure of biological systems. The interaction of lipids with other cellular components, including proteins and metabolites, enables a greater understanding of the mechanisms behind lipid metabolism and homeostasis.

The relationship between metabolic processes and regulated cell death has been extensively studied in cancer. However, despite initial clinical responses to inhibition of known targets, complete and durable responses to these agents are rare, and eventual resistance to each agent is nearly universal (median time to progression of 8 to 11 months). In this project, the metabolic changes, specifically aberrations in lipid metabolism, was examined as a potential mechanism for the development of resistance to targeted therapies. Utilizing mass spectrometry, we conducted global (i.e., untargeted) lipidomics, proteomics, and metabolomics on human kidney cancer cell line (ACHN) treated with drugs CYT387+MK2206 (CM), a combination of JAK and AKT inhibitor, which results in potent inhibition of the PI3K-AKT-mTOR pathway, and drug RSL3 that inhibits GPX4 and results in ferroptosis, a form of non-apoptic cell death.

Using mass spectrometry, 469 lipids, 5,903 proteins, and 75 polar metabolites were identified and quantified. These measurements in combination with bioinformatics approaches lead to an integrative omics characterization of CM, RSL3, and CM+RSL3 treated cells. RSL3 treated cells underwent minimal alteration with principle component analysis clustering RSL3 closest to the controls (no drug treatment). CM alone and in combination with RSL3 underwent extensive alteration and were more like each other than the controls and RSL3. Given the similarity of CM and CM+RSL3, results from the CM treatment will be the focus of the report unless otherwise noted.

Alteration in lipid metabolism was identified in each of the ’omics platforms. Metabolomics identified oleamide, a lipid signaling molecule, which decreased and underwent the greatest log2 fold change of any identified metabolite. The significance of the decrease in this lipid is still being investigated; however, oleamide has known roles with roles in gap junction inhibition and is responsible for causing sleep. In cancer, it has shown to have inhibitory effects on tumor extravasation and lessen metastasis.

Proteins related to lipid metabolism comprised 8.6% of the statistically significant proteins in the treated cells. Functional enrichment analysis of all statistically significant proteins with CM treatment highlighted increases in lipid metabolism, specifically fatty acid degradation (including beta-oxidation), as well as lysosomes. This may indicate greater instances of autophagy, which is associated cellular stress, survival as well as cell death. Enrichment analyses also identified decreases in cell division, which is expected with the inhibition of the PI3K-AKT-mTOR pathway.

Surprisingly, lipidomics analyses revealed minimal statistically significant changes. This may due to neutralizing effects of global analyses, meaning that alterations in one of the areas of the cell may be masked by alterations occurring in another region. Despite this, global trends in the sphingolipids revealed that complex sphingolipids with a specific chain composition were increasing with treatment, whereas those with a different chain composition

decreased. Upon investigation of proteins involved in sphingolipid metabolism, it was discovered that proteins involved in *de novo* synthesis of ceramides, the precursor lipid of more complex sphingolipids, correlated with the lipidomics trends. One of these proteins may be of interest, as the particular biological roles, such as acting as an indicator of oxidative stress and hypoxia, as well as being influenced by vitamin E, aligns with known changes resulting from drug treatment.

In summary, a multi-omics approach was used to characterize lipid alterations upon drug treatment resulting in the inhibition of the PI3K-AKT-mTOR pathway of kidney cancer cell lines. The strength and unique finding of this works resulted from integrating the ’omics data providing a couple molecules of interest of drug targeted therapies.

Microbiome-Exposome Interactions

Aaron T. Wright
PN15073/2748

This project is determining xenometabolic activities at the host-gut microbiome interface and delineating how exposures create metabolic susceptibilities and impact host physiology.

Environmental exposure to xenobiotics contributes to the shaping of the gut microbiota in hours immediately following birth and throughout childhood development. For the gut microbiota, some chemical exposures represent a potential carbon and energy source, but it is unclear how the microbiota interact with these contaminants and how microbe-mediated metabolism may alter bacterial functions or composition, and/or contribute to the negative consequences of chemical exposure.

Prior research suggests that compositional changes occurring within the gut microbiota do not accurately reflect alterations to function due to the chemical exposures. This is likely even more pronounced through development, as microbiome composition and function are both impacted by exposures. Therefore, to understand the functional consequence of chemical (xenobiotic) exposures throughout development on the gut microbiome and how these functional alterations may impact the susceptibility for disease onset, new function-dependent approaches must be applied that are irrespective of microbiome composition. We have developed activity-based protein profiling (ABPP) approaches and demonstrated how they can be used to characterize cell and enzyme level functional capacities and their susceptibilities to chemical exposures.

The human gut lacks a well-defined core set of organisms that span all human populations, yet microbiota across healthy individuals have common functional capacities for metabolism that arise from disparate combinations of more than 1,000 microbial taxa. Even within an individual, metabolism in the microbiota is largely maintained despite shifts in microbial composition during a lifetime, but susceptibilities during early life development due to chemical exposures are not clear. This suggests that understanding the molecular basis for gut microbiota-enabled susceptibility to chemical-induced toxicity and disease can not readily be inferred from metagenomes alone. It also suggests that inter-individual differences in phylogenetic composition may not produce varied metabolic function; rather, functional redundancy within the microbiota may compensate for compositional differences.

A more accurate model of microbial metabolism within the gut considers metabolism at three structural levels: community metabolism, taxa-level metabolism, and enzyme-level metabolism. Complex metabolic pathways will likely emerge through interactions within and across these hierarchical scales. At the community level, the spatial and compositional structure influences proliferation, activity, and survival of specific taxa. At the species level, the expression of enzymes for metabolism is controlled by various regulatory mechanisms. Finally, at the enzyme level, the actual biotransformations are performed. Current approaches, such as metagenomics and metatranscriptomics, can address the first two levels but are intrinsically unable to address the third. The methods we have developed directly incorporate enzyme-level functional measurements to enable more accurate predictions of how xenobiotic exposures can induce susceptibilities in the microbiome and host during development, leading to the onset of disease.

Activity-based protein profiling can isolate functional subpopulations of microbial taxa and enzymes from the gut microbiome. Fluorescence-assisted cell sorting (FACS) followed by DNA sequencing is a valuable tool to study function within microbial communities. We have developed an ABPP-based FACS platform (ABPP-FACS) for application in complex microbial communities, including the gut. The use of ABPP has multiple advantages. Because the probes measure enzyme activity regardless of protein source, these tools are not limited to specific taxa in the microbiome. Furthermore, the use of a clickable reporter tag

allows incorporation of a variety of fluorophores, making it easier to avoid spectral overlap with additional reagents. We have utilized ABPP-FACS to isolate microbes possessing β-glucuronidase, serine protease, and glycoside hydrolase activity from the gut microbiome. With regard to bacterial β-glucuronidases, they hydrolyze the glycosidic bond between glucuronic acid and xenobiotics, such as the chemotherapeutic irinotecan, and can lead to regeneration of the parent compound, altered pharmacodynamics, and side effects. Despite the medical importance, the specific microbial taxa and enzymes involved in its metabolism have not been known.

Using ABPP-FACS, we have enabled isolation and characterization of microbes that possess active β-glucuronidases and characterize the taxa by 16S sequencing and the enzymes by proteomic analysis.

To do this, microbes were freshly isolated from the mouse gastrointestinal tract and immediately labeled with a glucuronidase activity-based probe (GlcA-ABP), recently designed and synthesized by our group. A control of vehicle only (No Probe) was also included. Cells from both samples were washed, fixed, and a fluorophore (CF-640R) was attached to labeled proteins via click chemistry. Cells were then analyzed via flow cytometry. Gates were drawn based on the No Probe sample to detect cells with increased fluorescence for cell sorting. For both samples, events in “Probe Positive” and “Probe Negative” gates were sorted. DNA was isolated from all populations and used as a template for 16S sequencing. Taxa that were significantly more abundant in the GlcA-ABP Probe Positive population or the Probe Negative population were identified using Aldex2 and are taxa, which produce active β-glucuronidase within the gut. The probe labeled cells were also lysed, and the labeled enzymes were enriched and characterized by proteomic analysis, resulting in the identification of 10s of glucuronidases mapping back to the taxa isolated by flow cytometry.

To our knowledge, this proof-of-concept work is the first to sort and identify cells and enzymes based on a specific metabolic function within the gut microbiome. Importantly, this platform can be used with ABPs for other gut microbiome metabolic functions of interest as follows: serine and cysteine proteases (developed), glycoside hydrolases (developed), bile salt hydrolases (developed), β-glucuronidases (developed), sulfatases, and β-cysteine lyases.

Molecular Mechanisms of Drought Mortality and Survival

Nate G. McDowell
PN17094/2984

This project allows, for the first time, direct understanding of the molecular underpinnings of drought-induced mortality in agricultural species. This enables future application of 'omics solutions to minimize drought-induced impacts to yield and survival of crops critical to the United States and its citizens.

The carbon starvation and hydraulic failure theories advanced the field of ecology by stimulating intense research on the coupling of plant carbon and water metabolism. In parallel, 'omics work on model plants has led to great understanding of carbon and hydraulic metabolism in relation to stress, but mortality theory has not yet benefited from this type of study. There is great debate regarding the regulation of carbon and hydraulic metabolism during drought-induced death; these debates could be addressed with one experimental study combining drought-induced mortality with proper 'omics measurements.

Brachypodium plants exhibited large shifts in water stress during drought, which was visible both optically and through direct measurements. Large metabolomic shifts were observed, all associated putatively with survival mechanisms at the leaf level. For example, the large increases in sugars, organic acids, and amino acids are known to maintain turgor (e.g., prevent leaf wilting).

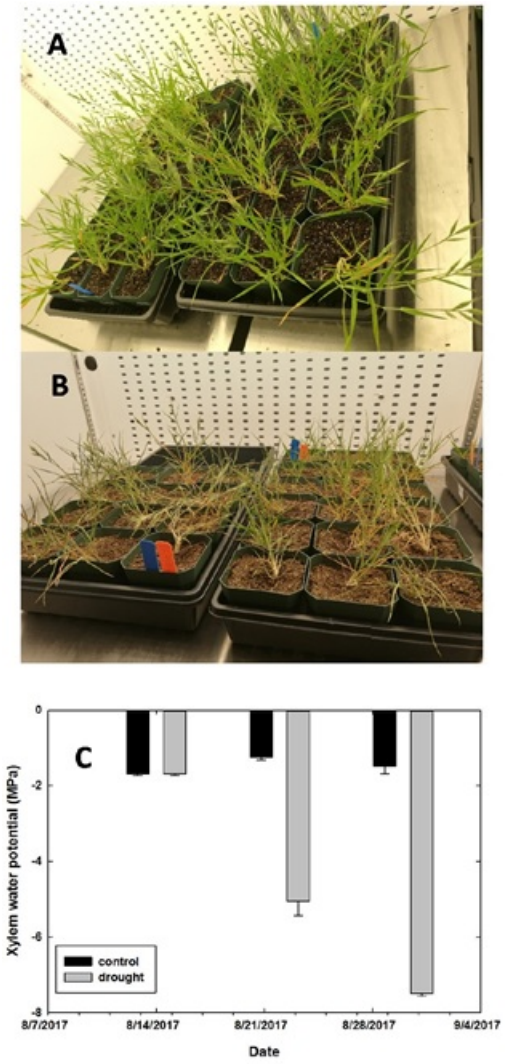

A) Well-watered *Brachypodium* (control plants), B) droughted *Brachypodium*, and C) water potential measurements (and standard errors) for the two treatments during experiment. More negative values mean greater water stress.

Multiscale Plant Modeling

Venkatraman Srinivasan
PN18029/3028

This project brings together cutting-edge advances in experimental and computational modeling and optimization of plant systems to study the impact of abiotic stresses induced by drought, salinity, and rising atmospheric CO_2 on plant performance and yield. The outcomes of this project will provide critical input for crop breeders to move towards achieving food and bio-energy security in a rapidly changing future climate and environment.

Prior research studies on crop modeling and experiments have focused on food crops with traditional targets such as seed or grain yield improvements. Bioenergy crops, on the other hand, are targeted towards improving biomass (e.g., stem and leaves). Here, we developed a state-of-the-art model for plant growth under various abiotic stress conditions and tested it in a lab environment and outdoor field plots. The validated and tested model is applied to predict optimum agronomic practices for maximizing biomass, water, light, and nitrogen use efficiency under various climatic conditions.

Two species of annual model grasses (*Brachypodium distachyon* and *Setaria viridis*) representing the two major photosynthetic pathways (C_3 and C_4, respectively) were grown in controlled growth chambers under ambient conditions and elevated atmospheric CO_2 (850 ppm). Biomass, yield, and photosynthetic activity were measured throughout the growth period (seed to maturity) and used to parameterize the computational model.

Model simulations indicated experimental anomalies and these were used to modify and test the controlled experiments.

Experiments were also performed in controlled growth chambers under ambient conditions to test the effect of short-term drought and salt stress on *Setaria* plants. Data suggest that *Setaria* exhibits notable tolerance to saline conditions while being highly susceptible to drought stress.

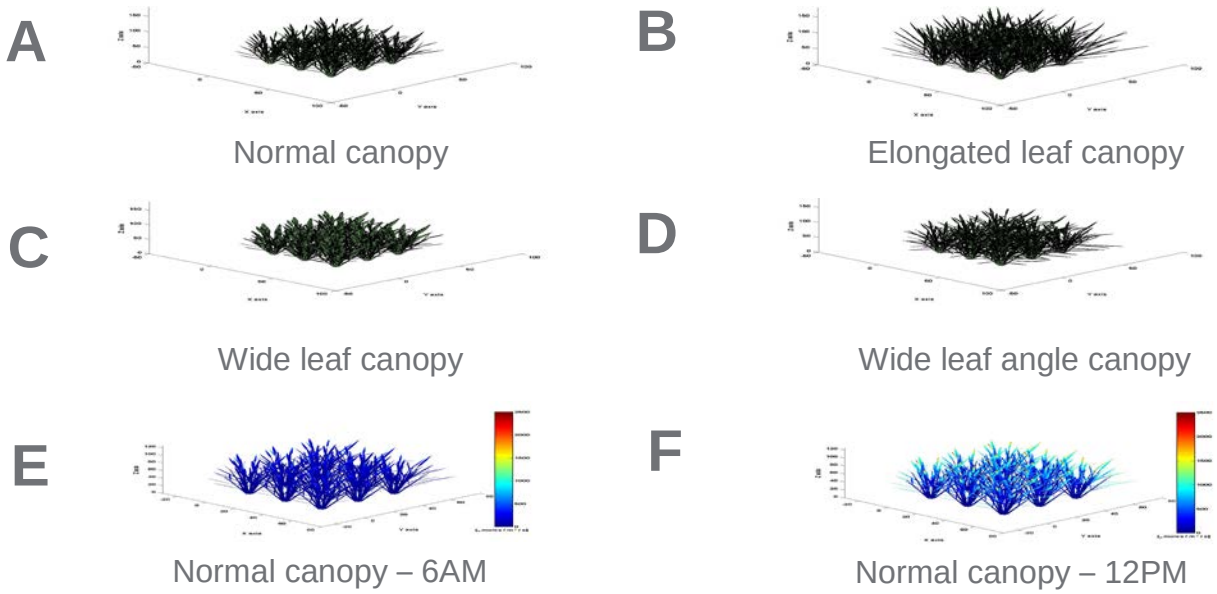

Sample model simulations of a canonical grass canopy 3D architecture with different canopy properties (A through D). Model simulations of light attenuation in a canonical grass canopy at two different time points (E through F). Color indicated the intensity of photosynthetically active radiation absorbed by the canopy.

Permafrost Microbiome Responses to Hydrologic Perturbation and Subsequent Alteration to Ecosystem Function

James C. Stegen

PN16030/2807

This project uses laboratory incubations and molecular characterization of field-collected permafrost to deepen understanding of how permafrost microbiomes respond to hydrologic perturbations and connects these responses with shifts in greenhouse gas emissions. This is vital, as increased greenhouse gas emissions due to permafrost thaw could produce positive feedbacks that accelerate the rate of climate change, yet there is a high-degree of uncertainty in model predictions because fundamental processes are poorly understood.

Microbial communities play a central role in the functioning of natural ecosystems by heavily influencing biogeochemical cycles. A major scientific challenge is to use knowledge of those influences to improve the predictive ability of microbially explicit models by incorporating feedbacks between environmental change, microbiome responses, and biogeochemical rates. Understanding how shifts in the environment are tied to shifts in biogeochemical rates via changes in microbial communities is particularly relevant in permafrost systems due to vast carbon stocks currently stored within thawing permafrost.

The primary research objective of this study is to reveal processes governing the response of permafrost microbiomes to hydrologic perturbation. These modeling efforts aim to build a predictive modeling framework that explicitly represents key members of soil microbiomes and the redox-associated processes they drive and feedback with.

Field-collected permafrost is being characterized using advanced molecular tools (multi-omics) and incubated in the laboratory under different redox and hydrologic conditions. In addition, permafrost is being thawed *in situ* across a naturally occurring hydrologic gradient.

Laboratory experiments are specifically designed to link permafrost microbiomes and associated biogeochemical processes to shifts in soil moisture conditions.

An initial scoping experiment was undertaken that provided key insights into microbiome response-to-thaw and other information (e.g., variability across replicates and the time-scale of microbiome responses). Those insights were used to design follow-on experiments.

The initial experiment did not attempt to manipulate moisture, but instead thawed permafrost under either aerobic or anaerobic conditions. The reason was to mimic redox conditions that might arise under different moisture conditions; drier soil generally leads to aerobic conditions, while saturated soil generally leads to anaerobic conditions.

Permafrost cores were incubated across a time series that allowed biogenic greenhouse gases to be repeatedly sampled. Replicate cores were also destructively harvested at multiple time points. The results showed that redox conditions had a strong influence over microbiome response-to-thaw and biogenic gas emissions. In particular, under aerobic conditions, the microbiome became dominated by one species: *Rhodoferax ferrireducens*. This organism can grow across a broad range of conditions and likely contributes significantly to system-scale biogeochemical function. One important aspect is that it can couple fermentation products to the reduction of Fe(III). This suggests that it has the potential to inhibit production of CH_4—a process that also relies on fermentation products. In turn, conditions that favor *R. ferrireducens* likely shift biogenic gas production toward CO_2 and away from CH_4. This provides new insight into factors governing the balance between CO_2 and CH_4 following permafrost thaw, which is a critical uncertainty due to CH_4 being a far more potent greenhouse gas than CO_2.

In addition to the microbiome, we observed shifts in metabolite profiles following thaw. The

data revealed significant increases in protein-like metabolites associated with phosphorylation molecular transformations under conditions where *R. ferrireducens* became dominant. *R. ferrireducens* is likely a dominant driver of biogeochemical cycling and microbe-microbe interactions in thawing permafrost, at least under conditions that facilitate its growth. We hypothesized that conditions in which there is significant spatial or temporal variation in redox potential facilitate *R. ferrireducens* due to its ability to grow both aerobically and anaerobically.

We tested this hypothesis with an additional experiment, which revealed that redox conditions are indeed important, but that pre-thaw geochemistry is potentially more influential over *R. ferrireducens* response to thaw. This points to the strong influence of environmental history.

We additionally performed the most spatially extensive field characterization of permafrost microbiomes to date, revealing key influences of carbon chemistry and spatial isolation.

Probing Complex Microbiomes Using Mass Spectrometry and Sequencing Capabilities to Understand How Microbiomes are Influenced by Their Environment

Stephen J. Callister

PN16031/2808

We are developing and applying a suite of 'omics measurement and bioinformatics capabilities to better understand how microbiomes present in the soil are influenced by their environment. Soil microbiomes are important contributors to the biotic cycling of nutrients required for all living things.

The goal of this project is to develop next-generation sequencing bioinformatics tools and mass spectrometry capabilities to address key knowledge gaps in our understanding of how complex microbiomes function within the environment. Microbiomes in the environment are responsible for key biogeochemical processes such as carbon and nutrient cycling. Predictive models concerning these nutrient cycles can be improved through better functional characterization of microbiomes at a molecular level. This molecular investigation can only be achieved through the development of sophisticated workflows for measurement of the metaproteome.

Unfortunately, empirical measurement of the environmental microbiome metaproteome by current analytical workflows result in a low depth of coverage (i.e., a relatively small number of proteins are measured compared to what is predicted by metagenomic sequencing). To address this challenge, we are evaluating and improving metaproteomics workflows combining both demonstrated and emerging bioinformatics and empirical capabilities. These workflows are being systematically evaluated, first on simplified constructed microbiomes and then on complex natural microbiomes.

Retro-fitting Non-traditional Microbes with State-of-the-Art Synthetic Biology Tools: Towards the Next Generation of Engineered Microbial Biosensors

Hans C. Bernstein

PN17001/2891

We are re-engineering microorganisms to act as autonomous, microscopic sensors using state-of-the-art synthetic biology tools. Ultimately, this will lead to new biotechnologies that help us monitor and protect our nation's critical water and agricultural infrastructure from contamination and disease.

New technologies made possible by modern synthetic biology are strengthening our nation's ability to continue addressing priority focus areas in energy and security. Rapid breakthroughs resulting from new developments in genome editing and gene synthesis now make it possible to build and program functions into living cells. This renaissance in molecular biology and genomic sciences has enabled us to construct genetic parts with circuit-like connectivity that can process logical operations, sense chemical threats, and store encrypted memory. However, almost all successful examples of these capabilities to date have been demonstrated using well-characterized "laboratory" organisms.

While useful for the development and demonstration of capabilities under stable conditions, these species do not survive well in most "real-world" chemical sensing applications. These traditional organisms are also limited in their metabolic activity, preferring substrates, such as sugars, that are typically not available in settings relevant to chemical threat detection such as surface water or soil.

A key challenge that applied researchers currently face is to be able to manipulate the best suited organisms for the particular environment or purpose. To effectively harness new developments in programmable genetic circuits for national security applications, such as environmental sensing of chemical warfare agents, we must expand our collection of programmable host chassis beyond the limited set of species that constrain the current state of the art.

Our new devices are specifically designed to operate within metabolically versatile soil microbes, *Pseudomonas fluorescens*, *Rhodobacter capsulatus*, *Arthrobacter chlorophenolicus*, *Burkholderia thailandensis*, and *Cupriavidus necator*. These hosts can grow and persist in a wide range of environments, which include dynamic soil and agricultural habitats, making them ideal sensors for a future capability to protect some of our nation's most critical infrastructure.

One of the fundamental challenges of bootstrapping novel synthetic biological parts into new microbes is in optimizing cellular competence, or uptake of exogenous DNA. A key technical accomplishment this year was the development of standardized, broad host engineering vectors for recombinant DNA transformation. Many broad host plasmid vectors are extremely long (more than 10 kilo-basepairs) and, therefore, unwieldy for genetic engineering. We tested a small library of broad host range plasmids and streamlined an approximately 7-kilo-basepair plasmid to a 4-kilo-base pair plasmid.

A second technical accomplishment was the characterization of two inducible systems in a range of non-traditional microbes, namely the LacI and TetR system. Genetic cassettes expressing LacI and TetR were cloned into *P. fluorescens SBW25*, *A. chlorophenolicus*, *B. thailandensis*, *P. putida*, and *V. natriegens*.

In at least three of these microbes, we showed that both LacI and TetR functioned as inducible transcription factor systems (titration response of the event detector shown for induction of LacI with isopropyl-beta-thiogalactopyroside, i.e., IPTG). Moreover, we constructed, cloned, and screened for at least one functional fluorescent reporter in each strain. Implicit in the

demonstration of these titration assays was the demonstrated functionality of classical promoters and ribosome binding sites from existing *E. coli* synthetic biological parts collections. In short, many extant synthetic biological parts function in both *E. coli* and in soil, marine, and aquatic microbes. This suggests a continuing model for advancement of synthetic biology in non-model microbes: 1) construction and characterization of biological parts in *E. coli*, 2) genetic manipulation and transformation of select biological parts into non-model microbes, 3) development of libraries of novel biological parts in non-model microbes where necessary, and 4) characterization of synthetic gene circuit performance in a non-model host.

A fascinating discovery emerged in the characterization of an integrase-based event detector circuit using population measurement assays (flow cytometry). The event detector is a biological circuit that activates the literal rewriting of DNA in the presence of a relevant environmental compound or target analyte. The compound could be a pesticide, a sugar, or any compound coupled and transduced through the genetic circuitry. What was interesting was that the mode of response, activation, and state latching of the circuit varied significantly across microbial host populations, depending on which host carried the circuit.

The emergence of circuit-host interactions in synthetic biology has launched a new frontier at the intersection of synthetic and systems biology. How do we engineer biological function that maximizes utility from the surrounding host, while leaving a minimal footprint on the housekeeping processes of the cell. The tension between engineered optimality of function and engineered stability of function in the context of evolutionary pressure is the subject of current research at PNNL.

Single-cell Proteomic Analysis of Developing Chick Vestibular Hair Cells

Ying Zhu
PN18084/3083

The objective of this project is to employ ultrasensitive, single-cell proteomics technology to characterize cellular heterogeneity and reveal developmental trajectory of inner-ear sensory hair cells. Understanding the developmental of hair cells is critical for investigation of hair cell regeneration as a cure for hearing loss.

Multicellular organisms have evolved highly specialized sensory cells to mediate between environmental signals and cellular processes. Understanding the developmental processes resulting in these highly specialized structures is key to any future efforts to manipulate these processes. To reveal the complexity of these multicellular structures, the Barr-Gillespie lab (OHSU) has used single-cell transcriptomics to analyze more than 1,000 chicken utricle hair cells and have organized those cells into a branching developmental trajectory. However, given the variable concordance between mRNA and protein levels, profiling protein expression at the single-cell level would be useful.

Because of the lack of a protein-amplification method, however, single cell protein analysis is extremely challenging. Conventional immunofluorescence assays are limited to measuring a handful of proteins in single cells due to spectral overlap. Microfluidic immunofluorescence techniques have enabled simultaneous detection of up to 42 secreted proteins from single cells by combining spatial and spectral encoding approaches. Mass cytometry can quantify up to 38 proteins, but the quantification accuracy is largely limited by antibody specificity.

At PNNL, we have developed nanoPOTS (nanodroplet Processing in One-pot for Trace Samples), which significantly improved the sensitivity of proteomic measurements and enabled us to identify more than 700 proteins from single mammalian cells. Based on this unique capability, we aimed to profile the global protein expression in single E15 hair cells isolated from chick utricle.

NanoPOTS chips with patterned nanowells were fabricated in a PNNL cleanroom and shipped to the Barr-Gillespie lab for cell collection. Hair cells were dissected from the utricles of E15 chicks. FM1-43 was used to specifically label hair cells, distinguishing them from supporting/progenitor cells. SYTOX Red Dead Cell Stain was used to distinguish live cells from dead ones. Cells were then separated and deposited into nanowells with a FACS Influx II instrument (BD Biosciences) set to “single cell” mode and equipped with a 100 µm nozzle. A total 30 samples were collected, including 20 cells as libraries, as well as samples of 5 cells, 3 cells, and 1 cell used to evaluate the sensitivity.

The collected cells were processed in nanoPOTS with a total volume of about 150 nL. Two-step enzyme digestions were used to improve efficiency. Samples were analyzed by ultra-low flow liquid chromatography running at 50 nL/min and an orbitrap Fusion mass spectrometer. Data were collected using a data-dependent acquisition approach. High AGC level and long ion accumulation time were used to increase mass spectrometry (MS) sensitivity. MaxQuant with Match Between Runs was employed for protein identification and label free protein quantification.

To improve the overall sensitivity of LC-MS, we evaluated the effect of column inner diameters (*i.d.*) on proteomic identifications of single cell level (approximately 0.2 ng) protein digest. We tested two different columns, 20 µm *i.d.* and 30 µm *i.d.*, which were run at flow rates of 20 nL/min and 50 nL/min, respectively. On average, 700 and 528 proteins were identified, respectively, demonstrating the smaller *i.d.* column has improved sensitivity.

With the increase of cell number, number of proteins or protein groups increased from 47 to 550. We observed lower protein numbers

from low FM1-43 level cells, which we attributed to the relative smaller cell sizes. Interestingly, by examining all the single-cell data, we can distinguish two cell types, including hair cells and supporting cells, based on label-free quantifications. TMSB4X (thymosin beta) is highly enriched in supporting cells, not in hair cells. Two Ca2+ buffers, OCM and CALB2, are much higher in hair cells than in supporting cells, and their concentrations are considerably higher than we previously thought. Several proteins are in hair cells but not at all in supporting cells (CRABP1, GPX2, GSTO1, AK1, VAMP3, OTOF). Together, these results demonstrated the great power of nanoPOTS for single-cell analysis.

Spatially Resolved Quantitative Gene Expression Analyses Applied to Transitioning Mouse Gut and Soil Microbiomes

Galya Orr
PN16110/2887

Quantitative gene expression analyses of complex microbial communities have been done exclusively by population measurements, which lump the behavior of an entire population into a single average value. These approaches ignore the impact of the diverse local environments on the responses of individual organisms and the complex spatial relationships between them, which govern the formation of functional units that ultimately dictate the community function as a whole. Adding a spatial context to gene expression analyses will be vital to understanding fundamental rules by which complex communities function and evolve under changing environments. To address this gap, we have established quantitative gene expression analysis in individual intestinal microbial and host cells while preserving spatial context within their native tissue or environments.

The function of individual organisms within a microbial community or individual cells within the tissue is governed by the local environment and interactions with neighboring organisms or cells. In complex spatial organizations of communities that consist of hundreds or thousands of different species, individual cells of a given clonal population of organisms can experience vastly different local environments and are likely to express very different genes in response. Likewise, individual cells within a tissue can experience fundamentally different local environments and are likely to express very different genes in response.

The spatial relationships between individual organisms within the community or individual cells within the tissue are, therefore, key to understanding the role of the individual organism or cell and, ultimately, to deciphering how the community or tissue functions as a whole. Meta-transcriptomic analyses have gained important insights into processes that take place within the community and suggested functional roles for different species. However, this averaged cell population approach lumps the behavior of an entire population into a single average value while ignoring the impact of the diverse local environments on the responses of individual organisms and the complex spatial relationships between them.

While single-cell RNA-Seq analysis has become established by many groups, it is applied to isolated cells with little or no information about the original location of the cells within the tissue. Adding a spatial context to gene expression analyses will be vital to understanding fundamental rules by which complex communities or tissue function and evolve under changing environments. Recent advances in single-cell analysis have enabled quantitative gene expression analyses in individual cells while preserving their spatial context within the tissue. To date, these approaches have been demonstrated only in eukaryotic cells. The translation of these techniques to bacterial cells presents multiple challenges due to their small size and content, as well as their complex environments within microbiomes. Building on our experience in single-molecule fluorescence imaging techniques, we will apply novel quantitative fluorescence *in situ* hybridization (FISH) approaches to enable multi-gene expression analysis in single cells while preserve the spatial context of the individual cells. When applied using single molecule fluorescence imaging techniques, FISH enables the quantification of single transcripts in intact cells with high accuracy.

Our project is designed to establish challenging techniques for quantitative multi-gene expression analysis in individual gut microbial and host cells while preserving the context of their local environments and spatial relationships within the microbiome or the tissue. Building on our expertise in single-molecule localization-based super resolution fluorescence imaging, we combined Stochastic Optical Reconstruction Microscopy (STORM) and single-molecule FISH

(smFISH) to achieve transcript counts in single cells with unprecedented accuracy and specificity. Our novel approach was termed “fluctuation localization imaging-based fluorescence *in situ* hybridization,” or in short, fliFISH. We applied the novel approach to understand the spatial relationships between native or perturbed gut microbiome and host cell physiology by 1) co-localization of specific microbes and 2) quantification of gene expression for receptors governing bile acid production.

To establish fliFISH in mouse gut cryo-sections, we focused on Cyp7a1 and Fgf15, which are two reporter genes indicative of the activation of the bile acid nuclear receptor, FXR, which governs bile acid production. The next step would be to quantify Cyp7a1 and Fgf15 expression in host cells in native and perturbed microbial communities, while characterizing community structure by targeting ribosomal RNA (16S). This would allow us to identify the spatial relationships between the community structure and host cells showing differential expression of the two reporter genes. Ultimately, this effort would identify fundamental rules and mechanisms by which microbiomes operate with details that cannot be achieved by averaged cell population measurements that ignore the local environments and spatial organization among the community members and the host.

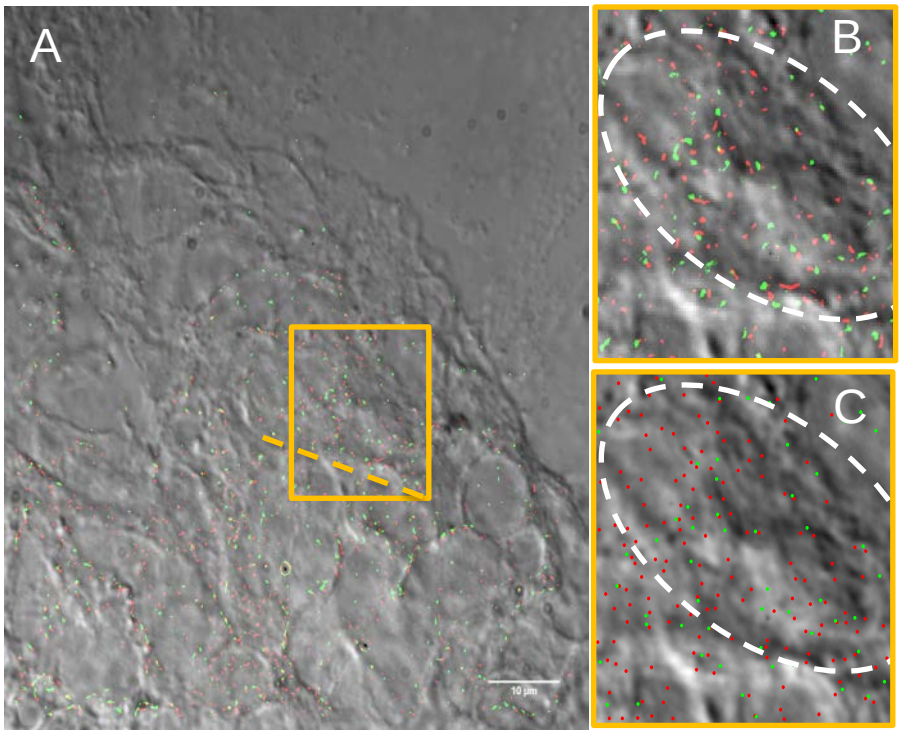

Application of fliFISH to quantify the expression of two reporter genes in single intestinal epithelial cells. A) Differential Interference Contrast image of a mouse gut cryo-section treated with FISH probes targeting Fgf15 (red) and Cyp7a1 (green). B) STORM image of the area marked by the orange square in A. C) Precise identification of transcripts (green and red dots) for the two genes using fliFISH.

Statistical Integration of Omics Data from Microbiomes

Joseph M. Brown
PN15077/2752

We will develop an infrastructure and computational tools designed to process, analyze, and visualize microbial community sequence data to address the challenge of computational analysis.

Microbes exist and function in communities. Studies of natural environmental or human-associated sites often reveal hundreds to thousands of microbial species co-existing (i.e., a microbiome). The interactions between microbes within such a microbiome are often complex, as is the impact the microbiome as a whole has on its environment. Deciphering microbial activities in their natural environments is a prerequisite to understanding their functional role in environmental processes. Research efforts to understand the vital roles these communities of microbes play in human health and environmental sustainability have thus turned to high-throughput technologies to measure the various biomolecules extracted from a sample (nucleic acids, protein, and metabolites) to infer the functional capability and emergent properties of the microbiome.

One of the most readily available data types for microbiome research is nucleic acid sequence data. It is feasible to sequence the DNA extracted from natural microbial communities consisting of many species. However, such DNA samples consist of a composite mixture of the genetic material of the community members (i.e., a metagenome), and inferring the functional capability or assigning taxonomy from complex mixtures of genetic material has proven challenging. Further, sequencing technologies can generate approximately a terabyte of data in a week, requiring the need to develop novel analytical tools. Robust analysis of complex data from microbial communities in human hosts and in the environment will be key to understanding their vulnerability to change.

We have built a sequencing capability and data delivery process at PNNL around industry best practices. Data obtained from our instrument go through rigorous quality scrutiny facilitated by an interactive and extensible dashboard that we have developed and released to the open source community. Our automated protocol allows us to utilize institutional computing for archiving, processing, and data delivery to accelerate the pace of data distribution to researchers.

Processing nucleic acid sequence data derived from microbial communities can be time and resource intensive in terms of both compute and employee labor. We designed and implemented a protocol to automate large amounts of processing into a simple configuration, single-command execution. This dramatically increases speed of annotation and, more importantly, saves critical configuration data to ensure scientific replicability.

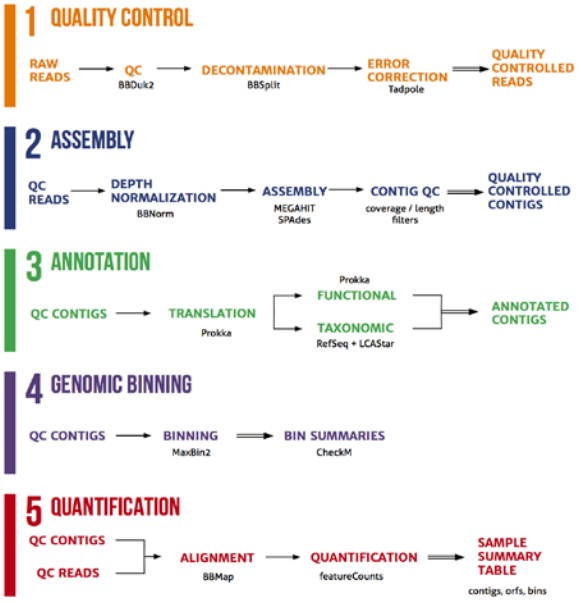

ATLAS workflow diagram. Raw sequence data is quality controlled, annotated functionally and taxonomically, and finally compiled into sample summary tables ready for downstream analyses such as differential expression or incorporation into environmental modeling efforts.

The infrastructure developed for ATLAS to process sequence data was also leveraged to build a tool to rapidly annotated raw sequence data without first assembling those sequences. Its application fills a void where rapid characterization of sequence data is preferred over sensitivity. PerSeq facilitates verification of sequence content so that our team can effectively identify contamination, communicate our findings with sequencing facilities, and work with those facilities to re-sequence samples and provide higher quality data.

Using Modified Proteins for Forensic Deconvolution of Xenobiotic Dose Quantitation and Timing

Jordan N. Smith
PN16023/2800

A novel biomonitoring approach utilizing modified-protein fingerprints to reconstruct dose and timing of dose is being developed. To support this approach, we developed a multipronged technique to identify protein modifications caused by chemical exposures and measured global protein turnover rates in rats. This novel biomonitoring approach could allow for dose reconstruction with greater accuracy and precision than current methods and discovery of novel toxicity targets.

Humans are exposed to a broad mixture of chemicals from occupational settings, consumer products, accidental releases, and the environment. Many chemicals are known to cause or have been linked to adverse health effects. To better understand the potential risks associated with these exposures, efforts are underway to biomonitor targeted human populations for chemical exposures, as highlighted by the National Research Council of the National Academies report, *Exposure Science in the 21st Century: A Vision and a Strategy*.

Current state-of-the-art methods to predict how much of a chemical or when exposure occurred (i.e., dose reconstruction) require *a priori* knowledge of one of two factors: dose or timing of dose. Blood or urine samples are analyzed for biomarkers of exposure, usually the chemical of interest or a metabolite of that chemical. Computational models are used to reconstruct a dose that may have caused a measured biomarker concentration. Biomarker concentrations are highly dependent on time and dose, and without some information about one of these factors, the most sophisticated dose reconstruction strategies can only conclude dose occurred. For compounds that are rapidly cleared from the body, even robust *a priori* information may not be sufficient to reconstruct doses without a high level of uncertainty, since biomarkers can only provide adequate information over a few biological half-lives.

We are developing a new approach to reconstruct dose and timing of dose using chemical adducts on proteins. Many highly reactive chemicals (which are typically toxic chemicals and are difficult to biomonitor) will react with proteins in blood to form chemical-protein adducts. Since there are many proteins in blood, exposure to a chemical will result in the formation of chemical adducts on many proteins. Different proteins have different natural turnover rates, which means each chemical exposure will create a modified-protein fingerprint that is unique by dose and time after the dose occurred. The goal of this project is to identify, measure, and utilize modified-protein fingerprints for dose reconstruction.

In our first aim, we developed a multipronged approach to identify protein adducts. First, global proteomic measurements were used to search for protein adducts in purified proteins, plasma, and whole blood treated with reactive chemicals. Custom bioinformatics software was developed to aid in verification of protein adducts from mass spectrometry data. Second, activity-based protein profiling was used to search for protein adducts. This technique utilizes chemical probes designed to enrich specific protein targets, which we used as an inverse indicator of targets for protein adduct formation. Used in tandem, global mass spectrometry and activity-based protein profiling were used to identify and confirm protein adducts caused by organophosphate pesticides, herbicides, fumigants, and other environmental chemicals.

As a second aim, we measured turnover rates of plasma proteins in rats. Rats were fed isotopically labeled lysine to label proteins. Then feed was changed to an unlabeled equivalent feed, and blood was repeatedly sampled from these rats. Global proteomics and activity-based protein profiling were used to measure changes in isotopic ratios of proteins. Using this

approach, we were able to identify 273 proteins and measure turnover rates of 174 proteins. This study is the first to measure global plasma protein turnover rates in rats, measure variability of protein turnover rates in any animal model, and utilize activity-based protein profiling for enhancing turnover measurements of targeted, low-abundant proteins. Together with our ability to identify protein adducts (Aim 1), these protein turnover measurements allow us to utilize protein adducts for advanced dose reconstruction.

In the last year, we extended our work in plasma to tissues. Identification of protein adducts in tissues allow us to discover and study novel mechanisms of toxicity. Protein adducts were identified in brain tissues of rats exposed to reactive chemicals using recently developed global proteomics and activity-based protein profiling. Adducts were identified on enzymes at lower doses than primary mechanisms of toxicity, suggesting possible novel toxicity mechanisms. The ability to identify protein adducts in tissues will allow for discovery of novel toxicity targets and provide insight on disease initiation and progression in tissues.

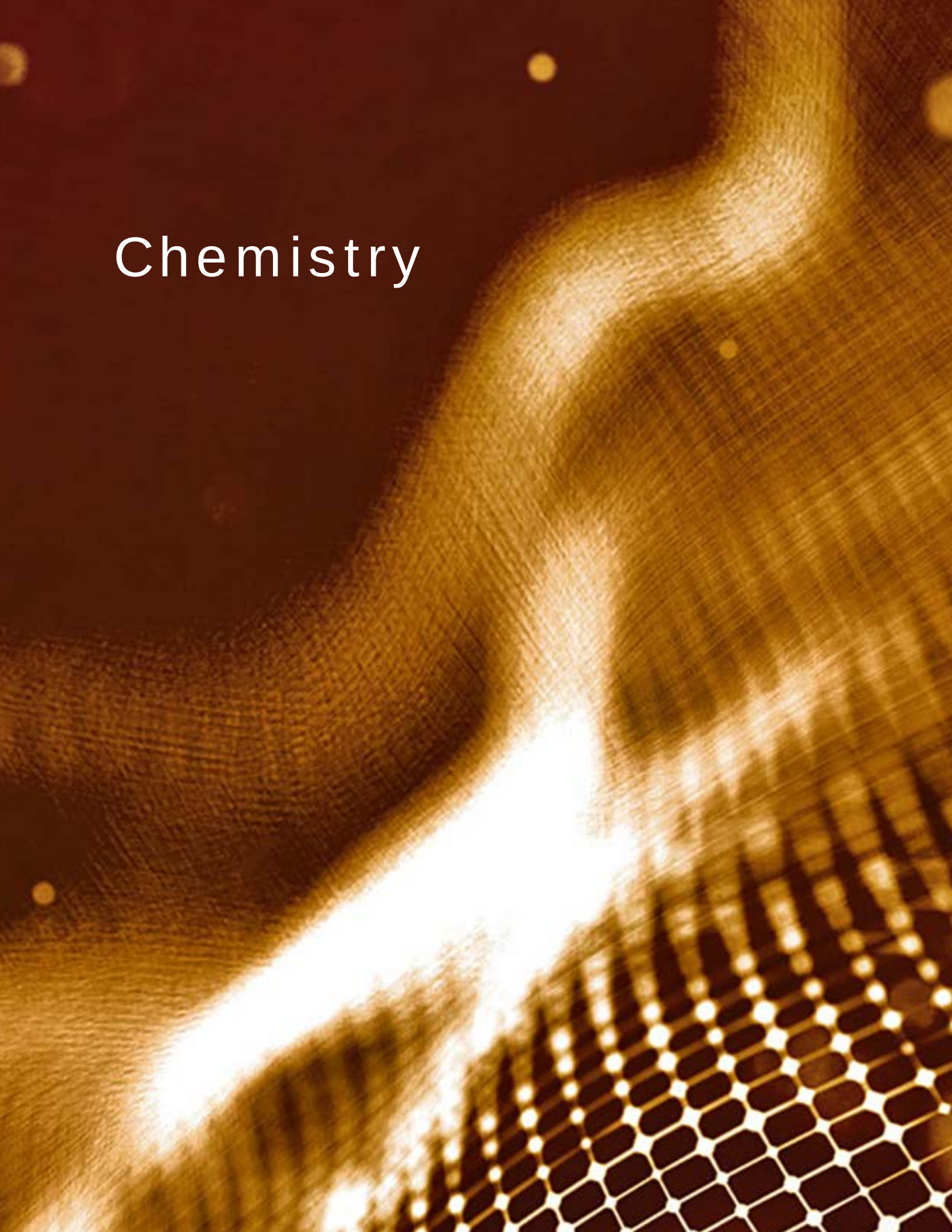
Chemistry

Chemical Bonding in Uranium Oxides Studied by Uranium-233 (^{233}U) and Uranium (^{235}U) Nuclear Quadrupole Resonance Spectroscopy

Herman M. Cho
PN17029/2919

The aim of this project is to develop a novel method to study the unique and distinctive way the actinide elements, which include uranium, neptunium, and plutonium, combine with other atoms. The discovery of an explanation for the interatomic interactions of the actinides would be a major advance in the understanding of the complex chemistry and physical properties of these elements, with significant implications for national security, nuclear energy, and environmental remediation.

Soon after the synthesis of the first transuranic elements, Seaborg proposed that the actinide elements were analogs of the lanthanide series and recommended the placement of the actinides below the lanthanide row in the Periodic Table. In the 70 years since then, however, a more complex picture has emerged, with the elements below plutonium (Z = 94) often being found to behave like transition metals rather than lanthanides. The validity of the lanthanide analogy continues to be a ubiquitous theme in actinide science, with far-reaching relevance. The purpose of this project is to construct a first-of-its-kind pulsed nuclear quadrupole resonance (NQR) spectrometer designed to probe actinide elements for insights on the similarities and differences of these elements with lanthanides and transition elements. The feasibility of actinide NQR spectroscopy will be evaluated with experiments on uranyl salts. The goal is to achieve the first ever detection of NQR signals from an actinide isotope, which would open a new avenue for investigating electronic structure in actinide complexes. Uranium isotopes are the focus of this project, but almost every actinide element up to curium has a long-lived isotope theoretically detectable by NQR methods.

Instrumentation has been assembled and tested for frequency-swept time domain NQR experiments in the requisite spectral range (0.1 to 3.0 GHz). The main components include a pulsed console and a broadband cryogenic probe with a 5-mm resonator. A cryostat has been procured, allowing measurements down to 4.2 K. Lower temperatures will enhance the sensitivity of the measurements, as well as reduce lifetime (T_1) broadening of the ^{235}U NQR lines. Custom sample capsules were fabricated for containment of radioactive material.

With theoretical electric field gradient calculations provided by Professor Jochen Autschbach's group at the University of Buffalo, a range of different uranyl compounds were surveyed as candidates for an initial demonstration of this approach. Their results made possible calculations of NQR transition energies that guided the choice of $Cs_2UO_2Cl_4$ as the most promising first candidate due to its favorable NQR transition energies and the potential for measuring spectra of neighboring ^{35,37}Cl- and ^{133}Cs-occupied sites.

Large crystals of $Cs_2UO_2Cl_4$ in quantities sufficient for NQR experiments have been synthesized and verified by X-ray crystallography. Samples have been made with both depleted and 95% ^{235}U-enriched uranium.

With samples in hand and the completion of the spectrometer, ^{35}Cl and ^{37}Cl nuclear magnetic resonance and NQR experiments were initiated to test both the performance of the NQR instrument and the electronic structure parameters predicted by the University of Buffalo group. The search for ^{235}U NQR signals of $Cs_2UO_2Cl_4$, which is predicted to consist of three lines near 461.2, 922.5, and 1383.7 MHz, has been initiated at room temperature.

Left: Uranium-235 enriched $Cs_2UO_2Cl_4$ crystals; Middle: cryogenic broadband NQR probe, with a meter stick for scale; Right: resonator section of the NQR probe, revealing the 5-mm sample tube in the solenoidal coil detector.

Development of Integrated Framework for High-accuracy Excited-state Simulations of Dynamical Processes

Karol Kowalski
PN17019/2909

This project will enable highly accurate excited-state simulations capable of utilizing existing peta- and soon-to-be exa-scale computer architectures. New excited-state capabilities will significantly advance our ability to describe processes related to energy conversion, photo-catalysis, light harvesting systems, and various spectroscopies. Additionally, new functionalities will be used to interpret data produced by Department of Energy light sources.

One of the prominent frontiers in computational chemistry is the study of excited-state-driven chemical transformations. The main challenges to be addressed are the inclusion of the appropriate level of accuracy to describe complicated structure of excited-state potential energy surfaces and interactions between them, including avoided crossings, barriers, and conical intersections. This can only be achieved by employing excited-state wave-function-based approaches that can properly capture a vast array of excited-state correlation effects. Although these methodologies are known to be accurate, the main challenge is posed by their steep numerical overhead. To address this issue, we plan to integrate the state-of-the-art theoretical Equation-of-Motion Coupled-Cluster (EOMCC) formulations with emerging programming models that will enable efficient utilization of high-end peta- and near-exa-scale computational platforms.

We are hoping to achieve significant progress in the development of parallel EOMCC formulations to enable them for systems composed of hundreds of atoms. Proposed development will also significantly extend the area of application of the EOMCC formalism. We are planning to develop an integrated environment to tackle excitations in various energy regimes for closed- and open-shell systems. We are also hoping that the proposed development will pave the way for the future extension of the EOMCC formalism to linear response coupled cluster (LR-CC) and closely related CC Green's function formulations.

The above-mentioned goals will be achieved through the integration of the theoretical developments with state-of-the-art programming models. In particular, the availability of specialized tensor libraries plays a critical role in this project. For this reason, the effort associated with providing a certain class of capabilities to Tensor Algebra for Many-Body Methods (TAMM) is an extricable part of this project. TAMM is a framework designed to support quick development of performance portable CC methods. This effort will include efficient implementations for tensor data structures, element-wise tensor operations, and optimized operations of blocks of tensors.

In FY 2017, we developed ionization potential (IP)/electron affinity (EA)-EOMCC TAMM approaches, improved scaling and performance of IP/EA EOMCC methods, completed the largest up-to-date simulations of IP/EA with EOMCC methods, explored the possibility of modeling excited-state processes in open-shell systems, and completed a large CC scale calculation with 1,658 basis set functions.

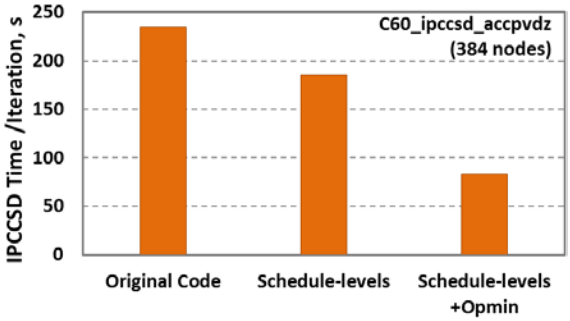

Speed-up of the TAMM-generated IP-EOMCCSD code compared to the existing (NWChem) implementation.

In FY 2018, we have further extended the performance of the CC modules on the leadership class computer architectures. In particular, we have demonstrated significant progress in enhancing the performance of IP-EOMCC singles and doubles (EOMCCSD) and CCSD perturbative triple (CCSD[T]) modules on Oak Ridge National Laboratory's Summit supercomputer. For example, with TiO_2 clusters, we have demonstrated that novel schedulers and operation minimization procedures can provide a three to six times speedup of the IP-EOMCCSD code compared to the existing implementation in NWChem. It also has been shown that the CCSD(T) can take advantage of the graphics processing unit technology offered by the Summit system, which resulted in very good scaling across a quarter of the system (1,024 nodes). In a similar way, CCSD(T) has been demonstrated on the Cori KNL system at Lawrence Berkeley National Laboratory.

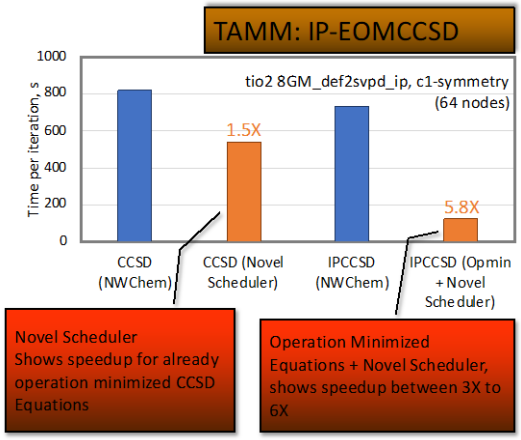

Speed-ups of the TAMM-generated IP-EOMCCSD codes achieved with the Summit architecture.

Electrochemical Reactor and Process: Oxidation Electrocatalysis for Increasing the Value of Renewable Carbon

Robert S. Weber
PN18086/3085

This short project was intended to initiate research on oxidation catalysis and membranes that would be appropriate for use with basic electrolytes or basic anolytes and acidic catholytes, such as may facilitate the depolymerization, defunctionalization, and mineralization of species that report to the aqueous phase in hydrothermal processing of renewable feedstocks such as biomass.

We are exploring the use of electrocatalysis to convert bio-oil into more valuable fuels and chemicals. Those upgrading reactions principally involve electrochemically activated reductions. Evidently, an electrochemical cell must simultaneously perform both reduction (cathodic) and oxidation (anodic) reactions. To date, however, we have been able to ignore the anode processes by employing unrealistically easily oxidized species in high concentrations. This project will research total oxidation and peroxidation of water-borne chemical species that accompany bio-oil, which are now disposed as waste. Examples include organic acids, aldehydes, and alcohols.

We have identified several suppliers of potential anode catalysts, including powders of boron-doped diamond, boron-doped nanotubes, and nitrogen-doped nanotubes (from NanoTech Labs); and powders consisting of mixed metal oxides, in which the mixed metal oxides will be doped PbO_2 (e.g., TiO_2-NTs/Sb-SnO_2/PbO_2).

The catalysts will be mounted on carbon supports using facilities resident in our laboratories in work done on other projects. Those materials promise to be usable at the high positive (oxidizing) potentials needed to activate the expected refractory polar organics.

We have also identified several suppliers of potential membrane materials, including anion exchange membranes from Tokoyuma and from Dioxide Materials, as well as bipolar membranes from Fumasep.

In addition, instead of using an ion-selective membrane, we have considered whether we can operate the cell with a microporous membrane (i.e., a diaphragm), for example Celgard from Asahi Kasei, an expanded polyethylene. Those materials (catalysts and membranes) will be tested in subsequent work.

Finally, this project purchased analytical instrumentation that will be used to identify and quantify the products and conversions affected by the electrochemical transformations. We specified two liquid chromatographs: one equipped with a refractive index detector and an automated six-port sampling valve that will be used, at-line, to monitor the effluent flow from an electrolysis cell; the other chromatograph has a manual injection system and a mass sensitive detector for use in methods development.

Fundamental Understanding of Nucleation Processes to Assess Solution Stability and Phase Growth and Genesis

Gregg J. Lumetta
PN15085/2760

We are developing a physicochemical framework for predicting and manipulating precipitation reactions relevant to nuclear materials processing and nuclear forensics.

Nucleation and crystal growth are fundamentally important to processing nuclear materials and radioactive wastes, but information is lacking regarding the basic science underlying these transformations. Many chemical processes used in the nuclear industry—both for recovering special nuclear materials and for disposing of radioactive wastes—involve manipulating highly concentrated salt solutions. Precipitation of solids from such solutions is often a concern. In this context, precipitation might be desired (e.g., of plutonium oxalate during plutonium oxide synthesis) or not (e.g., during ion exchange or solvent extraction processes).

We are developing a framework based on recent developments in crystal growth that have provided insight into two distinct pathways for nucleation and growth. In the "classical" pathway, nucleation occurs through ion-by-ion addition to a growing cluster with increasing free energy of formation until a critical size is reached. At this point, the free energy change for further growth becomes negative and occurs via ion-by-ion addition to kink sites at atomic steps on the crystal surface.

Dependence of crystal morphology and growth rate on applied supersaturation is well understood for both nucleation and growth. These dependencies are distinct from crystals formed through the second, "non-classical" pathway, broadly described as "particle-mediated growth." In the latter scenario, nucleation and growth occur via addition of higher order species ranging from oligomeric complexes to liquid droplets to amorphous or crystalline nanometer-scale particles. Detailing the morphologies, internal structures, and dependencies of growth rates on supersaturation allows the formation mechanism to be determined and related to process conditions. Moreover, rate measurements versus supersaturation and temperature allow us to determine activation barriers controlling nucleation and growth processes.

Our research is focused on precipitation of oxalate salts of trivalent f-element ions, with the general formula $M_2(C_2O_4)_3\ xH_2O$ (M = a lanthanide or actinide element; x is usually = 10). These salts are precursors to corresponding metal oxides, making them technologically important and, in the case of actinides, of interest to the nuclear forensics community. Due to the challenges working with highly radiotoxic plutonium, most studies were performed using Eu(III).

A combination of theoretical and experimental techniques is used to develop a framework for explaining nucleation and subsequent crystal growth of the metal oxalate systems, from the atomistic to hundreds of micrometers scale. In FY 2018, experimental work focused on measuring crystal growth kinetics for $Eu_2(C_2O_4)_3\ 10H_2O$ using a combination of optical microscopy and image analysis software. The measured crystal growth rates were evaluated theoretically to deduce crystal growth pathways involved. Other computational work was performed in which the nano-potentials and fields experienced by the Na^+ and Cl^- ions in NaCl were calculated to characterize electric properties of small NaCl cubic crystallites. It is hypothesized that this approach can be used as a basis for developing novel order parameters to describe the crystallinity of the salt clusters underlying nucleation and crystallization processes.

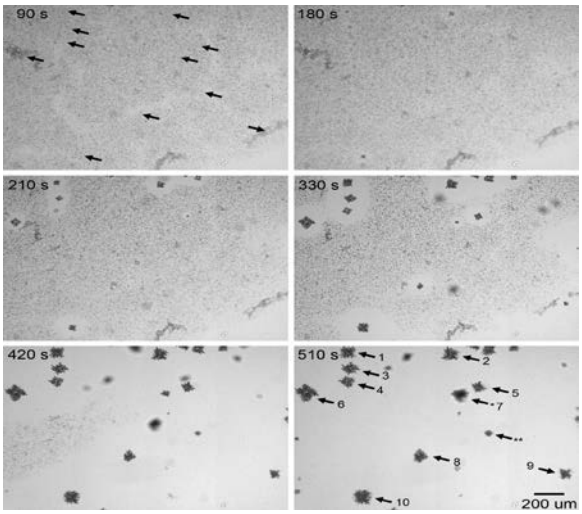

Optical micrographs of europium oxalate crystals growing in solution. Numbered arrows in the frame labeled “510 s” identify the particles that were measured to determine growth kinetics. The same arrows appear in the 90-s frame to provide a spatial reference earlier in the reaction.

Three cases were considered for interpreting $Eu_2(C_2O_4)_3\ 10H_2O$ growth kinetics, which were determined by optical microscopy: 1) interface limited growth, 2) diffusion limited growth, and 3) the Ostwald ripening model. These three models can be distinguished by plotting the effective particle radius versus time, square root of time, or cube root of time; linear plots would indicate interface limited growth, diffusion limited growth, or Ostwald ripening, respectively. Our results clearly show that $Eu_2(C_2O_4)_3\ 10H_2O$ crystal growth is not interface limited under the conditions examined. Diffusion limited growth or Ostwald ripening both would fit the crystal growth rate data, but diffusion limited growth is most likely, since further analysis of the Ostwald ripening model suggests unreasonably high surface tension for the evolving crystal.

In situ optical microscopy investigation of $Eu_2(C_2O_4)_3\ 10H_2O$ crystal growth also revealed two distinct growth regimes, apparently driven by inhomogeneities in the system. Early in the process, there are localized regions with high concentrations of small initial particles. These initial particles dissolve and re-precipitate into larger observed crystals.

In addition to study of $Eu_2(C_2O_4)_3\ 10H_2O$, theoretical models were used to characterize electric fields and potentials experienced by NaCl nanocrystals where these electrical properties can be used as signatures of the new phase. We paid attention to examining deviations of the potentials experienced in the nanocrystal (nanopotentials) from the potential experienced within an infinite crystal (the Madelung potential, approximately 8.95V). Interfacial surface tension can be computed from the difference between interior and surface electric potentials, which is the critical property influencing kinetics of nucleation and crystallization processes within the classical nucleation model.

By examining a sequence of cubic NaCl nanocrystals, ranging from 2 to 19 atoms on an edge (2^3 to 19^3 ions), with computational models, we can track the behavior of potentials and fields as a function of particle size. We found overall average potential converges toward the bulk limit, but ions on the surface of the nanocrystal experience very different potentials (with corners having lower potentials than edges, which were lower than ions on the face).

We also computed equivalent quantum mechanical electric potentials and found they are quite different from classical potentials. It was challenging to reproduce quantum potentials using an atom centered classical point charge model, unless the atomic point charges had been derived from a charge fitting scheme that utilized the potential information to obtain the atomic charges.

The performance of two canonical NaCl force fields was compared to high-level *ab initio* Symmetry Adapted Perturbation Theory calculations, which can decompose the interaction energy into intuitive physical components (electrostatic, induction/ polarization, dispersion, exchange-correlation) and be used as a basis to compare force field parameterization. These calculations are important to quantify the nucleation pathway, surface tension, and crystal lattice energy. Extension of these computational techniques to the $M_2(C_2O_4)_3\ xH_2O$ systems is being examined.

Fundamentals of Electrocatalytic Hydrogen Addition

Oliver Y. Gutiérrez-Tinoco
PN17022/2912

This project aims to use renewable electricity to convert biomass feedstocks into fuels at conditions much milder than those used by current technologies. In order to achieve this ambitious goal, we need to discover the fundamental principles of this fascinating chemistry.

Sustainable growth requires effective ways of converting biomass-derived feedstocks into valuable chemicals and transportation fuels. However, state-of-the-art technologies, designed to constantly convert large amounts of fossil oil feedstocks, are impractical for biomass treatment. Thus, new, low-scale technologies are needed that produce chemical energy from intermittent and seasonal renewable sources, or even from waste biomass.

At PNNL, we are doing early-stage research to invent technologies for low-scale chemical conversions powered by electricity. This approach has the potential of decreasing the need for thermal inputs while producing H_2 (another valuable energy carrier) in a sustainable way.

Our goal is to learn how to manipulate the fate of hydrogen produced at the electrode. We seek to control the rates of hydrogenation of biomass compounds and of H_2 formation through adjusting the electric potential, reaction environment, and electrocatalyst composition. Upon developing the capabilities needed to accomplish this challenging task (in FY 2017), we have made major advances in our scientific research, such as mapping the reactivity of diverse families of molecules and determining reaction mechanisms by a combination of kinetic and *in situ* spectroscopic measurements.

One of the major achievements of FY 2018 has been the complete mapping of the reactivity of biomass compounds and the activity of different metals toward electrocatalytic hydrogenation. With this mapping, we discovered that the rates of hydrogen addition to the organic compounds and H_2 evolution (the prevalent side reaction) are linked. Specifically, the faster the reaction of the organic compound with hydrogen (electrochemically produced) is, the higher the fraction of current utilized to transform the organic. However, different compounds have different reactivity. For instance, the aromatic aldehydes and ketones are converted to alcohols faster than the phenolic compounds are converted to cyclic alcohols. Bulky molecules, such as aryl ethers, have relatively low reaction rates, although hydrogen addition to the C-O, leading to oxygen-free olefins and alkanes as well as to the aromatic C=C bond, occurs. Aliphatic aldehydes and ketones are relatively unreactive compared to their aromatic analogs, which suggests that aromaticity is the molecular property that fosters reaction at ambient conditions.

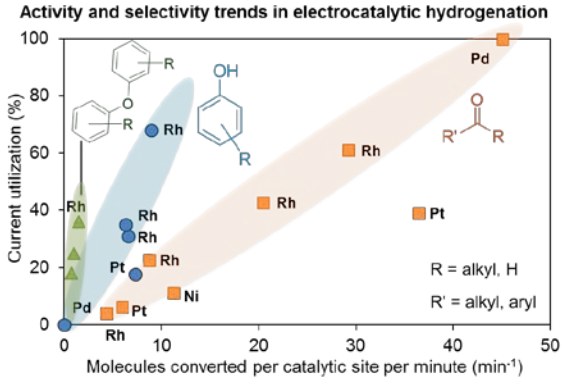

Correlations observed between the percentage of current utilized to convert organic compounds (current utilization) and rates of molecular conversion. The results are grouped in three families of compounds converted by the metals indicated in the plot.

Our kinetic and spectroscopic investigations have helped us explain why the hydrogenation rates and current utilization are correlated. For hydrogenation of aromatic rings, hydrogen is electrochemically produced on the catalyst and then transferred to the aromatic ring. This last step (hydrogen transfer) determines the overall reaction rate and is the same for electrocatalytic reactions as for reactions

performed with externally supplied H_2. We have even “seen” reactive species (including adsorbed H) interacting with the metals via sophisticated X-ray adsorption spectroscopy experiments performed in the Advance Photon Source at Argonne National Laboratory. In those experiments, we determined the state of the catalysts during operation and observed unique features attributed to interactions of the metal with the reactants, which we interpreted with the help of theoretical chemistry. As a result, we positively demonstrated that the conversion rate depends on the amount of hydrogen produced on the metal. The amount of this hydrogen-on-metal, in turn, can be manipulated by varying external hydrogen pressure or cathodic potential.

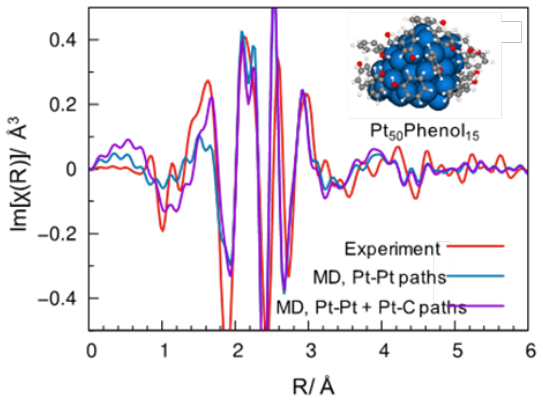

Experimental X-ray spectrum of a working platinum catalyst (red line) and spectra modeled (blue and purple lines) after the structure shown in the top-right corner.

In contrast, the hydrogenation of C=O bonds (ketone and aldehyde conversion to alcohols) follows a true electrochemical reaction pathway, which means that electrons and protons are directly added to the organic compound instead of indirectly via transfer of hydrogen atoms from metal to the C=O bond. H_2 production and hydrogenation are still linked due to competition between the metal and adsorbed carbonyl groups for the protons. The practical consequence of this newly discovered mechanism is that electrocatalytic rates of conversion of C=O bonds are much higher than rates obtained with hydrogen supplied externally. This is an important potential advantage of the electrocatalytic approach over typical thermal operation.

For all the compounds tested in our research, kinetic modeling and calorimetric experiments have shown that the strength of interaction between the organic compounds and the metal determines both the rates of hydrogenation and H_2 evolution. This identification and quantification of organic-metal interactions is an important contribution to the field of electrochemistry for organic reactions.

Heterogeneous Catalyst Development for Crotonaldehyde from Acetaldehyde

Karthi Ramasamy
PN18019/3018

Crotonaldehyde is an intermediate compound to several valuable commodity chemicals and currently produced using homogeneous catalyst with a sequence of complex processing steps. Our project aims to simplify that process, which also will reduce capital and production costs, as well as the amount of waste produced.

At present, crotonaldehyde (α, β-unsaturated C4 aldehyde) is commercially synthesized using a homogeneous catalyst in a complex sequence of processing steps. In the first step, acetaldehyde is aldolized to 3-hydroxybutanal in the water-cooled reactor with aqueous NaOH as catalyst. In this step, the conversion is limited to between 50% and 60% to restrict the secondary reactions. Next, the aldolized product stream is neutralized with acetic acid and sent to a stripping column for acetaldehyde recycle. Then the 3-hydroxybutanal is dehydrated to generate crotonaldehyde and sent through the distillation column for purification. The current crotonaldehyde synthesis process uses many processing steps and homogeneous catalysts, making this process very complex and expensive.

Developing a single-step heterogeneous catalytic process to produce crotonaldehyde will reduce the overall capital and production costs and minimize undesired product generation. Dual functionality, carbonyl function and the conjugated olefinic double bond within the aldehyde, of the crotonaldehyde enables various chemical reactions and production of high value chemicals. Currently, the complexity and the synthesis cost limit crotonaldehyde's role in the commodity chemicals world. Developing a simple and inexpensive process with a heterogeneous catalyst to synthesize crotonaldehyde from renewable feedstocks, such as ethanol (ethanol → acetaldehyde → crotonaldehyde), will be beneficial to creating an economical and sustainable chemical and fuel industry.

Over a heterogeneous catalyst, acetaldehyde conversion to crotonaldehyde occurs via a sequence of two cascade steps in a single catalytic bed. The sequence is the base catalyzed aldolation to form 3-hydroxybutanol, followed by the acid catalyzed dehydration to form crotonaldehyde. Accomplishing this chemistry in a single catalytic step requires a bi-functional acid-base mixed oxide catalyst. Both the 3-hydroxybutanol and crotonaldehyde are very reactive, so maintaining the optimum balance between the active sites and identifying the operating conditions (e.g., temperature, pressure, weight hourly space velocity) is imperative to achieving the high crotonaldehyde yield.

In this work, several mixed catalyst catalysts containing both acidic and basic properties $MgO\text{-}Al_2O_3$, $MgO\text{-}ZrO_2$, CaO-P, $MgO\text{-}SiO_2$, $MnO\text{-}ZrO_2\text{-}ZnO$, and $ZnO\text{-}ZrO_2$) were tested in a plug flow experimental system. In general, bulk mixed-oxides are widely employed in industry as heterogeneous catalysts for selective oxidation, so the cost of the materials, as well as the catalyst synthesis, is economical for these catalysts.

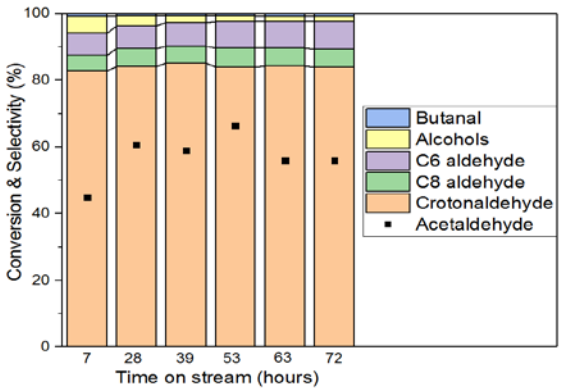

Conversion of acetaldehyde and selectivity to crotonaldehyde and other byproducts over mixed oxide catalyst.

Among the various mixed oxide catalysts tested, ZnO-ZrO_2 (composition of 1:2 between the ZnO and ZrO_2) provided the best conversion, selectivity, and catalyst stability for the crotonaldehyde synthesis from acetaldehyde. The highest selectivity to crotonaldehyde achieved was around 82%, with an acetaldehyde conversion around 60%. The rest of the 18% selectivity is made up of the high molecular weight unsaturated aldehydes (C6 and C8) and the hydrogenated product of the respective aldehydes (e.g., butyraldehyde). This catalyst is very stable, and it is demonstrated beyond 70 hours of time on stream in a plug flow reactor arrangement without any deactivation signs for both the acetaldehyde conversion and the selectivity to crotonaldehyde.

Investigation of the Signatures of Additively Manufactured Objects Using Advanced Chemistry and Materials Science Techniques to Identify Counterfeits

Chris Barrett
PN17036/2926

The purpose of this project was to develop a focused capability to address the need for additively manufactured device forensics, identify signature-rich aspects of different build processes that can be used to distinguish counterfeits, and to determine provenance and predict performance.

The rise of additive manufacturing (AM) in recent years is, in part, due to the open-sourced nature of the printing processes and reduced cost and capital barriers relative to traditional manufacturing. The advent of "desktop," three-dimensional (3D) printers has, quite literally, brought manufacturing to the masses. Thus, it is reasonable to assume that AM will lead to an increase in objects of importance to national security, which could be fabricated at a point of use, and to global markets, where an influx of parts and products of unknown origins could lead to rapid destabilization. This democratization of manufacturing has spurred a growing demand from producers and end users to verify the authenticity and quality of individual parts.

To this end, we have developed an anti-counterfeiting approach that utilizes both intrinsic and extrinsic properties of a 3D-printed part that can be non-destructively interrogated to validate authenticity. Our parallel efforts to identify and study signatures of AM objects were directly leveraged in generating part-specific chemical signature data that can be linked to a securitized, distributed, and time-stamped blockchain ledger entry. Validation was facilitated by a QR (Quick Response) code, printed directly to the part, which provides a searchable reference to an Ethereum-based blockchain entry using a standard smart phone.

Tasks for the initial phase of the project were split between identification and attribution of intrinsic signatures of objects fabricated by AM and the incorporation and measurement of additives with unique extrinsic signature profiles. The merits of the first task not only support the anti-counterfeiting objective, but also offer a mechanism by which counterfeits can be identified and provenance determined. Using techniques, such as computed tomography, coupled with focused ion beam milling and electron microscopy, particulates inherently incorporated during Fused-Deposition-Modeling-(FDM)-style printing were studied as a means of correlating parts to specific printers. Pyrolysis gas chromatography mass spectroscopy was also evaluated as an ideal technique for not only polymer identification in selective laser sintering (SLS) prints, but also detection of trace additives and impurities that can be sourced to specific printer feedstock and their associated supplier.

Using a QR code printed onto a part to validate its authenticity.

In the second case, we published a new, low-cost, anti-counterfeiting method for 3D-printed parts by use of a blockchain platform, where inclusion of measured fluorescence data with a digital thread, enhanced part security. Nanocrystals were uniformly doped into polylactic acid and printed in selected areas of an object. Example objects were designed to

contain QR codes with raised features printed with the polylactic acid composite material. While the measured emission color data is not particularly complex, it becomes significantly more powerful when archived as a component of the digital twin on a blockchain ledger.

Incorporating chemical signature data from extrinsic tags, or intrinsic signatures of a printed part, to complement other digital part metadata on a blockchain database may provide end users, intermediaries, and manufacturers with an easy and low-cost verification tool. As such, future efforts may explore this approach further, expanding to new methods of handheld interrogation, direct attribution of certain signatures, and production of AM standards for model validation.

To briefly summarize the work carried out by this project, we investigated the use of advanced measurement techniques to study unique structural and chemical characteristics within AM objects. Some of our initial efforts centered on X-ray computed tomography, a non-destructive evaluation technique that allows for the examination of microstructure within an object, with little need for sample preparation. This capability allowed us to study unique artifacts of a build process, such as porosity, density variations, and particulate incorporation. For instance, the porosity of an SLS-printed object has been found to correlate directly with build direction, while filament materials of FDM systems exhibit significant incorporation of high-Z metals or metal clusters as a result of both extrusion and printing. Under the framework of a relative strength index and based on the strength of the results gathered from this project, a scanning electron microscope integrated μCT was procured and installed, allowing expansion of this technique to smaller length scales (sub-micron). Coupling techniques, such as computed tomography, focused ion beam milling, and electron microscopy, particles embedded during FDM printing were successfully mapped, extracted, and then isolated for discrete analysis by scanning transmission electron microscopy and electron energy loss spectroscopy. In addition, pyrolysis gas chromatography mass spectrometry was tested and evaluated as an ideal technique for not only polymer identification in SLS prints, but also for detection of trace additives and impurities that can be sourced to a specific printer feedstock and their associated supplier.

Building upon our established expertise and capabilities with measurement and trace detection, the goal for this line of research going forward will be to focus more heavily on a model-prescribed measurement strategy tailored to phase-field and finite element analysis, affording better correlation between the two areas and greater insights from data analytic techniques. In this way, more applied science challenges from various sponsors could be tackled in the future.

Mimicking the Function of the Enzyme Scaffold

Molly J. O'Hagan
PN17061/2951

Natural enzymes catalyze many reactions that can be used for sustainable energy applications, such as the interconversions of H_2 and H^+, O_2 and H_2O, or CO_2 and CO using earth abundant metals and mild conditions, with performance unmatched by synthetic catalysts. We aim to create synthetic catalysts with performance that can rival that of the natural systems by using hybrid systems (i.e., synthetic catalysts attached to protein scaffolds) to identify design principles by which the protein matrix can be used to control reactivity and increase performance. This has the potential to revolutionize catalysts and advance chemical transformations.

The chemistry that enzymes catalyze occurs at a specific active site within the protein matrix, but that active site, in the absence of the protein scaffold, cannot do the same chemistry. The protein scaffold has been shown to control important properties such as stabilizing the active site geometry, transport of products and substrates, controlling acid/base chemistry, creating the environment around the active site, and altering redox properties.

Many studies on molecular functional mimics of enzymes have been focused on the role of the first and second coordination spheres, showing a tremendous impact in moving protons, stabilizing structures, and delivering substrates. However, there is still a significant performance gap between the function of these complexes and enzymes performing the same reaction. By incorporating existing molecular catalysts into protein scaffolds, we can make systematic changes that enable the identification of design principles by which the protein scaffold influences efficiencies. The design principles can then be directly translated to create new efficient molecular catalysts and, ultimately, heterogeneous catalysts.

We are covalently linking a synthetic catalyst to a well-defined protein using bioconjugation techniques. Our strategy for covalent linkage uses a maleimide functional group that reacts with cysteine side chain thiols within the protein to attach the catalyst. We have successfully synthesized a nickel catalyst that has the bioconjugation linker within the ligand backbone characterized by nuclear magnetic resonance (NMR) spectroscopy. We have also successfully expressed and purified three protein targets with cysteine mutation that maintain their native structures. We have successfully covalently coupled the nickel catalyst to the first target, Lactococcal multidrug resistance regulator (LmrR) protein. The resulting protein-containing catalyst is active for CO_2 hydrogenation, while the catalyst alone is not—the protein scaffold enabled catalytic activity, indicating a clear and positive impact of the scaffold. Higher pressures increased catalytic activity for the protein-complex, while higher temperatures lowered catalytic activity, thought to be due to protein denaturation.

A summary of the reactivity results.

Reactivity Summary				
Complex	Pressure (atm)	Temp. (K)	CO_2: H_2	Rate (hr^{-1})
No scaffold	34	298	1:1	N.R.
No scaffold	58	298	1:1	trace
Scaffold	1.7	298	1:1	0.021
Scaffold	17	298	1:1	0.14
Scaffold	34	298	1:1	0.23
Scaffold	58	298	1:1	0.37
Scaffold	34	323	1:1	0.081
Scaffold	34	353	1:1	N.R.
Scaffold	17	298	0:1	N.R.
1 + LmrR*[a]	58	298	1:1	N.R.

Conditions were 0.3 mM complex, 0.5 M sodium bicarbonate, at pH 8.15 with propane sulfonate as an internal integration standard. N.R. indicates no detectable product formation.
[a]1, peptide coupling reagents, LmrR* without maleimide for covalent attachment.

In order to determine how the scaffold is influencing catalysis, we performed several structural studies. We successfully expressed ^{15}N labeled LmrR and used NMR to examine the structure. Unfortunately, the helices close in space to the molecular complex are too mobile to characterize by NMR. We were able to crystallize one oxidation state of the protein-complex; however, the complex had significant disordered, resulting in limited quantitative structural data. Despite the mobility, extensive NMR and spectroscopic data indicate that the metal site is not significantly altered when it is placed within the scaffold. Further, a mechanism in water was modified from the mechanism observed in organic solvents, where the dihydride binds CO_2 and releases formate, rather than deprotonation occurring first.

Further work would emphasize examining the dynamic structures using NMR or spectroscopic techniques, as well as extending the techniques to more structurally restricted scaffolds or molecular complexes to facilitate structural characterization. Further, directed evolution techniques would also be considered to try to achieve even faster catalysis.

Ultimately, understanding how to control substrate delivery, dynamics, pK_a, and catalytic redox potentials could be achieved using the protein scaffold. Identification of these design principles will enable the design of synthetic homogeneous and heterogeneous catalysts with performance that can match or exceed that of native enzymes.

Multimodal Approach for Rapid, Robust, Reliable, and Economic Environmental Monitoring

Dev Chatterjee
PN17051/2941

Availability of a universal, field-deployable sensor platform for rapid monitoring of multiple subsurface analytes will streamline the Department of Energy's (DOE's) environmental remediation and clean-up efforts. This project utilizes a multimodal analytical approach to develop a single, integrated sensor platform for continuous* in situ *monitoring of multiple contaminants. The proposed approach is based on electrochemical and optical luminescence techniques, enabling measurements of the analytes of dissimilar nature in wide concentration ranges.

Simultaneous rapid detection and quantification of multiple analytes remain a great challenge in environmental sensing. Detection of an analyte is achieved via recognition by a sensor of its unique property (i.e., intrinsic or acquired), producing a selective response. As the distinguishable properties of dissimilar analytes vary, finding a single sensor module for the detection of different classes of analytes (e.g., chemical versus biological, organic versus inorganic compounds, ions versus neutral species) is challenging.

One approach to designing a sensor that can detect multiple analytes having diverse characteristics is to translate the different responses into a common form of expression, irrespective of the properties of the analytes. To achieve this, the target analytes can be selectively captured by specific probes immobilized on a single electrode platform, resulting in a marked increase of its electrochemical impedance proportional to the analyte concentration. The sensitivity and detection limit of the electrochemical response can be enhanced through a secondary optical luminescence detection mode, which monitors the luminescence intensity during a simultaneous redox conversion of a non-luminescent molecule (NL) to its luminescent form (L) at the electrode; analyte capture inhibited this conversion through electrode passivation, proportionally lowering luminescence intensity.

A key feature in this approach is that the capture can take place through multiple different mechanisms, so long as the end result of the capture is a change in impedance or luminescence. Therefore, such detection is not limited to any analyte-specific properties and can be applied to a wide array of analytes. The sensor platform universally translates these diverse responses to a common output signal (i.e., impedance and/or luminescence), enabling simultaneous quantification of multiple analytes.

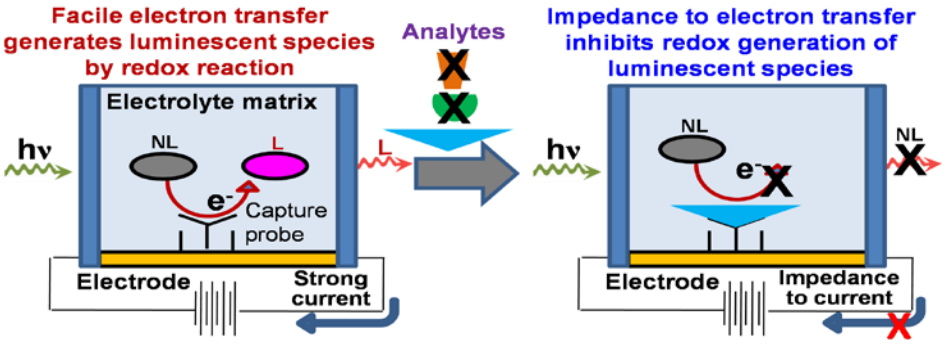

Schematic representation of biomodal analyte detection.

FY 2017 research demonstrated a proof-of-concept of the universal sensor approach using three chemically diverse contaminants. Their detection using the same impedance platform methodology illustrated possibility of extension of this approach to other analytes of interest relevant to DOE missions. Three contaminants found at the Hanford Site and many other DOE sites nationwide, including CCl_4, TcO_4^-, and NO_3^-, were selected based on their significant chemical diversity.

The following model analytes exemplify key challenges likely to be encountered in the integrated detection of the multiple analytes by a common platform: 1) no reported *in situ* technique for CCl_4 detection and quantification exists; 2) established methods for *in situ* detection of TcO_4^- and NO_3^- are not suitable for sensing using integrated platform; 3) while NO_3^- detection is most studied due to its ubiquitous nature within environmental, food, and industrial systems, no existing sensor for NO_3^- allows its quantification in wide enough range.

In FY 2017, major project accomplishments include identification of a capture probe for unique recognition of each contaminant and translation of the obtained responses to the common impedance detection. It was discovered that phenylene oxide polymers or cobalt(II) porphyrin complexes incorporated on an electrode surface can serve as selective probes for CCl_4; to the best of our knowledge, these are the first reported examples of the sensor media for CCl_4. Thioalkanes and polypyrrole polymers were identified as selective probes for TcO_4^- and NO_3^-, respectively. Each capture probe recognizes CCl_4, TcO_4^-, or NO_3^- through a different mechanism but generates a common impedance response when incorporated onto the electrode surface, thus, validating our approach for the universal sensor platform. Also in FY 2017, we demonstrated the broad applicability of our approach using chemically diverse targets, as well as the selectivity of our approach in real systems.

FY 2018 work consisted of two main parts: 1) designing a portable, field deployable platform for selective detection, and 2) demonstrating the sensitivity of detection. The platform design of our FY 2018 work employed interdigitated microelectrodes within a microfluidic channel. Capture probes were aligned in the channel on top of the electrodes, and targets were captured as a solution was passed through. The design also allowed integration of multiple targets on the same platform. The microelectrodes were instrumental in lowering the limits of detection by allowing a high signal to noise ratio via confinement of the ionic flux within the electrode nano domains. Thus, using this set-up we achieved limits of detection lower than Environmental Protection Agency (EPA) advisory limits for all three analytes (CCl_4: our limit = 5 ppb, EPA advisory limit = 5 ppb; TcO_4: our limit = 750 pCi/L, EPA advisory limit = 900 pCi/L; and NO_3: our limit = 0.05 mM, EPA advisory limit = 0.16 mM). We further tested out the approach for the detection of perfluorooctane sulfonate, which is one of the key harmful offenders at various EPA sites; our detection limit was significantly lower than the EPA advisory limit (our limit = 5 ng/L, EPA advisory limit = 70 ng/L).

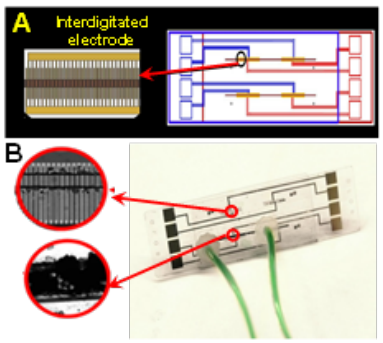

A) Schematic representation of the interdigitated electrode. B) Zoomed-in images of the chip with packed porous probes (bottom) and blank (top).

Overall, the investigated approach to the universal sensor platform addresses DOE needs for monitoring of relevant contaminants within the dynamic, multicomponent matrices of Hanford Site vadose zone and groundwater. It opens possibility of detection and quantification of multiple contaminants and analytes of interest on one platform through the ability to translate dissimilar stimuli to a common response (i.e., electrical or optical). The approach can be readily extended to other contaminants, as well as for detection of and predictive monitoring of co-mingled contaminants.

Spectrally Resolved Nanoscale Imaging of Single Molecules, Plasmons, and their Interaction

Patrick Z. El-Khoury
PN16093/2870

This project aims to develop ultrasensitive multimodal (bio)chemical imaging technologies that can be used to interrogate single molecules and metallic nanostructures, as well as to advance our understanding of molecule-plasmonic metal interactions. The potential applications of the developed technologies span the realms of several scientific disciplines.

The proposed research efforts were conceived with a hypothesis that a single molecule is the ultimate probe of its local environment. Currently, it is possible to establish the chemical identity of some substances at the ultimate detection limit of a single molecule (i.e., the sensitivity required to identify 1.66 yoctomoles [10^{-24} moles]), using surface-enhanced Raman scattering (SERS). Recent work has also demonstrated the possibility of recording chemical images of select classes of individual molecules using tip-enhanced Raman scattering (TERS) with sub-molecular resolution. Nonetheless, the mechanisms involved in attaining single molecule detection sensitivity using both techniques are not fully understood; the unique interplay between individual molecules and their distinct and complex local environments complicates their optical signatures and images. In this regard, persistent gaps in knowledge in this field significantly hindered efforts aimed at generalizing and transcending these most promising techniques beyond their proof-of-principle stages. This is particularly the case for measurements performed under ambient laboratory conditions.

Our above-stated hypothesis and proposed approach to SERS/TERS are unique. Namely, rather than using these spectroscopic tools to probe molecular properties, we employed the SERS/TERS signatures of a single molecule to probe its local environment and to expose some of the mechanisms involved in attaining yoctomolar detection sensitivity in Raman spectroscopy. Our work enabled 1) fingerprinting libraries (e.g., [bio]chemical agents) with single molecule detection sensitivity, 2) monitoring chemical reactions (e.g., bond breaking and making) with single bond detection sensitivity, and 3) probing charge flow across metal nanojunctions with single electron detection sensitivity.

Several noteworthy technological and conceptual advances were enabled through this project. For instance, we developed and demonstrated a unique approach to hyperspectral optical microscopy, achieved by coupling a hyperspectral imager to various optical microscopes. Hyperspectral fluorescence micrographs of isolated fluorescent beads were first employed to ensure spectral calibration of our detector and to gauge the attainable spatial resolution of our measurements. Subsequently, different science applications of our instrument were described. Namely, spatially over-sampled absorption spectroscopy of a single lipid (18:1 Liss Rhod PE) layer revealed that optical densities on the order of 10^{-3} can be resolved using our setup by spatially averaging the recorded optical signatures. This was followed by three applications in the general areas of plasmonics and bioimaging. Notably, we deployed hyperspectral absorption microscopy to identify and image pigments within a simple biological system: namely, a single, live *Tisochrysis lutea* cell. Overall, our initial work paves the way for multimodal spectral imaging measurements targeting a broad variety of systems ranging from single cells to plasmonic metal nanostructures.

We coupled the above-described hyperspectral optical microscopy module to a custom-built Raman nanoscope. Using this multimodal chemical and topographic imaging platform, we illustrated how molecular Raman scattering (in the TERS scheme) may be used

to visualize several aspects of the local environments in which molecules reside. More specifically, we demonstrated a non-standard application of TERS, whereby various aspects of plasmon-enhanced electric fields localized at nanometric asperities sustained on a sputtered silver substrate were imaged. This unique approach comprises a logical extension to classical TERS spectroscopy and imaging measurements, in which practitioners are primarily focused on nanoscale chemical imaging applications. We demonstrated ultra-high spatial resolution (sub-nanometer) using atomic-force-microscopy-based TERS electric field imaging measurements performed *under ambient laboratory conditions*. We further illustrated that molecular charging at plasmonic tip-sample nanojunctions play a significant role in TERS spectroscopy and imaging.

The above-described results alluded to the exciting prospect and possibility of imaging the vector components of plasmon-enhanced local electric fields through TERS with nanometer spatial resolution. This was illustrated through ambient TERS measurements recorded using silver atomic force microscope tips coated with 4-mercaptobenzonitrile molecules and used to image step edges on an Au(111) surface. The observed two-dimensional (2D) TERS images uniquely mapped electric fields localized at Au(111) step edges following 671-nm excitation. Notably, we established that our measurements are not only sensitive to spatial variations in the enhanced electric fields but also to their vector components. We also experimentally demonstrated that 1) few nanometer precision is attainable in TERS nanoscopy using corrugated tips with nominally radii of about 100 to 200 nm, and 2) TERS signals do not necessarily exhibit the expected dependence on localized electric field magnitudes. Overall, we illustrated the concept of electric field imaging via TERS and established the connections between our observations and conventional TERS chemical imaging measurements.

On the theoretical/computational front, we explored underappreciated chemical phenomena in ultrasensitive SERS and TERS. We observed a fluctuating excited electronic state manifold, governed by the conformational dynamics of a molecule (4,4'-dimercaptostilbene [DMS]) interacting with a metallic cluster (Ag_{20}). This affected the simulated single molecule Raman spectra, as the time trajectories of a molecule interacting with its unique local environment dictates the relative intensities of the observable Raman-active vibrational states. *Ab initio* molecular dynamics (AIMD) of a model Ag_{20}-DMS system were used to illustrate both concepts considering experimental results. Ongoing work is focused on bridging the gap between conventional (statistically sound), AIMD-based Raman spectral simulations aimed at recovering the spectral response of molecular ensembles, on one hand, and non-standard, time-domain simulations that are needed to recover the optical response of a single scatterer. Furthermore, as similar effects govern ultrasensitive TERS nanoscopy measurements, we are currently developing this framework to understand nanoscale chemical images recorded using TERS.

Synthesis of Tunable Electro-catalysts for Biomass Conversion

Miroslaw A. Derewinski

PN17024/2914

The objective of this project is to develop a robust heterogeneous electrocatalyst composed of metal nanoparticles supported on conducting carbon felts capable of electrocatalytically hydrogenating (ECH) biomass derived oxygenates such as aromatic aldehydes, ketones, and phenolic compounds primarily present in the lignocellulose and waste oil. To develop effective catalysts for electrocatalytic hydrogenation, we tune the catalysts by changing the metal properties and its environment on conductive carbon support.

Low temperature ECH is a plausible method to convert bio-oil to transportation fuels. ECH can be achieved by producing hydrogen on the catalyst surface by coupling electrocatalytic water splitting that reacts with organic substrates. Due to complexity of the feedstock in composition and functionality, design and synthesis of catalysts often have several challenges, such as stability, activity, and reproducibility, that limit viability of commercially available catalysts.

To address these challenges, we synthesized electrodes containing metal nanoparticles. The properties of deposited metal were achieved by controlling properties of metal nanoparticles and modifying carbon support. Three different approaches were applied: 1) impact of synthetic parameters on effectiveness of wet impregnation method, 2) effect of size and morphology of nanoparticles on their ability to catalyze electrochemical reduction, and 3) surface modification of carbon felts to optimize interaction between metal and supports. We have studied the impact of preparation methods, notably thermal treatments (temperature, duration, and atmosphere) and weight loading.

In FY 2018, we accomplished the synthesis of size-controlled metal nanoparticles and correlation between the metal dispersion and ECH of oxygenates. Chemical reduction methods were used to synthesize four different sizes of palladium (Pd) metal nanoparticles (2 to 6 nm). The colloidal nanoparticles were impregnated on carbon felts, followed by thermal treatment to remove the capping agent. Investigation on the effect of metal particle sizes after thermal treatment (increased to 4 to 9 nm) showed the intrinsic activity (time of flights [TOFs]) of hydrogenation of benzaldehyde decreases with increasing Pd particle sizes.

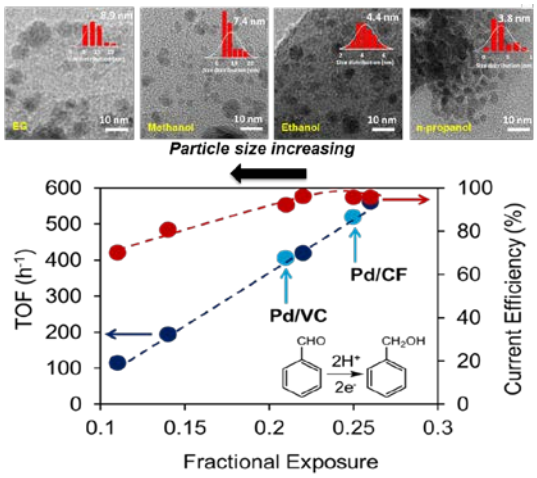

Transmission electron microscopy images of Pd nanoparticles on carbon felts (top) and correlation between initial TOFs and fractional exposures (down).

Due to limitation of carbon felts, such as low surface area (1 m^2/g) and hydrophobicity, the resulting lower metal loading and dispersion are often considered a major drawback. To determine an impact of carbon support on deposited metal, we modified the carbon surface to see how intrinsic properties of metal changed depending on surface functionality of carbon. Three different surface modifications were used to improve the carbon support's surface properties: 1) deposition of oxygen or nitrogen modified mesoporous carbon species to increase

surface area, 2) nitric acid treatment, and 3) oxygen plasma treatment. Modified carbon felts were subsequently used for preparation of Pd nano catalysts and tested for ECH of benzaldehyde. The recorded activity in ECH is correlated with changing surface area and functionality by tuning surface chemistry to introduce basic or acidic properties.

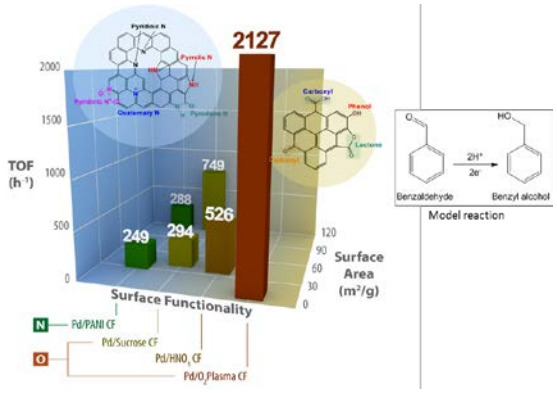

Graphic correlation between surface functionality, surface area, and ECH activity benzaldehyde reduction.

In summary, we developed synthesis of electrocatalysts by tuning the synthetic treatment parameters, changing metal properties, and modifying carbon surface to see the impact on deposited metal. Main achievements in ECH catalytic activity include 1) highly dispersed catalyst showing an increase of ECH activity and 2) providing acidic sites on the carbon surface (O_2 Plasma CF) enhances the ECH activity compared to basic properties.

Theoretical Studies of Metal Complex Degradation Products and Their Associated Signatures in the Plutonium Separations Process

Neil J. Henson
PN17090/2980

Understanding the degradation of chemical species used in the plutonium production processes can be used to better elucidate the dominant chemical pathways present in the processing of nuclear material and enable increased efficiency through improved process design.

A full elucidation of the chemical pathways resulting from breakdown of the coordinating ligands used in the PUREX process has not been performed. The degradation products from these reactions potentially allow a better understanding of why breakdown occurs and the consequences of these species on the efficiency of the overall separations process. This project aims to study computationally possible chemical reaction pathways and compare predicted spectral signatures with available experimental data.

In the final months of the project, we focused on calculations of the electronic structure and properties of the tributyl phosphate (TBP) ligand coordinated to actinide species using the NWCHEM software. Spectroscopic and crystal structure determinations have suggested several possible structural motifs for coordination of TBP in non-polar solvents. For example, for the uranyl cation, $U^{VI}O_2^{2+}$, a coordination mode with two nitrate anions (to make the overall complex neutral) in the equatorial plane (with the UO_2^{2+} species) and two TBP ligands occupying axial positions is thought to be likely. The neutral charge state of the complex is favored in non-polar solvents. We used this coordination geometry as a starting point for a calculation on the $(UO_2)(NO_3)_2(TBP)_2$ complex. The calculation showed this complex to be stable. The two TBP ligands are predicted to assume an eclipsed conformation looking down the axial direction. The U-O bonds lengthen slightly from 1.74Å to 1.76Å on coordination of the ligands, which is inconsistent with previous observations indicating the relative insensitivity of this structural parameter to the nature of the coordinating ligands.

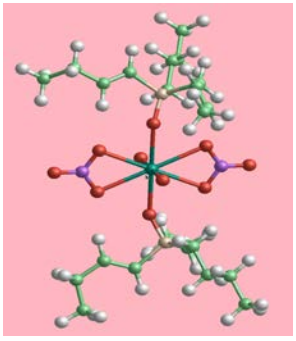

Calculated structure of $UO_2(NO_3)_2(TBP)$ complex.

In contrast for the Pu(IV) cation, previous work has suggested two possible complexes that form with TBP ligands 1) $Pu^{IV}(NO_3)_4(TBP)_2$ and 2) $Pu^{IV}(NO_3)_4(TBP)(TBP.HNO_3)$. The former of these is similar to the uranyl complex described above with an additional two nitrate anions needed to balance the charge, effectively replacing the uranyl oxygens. For comparison with our previous calculation on the uranyl system, this complex was chosen for our initial study. This coordination geometry is predicted to be stable. The calculated N-O bond lengths are significantly shorter than for the uranyl complex indicating less charge transfer to the central cation for this complex, but similar to that observed in other Pu(IV) systems. The Pu-O bond length to the TBP ligand (2.28Å) is shorter than in the uranyl system (2.35Å), reflecting the increased positive charge on the actinide center.

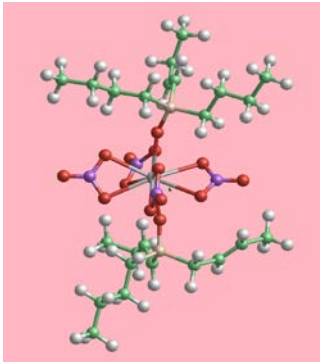

Calculated structure of $Pu(NO_3)_4(TBP)_2$.

Unveiling the Dynamic Microbial Biofilm and Plant Root Interface Under Extreme Conditions

Xiao-Ying Yu
PN16071/2848

Biofilm formation on plant roots is known to be associated with biological control and pathogenic response; however, how plants regulate this association is not well known. We propose to enable unique PNNL multimodal chemical imaging capabilities to investigate the dynamic biofilm-plant root interface under environmental conditions to obtain measurements ranging from molecules to cells and associated communities.

Plant growth promoting bacteria (PGPB) are a prerequisite for biofilm formation and adhesion to plant roots. Single cells play a complex functional role in bacterial biofilm surface components and extracellular factors in plant-bacterial association. Our knowledge of the identification and functions of extracellular proteins, DNA (eDNA), and lipids in the biofilm matrix of plant-associated bacteria remain limited. Cell-cell communication in bacteria-plant systems involves bacterial quorum sensing and the synthesis, release, and recognition of diffusible molecules such as indole. Production, perception, cellular sensitivity, and response, as well as stability of signaling molecule(s), are key criteria to defining how these molecules can be monitored dynamically.

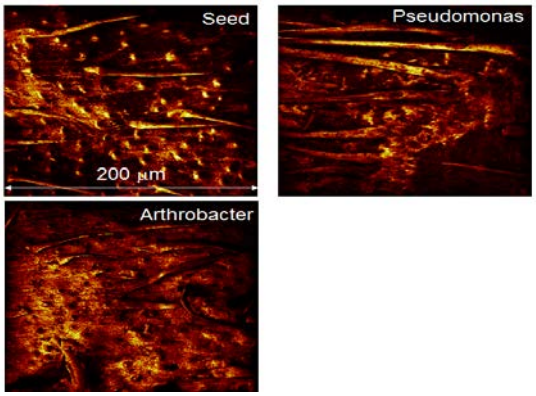

Positive total ion images of the seed top sections with and without interactions with *Pseudomonas* and *Arthrobacter*.

This research aims to provide *in situ* dynamic multimodal chemical imaging of the interface between plant roots and microbial biofilms enabled by a versatile microfluidic reactor, namely System for Analysis at the Liquid Vacuum Interface. The following three tasks are proposed: 1) study the collagen-like proteins (Clps) and bacteria cell attachment at a surface, 2) obtain molecular distributions of key metabolic species in single bacterial cells at the biofilm-root interface, and 3) determine localized flux and mass transfer in biofilm cell-cell communications at different simulated extreme conditions.

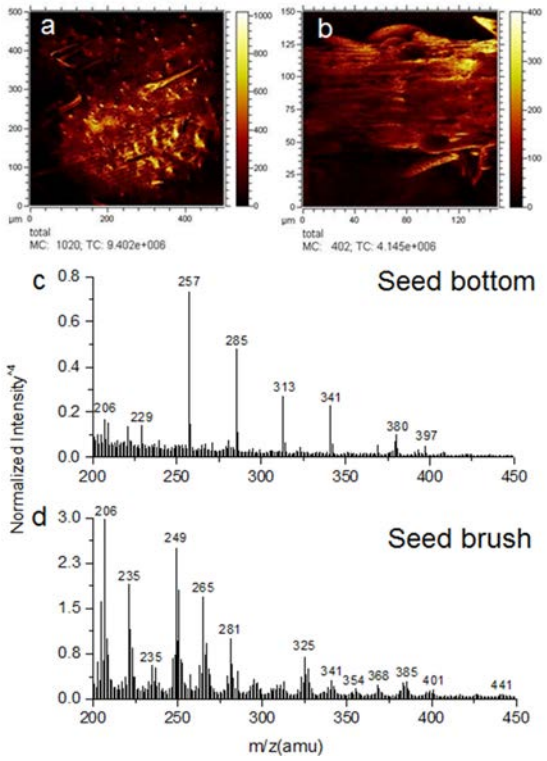

Positive SIMS imaging of a) seed bottom and b) brush and their corresponding mass spectra in c) and d).

In FY 2018, we first focused on the characterization of two PGPBs—*Arthrobacter* gram positive and *Pseudomonas* fluorescens gram negative species—that are commonly found in soil for culture. We investigated their

biofilm formation and adhesion to model solid surfaces. We hypothesize that the gram positive and gram negative species would have different effects on plant seed growth.

Secondly, we utilized delayed image extraction mode in time-of-flight secondary ion mass spectrometry (ToF-SIMS) to chemically map the seed surfaces after the seed was interacted with *Arthrobacter* and *Pseudomonas* under seeding conditions.

Our results demonstrated that gram positive and gram negative PGPBs have different effects on the seed on both changing the surface physical structures and chemical distribution. Both features reflect the results of mass transfer at the dynamic seed-PGPB interface. We provide a new approach to study plant biology and further expand high-resolution imaging capabilities in biological studies.

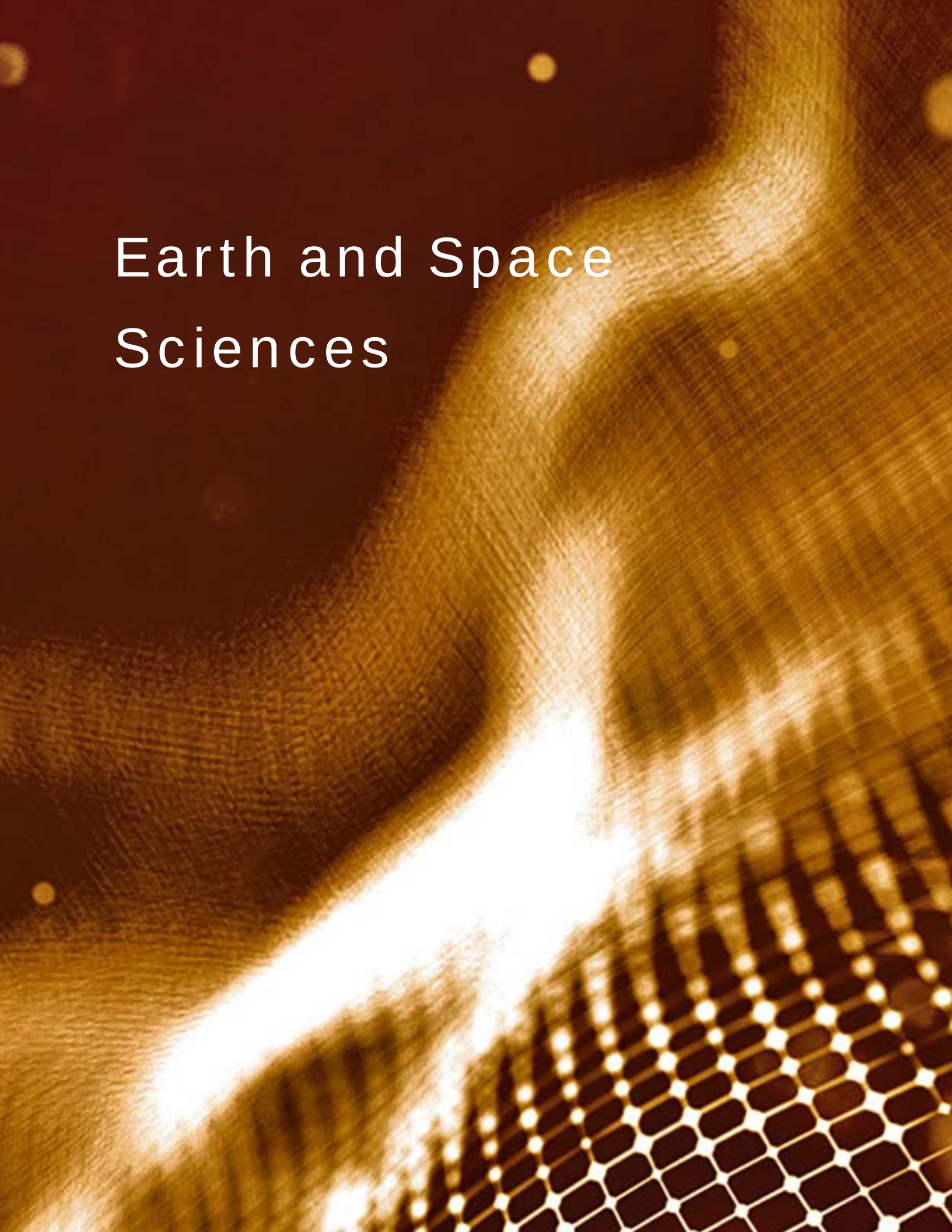
Earth and Space
Sciences

Assessing Climate and Human-exposure Impacts of Polycyclic Aromatic Hydrocarbons (PAHs) and Secondary Organic Aerosol (SOA) Particles

ManishKumar B. Shrivastava
PN16001/2778

Based on the latest advances in measurements, we developed novel modeling algorithms showing that health-relevant PAHs are shielded in the atmosphere by naturally occurring, highly viscous SOAs. We also show that PAH-related lung cancer risk is expected to increase by up to 100% in 2050 in developing regions of Africa and South Asia due to increased agricultural waste burning and shifts to traditional biomass for energy.

Despite decades of research, the long-range transport of PAHs is not well understood, mainly due to incomplete knowledge of gas-particle partitioning and chemical loss rates of PAHs.

Previous modeling studies have indicated that particle-bound PAHs like benzo[a] pyrene (BaP) need to undergo much slower heterogeneous loss to explain their observed atmospheric long-range transport. However, a mechanistic understanding of processes that cause this slow heterogeneous loss has been largely missing. Based on measurements that show that SOAs embed and shield PAHs from atmospheric chemical degradation, we developed new modeling paradigms in a global chemistry/atmospheric model, wherein a shell of highly viscous (glassy) SOA forms around BaP that is adsorbed on the surface of soot/black carbon core. This shell effectively shields BaP from heterogeneous oxidation by ozone, at relatively cold/dry conditions. Using a global three-dimensional atmospheric model, we demonstrated how this new model treatment largely increases BaP concentrations, lifetimes, and their long-range transport, globally. This work was published in the *Proceedings of the National Academy of Sciences (PNAS)* in 2017.

In the current work, we extended our initial modeling studies of toxic PAHs in the atmosphere to address new and very important aspects of PAHs that were not considered in the first two years of this project.

First, we designed and implemented new modeling algorithms to investigate whether the rapid formation of oligomers (bonding of smaller molecules to form larger molecules) catalyzed by PAHs could explain the large increase in SOA mass and number observed in the laboratory. We found that just particle-phase oligomerization cannot explain the increase in SOA mass and number. We found that chemistry in gas-phase followed by uptake on particle surfaces and particle-phase chemistry are all needed to explain the observations. This work has motivated a need for new measurements to elucidate the catalytic effects of PAHs on SOA.

Second, we explored how the exposure to PAHs and related lung-cancer risks would change by 2050. Our results show that developing regions in Africa and South Asia would likely have up to a 100% increase in PAH lung-cancer risk due to increased agricultural waste burning and shifts to traditional biomass for energy.

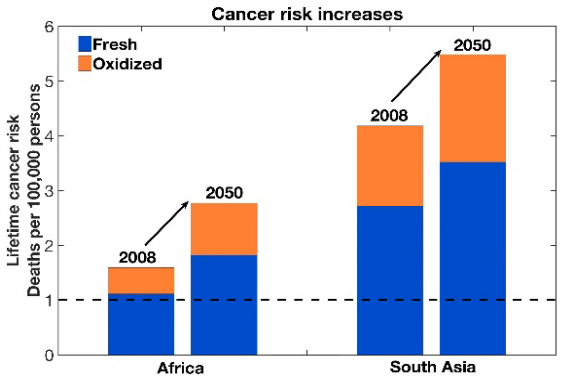

This figure shows that model-predicted PAH lung-cancer risk is expected to increase by up to 100% in developing regions of Africa, as well as South Asia. A significant fraction of PAH lung-cancer risk is attributed to oxidized PAHs (heterogeneous PAH oxidation products), which are often neglected in cancer-risk evaluation strategies. Our modeling study represents the first attempt to quantify global exposure and lung-cancer risk due to PAH oxidation products.

We also found that toxic oxidation products of PAHs, often neglected in current cancer risk evaluation strategies, contribute significantly to cancer risk, especially over warm and humid tropical regions. We compared two different PAH shielding mechanisms and showed that the conversion rate from parent to oxidized PAHs strongly depends on the shielding mechanism varying with the viscosity of SOA coatings (depending on temperature and relative humidity and PAH catalytic effects).

Assessing the Feasibility of Modelling Soil Organic Carbon Contributions to Atmospheric Ice Nuclei

Susannah M. Burrows
PN18049/3048

Freezing of cloud droplets is controlled, in part, by the presence of ice-nucleating particles (INPs), and cloud ice, in turn, impacts the formation of precipitation and the amount of sunlight clouds reflect. This seed project aimed to better understand an underexplored source of atmospheric INPs: soil organic carbon associated with agricultural activities.

Previous studies showed that soils containing large fractions of organic matter were more effective as atmospheric INPs than purely inorganic soils, such as those from deserts. However, the chemical properties controlling the effectiveness of agricultural soils as INPs, and the contribution of soil organic carbon to variability in atmospheric INP concentrations, are not well understood. This project aimed to improve that understanding by characterizing the chemistry of soil particles that act as INPs and estimating their contributions to atmospheric INP concentrations.

Agricultural soil samples were analyzed from two locations: Richland, Washington, and from the Department of Energy's Atmospheric Radiation Measurement Southern Great Plains site in Oklahoma.

Scanning electron microscopy with energy dispersive X-ray spectroscopy (SEM-EDX) was used to characterize the chemical composition of total aerosolized soil particles and of INPs sampled from those soils at -34° Celsius. The analysis revealed that for these samples, INPs were less likely to contain organic matter and more likely to resemble inorganic mineral dust, compared to the overall particle population. This finding contradicted earlier published work, and additional study will be needed to better understand the reasons for the apparent contradiction and, thus, understand which properties of agricultural soils control their ability to act as INPs.

Additional measurements of aerosol composition were conducted at the Advanced Light Source at Lawrence Berkeley National Laboratory using scanning transmission X-ray microscope near edge X-ray absorption fine structure.

Estimated typical atmospheric concentrations of agricultural soil INPs in the atmospheric boundary layer were compared with typical concentrations of other atmospheric INPs for near-surface air. In agreement with previous studies, we find that agricultural soils are potentially a quantitatively relevant source of INPs in near-surface air.

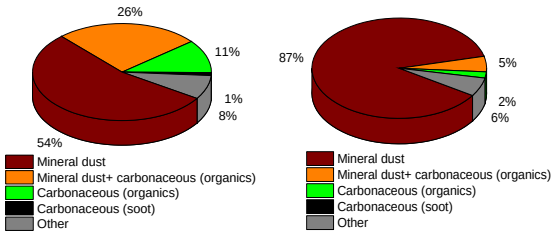

Classification of soil particles, depending on their elemental composition as determined by SEM-EDX analysis. Samples of agricultural soils collected in Richland, Washington, were dry-dispersed for analysis. Left: total soil sample; Right: ice-nucleating particles as sampled by the Environmental Molecular Sciences Laboratory Ice Nucleation chamber, operating at -34° Celsius. The chemical composition of the ice-nucleating particle sample differs from the total particle sample, indicating that the particles triggering ice nucleation in these samples may be chemically distinct.

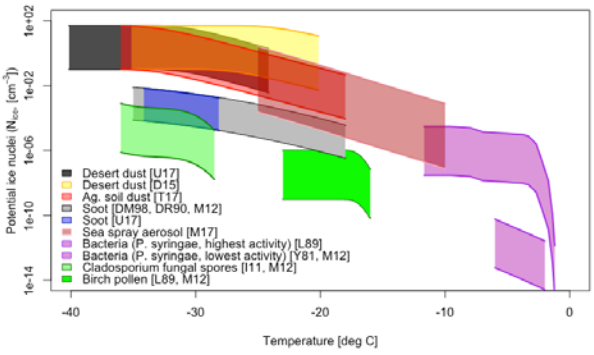

Summary of typical atmospheric concentrations of potential INPs in near-surface air, as a function of atmospheric temperature.

Breaking the Curse of Dimensionality in Atmosphere Modeling: New Methods for Uncertainty Quantification and Parameter Estimation

Xiu Yang
PN17009/2899

The goal of this project is to develop a new computational framework that uses cutting-edge signal processing techniques to efficiently quantify uncertainties associated with empirical parameters in numerical models designed for weather prediction and Earth system research.

Numerical models that simulate the global-scale dynamical motions of the Earth's atmosphere are essential tools for weather forecasting and Earth system research. These models contain many empirical parameters that are inherently uncertain, resulting in large uncertainties in their predictions. Standard uncertainty quantification (UQ) methods suffer from the so-called "curse of dimensionality," (i.e., the required number of simulations increases exponentially with the number of uncertain parameters). The numbers of simulations required by those methods are impractical to achieve due to the very high computational cost of each simulation. This has resulted in a major obstacle to effective application of UQ techniques to atmosphere modeling. This project aims to establish a new, sparse sampling framework specifically designed for the very complex problem of atmosphere model development to allow for accurate characterization of parametric uncertainties from an affordable number of simulations.

FY 2017 was the first year of this project. We designed a strategy that used compressive sensing to construct surrogate models describing the relationships between the uncertain parameters and the large-scale (global or regional) features in DOE's new global atmosphere model. Validation results indicated that, compared to the commonly used method of least squares fitting, compressive sensing significantly reduced the error in the surrogate models. In situations where the number of atmosphere simulations was significantly smaller than the number of degrees of freedom in the surrogate model, compressive sensing effectively played the roles of both parameter screening and surrogate model construction. This suggests that our algorithm is not only more computationally efficient, but also more objective, since it requires far less prior knowledge from experts in the specific domain of research. Another highlight of our results was that the excellent performance of compressive sensing was consistently seen in a wide range of physical quantities, suggesting that our methodology is likely to be applicable to other atmosphere models as well.

In FY 2018, we reached three important milestones. First, the compressive-sensing-based surrogate construction algorithm was further evaluated with a different set of atmospheric simulations and was again demonstrated to be substantially more accurate and efficient than the traditional method. Initial efforts were also made to construct surrogate models for spatially distributed features of the atmosphere.

Second, our surrogate models were used to perform parameter sensitivity analysis, an investigation that the atmospheric scientists often need to do when developing a new model or upgrading an existing version. We demonstrated that our surrogate models were able to provide accurate answers using only a quarter of the simulation samples required by the traditional method, implying a substantial saving of the CPU time needed for expensive atmospheric simulations.

Third, we made an initial effort in parameter estimation. A method was developed to successfully identify multiple sets of parameters that led to atmosphere simulations with the desired global-mean features. This provided a proof of concept that our surrogate models can be used for to obtain efficient and objective parameter estimation for the highly nonlinear and complex global atmosphere models.

Ecosystem Transitions and Associated Greenhouse Gas Fluxes Following Salt-water Intrusion from Relative Sea Level Rise

Heida L. Diefenderfer
PN16076/2853

The overarching goal of this project is to quantify, mechanistically understand, and predict shifts in CH_4, CO_2, and N_2O fluxes from an intact wetland community in response to salt-water intrusion. Understanding the effects of these large-scale disturbances, predicted to occur increasingly in coming decades, on greenhouse gas sources and sink function is critical to improving process-rich models of climate change effects on coastal wetlands.

Coastal and fluvial ecosystems bordering the landward limits of salt water are key depositional regions for terrestrial nitrogen (N) and carbon (C) bound for the ocean. These highly productive and globally distributed ecosystems are dominated by herbaceous, shrub, and/or forested vegetation. Yet, long-term trends indicate that the zone of tidal freshwater will migrate substantially in the landward direction in coming decades. Soil chemistry will be disturbed by shifting hydrologic and salinity regimes at the intersection of river basin and coastal nearshore processes, changes in porewater salinity may overwhelm the salt tolerance of plant and microbial communities, and the microbial community will exert functional controls on the decomposition of legacy material from disturbance-induced rapid succession. However, the time lags and magnitude of responses by microbial communities to salt-water intrusion, as measured by greenhouse gas flux function, currently remain unknown, which limits the robust prediction of ecosystem functional shifts because of altered salinity regimes.

Understanding the controlling factors on these complex ecosystem processes is fundamental to Department of Energy Biological and Environmental Research missions related to global elemental and water cycles. Thus, this project sought to discern the sensitivity of soil microbiome molecular processes and gas exchange to altered salinity regimes.

This study utilized *in situ* characterization coupled with hypothesis-driven experiments on intact soil cores in the ambient coastal environment. It focused on a tidally influenced, forested wetland near the mouth of the Columbia River in Washington State. Climate change is altering the hydrologic regime in this, and similar, tidal freshwater regions, such that historically river-dominated conditions are being increasingly affected by nearshore-ocean conditions, including salt-water intrusion. Coastal wetlands like this one are particularly susceptible to storm events, salt-water intrusion, and increasing water levels.

We hypothesized that sudden changes in salinity regimes will strongly select for particular microbial taxa, likely producing mortality events and, thereby, affect community functions, including the emission of greenhouse gases. To address hypotheses like these, however, we needed to improve upon the standard experimental and monitoring systems that have been used for decades: static chambers that are sampled by hand with syringes and then analyzed at a gas chromatograph. The frequency and timing of such sampling was limited and produced a publication record that appeared to be skewed toward summer, daytime, calm weather, and C not N. This aspect of the research leveraged recent technical advances in autonomously deployed sampling systems, specifically a coupled cavity ring-down spectrometer and autochamber system capable of high-frequency data collection in frequently flooded marshes.

In the present study, we first exhaustively quality-control tested the system for laboratory use, in a series of three laboratory experiments and a fourth quantitative experiment, in coordination with the manufacturer. This led to the repair of defects, and development and publication of R-code to identify and flag data associated with malfunction events and to estimate the most precise slopes and, thus, fluxes from the data.

Subsequently, we conducted a laboratory greenhouse gas flux experiment in three 4-month phases, each including six large-diameter cores from wetland soils: 1) compared

freshwater (control condition) and 4-ppt (parts per thousand) salinity conditions on cores under saturated conditions, 2) compared saturated and tidal (periodic saturation) conditions on cores at 4-ppt salinity, 3) compared freshwater and 4-ppt salinity conditions on cores under tidal condition.

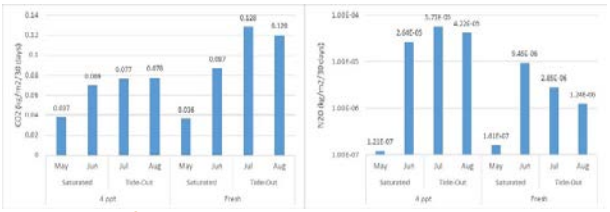

Mass (kg m^{-2} $month^{-1}$) of CO_2 (left) and N_2O (right) as a function of salinity and month.

These experiments were made possible by utilizing the seawater plumbing at the Marine Sciences Laboratory and freshwater brought from the wetland, mixed together to simulate the oligohaline range of diluted seawater similar to model-predicted effects of climate change in tidal freshwater wetlands. Moreover, we conducted the experiments outside, at sea level, a few meters from the Pacific Ocean, so changes in pressure, temperature, atmospheric CO_2, and other environmental factors are not simulated but real; monitoring data from the Marine Sciences Laboratory weather station and other local sources, such as sea level buoys, were used as covariates for data analysis.

We also initiated characterization of *in situ* conditions at the study site to support eventual development of a core-scale reactive transport model incorporating the saturation rates observed in laboratory experiments and analytical results on field-collected soils for total carbon, total organic carbon, total inorganic carbon, bulk density, particle size distribution, and total solids. During the core-incubation study, replicate cores were also sacrificed for porewater analyses (i.e., pH, specific conductance, carbonate, chloride, sulfate, nitrate, total calcium, iron, manganese, potassium, and sodium) to support parameterization of this model. Analysis of data from piezometers deployed between June 28 and November 1, 2017, at the site to develop a flow field model indicated that the variability in the depth of the ground water was small (coefficients of variation [CVs] less than 5%) compared to a nearby channel (CV = 66%). The average ground water depth at the site was 50% greater than the average water level in the channel, and the site was inundated by surface water 0.5% of the time.

In Phases II and III at temperature-corrected conductivities of 0.2 and 0.3 S/m (measured at 5 cm below the surface of the sediment cores), the flux of N_2O significantly decreased (p less than 0.003) with increasing soil moisture. At conductivity of 0.4 S/m, the relationship with percent moisture was muted (p = 0.18) and was not different from the fresh water. At conductivities of 0.3 and 0.4 S/m, fluxes significantly increased (p equal to or less than 0.01) with temperature and at conductivity equal to 0.2 S/m, generally increased with temperature (p = 0.08). The contribution of N from N_2O was very low (most flux less than 0.2) in the fresh treatment (conductivity equals 0 S/m) at all temperatures and soil moistures compared to saline conditions. One extreme value was removed.

In contrast, the freshwater treatment had greater fluxes of CO_2 at higher temperature and soil moisture levels than the saline treatments. For all conductivity levels, the flux of CO_2 decreased with increasing soil moisture (p less than 0.001) and increased (p less than 0.001) with temperature. One extreme value was removed from analysis.

Fluxes of CH_4 were variable and inconsistent across levels of moisture, temperature, and conductivity. Soil moisture and temperature explained less than 17% of the variability in flux over all values of conductivity.

Modeled results indicate that under a sea level rise scenario, salt-water influx at a 4-ppt level would suppress C evolved as CO_2 but not as CH_4. In contrast, N evolved as N_2O would increase with salt-water intrusion.

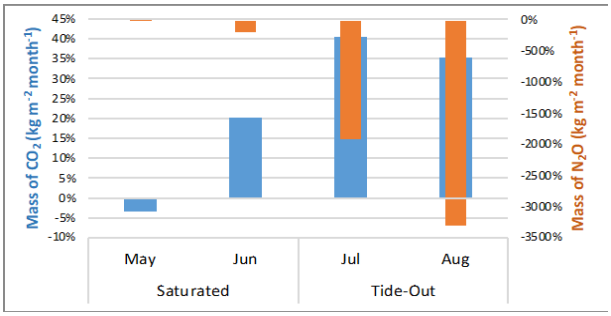

Percent difference (fresh - saline/fresh) in the mass of CO_2 and N_2O evolved from soils with saturated and receding (ebb-tidal) water conditions.

Geochemical Controls on Fracture Growth

Jeff Burghardt
PN18035/3034

In most cases in natural and manufactured structures, fracture growth is at least in part controlled by chemical reactions through a process that is poorly understood and, thus, relatively unpredictable. This project aims to develop a laboratory apparatus that allows the fundamental, molecular-level mechanisms responsible for this process to be observed for the first time.

The controls that chemical factors exert on fracture growth have been studied for several decades, in a wide variety of materials. However, to our knowledge, all previous studies of these mechanisms have utilized only mechanical instrumentation during active fracture growth. The most sophisticated previous studies utilized chemical measurements / observations only *ex situ*—after the stress that was driving the fracture had been released. This project sought to leverage existing *in situ* chemical instrumentation capabilities to be the first to deploy *in situ* chemical diagnostic tools together with traditional mechanical instrumentation to a stressed/growing fracture. The objective was to provide a means of testing the various hypothesized mechanisms for chemically controlled fracture growth.

We designed and fabricated a double-torsion fracture testing apparatus that is integrated into an existing high-pressure, high-temperature reaction vessel with optical windows. The double torsion apparatus allows a fracture to be initiated and carefully propagated in a plate-shaped sample. Instrumentation was installed that allows the fracture growth rate and stress intensity to be measured. A fixture was constructed for mounting this vessel/fracture testing apparatus to allow Raman spectroscopy measurement of the fracturing sample. This fixture allows the spectrometer probe to be moved via a motion control system to probe different locations on the sample (i.e., different distances away from the fracture tip).

After the double-torsion apparatus was constructed, it was tested by measuring the fracture velocity using a set of soda-lime glass samples. Soda-lime glass is a common benchmark material for this type of testing. We verified that the fracture velocities for a given load magnitude that we measured were consistent with those reported in the literature.

Our initial results indicate an increase in some of the Raman spectral peaks near the fracture tip. This result supports two hypothesized phenomenon associated with and thought to be responsible for subcritical fracture growth in this material: the migration of cations and molecular water to the zone of high tensile stress, which disrupts the SiO_4 structure.

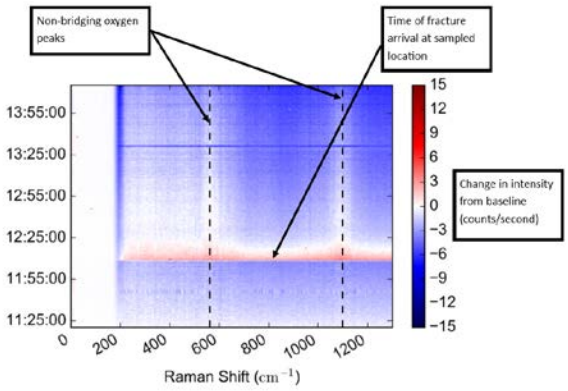

The peaks that increase in intensity are associated with bending and extension of non-bridging oxygen atoms in the SiO_4 structure of the glass.

While soda-lime glass was ideal for a first material to test, because its subcritical fracture growth behavior is so well studied, with well thought-out hypotheses to be tested, it turned out to be a difficult material to work with, because the Raman peaks are relatively broad due to the structural complexity of the glass. The primary signal that was anticipated based on the literature was a shift in the spectral location of the bending-mode peaks. However, the broad peaks and the limited spectral resolution of the spectrometer available has not made any shift in the spectral location of the peaks to be detectible thus far. In the future, we hope to test materials with sharper peaks and with a more modern spectrometer.

How Do Non-linear Microbial Processes Lead to Linear Ecosystem Fluxes?

Kathe Todd-Brown
PN15094/2769

This project incorporates new measurements and understanding into soil carbon models, advancing predictive capabilities of biogeochemical models and bridging the gap between microbial processes and ecosystem observations.

Modeling soil carbon dynamics is critical to predicting how much carbon dioxide will be in the atmosphere to drive future climate change. Soil carbon models have remained essentially unchanged for decades. These models partition soil carbon into one to nine pools; carbon leaves these pools at a rate proportional to the amount of carbon in the pool (i.e., first-order linear decay)—some of the exiting carbon is diverted to other pools, and the rest leaves the system as carbon dioxide. This model type tends to statistically fit observed soil carbon emissions using laboratory incubations. However, despite extensive attempts to characterize the environmental sensitivity, parameters must be re-calibrated for each location, making it difficult to confidently generalize these models to global projections.

In the past 15 years, new microbial and chemical characterization methods have led to a growing interest in the biogeochemistry community in process-rich decomposition models. In these models, soil carbon must first pass through a microbial pool before leaving the system as carbon dioxide. In addition, other explicit processes, such as extracellular enzyme mediated breakdown of organics and mineral-organic interactions, are also considered. These models are appealing, not only because they can describe a more fundamental understanding of soil decomposition, but also for their potential to incorporate new 'omic and high-resolution chemical measurements. There are mathematical and computational challenges due to the non-linearity of the new models, in addition to traditional issues around parameter and driver heterogeneity.

The objectives of this research are 1) to develop better soil carbon models in the short-term via model-data integration of realistic field data into traditional decomposition models and 2) contribute to long-term improvements by capturing process-explicit representations of our evolving understanding of soil decomposition in new models.

This project provided statistical and modeling support for a study evaluating novel ways to examine temperature sensitivity of soil carbon stocks across multiple field-warmed manipulations. Soil carbon changes are generally considered to be too noisy to use for temperature sensitivity calculations; previous studies have instead relied on changes in soil respiration over time. We have shown that it is possible to calculate a temperature sensitivity using soil carbon stocks directly, given a large enough sample size, and can, thus, constrain Earth system model results post-hoc to reflect the field data. We also showed that, under specific conditions relevant to Earth system models, the current soil carbon models are overly complex and propose an equivalent simplified model. This simplification is controversial but robust and has profound implications for how soils are modeled at the ecosystem scale.

On the process-explicit modeling front, we have developed and parameterized a new model from the literature: JAM (Just Another Microbial) model. Preliminary results suggest that different subsets of parameters control the long-term field soil carbon dynamics versus short-term lab incubation carbon dioxide flux from the system, and that biological, chemical, and geophysical properties equally influence long-term soil carbon dynamics. While these results intuitively make sense from a soil science prospective, this is the first time that this has been demonstrated in a model context.

SWEEET – SeaWater Electrochemical Element Extraction Technology

Matthew Asmussen
PN18028/3027

As our energy sector diversifies, the materials required (e.g., lithium [Li], rare earth metals) for new technologies are both increasing in price and widely sourced from other countries. Many of these materials are present in seawater and the development of technologies to harvest them directly from the sea can open a new market, potentially lower costs of these critical elements, and relieve reliance on foreign countries for materials crucial to the USA's growth.

There are currently no commercial-scale efforts to extract elements directly from seawater. Diminishing terrestrial reserve-supply ratios of many valuable elements make seawater mining an intriguing technology. An example of this potential is the extraction of Li. Li is currently recovered in slow (several years) and inefficient (less than 50% recovery) evaporation and chemical treatment processes of brines, primarily in South America. Li concentration is too low in seawater to use the same evaporation/chemical treatment processes, but alternate methods are possible.

Li-ion batteries function by electrochemically moving Li-ions through an electrolyte solution into the structure of an electrode. Most Li-ion batteries use a non-aqueous electrolyte for the transfer of Li-ions due to limited stability of most Li-ion battery electrode materials. However, select materials that can be used in Li-ion batteries are stable in aqueous environments and can carry out the same Li-insertion processes. On a large scale, this type of process can be powered locally at a marine hydrokinetic platform. Several goals were set out at the start of the project:

1. Identify electrode materials that are stable in aqueous environments can be used in a demonstration system.
2. Confirm the stability of these electrode materials in seawater.
3. Construct a system to allow testing of element extraction from a raw seawater source at the Marine Sciences Laboratory (MSL).
4. Retrieve Li from raw seawater.

The project began with selection of electrode materials to be used. A down-selection was made to two electrode materials to pursue testing with: 1) electrolyzed manganese dioxide (EMD), selected to provide a stable material in aqueous solution and be (apparently) Li-free, and 2) Li titanium oxide (LTO), a lithium containing electrode with theoretical higher efficiency than EMD.

The electrodes were initially screened in bench scale tests using solutions spiked with high levels of Li and various salts. The proposed collection method for the Li would be placing the electrodes in solution (or seawater) and passing a current through the system to collect Li at the cathode. The electrode is then placed in a fresh NaCl solution and the current reversed to discharge the Li. Stability issues were observed that led to dissolution of the pouch-style electrodes in the discharge step. This was overcome by limiting the duration of the discharge cycle (30 minutes) and changing system control from a DC power source to a potentiostat.

Initial testing focused on the EMD electrode showed the expected response for Li insertion to the electrode and decreasing concentration of Li (capture of about 4 µg Li/g electrode) in solution. The electrodes were moved for testing in simulated seawater spiked with Li. In these tests, the discharge solution was measured to have Li released from the electrode (about 100 µg recovery).

The next step was construction of a system to perform tests in the raw seawater flumes at the MSL. A cartridge electrode design was developed and fabricated to hold a three-electrode cell system within the seawater flume. Coupled with a workstation, this design established a new capability at MSL to perform testing in raw seawater.

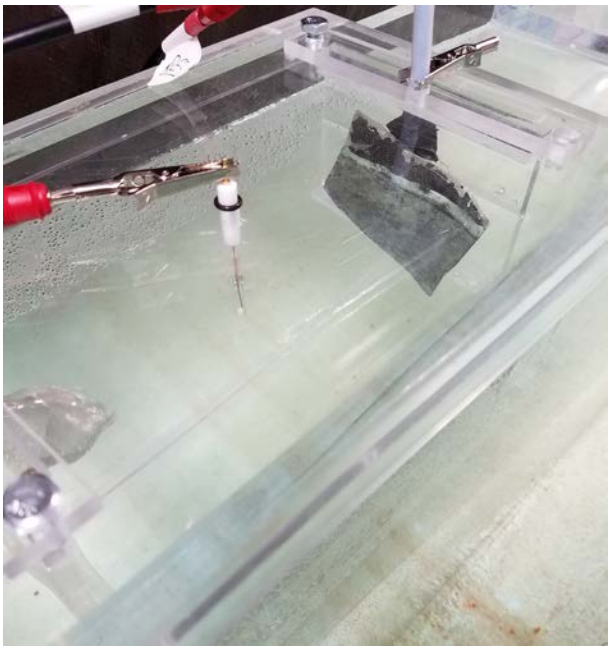

The electrochemical system used for testing in the raw seawater flume at MSL.

The first testing of EMD and LTO at MSL was carried out using the same loading/discharge method. After exposure to the raw seawater feed, the electrodes were discharged, and Li was measured in the discharge solution. After the test, the EMD and LTO electrodes showed large white deposits on their surface, which were found to be $Mg(OH)_2$ that would cover the surface with increasing exposure time.

An expanded suite of testing was initiated at MSL to investigate the response of various collection times (4 h through 120 h) and recycling of the electrodes. It was observed that the EMD electrodes were yielding comparable discharges of Li after differing exposure time frames. Blank experiments were performed to discharge fresh electrodes prior to exposure to seawater, and Li was detected from the EMD. This was a highly surprising observation, considering the EMD was the “Li-free” electrode. Digestion of the electrodes proved that a nominal Li contamination was present in the EMD material. The amount of Li released by the EMD after the loading in seawater could not be statistically separated from the contamination Li released in blank testing.

In summary, the project highlighted several challenges and a need for optimization with Li-extraction. An improved method of electrode discharge/collection needs to be determined, Mg deposition on the surface during collection in raw seawater needs to be limited, and alternate Li-free electrode materials should be investigated. However, this project, despite the challenges, has established a new capability to investigate materials for recovery of elements from seawater.

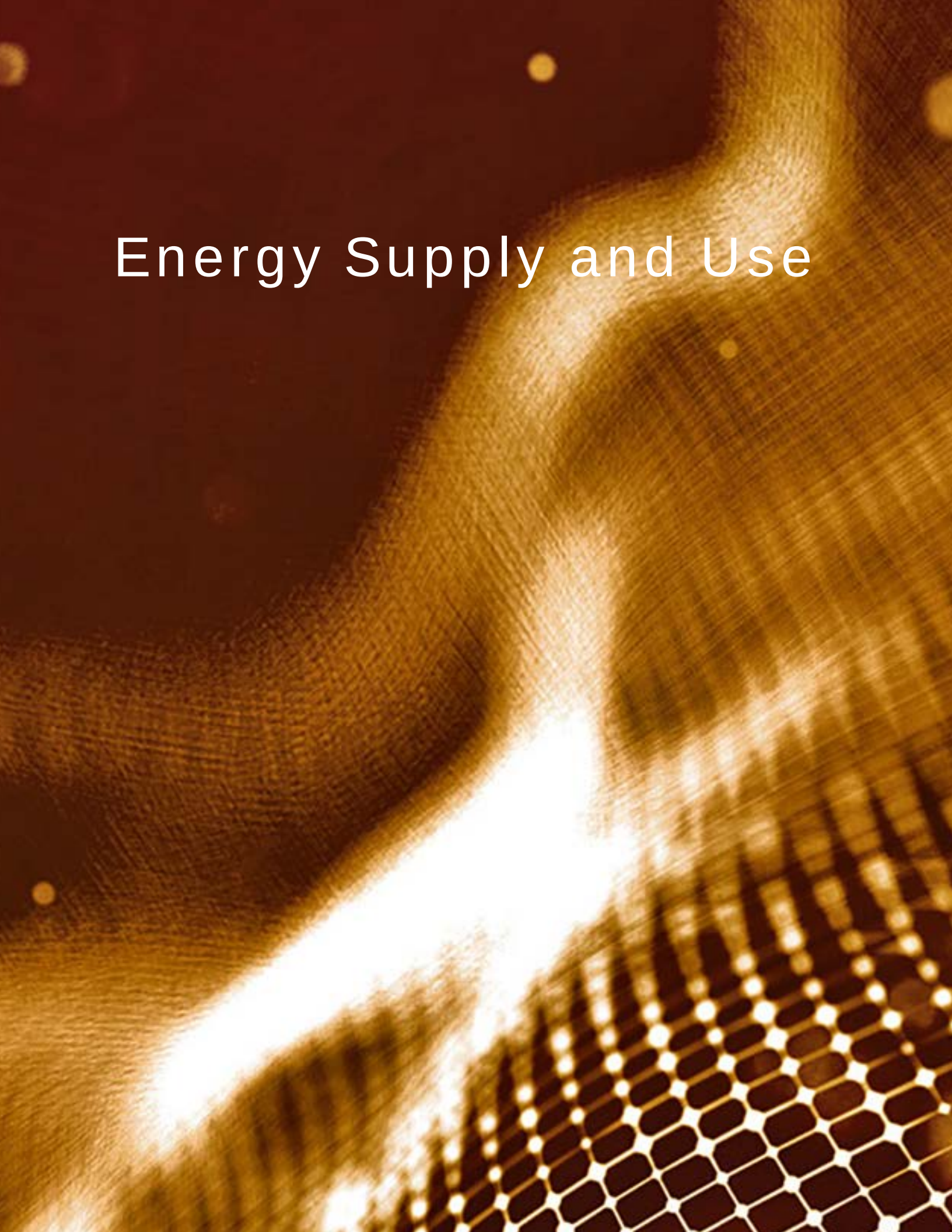
Energy Supply and Use

Blockchain for Building Identification and Data Exchange

Nora Wang
PN18046/3045

Buildings are the single largest users of electric power in the country; however, difficulty in joining data from disparate sources in a single location due to the different ways of identifying buildings becomes a major obstacle to information and knowledge exchange for energy research and policy. This project has designed a blockchain application that will enable any building stakeholders to participate in a global database that can store an unambiguous permanent record of building transactions.

Previously, the project team created the Unique Building ID (UBID) that serves as a natural, location-based key used to identify buildings uniquely, world-wide. We created a prototype blockchain solution that shows how UBID records can be asserted and globally shared without a central authority and how records of the building can be stored and shared efficiently and securely referencing the UBID.

We created a database schema for building information keyed to the UBID and adapted to blockchain deployment. We created a series of use cases designed around the needs of system users. To elicit requirements, we created a separate user experience prototype that described how the user would interact with the system to accomplish the use cases. We then implemented a prototype blockchain application in Hyperledger™ Fabric that demonstrated how a real blockchain would implement selected use cases. Finally, we hosted a visiting professor and his student who helped us devise an approach for automatic validation of smart contracts in a blockchain.

As part of our requirements elicitation process, we engaged a team of volunteers from the Berkeley Innovative Solutions Consulting group out of the University of California, Berkeley. The students identified stakeholders in the cities of San Francisco; South Burlington, Vermont; and Seattle, Washington. Other stakeholders included the U.S. Green Building Council (USGBC) and Ecotope, Inc. The student team discovered that stakeholders do have problems with multiple conflicting identifiers for the same building stock across different departments. Based on the UBID methodology and the blockchain implementation, the team determined that the UBID blockchain solution would result in substantial cost savings in database generation, operations, and maintenance in the cities surveyed and the customer cities of the other organizations surveyed.

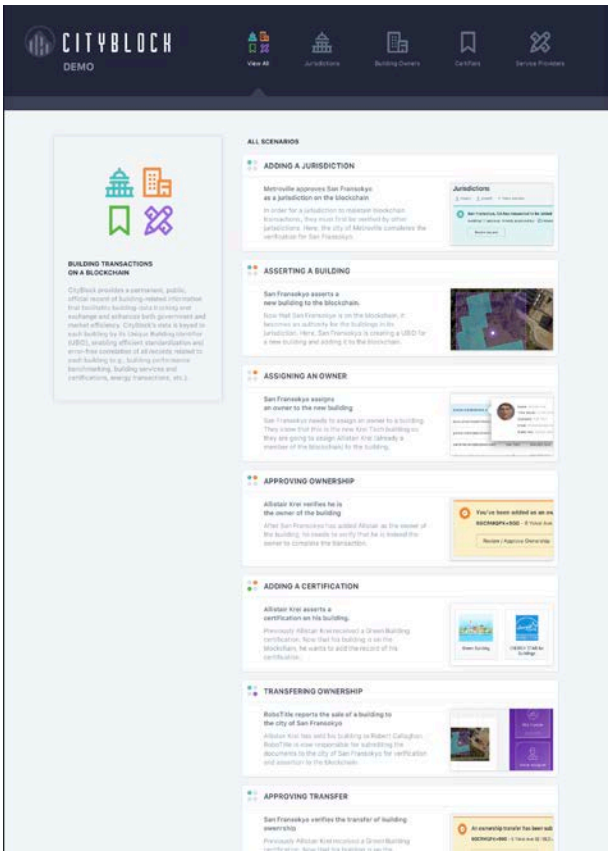

This is a screenshot of the CityBlock user interface mockup.

We devised six use cases: 1) joining the UBID blockchain, 2) asserting a UBID for a building initially, 3) issuing a green building certification, 4) revoking a certification, 5) changing building ownership, and 6) issuing a building permit. We mocked up a user interface for four of these use

cases. Then we showed this interface (named CityBlock) to potential users, and it was enthusiastically received.

We implemented a prototype blockchain application in Hyperledger Fabric for the second use case. We found Hyperledger Fabric Composer too immature to create a full prototype, but we proved with it that a blockchain application is possible using real-world tools. In the future, if funding permits, we hope to implement our use cases on a different blockchain.

Smart contracts are used in blockchain applications to obtain goods and services without requiring a trusted middleman. We expect that the UBID blockchain will make it possible for users to offer trusted services like certification, energy benchmarking, and permitting for buildings. However, it is critical that the contracts not have loopholes, because they run as a computer program without human oversight. Smart contracts can be verified using Microsoft's Temporal Logic Analyzer.

Our most important findings of the year included that a UBID blockchain would save money and effort, and that it is, indeed, feasible, although the current state of blockchain technology seems immature. We found ways that users would like to interact with such a blockchain-based system for building IDs and laid the groundwork for verification and validation of smart contracts based on the UBID blockchain.

Blockchain Transactive Energy Application: Increasing Speed, Scale, and Security at the Grid's Edge

Michael E. Mylrea
PN18039/3038

This project resulted in running an open source blockchain node at PNNL to execute various auction-based smart contracts. Through the achievement of this novel and timely goal, PNNL is the first national laboratory to set up a grid-specific blockchain node to advance grid cybersecurity blockchain research and experimentation. Realizing these goals resulted in a blockchain platform for grid cybersecurity and transactive energy researchers to perform realistic, utility-scale experiments. Such advanced research coupled with these research outcomes could potentially improve the security, speed, and scalability of complex energy exchanges at the grid's edge.

The primary focus of this work was to investigate and test how the application of permissioned and private proof-of-authority (PoA) blockchains can improve the security, speed, or efficiency and scale in both transactive control and supply chain applications.

Blockchain technology comes with several potential benefits that can improve the current processes in energy utility space. One of those critical areas is associated with security and implementation platforms of the transactive control and systems. There are various types of transactive control mechanisms. This research is to evaluate the efficacy of blockchain technology in transactive energy applications and to demonstrate its potential through table-top experiments.

There has been some work in this area, primarily using permissionless and public proof-of-work (PoW) blockchains. In the transactive energy system, since the participants are consumers attempting to bid and buy energy, these transactions cannot be executed in a public consensus model. In addition, the utility should have the authority to permit the consumers that can be part of the energy transaction platform. Therefore, permissionless and public blockchains may not be the right path.

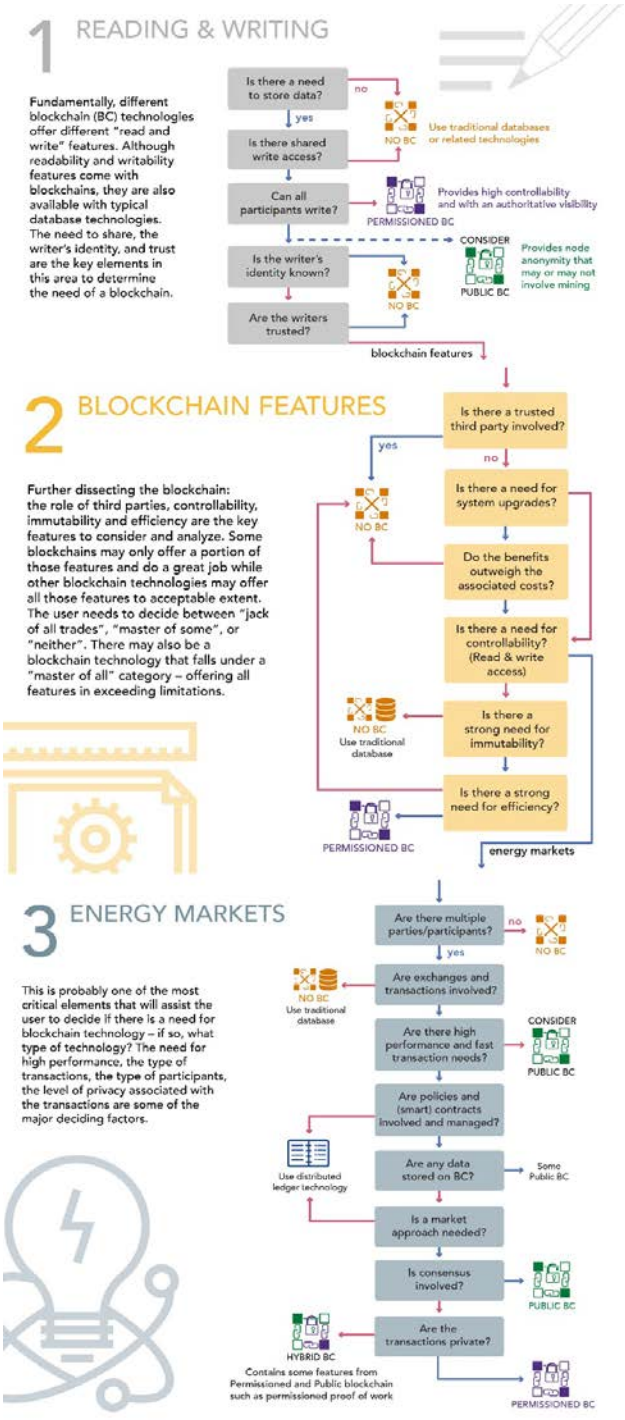

Roadmap depicting information to help end users determine which type of blockchain they will need, focused on the following: 1) read and write features, 2) blockchain features, and 3) energy markets.

Some high-level objectives of this research were to 1) develop a roadmap to determine the type of blockchain that should be used for an application, 2) understand technical aspects of permissioned PoW and PoA blockchain applied to the energy space, 3) identify and address organizational network challenges in deploying and running a blockchain node, and 4) execute smart contracts—generate token, commodity transfer, and open and Vickrey auctions.

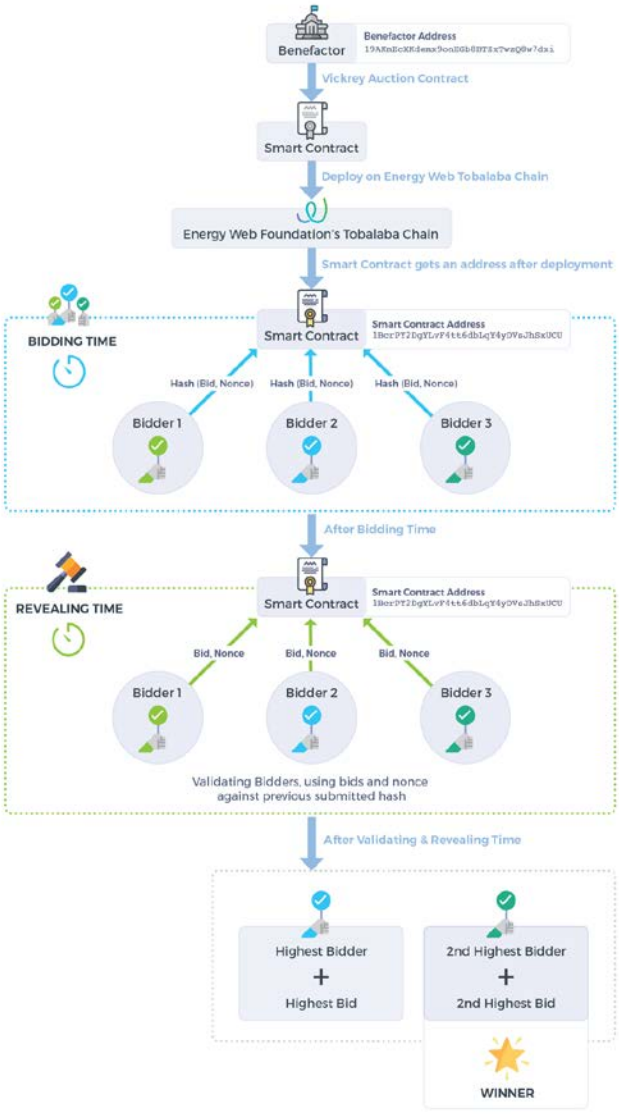

Roadmap depicting information to help the end user determine which type of blockchain they will need; this section focuses on executing smart contracts.

Before optimizing or securing electricity infrastructure with blockchain technology, it is important to determine what technology is going to be applied and what problem will be solved. Some blockchain solutions create more problems than solutions, expand security gaps more than mitigate them, increase costs rather than efficiencies, increase latency rather than optimize it, and increase energy use rather than reduce it. Blockchain solutions that help track and secure large data sets also need to be energy efficient, economic, and interoperable. Cost, functionality, scalability, and cyber resilience were all important factors in considering the functional requirements for grid cyber use cases that were explored.

Results of the project are that we 1) developed a roadmap to help end users determine when to use blockchain to increase the cybersecurity of electricity infrastructure, 2) addressed organizational network challenges and established blockchain nodes to enable testing of various real-time transactive experiments, 3) successfully executed multiple auction-based smart contracts, 4) engaged with 15+ industry and utility vendors, and 5) engaged with the Energy Blockchain Consortium to identify grid-related use cases.

Campus as a Laboratory

Paul W. Ehrlich

PN17040/2930

The ability to connect to and test on physical hardware enables control method developers to better validate the behavior of systems under control of the methods they develop and the models they use in simulations at scale.

This project continues the development of new physical testbed capabilities, while ensuring that the resulting testbed is flexible, scalable, and expandable so that new, advanced control technologies can be experimentally tested. The project focuses on expanding the existing testbed infrastructure to include additional hardware, equipment, and buildings and includes testing and validation of the new testbed capabilities implemented. The project also includes documenting the components, structure, and operation of the testbed and providing support to experimenters in defining, configuring, and executing experiments.

During FY 2017, project work focused primarily in two areas: 1) integrating external data source connections into the test bed and 2) reintegrating the relocated Building Diagnostics Laboratory into the tested and supporting use of it for an integrated demonstration.

The external data sources integrated included data streams for wind and balancing authority load from Bonneville Power Administration, several data sources from the Midcontinent Independent System Operator, data from the New York Independent System Operator, data on system status of the California Independent System Operator, and price data from the Commonwealth Edison Company's Residential Real-Time Pricing Program. The data from these sources can be used as input to control experiments.

Re-integrating the laboratory focused primarily on establishing network connections and commissioning and enhancing the laboratory equipment and controls. This laboratory includes a complete commercial heating, ventilation, and air-conditioning (HVAC) system (chiller, air handler, variable-air-volume terminals, and controls) that would normally serve a small office building or school. The lab was relocated from its previous location in FY 2017, as part of a PNNL move-out of some old facilities, and enhanced with new controls, metering, and sensors, as well as the ability to false load a set of small test rooms conditioned by the HVAC system. This new Advanced Building Control Test Facility can readily be used to simulate a series of building sizes and system types.

Testing in the facility is achieved with the use of a commercial control system that uses BACnet® communications. These controls are connected to the testbed via a VOLTTRON™ server and a bridge between VOLTTRON and the Framework for Network Co-Simulation™ (FNCS, pronounced "phoenix") environment, enabling researchers to perform hardware-in-the-loop simulation experiments.

This flexible facility began to support experimentation on new methods of control implemented on the HVAC system in the laboratory, the laboratory system in conjunction with operating buildings on the PNNL campus, and hardware-in-the-loop together with simulations that enable experiments on large-scale building-grid systems.

During FY 2018, the project continued in several areas: 1) continued enhancements to the Advanced Building Control Test Facility, 2) expanding the capabilities of the VOLTTRON platform to better support the testing process, 3) developing documentation and training on the use of PNNL facilities for hardware-in-the-loop testing, and 4) testing these processes with research teams.

Work related to the test facility included installation of false loading to allow for researchers to simulate both weather and occupancy, as well as detailed sub-metering to allow for improved testing capabilities. Mechanical updates were also made to the chiller and air handler systems, including larger

fans and a more reliable chilled water system. Finally, a detailed facility reference guide was developed, as well as a training program for researchers on how to utilize the facility.

Efforts were made to enhance the VOLTTRON platform and to improve its capabilities to support hardware-in-the-loop testing. We updated the infrastructure to VOLTTRON 5.0 to make use of new features. This included the addition of multiplatform support to provide the potential to simplify interactions with data across multiple instances. We implemented the BACnet Change of Value subscriptions, which is a more efficient method to collect data, reducing the amount of storage required, as well as the effort needed to support data exchange, both on the control system and network. We improved FNCS integration: FNCS is now a subsystem that VOLTTRON agents can utilize with no setup needed on their part. We also deployed a new database (Crate) in VOLTTRON that includes the ability to readily export data using flat files that researchers can store in Pacifica.

Equipment in the Advanced Building Controls Test Facility.

In order to support current and future testing efforts, documentation was developed that can be used to assist researchers in understanding the testing process, systems, and procedures. This included a detailed manual that explained the intended systems and usage for the Advanced Controls Test Facility. This document describes both the systems in place, as well as the process to utilize simulated loading. A second document was developed that covered the general process for hardware-in-the-loop controls testing on the PNNL Richland campus, which includes an overview of the systems, usage of VOLTTRON, the process for interacting, and gaining approval of the PNNL Facilities and Operations group. This is part of a larger volume of documentation that includes control diagrams, mechanical descriptions, energy models, and other tools designed to assist in the process of testing in PNNL facilities. All of this documentation will be available for future controls research teams.

Control Framework for Large-scale Complex Systems

Enoch H. Yeung
PN16063/2840

This project is developing a framework for system analysis, decomposition, and engineering of distributed control for infrastructure systems.

With rapid technological advancement in communication, computing, and control, dynamical systems become increasingly complex (e.g., large-scale, dynamically coupled, and uncertain), posing new challenges to the current control engineering paradigm. This project develops analysis and synthesis methods to systematically architect and design control hierarchies for large-scale complex systems. The outcome of this investigation is a set of requirements that will inform control architecture definition and algorithm selection for a given system size and physical shape, as well as communication and computation architectures.

In FY 2018, we developed novel algorithms for: 1) selection of control nodes in large-scale networks using submodular optimization, 2) identification of coupling strengths in large dynamical networks for optimal partitioning using Lyapunov-based methods, and 3) extension of Koopman operator-based learning approaches to switching hybrid systems.

Submodular optimization provides for a principled and scalable approach to select an optimal subset from a ground set of entities under certain conditions, whereas the brute-force approach suffers from exponential complexity. In FY 2018, we focused on the application of submodular optimization approaches for selecting (control) input nodes in networked multi-agent systems. By formulating the controllability criteria as matroid constraints, we tackled the problem of performance optimization while ensuring controllability. We developed accelerated greedy algorithms with accelerated computation oracles and demonstrated significant speedups. Noting that the stochastic greedy algorithm does not result in significant degradation of the solution performance objective, we further accelerated the flow by applying low-rank updates to the objective function computation. The scaling results show more than two orders of magnitude speedup for systems of size 2,000 nodes. In sparse networks with densely connected clusters, we achieved nearly three orders of magnitude speed-up by applying a two-stage algorithm with domain-decomposition.

Distributed analysis and control relies on the separability of large networks into weakly interacting subsystems. Understanding the nature of coupling and interaction strengths in a dynamical network is critical, not only for distributed control design, but also to evaluate the resiliency of the network to failures.

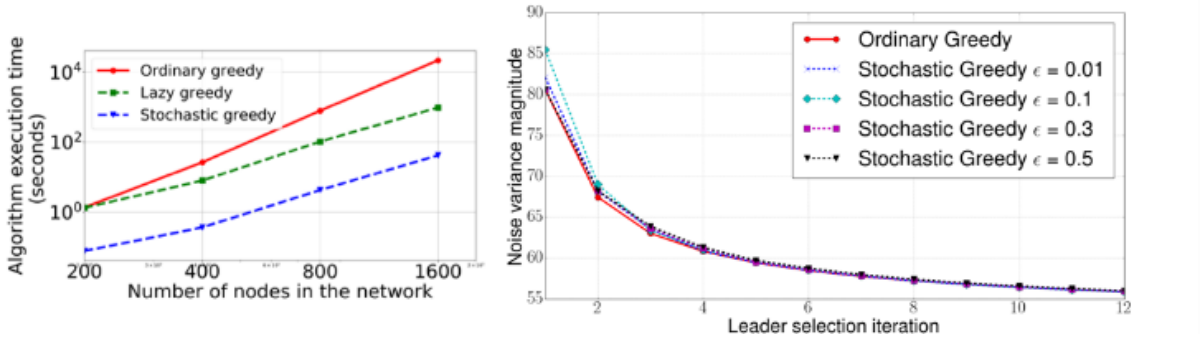

(Left) A comparison in run times between three variants of the greedy algorithm in selecting 5% of the number of nodes as leaders, with low-rank updates for oracle acceleration. (Right) Solution obtained by the stochastic greedy algorithm has very little degradation as compared to the greedy algorithm for an Erdős-Rényi graph.

We introduce a notion of generalized power and energy-flow in dynamical networks applying the theory of vector Lyapunov functions. Moreover, we develop an algorithm, based on sum-of-squares programming, to estimate the energy-flows across polynomial networks via a comparison systems analysis. Energy-flows vary as per the initial conditions, allowing dynamic partitioning of the networks that best suits the operating conditions. We extended the algorithm to the analysis of networks with multi-timescales, such as power networks, using singular perturbation theory. To illustrate its versatility, we applied the algorithm to compute the energy-flow and obtain dynamic partitioning of a Lotka-Volterra population dynamic model and differential-algebraic power system models.

Finally, we extended the Koopman operator-based methods to the learning of the phase space of switching hybrid systems. The genetic toggle switch is formed in a synthetic bi-stable system by two repressible promoters arranged in a mutually inhibitory network. We proposed a phase space stitching method to construct the unified Koopman operator from the deep-Koopman operators for each stable state (on/off).

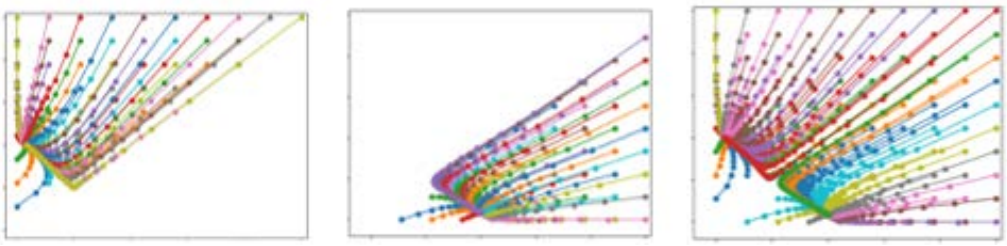

(Left and Center) Learned phase portrait of the individual invariant subsystems. (Right) Learned phase portrait of the entire phase space of a bistable toggle switch using deep Dynamic Mode Decomposition.

Development of High Energy Lithium Ion Sulfur Batteries

Dongping Lu
PN18044/3043

This project aims to demonstrate a new prototype lithium ion (Li-ion) sulfur battery technology and identify potential scientific and technical challenges to be addressed. This technology would accelerate battery application in large-scale energy storage by taking advantages of high-energy and low-cost sulfur cathodes, as well as long-cycle-life intercalation-based anodes.

Lithium-sulfur (Li-S) battery technology has the potential for high-scale energy storage by delivering two to three times higher energy at a much lower cost, compared to state-of-the-art Li-ion batteries. However, its deployment is hindered by the limited cycle life, which is caused by the unstable Li metal anodes. Replacement of the Li anode by using stable, intercalation-based compounds, such as graphite or alloy-based silicon, could circumvent the problems and, thus, extend cell cycle life with improved safety.

The objective of this project is to validate a new concept of high-energy Li-ion sulfur batteries and identify key challenges in developing such a high-energy and long-cycle battery technology.

Before deployment of experimental research, energy prediction of Li-ion sulfur battery system was performed based on a practical pouch cell configuration. To reach the system energy over 250 Wh/kg, the areal capacities over 6 mAh/cm^2 are required for both sulfur cathodes and graphite anodes, and the latter should be even higher for an optimal negative/positive capacity ratio. The project's efforts are focused on preparation and performance evaluation of high loading electrodes, development of compatible electrolytes, and understanding the scientific and technical challenges in the system integration.

One of the targets of the project is to identify the optimal graphite electrode composition and architecture and achieve extremely high areal capacity in the thick electrodes. The graphite electrodes with mass loading of 22 to 40 mg/cm^2 (corresponds to 8 to 14 mAh/cm^2) have been developed after optimizing material types and contents for graphite, carbon additives, and binders. Seven electrolytes composed of different solvents, additives, and combinations were prepared and screened by using the high loading graphite anodes and sulfur cathodes in Li half cells. Two electrolyte recipes were identified as suitable for Li-ion sulfur fuel-cell demonstration by considering cell cycling stability, viscosity, and ionic conductivity properties. Another focus of the project is to identify scientific or technical obstacles in adopting the proposed concept for practical applications. Li-ion sulfur cells have been successfully demonstrated by using relatively low loading graphite anodes (about 5 mg/cm^2). However, when the electrode loading is increased to a high level above 22 mg/cm^2, an accelerated capacity decay was usually observed.

Systematic study of electrochemical performance, X-ray powder diffraction, scanning electron microscopy, and *in situ* electrochemical impedance analysis indicates that gradual passivation of thick graphite electrodes is one of the dominants for the capacity decay. A thick solid electrolyte interphase (SEI) layer was found to form on the graphite anode upon cycling, which is due to polysulfide shuttle reactions and Li sulfide deposition. This thick SEI was believed to be responsible for the permeant Li loss, increased cell resistance, and rapid capacity fading in Li-ion sulfur batteries.

To minimize the passivation of graphite anodes from Li polysulfide/sulfide deposition, a proactive surface passivation approach was employed by coating a 2 nm thick Al_2O_3 layer on the graphite electrodes by atomic layer deposition method. Post-cycling analysis revealed that the Al_2O_3 passivation layer reduced the polysulfide shuttle reactions and decreased the polysulfide deposition on the graphite anode. In addition, a roll-to-roll graphite electrode lithiation approach was also proposed and employed. Thin Li foils were attached onto double-side coated graphite electrodes to obtain such Li/graphite anode

assemblies, which were used directly as anodes for full cell fabrication. This approach enables a simple and scalable graphite lithiation process. The residual of Li foil and the formed SEI on the Li surface help to mitigate the graphite passivation and, thus, extend cell cycle life.

Grid Architecture Analysis

Renke Huang
PN18033/3032

Currently existing methodologies for evaluating grid designs and grid architectures either model too much or too little about the interactions among different physical systems. This project developed an analytical evaluation tool to provide quantitative structural metrics for analytical comparison of multi-network grid designs and architectures, which do not exist now.

Currently existing methodologies for evaluating grid designs and grid architectures either model too much or too little about the interactions among different physical systems such as power networks, communication networks, and control networks. One of the existing approaches uses co-simulation. However, evaluation and validation of complex architectures, especially those that involve multiple interacting structures, is difficult in the early stages, because co-simulations require great amounts of detail that are not available at that stage, and any missing or incorrect design details can spoil the simulation.

On the other hand, some evaluations are done with spreadsheet models, which can mask unrealistic assumptions and overlook important bottlenecks. This project developed an analytical evaluation tool for different grid designs and grid architectures, which uses graph theory, modeling, and analysis to investigate the interactions among multiple physical systems. The developed tool provides quantitative structural metrics for analytical comparison of multi-network grid designs and architectures that do not exist now.

The novelty of this project comes from hitting the “sweet spot” between too much and too little detail, where there are no alternatives to support early analytical evaluation of grid designs and grid architectures. The method and tool developed provide fast modeling at the level of detail typically available in early stages of such work, combined with analytical measures that can provide real insight into structural choices that are the essence of architectural specification. The availability of this combination fills a gap that previously existed in architecture development work and was addressed only via *ad hoc* and intuitive approaches that often lead to mistakes and/or multiple time-consuming co-simulations that were only limited to specific models and use cases. The developed graph-based approach is more general in producing analytical structure metrics, in turn leading to greater insight and to opportunities for multi-system optimization.

In this project, we developed a conversion tool that builds graphic models of transmission power grids and distribution feeders from existing detailed models, as well as a synthetic tool that could build graphic models for communication and control networks from heuristics informed by the grid architecture work. Based on the graphic models we built, graph-oriented algorithms and solvers were developed to provide quantitative metrics for grid architecture and compare alternatives. The metrics include 1) algebraic connectivity/vertex connectivity for connectedness and synchronizability, 2) isoperimetric number and critical cut edges for bottlenecking, 3) endpoint scalability, and 4) application scalability.

Identified Critical Cutting Edges of power grids and communication network.

Furthermore, we developed two use cases to demonstrate the capabilities of the tools and algorithms we developed in this project. In the first use case, we synthetized the wide-area communication networks on top of a 700-bus

transmission power grid, computed the isoperimetric numbers for the networks, and found the critical cut edges to evaluate the quality and vulnerability of the networks. In the second case, we synthetized the wireless communication networks for collecting smart meter data on top of a distribution feeder, computed the graphic metrics for the networks, and found the vulnerable nodes to evaluate the networks' structural resilience to cyber-attack. Both the two use cases demonstrated the validity and effectiveness of the developed tools and method.

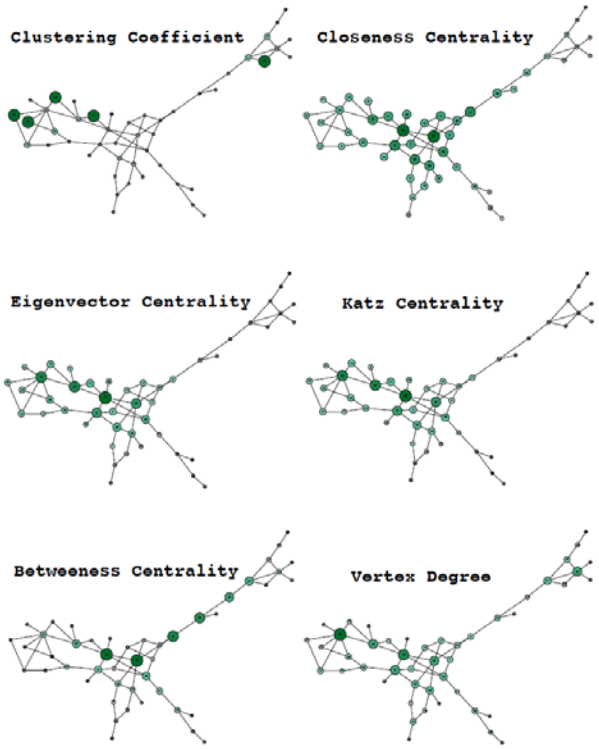

Vulnerable nodes identified based on different quantitative graphic metrics.

Integrated Control Testing Under Complexity

Jacob Hansen
PN17057/2947

This project investigates prototype-stage advanced control methods to understand their behaviors within large-scale interconnected energy systems via simulation and hardware-in-the-loop (HIL) experiments of unprecedented scale and complexity.

Power and energy systems are undergoing substantial changes, from highly predictable systems with central generation to systems with high penetrations of non-dispatchable, variable, renewable energy resources, increasing the overall system uncertainty and decreasing the controllability. These changes have necessitated the deployment of increasingly advanced control schemes to balance supply and demand, both short- and long-term, while maintaining operational costs at a competitive level. Such advanced control schemes are often designed using simplified models of the power system without considering the full complexity present in interconnected power systems, how the solution might work within the context of legacy control systems, or the structural position within a larger architectural framework. Neglecting this complexity makes these control schemes highly susceptible to unforeseen and potentially undesirable effects on the energy system as a whole. At low penetration rates of renewable generation, these assumptions are quite practical; however, envisioning a more active and distributed grid of the future requires examining the interactive nature of high renewable penetration cases in greater detail.

Previous efforts have developed advanced control methods targeted towards the power grid. The resulting algorithms have been tested on small test systems with assumed boundary conditions, showing tremendous performance improvement according to the objective of the control system. However, to rigorously assess the control system, this project evaluates the same control system using PNNL's testbed. This testbed is capable of simulating large-scale power systems using co-simulation capabilities to capture interactions in the power grid from the distribution system to bulk power operations.

In FY 2017, this project evaluated two control systems using the testbed. The first control system focused on distributed control, taking a transactive control approach consisting of price-responsive residential heating and air conditioning systems that react to changes in the wholesale locational marginal price (LMP) of electricity. The LMP was assumed to be a boundary condition and the wholesale markets were not modeled. In previous demonstration efforts, this boundary condition was removed, and a simple transmission system was modeled to create a co-simulation of transmission and distribution. In doing so, price oscillations were observed in cases with high penetrations of flexible loads. To address these price oscillations, this project added a new control layer that collects distribution system flexibility information and communicates it to the wholesale market. This allows the wholesale market to dispatch the flexible load and eliminate the aforementioned price oscillations. Furthermore, this project also expanded the complexity and scale of the systems for which the co-simulation capability could evaluate control systems. The current evaluation can simulate an interconnect-scale power system (e.g., the Western Interconnection, which serves the western United States) with highly detailed distribution system load modeling along with appropriate existing control systems to capture more realistic power system operations.

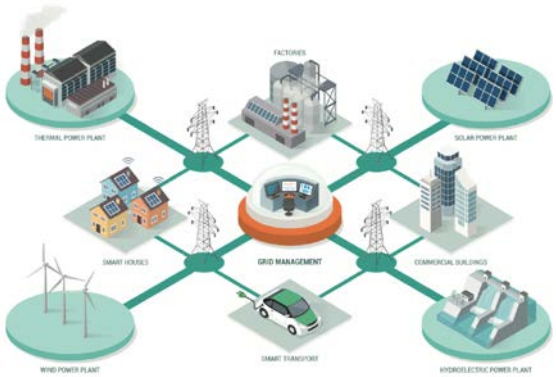

Smart energy infrastructure illustration.

The second control method evaluated during FY 2017 was focused on the impacts of communication networks on the performance of distributed control. The method uses a distributed consensus algorithm that is robust to communication imperfections. The algorithm was tested using simple models in a single simulator to represent the distributed control system. As part of this project, a distributed agent co-simulation framework was developed with every agent modeled as a separate simulator. This enables evaluating the control algorithm in a truly distributed manner. Because these are actual distributed simulators, they can even be installed in separate pieces of computing hardware. Using the control theory from an earlier project, this distributed co-simulation framework was used to solve the day-ahead economic dispatch problem. Individual agents communicated with each other and all messages between agents were routed through an advanced discrete network simulator, ns-3. Short and long network delays and both power line and fiber optic communication infrastructures were considered. These technologies were used to evaluate the impacts of communication imperfections on the control system performance. Simulation studies showed that communication imperfections do impact the time to solution, but overall, the control system can converge to correct solutions when ample communication paths are present between the distributed agents.

In FY 2018, this project focused on two major tasks 1) evaluating a PNNL-developed hierarchical control structure that incorporates transactive energy techniques to engage end-use load in the wholesale real-time energy market and 2) developing a web-based dashboard for deploying transactive control on buildings. The evaluation of the hierarchical control structure highlighted the ability of the architecture to integrate and control the inherent flexibility in loads in a stable manner, while honoring customer preferences and realizing benefits for the system as a whole. In order to evaluate the proposed control system, the project used the testbed that supports simultaneous experimentation on physical and virtual assets. This testbed facilitates data exchange between transmission and distribution systems simulators, while allowing control algorithms to be implemented at each level of the hierarchical architecture. This work evaluated the performance of the proposed transactive energy control algorithm on a close-to-real-life power system scale model that incorporates tens of thousands of individually simulated distribution systems with millions of controllable loads.

The web-based dashboard developed for deploying transactive control on buildings enables users to 1) adjust the operation status and parameters of the transactive control in runtime and 2) view how buildings respond to the transactive control in real time. It facilitates deployment by encapsulating technical details such that no technical background information is needed for users. The dashboard consists of three major components: a Docker, a Cloud Database, and a remote PC. Docker is a software container that operates different Python functions. Among those Python functions, the web framework coordinates the operation of other functions based on the information received from users. It contains an interface to receive http requests from users via web browsers.

The http requests can be divided into two categories, the commands for transactive control and the data querying for the building operation data. If receiving the commands for transactive control, the web Framework calls the Socket Client function to convey commands through the socket connection to the VOLTTRON™ instance that is running in a remoted PC. The commands are then implemented by the corresponding transactive control agents under the VOLTTRON instance. If the web framework receives the command for querying data, it calls the Database Query function to send the query request to the Cloud Database, which receives the streaming data from the VOLTTRON instance in the remote PC.

Once the queried data is collected, it is forwarded to the Visualization function to generate interactive plots. The plots are then embedded into an html file by the web framework and sent back to users' web browsers where the html file is translated into readable web pages. This dashboard expands the existing functionalities to allow interactive simulation, so the users can see the impact of changing controller parameters immediately.

Integrated Models for Energy Resiliency Planning

Vikas Chandan
PN18036/3035

This project seeks to develop an integrated resilience analysis system for buildings, campuses/installations, and communities by coupling buildings, power systems, renewables, and storage models.

Resilience has become high priority for the federal sector, state, and local governments and is moving into the commercial sector. Resilience is the ability of a system to prepare for and adapt to changing conditions and withstand and recover rapidly from disruptions. As resilience begins to take center stage, sophisticated tools and mechanisms are needed to accurately evaluate various elements of resilience in a connected way.

While several tools address specific pieces of the resilience puzzle, a single, consolidated tool that integrates available data, models, and tools into a comprehensive analysis framework and optimizes the solution sets has not been developed yet. The objective of this research project is to address this gap by developing an integrated analysis system for buildings and communities by coupling buildings, power systems, renewables, and storage modeling. The resulting framework will enable a seamless evaluation of the costs and benefits of a suite of measures, including energy efficiency and conservation, renewables, battery storage, and microgrids in the context of energy resilience.

We developed a proof of concept integrated framework that includes modeling and optimization components previously developed by PNNL and others: photovoltaic model, battery model, diesel generator model, building load model, optimal system sizing module, and dispatch optimization module. The integrated framework provides the ability to optimize component sizes, generator, and battery dispatch schedules, and building loads to minimize capital and operational costs while achieving resilience objectives.

We analyzed two specific test sites and developed representative scenarios reflective of resilience needs: PNNL campus in Richland, Washington, and Army Reserve site in Maui, Hawaii. Next, we developed a proof of concept demonstration by applying the integrated framework to the above scenarios. We successfully demonstrated that tools not originally designed for resilience can be integrated together for resilience analysis in a modular fashion.

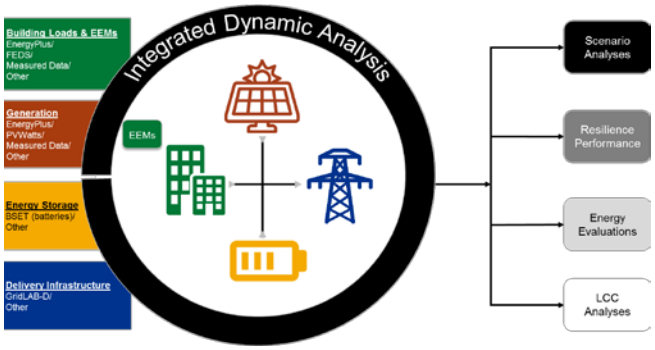

Vision of the integrated framework.

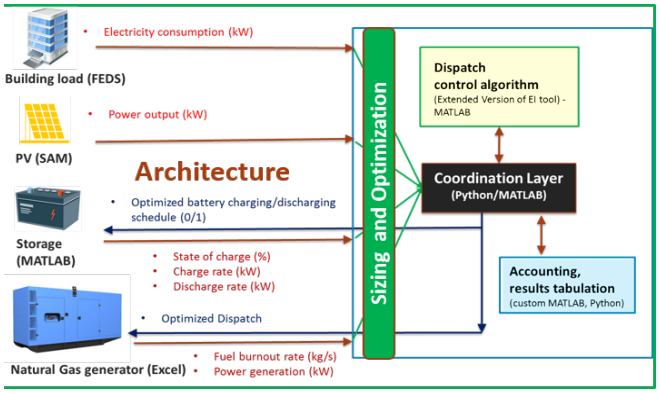

Proof of concept integration framework.

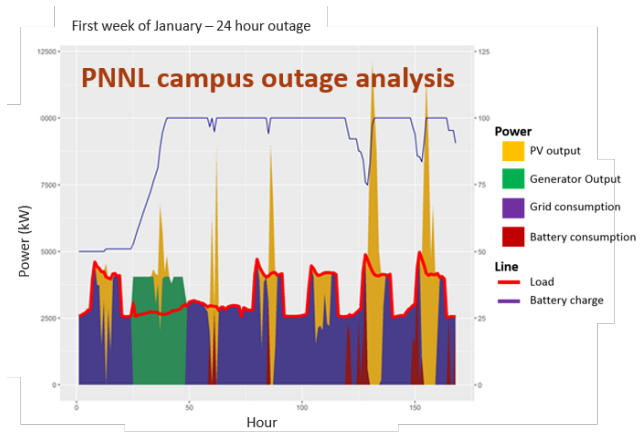

Simulation results for PNNL campus outage.

Nonflammable Electrolytes for Lithium-Ion Batteries

Wu Xu
PN18068/3067

Development of higher energy density lithium (Li)-ion batteries for electric vehicles (EVs) requires much higher safety than state-of-the-art (SOA) Li-ion batteries. Utilization of nonflammable electrolytes developed in this project will enable the SOA Li-ion batteries to meet the safety requirements for large-scale applications of plug-in hybrid EVs and pure EVs.

Normally the safety problems of SOA Li-ion batteries are mainly related to the high flammability of nonaqueous electrolytes used in the batteries. The development of nonflammable electrolytes (NFEs) for SOA Li-ion batteries is, so far, not very successful. The completely NFEs will seriously deteriorate other battery performances such as capacity and cycle life. The SOA Li-ion batteries are still using flammable electrolytes or low flammability electrolytes with slight sacrifice in other electrochemical performances. Therefore, there is an urgent need to develop NFEs that can maintain the same battery performances as the SOA Li-ion electrolytes do. Recently, we developed flammable and nonflammable localized high concentration electrolytes (LHCEs) for stable cycling of high voltage Li metal batteries, but such LHCEs have some compatibility issues with the graphite anode used in SOA Li-ion batteries. We propose to modify the nonflammable LHCEs so they are compatible with graphite anode. Through the research and development in this project, we expect to achieve at least one modified NFE formulation to maintain or outperform the same long-term cycling stability as the conventional electrolyte does.

In this project, we developed two low flammability electrolytes and five NFEs based on LHCEs for Li-ion batteries with graphite (Gr) anode and comparatively evaluated their cycling stability with two control electrolytes; one is a conventional electrolyte (E-control-1) and another is a regular NFE (E-control-2) prepared by adding a nonflammable solvent into the conventional electrolyte. The cathode materials are conventional ones, such as $LiNi_{0.80}Co_{0.15}Al_{0.05}O_2$, $LiCoO_2$, $LiNi_{1/3}Mn_{1/3}Co_{1/3}O_2$, and $LiNi_{0.8}Mn_{0.1}Co_{0.1}O_2$ (NMC811), respectively. The areal capacity loading for the anode was about 1.6 to 1.8 mAh cm^{-2}, while the cathode was 1.5 to 1.6 mAh cm^{-2}. The electrolytes were tested in coin cells in the voltage range of 2.8 to 4.3 V by using the standard protocol (i.e., two formation cycles at C/20 or C/10 rate) followed by cycling at C/5 for charge and discharge rate or C/2 charge and 1C discharge, where 1C is the current density related to the cathode areal loading.

In the studied four Gr||cathode cell systems, most developed LHCE-based NFEs show similar long-term cycling stability, like the conventional Li-ion electrolyte (E-control-1), and some even outperform the control electrolyte in terms of capacity, capacity retention, and cycle life. These LHCE-based NFEs definitely have much higher capacity and better cycling stability than the regular NFE by simply adding nonflammable solvent into the conventional electrolyte.

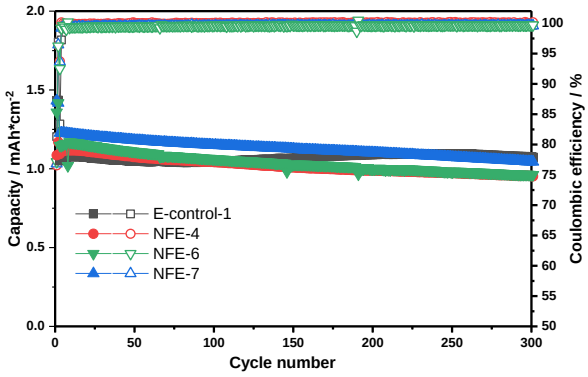

Cycling stability and efficiency of Gr||NMC811 coin cells with different electrolytes at the charge rate of C/2 and the discharge rate of 1C after two formation cycles at C/20 in the voltage range of 2.8–4.3 V at 30°C.

In addition, we also developed two LHCE-based NFEs for silicon anode-based Li-ion batteries and two for hard carbon-based sodium-ion batteries. These NFEs show much better cell performances than the control electrolytes (which are flammable) in these battery systems.

Reducing Cold-start Emissions

Kenneth G. Rappé
PN18073/3072

The reduction of emissions associated with cold-start has become a focal point for achieving ultra-low legislative standards and reaching CAFÉ targets, as these emissions can represent up to 95% of the total released from a vehicle. This work is focused on continuing the development and optimization of a material that can passively add heat directly to aftertreatment catalysts, thereby heating them up quicker, shortening the cold-start period, and reducing the associated emissions.

Current aftertreatment catalysts provide low activity at 200°C or less that fall short of the emission conversion target set by the U.S. Department of Energy and industry. This work pursues decreased cold-start emissions by continuing the development of a class of adsorbents that can passively heat aftertreatment catalysts directly by exothermic CO_2 capture, resulting in faster catalyst light-off. By leveraging the ability of higher temperature exhaust to drive endothermic CO_2 release and enable reversible operation, these materials can facilitate a strategy of exhaust energy recovery through the coupling of tunable and reversible exothermic and endothermic reactions. If successfully deployed, these materials would represent a paradigm shift in the ability to decrease cold start emissions.

Originally based on more than 3 years of previous PNNL work, this project builds upon initial development efforts focused on bulk MgO adsorbent coupled with a ternary or quaternary Na/K/Li nitrate/nitrite salt system as a eutectic promotor. The initial work demonstrated the ability to provide heat strategically to a catalyst to shorten the “effective” cold-start duration experienced. This was accomplished by coupling the highly exothermic CO_2 capture of the MgO sorbent with the tunable temperature properties associated with softening of the eutectic promotor. However, stable cyclic CO_2 capture (i.e., sorbent durability) remained elusive.

In this project, we identified that the previously observed challenges associated with sorbent durability included both capture phase morphological degradation, as well as eutectic promotor chemical changes. Regarding the former, we identified that surface area of the active MgO capture phase was significantly reduced following CO_2 capture, thereby decreasing the density of active triple-phase (gas-sorbent-eutectic) boundary sites necessary for CO_2 capture. Regarding the latter, we discovered that the $NaNO_2$ component in the ternary and quaternary eutectic promotor was decomposing. This was originally hypothesized based on literature information and subsequently corroborated with X-ray diffraction.

In pursuit of the former challenge, the effect of active-phase sorbent composition was evaluated for enhanced CO_2 adsorption and material stability. The result of this work is the development of a more stable active phase consisting of MgO and Na_2CO_3 that together form a $Na_2Mg(CO_3)_2$ double salt upon CO_2 capture. Studies showed that the presence of Na_2CO_3 facilitated sorbent stability and observed that a MgO:Na_2CO_3 weight ratio of 50:50 gave optimum CO_2 capacity and stability properties.

In pursuit of the latter challenge, evaluation of eutectic chemistry and content showed that 10 wt% $LiKNO_3$ gave the best combination of CO_2 capture performance and stability. In summary, the study showed that three different components were necessary for optimum stability and performance, including 45 wt% MgO, 45 wt% Na_2CO_3, and 10 wt% $LiKNO_3$.

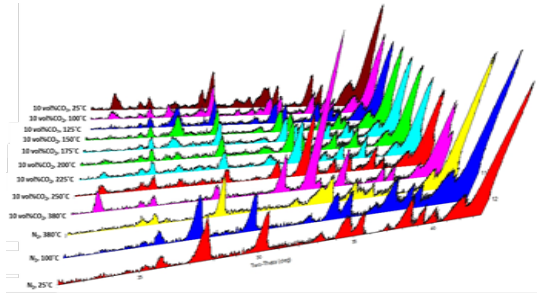

In situ X-ray diffraction micrographs of 20 wt% $LiKNO_3$ on MgO:Na_2CO_3 during CO_2 adsorption as a function of reaction temperature, showing the transition through an active capture phase and its regeneration.

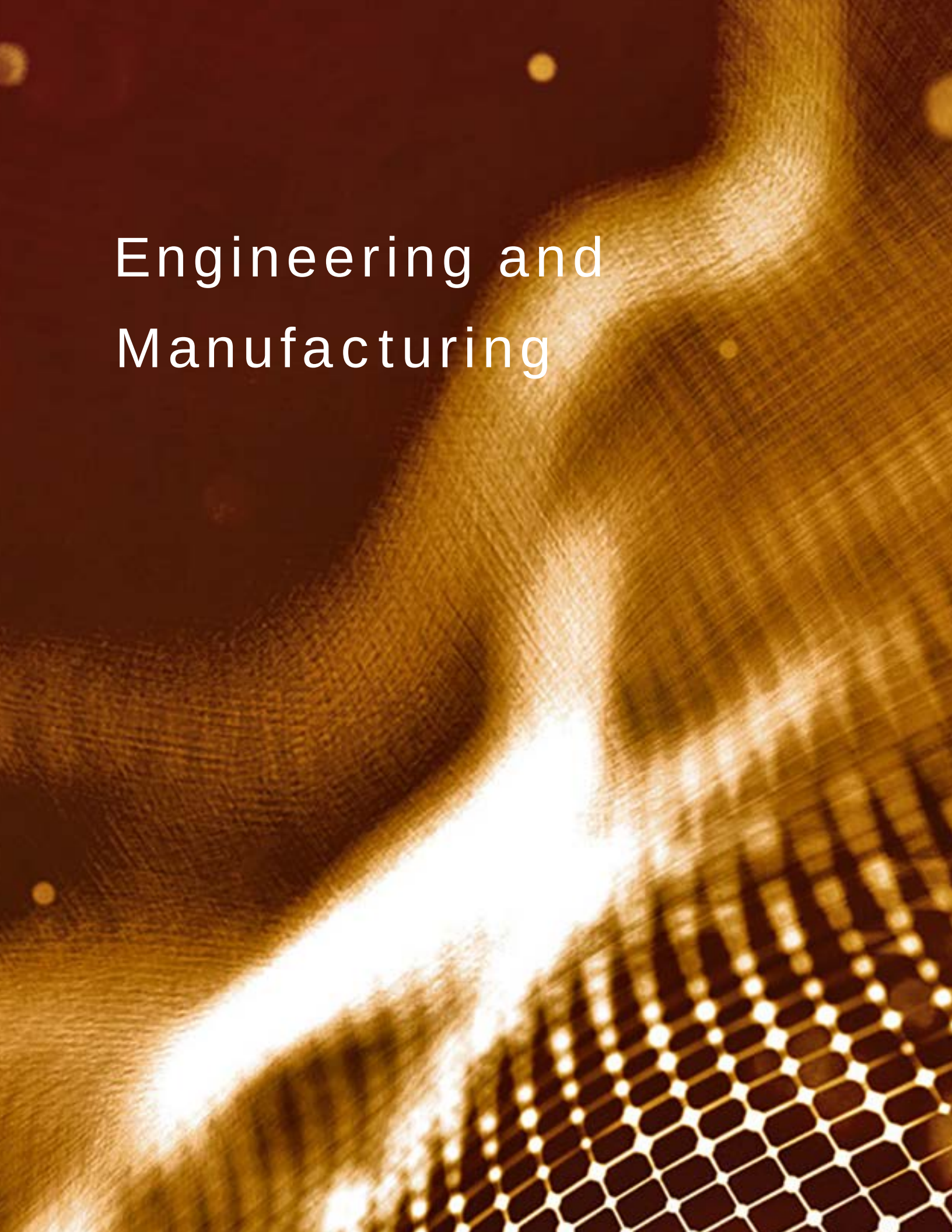
Engineering and
Manufacturing

Bulk Thermally Stable Nanocomposite Processing

Scott A. Whalen
PN16022/2799

In this project, we are developing the underlying science and engineering processes for fabricating bulk materials with thermally stable nanostructured features. Our research in far-from-equilibrium shear processing is envisioned to enable fabrication of industrial-scale products, with game-changing material properties that, before now, have only been achieved in powder, flake, thin-film, or very small specimens.

The work performed on Shear Assisted Processing and Extrusion (ShAPE™) was publicized through a PNNL press release and picked up by approximately 50 news outlets, including *R&D Magazine*, *ASM International*, *AZO Materials*, *The Engineer*, *IOM3*, and many others.

As a result of this press release, numerous companies contacted PNNL to inquire about the possibility of having their material processed by ShAPE. Three companies sent material in various forms including aluminum-transition metals powders, nanostructured aluminum powder, magnesium billets, and even pure rhodium billets. These materials, minus rhodium, were all processed with great success and returned to the companies for characterization. In one case, the mechanical properties were so impressive that SCM Metals partnered with PNNL on a DOE Technology Commercialization Fund proposal that was awarded through the DOE Advanced Manufacturing Office. This work will scale up extrusions to a 1.0-inch diameter bar and will focus on energy savings associated with bypassing conventional powder metallurgy processing steps.

A key technical accomplishment in FY 2018 was the successful processing of SCM Metal's gas-atomized Al-12.4TM powder directly into extruded rods using ShAPE.

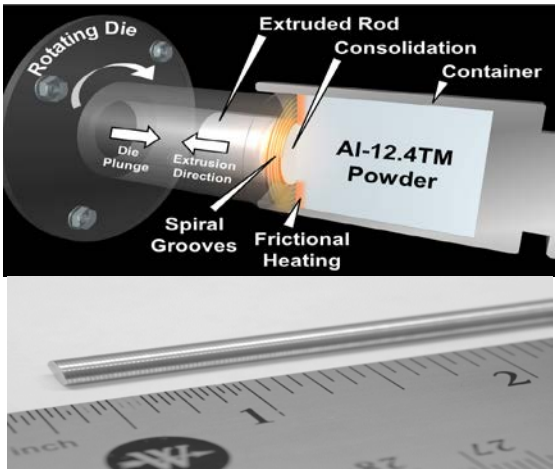

Schematic of the process and tooling (left), along with an example of a 5-mm-diameter extruded rod (right).

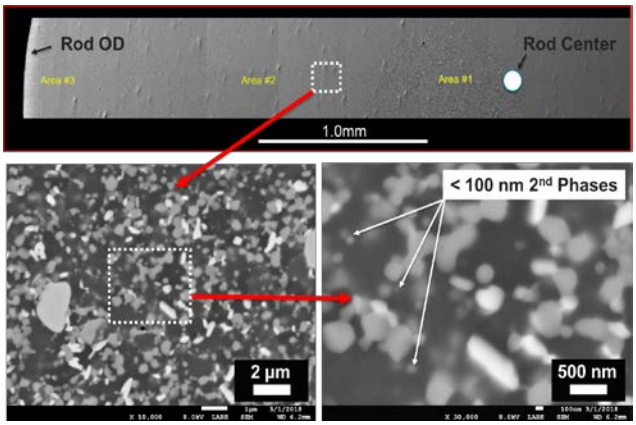

Al-12.4TM powder was consolidated into fully densified (top), with an extrusion force that was 50 times lower than conventional methods. Due to the lower process temperatures of ShAPE, nanostructured features within the powders were retained in the extrusion (bottom).

Mechanical test results gave an ultimate tensile strength (UTS) and yield strength (YS) of 480 MPA and 415 MPa, respectively, which are comparable to that obtained by conventional extrusion. However, the 16% elongation was double that obtained by SCM using conventional extrusion. High temperature testing at 200°C and 300°C gave a UTS/YS/Elongation of 326 MPa/316 MPa/8.6% and 240 MPa/238 MPa/9.4%, respectively.

Microchannel Reactive Distillation: Alcohol-to-Jet Application

Robert A. Dagle
PN18065/3064

We aim to develop the proof-of-concept principles for a new reactive separation process technology that offers energy savings, process intensification, and compact modular reactors, ultimately providing reductions to both capital and operating costs that can be applied to a host of energy applications

Here we are developing microchannel reactive distillation (MCRD) capability for alcohol-to-jet application: combining ethanol/water separation and ethanol dehydration in one-unit operation. Ethanol is first distilled into vapor phase, converted to ethylene and water, and then the water co-product is condensed to shift reaction equilibrium.

Process intensification is achieved through rapid mass transfer—ethanol stripping from thin wicks—leading to lower residence time and improved separation efficiency.

Energy savings are realized with integration of unit operations. For example, heat of condensing water can offset vaporizing ethanol. Furthermore, the dehydration reaction equilibrium shifts towards completion by immediate removal of the water byproduct upon formation, while maintaining aqueous feedstock in the condensed phase.

The operation enables low temperatures (less than 250°C) and mild pressures (less than 500 psig) compatible with conditions required for downstream ethylene oligomerization. This effort seeks to extend our microchannel distillation technology, enabling a new reactive distillation platform with integration of catalytic material.

Wicks (about 4 inches by 2 inches) used for transport of liquid ethanol were assembled from stainless steel shims, produced using photo-etching to cut a specified pattern, and diffusion bonded onto stainless steel screen. Holes were cut into the liquid headers to allow for liquid flow into the wick. Produced wicks were inserted into a previously constructed clam-shell device and used here for ethanol/water processing. Siphon height tests were performed in order to optimize MCRD placement. The test system balance of plant, including liquid effluent collection reservoirs, inlet/exit gas lines, and associated equipment was installed.

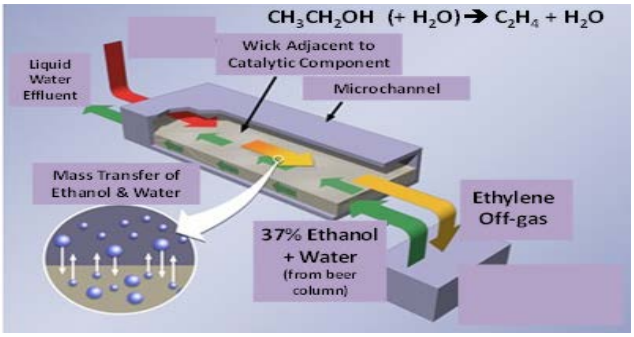

MCRD unit with catalyst loaded into vapor channel adjacent to the liquid wick.

Liquid and gas flows were varied to determine a suitable range of flow rates for the system. Separation tests were conducted with 40 wt% ethanol in H_2O feed at 100 to 210°C and 180 to 700 psig; approximate range of conditions targeted for simultaneous ethanol/water separation and conversion. With the system yet unoptimized, approximately two stages of ethanol-water separation were demonstrated with this device.

Catalyst performance evaluations were carried out in a separate flow-through reactor to identify a suitable ethanol dehydration catalyst appropriate for use under the conditions of operation required for MCRD processing. Low temperatures and high pressures are required; however, these conditions also restrict conversion for the equilibrium-limited ethanol dehydration reaction. Additionally, undesirable diethyl ether formation is problematic. Nine different solid acid catalysts were assessed, and a ZSM-5 (Si/Al 23) catalyst was identified for further parametric evaluation. Temperature, pressure, and space velocity studies were performed in order to understand operational characteristics.

The ZSM-5 (Si/Al 23) catalyst was loaded into the vapor channel port adjacent to the liquid wick. Demonstration of MCRD operation was initiated, and evidence for both ethanol/water separation and ethanol dehydration reaction was observed.

Non-signalized Intersection Control – a Collaborative Control for Traffic Flow Systems Composed of Connected Autonomous Vehicles (CAVs)

Hong Wang
PN18042/3041

This project has developed a novel framework for how the active collaborative control can be used to control the traffic flows near intersections without traffic signal infrastructure for CAVs. This will establish a new research area in transportation control perspective: to develop economical traffic flow systems for smart cities.

With the potential for increased penetration of CAVs, intersectional signal control faces new challenges in terms of its operation and implementation. One possibility is to fully make use of the communication capabilities of CAVs so that intersectional signal control can be realized by CAVs alone; this leads to non-signalized intersection operation for traffic networks where there is no need to implement expensive signal controls at intersections.

In this project, a full-state model of the CAVs approaching intersections has been developed by assuming that each concerned CAV has already been controlled autonomously by their own system. This leads to closed-loop linear dynamics for each CAV, where the sept-points of each CAV are just their position and speed. Using such a full state dynamic model, control requirements are formulated as an optimal control problem, so that each CAV is controlled to achieve its maximum allowed speed with safe distance between them. As a result, a linear quadratic control strategy is obtained. Some examples have been given, as well, to demonstrate the proposed algorithm together with the discussions on the future directions.

If each approaching CAV is taken to a non-signalized intersection as a subsystem (i.e., an autonomous agent), then these subsystems should work together in a collaborative way to maximize the throughput of traffic. We consider an N number of CAVs approaching a non-signalized intersection and assume that the dynamics of the *i*th CAV is a self-closed-loop system where position and speed are denoted in a two-dimensional plane:

$$x_i = \begin{bmatrix} p_i \\ q_i \end{bmatrix}; \frac{dx_i}{dt} = \dot{x}_i = \begin{bmatrix} \frac{dp_i}{dt} \\ \frac{dq_i}{dt} \end{bmatrix}; (i = 1, 2, \dots, N) \quad (1)$$

where p_i stands for the longitude movement and q_i represents the latitude movement (i.e., lane changes) of the *i*th CAV. In this case, the longitude movement is for the direction of the vehicle moving forward and the latitude movement is for lane changes.

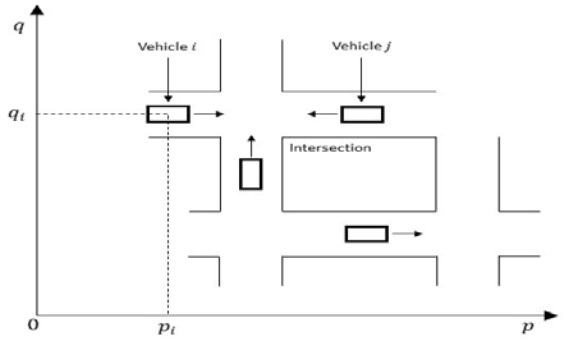

A simple intersection with CAVs.

Position and speed are the two groups of state variables defined as the following vector.

$$X_i = \begin{bmatrix} x_i \\ \dot{x}_i \end{bmatrix} \in R^4; \quad (i = 1, 2, \dots, N) \quad (2)$$

In this regard, the dynamics of the *i*th CAV (the *i*th agent or subsystem) can be expressed in the following form

$$\dot{X}_i = A_i X_i + B_i r_i + \sum_{i \neq j}^{N} C_{ij} X_j \quad (3)$$

where $\{A_i, B_i\}$ are the assumed known parameter matrices that represent the dynamics of the concerned CAV of appropriate dimensions, C_{ij} are the communication coefficient matrices that represent communication capabilities between the *i*th and the *j*th CAVs. If there is no communication between the *i*th and the *j*th CAVs, then $C_{ij} = 0$. In the equation, r_i is the set-point of the position trajectory of the *i*th CAV.

We need to select the set-points for each CAV in the group to achieve the following multi-objective constrained optimization.

$$\max_r \dot{x}_i; \quad (i = 1, 2, \dots, N)$$

s.t.

$$\|x_i - x_j\| > \delta; \quad i \neq j \text{ (Safe distance)}$$

$$\|\dot{x}_i\| < M; (i = 1, 2, \dots, N) \text{ (Speed constraints)} \quad (4)$$

As a result, to ensure an optimal passing through of all the CAVs near the concerned intersection with a guaranteed safety margin, the set-points must be selected for each vehicle to solve the following optimization problem.

$$\min_r J = \min_r \int_{T_1}^{T_2} [(\widetilde{M} - Hv)^T (\widetilde{M} - Hv) + \rho \dot{r}^2] dt \quad (5)$$

Subjected to the constraints, where $\rho > 0$ is a pre-specified weighting coefficient for energy consumption penalty, will lead to the following

$$r_{j \neq i_*} = r^*_{j \neq i_*} + \Delta r_{j \neq i_*}, \quad (6)$$

where the incremental change of set-point represented as $\Delta r_{j \neq i_*}$ is given by

$$\Delta r_{j \neq i_*} = \sum_{j \neq i_*} \theta_j X_j \quad (7)$$

where θ_j is an optimal fixed feedback gain matrix.

When fault occurs in one of the CAVs, for example sensor or actuator faults, then the other healthy CAVs should work together in a collaborative, fault-tolerant way to maximize their throughput of traffic. This belongs to a collaborative, fault-tolerant control for multi-agent systems subjected to various constraints, where modeling, fault diagnosis, and collaborative, fault-tolerant control should be carried out. In terms of fault diagnosis, we have the following adaptive diagnostic observer constructed for each CAV.

$$\dot{\hat{X}}_i = A_i \hat{X}_i + B_i r_i + \sum_{i \neq j}^{N} C_{ij} \hat{X}_j + E_i \hat{f}_i + L(x_i - \hat{x}_i) \quad (8)$$

where $\hat{X}_i$ is the estimate of X_i and $\hat{f}_i$ is the diagnosed (i.e., estimated) result of fault f_i, and L is a gain matrix. Define the state estimate error and the fault estimation error as

$$e_i = \hat{X}_i - X_i$$
$$\tilde{f}_i = \hat{f}_i - f_i \quad (9)$$

and then the following diagnosis of fault can be obtained.

$$\frac{d\hat{f}_i}{dt} = -(\hat{x}_i - x_i) \quad (10)$$

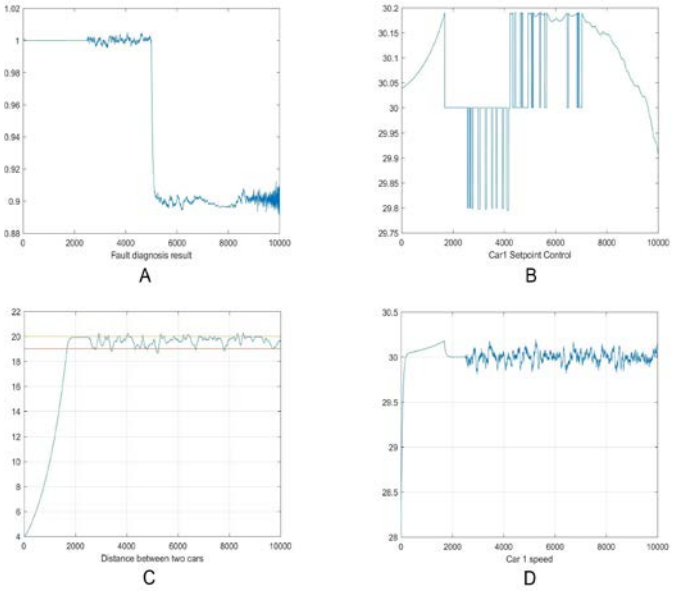

Simulation results for A) fault diagnosis, B) set-point control, C) distance, and D) max speed.

We have developed modeling and control for non-signalized intersections for 100% penetration of CAVs. Also, fault-tolerant control strategies have been obtained. The project has shown that regardless of faults occurring or not, the CAVs concerned can be made to pass smoothly and safely through the non-signalized intersection with maximum speed and minimized energy consumption. Future works involve control of multiple networked intersections and fault tolerant control at intersectional level.

Reactor and Process Design

Robert S. Weber
PN17023/2913

We are inventing and characterizing new chemical reactors that can convert regional- and community-scale quantities of waste into fuel or chemicals. The reactors must be able to deal with a wide range of feedstocks, they must be inherently safe, and they should not rely on external facilities for co-reactants or heat rejection and supply.

We have shown that hydrothermal liquefaction can treat a wide range of feedstocks and can produce a bio-oil that required much less upgrading than other ways of deconstructing biomass. We determined early that there was value in exploring the use of electrochemical processes for the further conversions needed to transform the bio-oil from hydrothermal liquefaction into fuel or higher value chemicals.

Examples from our own work and from the literature showed that electrochemical reduction offered adequate reaction rates and at least some of the necessary generality. In addition, an electrochemical reactor necessarily both oxidizes (removes electrons) on one side of the reactor and reduces (adds electrons) on the other side. Therefore, the two compartments could, in principle, be coupled to upgrade the bio-oil and polish the water that was employed as a reactant and a carrier in the upstream hydrothermal liquefaction.

This project was designed to devise reactors that could perform the required electrocatalysis by providing effective contact between the oil-water emulsions, the solid catalysts, and the electrode surfaces. We also worked to develop technical and economic models that would help focus on research that could address the most important remaining questions.

We fabricated a third, larger reactor to permit measuring transport rates and kinetics rates at a scale that could be readily numbered up to contend with pilot-scale deployment. We now have a set of reactors extending from bench to production scales, along with the quantitative models that will permit us to accurately estimate the performance and economics of these reactors.

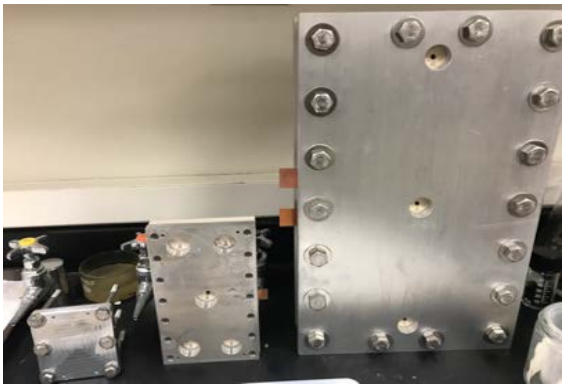

Three scales of reactors now available.

We developed a new way to count redox sites in supported electrocatalysts, which uses a gentle surface oxidation followed by a quantitative electrochemical reduction. The method is both sensitive and accurate: its results agree with other, *ex situ* estimations of the number of available redox sites.

Finally, we also refined a techno-economic model, which indicates that an electrolysis reactor should cost only about 15 to 25% of the total target cost of a waste-to-energy system that could handle the envisaged 1 to 100 barrels of oil per day.

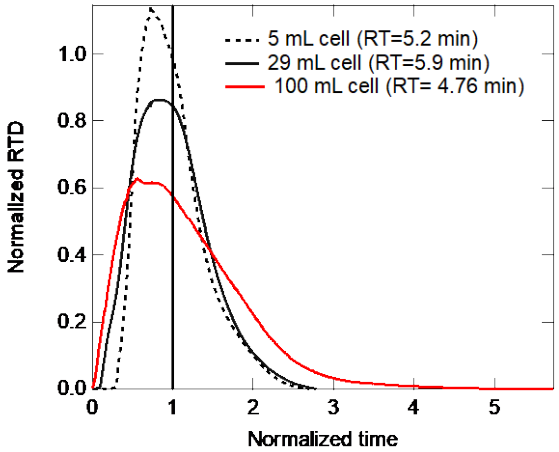

Residence time distributions show that the reactors have similar rheology.

Scalable Processing of Nanostructured Materials

Nicole R. Overman
PN16014/2791

We have developed novel and scalable processing methods for fabrication of unique structural and magnetic nanocomposites. This work was performed in to advance high-throughput manufacturing technologies and develop improved lightweight structural alloys and soft-magnetic materials.

Prior research on far-from-equilibrium alloy development has revealed several key factors that can have profound effects on improving material properties such as strength, toughness, corrosion resistance, and in some cases, magnetic properties. The basis for these advances has relied heavily on microstructural control and refinement. The underlying science behind them boils down to an ability to impart maximum disorder into the alloy at a microscopic level. The difficulty with this approach is in stabilizing the dis-ordered or far-from-equilibrium material enough so that it can be retained despite extreme environments encountered during processing and in service.

The key goals of this project are, first, to provide material for consolidation testing and, second, to understand and identify key processing parameters that can be exploited to produce and homogenize novel precursor materials on the nano-scale level. Processing regimes under investigation targeted two primary fabrication approaches: melt spinning and ball milling. Using this multi-faceted approach, we were able to take advantage of both thermodynamic and kinetic effects to produce precursor materials for consolidation that exhibit novel alloy compositions with enhanced homogeneity, processability, and thermal stability. Our approach focused on optimizing structural refinement through systematic evaluation of processing parameters for both these methods.

Significant progress was made in the key material systems targeted. Demonstrator alloys were identified and fabricated based on their ability to serve as game-changing material systems. Multiple crystal structures were incorporated to strategically align with the work of sister projects. Three Al-Mg based binary alloys were studied, with emphasis on thermal stability. For ShAPE™ process development, magnesium-based alloy AZ91 was produced and characterized. Last, Fe-Si (3 to 9 wt%) materials were also processed to evaluate magnetic properties. AZ91 and Fe-Si alloys were fabricated using melt spinning.

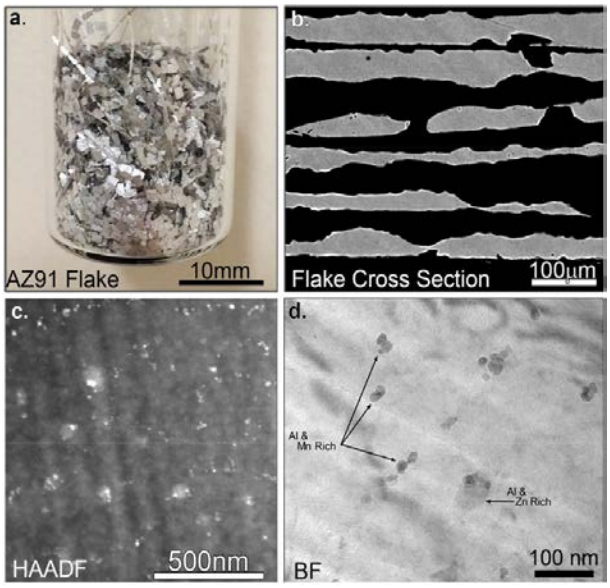

As produced, AZ91 RS flake material is shown in (a), along with a cross-sectional view of the flake via scanning electron microscope backscatter imaging (b); transmission electron microscopy images (c, d) show the presence of nanoscale second phases.

Evaluation of the melt spun precursor material has revealed key fabrication insights, showing fine distributions of nano-scale second phases. A unique outcome of the work performed has been an increased understanding of the effect wheel speed can have on the as-produced microstructure of melt spun ribbon. We have shown that in the case of the Fe-Si ribbons, the grain size and structure can be significantly refined when the through thickness width of the ribbon is decreased. This result was found to be highly dependent on the material system under evaluation; the Mg-based ribbons did not show the same behavior.

In Fe-Si systems, we have demonstrated an ability to tailor the as-processed microstructure based on the wheel speed employed during processing. Evaluation of resistivity and magnetization of the Fe-Si ribbons has clarified the impact wheel speed can have on these properties at varied silicon concentrations.

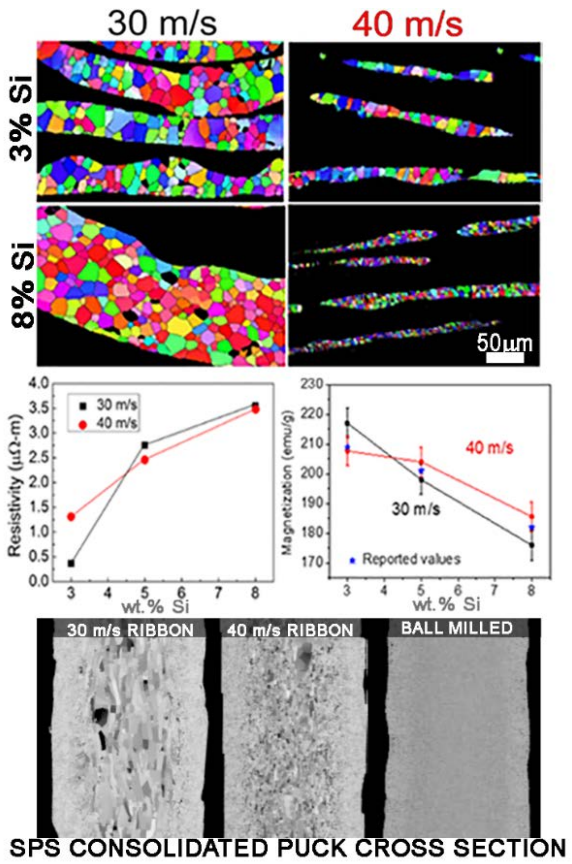

Electron Backscatter Diffraction of Fe-Si melt spun ribbon cross sections showing refinement due to increased wheel speed (top). Resistivity and Magnetization trends as a function of increasing silicon content (middle). Retained precursor microstructures following SPS consolidation (bottom).

Additionally, Mössbauer spectroscopic studies indicated Si content had a significant influence on the number of Fe sites, relative abundance of the Fe species, and internal magnetic fields/structural environments. This result is significant because it illustrates the ability to affect changes in the electronic structure of the material.

Analysis of Fe-Si precursor materials following consolidation by Spark Plasma Sintering (SPS) has revealed initial precursor microstructures can be retained despite the elevated temperature consolidation. Ball milling was identified as the preferred precursor processing method for Fe-Si, as it resulted in the most uniform structural refinement. SPS consolidation was also found to result in formation of a surface rind on the exterior of the consolidated puck, comprised of a refined grain structure.

Studies on the thermal stability of the melt spun AZ91 ribbons following ball milling have revealed precipitation of $Mg_{17}Al_{12}$ equilibrium phases occurs at milling times greater than 20 hours, illustrating a need for thermally stable, Mg-based alloy chemistries.

Fabrication and analysis of the aluminum binary alloy compositions Al-1, 5 and 10% Mg (identified for improved thermal stability and modeled in a sister project) revealed that increased magnesium concentration refined grain size and inhibited grain growth following annealing. Successful grain refinement was accomplished via melt spinning and maintained (about 2 µm) following heat treatment of 3 hours at 300°C.

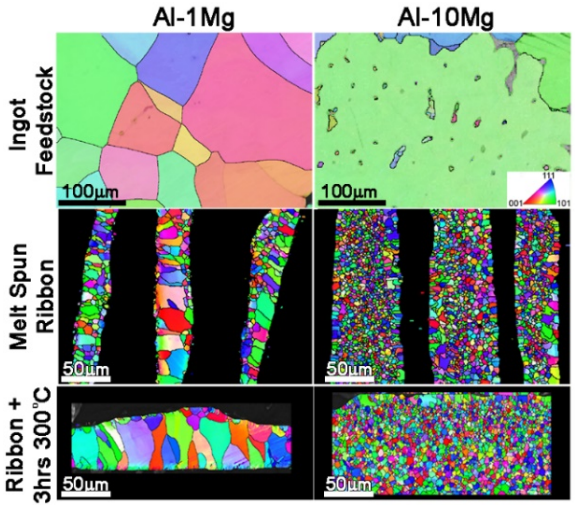

Electron Backscatter Diffraction of Al binary alloys showing starting ingot material (top), melt spun ribbon (middle), and heat-treated ribbon showing minimal grain growth.

To date, successful flake processing at scale has resulted in the fabrication of more than 3 kg of rapidly solidified Al-/Mg-based precursor material, which has supported in excess of 40 consolidation experiments.

Materials Science and Technology

Accelerating Lithium Ion (Li^+) Transport for Extreme Fast Charging Batteries

Jie Xiao
PN18041/3040

This project has systematically studied the fundamentals that hinder fast Li^+ transport in batteries under fast charging conditions. The electrochemical diffusion processes of Li^+ within different regions have been analyzed to determine the rate-determining step at different conditions. Appropriate strategies are accordingly proposed to accelerate Li^+ transport for extreme fast charging batteries.

While the cost for electrical vehicles, powered by Li^+ batteries, has been driven down remarkably in recent years, the battery charging time needs to be further shortened to reduce the mileage anxiety. However, when the charge rate is substantially increased, the high polarization on the anode side will lead to direct Li plating over the graphite anode. The exposed Li will quickly react with the electrolytes, irreversibly consuming very limited Li and electrolyte resources in the cell, leading to degraded performance after fast charging. Alternative anodes, such as $Li_4Ti_5O_{12}$, have been proposed to increase the charging capability of Li^+ batteries. However, the low capacity and high operating voltage of $Li_4Ti_5O_{12}$ significantly lowers the full cell energy. To meet the high energy goal, graphite still must be employed in Li^+ batteries. To improve the kinetics of the graphite anode, a silicon (Si) nanolayer was incorporated on the graphite surface, which demonstrated improved charge rate capability, although the effect of Si coating during repeated cycling is unknown.

During charge, Li^+ must transport continuously through three connected paths (i.e., electrolyte, solid electrolyte interphase layer, and graphite lattice). Simply modifying one or two of the diffusion paths will not significantly impact the observed anode performance since the rate-determining step changes at different conditions. To accelerate the Li^+ transport, all the three transport paths need to be considered. An integrated strategy must be developed to shorten the Li^+ diffusion paths and eliminate Li dendrite formation associated with a fast charging process.

Fast charging capabilities of Li^+ batteries are predominantly determined by how fast the anode can accept Li^+ ions. To simplify the study, an appropriate electrolyte (i.e., 1M $LiPF_6$-EC/DMC [3:7]) is selected, which will produce appropriate solid electrolyte interphase on graphite surfaces and thus not become the rate-determining step at least at moderate current densities. This project focuses on maximizing the capability of graphite anode to quickly accommodate Li^+ ions during fast charge.

Although Li^+ ions can be extracted very quickly from graphite lattice, they cannot intercalate into graphite sufficiently fast. As the lithiation rate increases from 0.1C to 4C, a fast capacity degradation is observed, indicating that graphite cannot accommodate Li^+ ion intercalation promptly at high rates. Note that the areal capacity of graphite anode is reasonably high at 1.9 mAh/cm^2, which is representative in a power-type battery.

The current density within the electrode is usually highest on the electrode surface (close to the separator side) and gradually decreases towards the interior electrode (towards the copper current collector). Accordingly, the electrochemical reactions are most intensive on the electrode surface toward the separator. The higher over potential within the top surface region of the anode easily triggers Li plating directly on graphite surface instead of intercalating into the lattice. Therefore, most of the Li “dendrites” are found on the electrode surface instead of the interior part.

In order to reduce the inhomogeneity of polarization across the whole graphite anode, the porosity of the electrode is increased appropriately. Appropriate additive X is, therefore, used during the electrode preparation process. Additive X is solid state and easily mixed with graphite and binder during slurry

making process. After the electrode is immersed by liquid electrolyte, additive X quickly dissolves, leaving pores across the whole graphite electrode. Through the control of the additive amount, the location and amounts of pores can be tuned conveniently.

The graphite electrode, after porosity modification, is further compared against the original one without any treatment in graphite/LiNiMnCo (NMC) full cells. The discharge capacities from the full cell with untreated graphite electrode decrease very fast when the charging rate is increased. Increasing graphite electrode porosity greatly mitigates this discharge capacity fading at high charging rates. Not only is the polarization largely reduced in the cell with higher graphite electrode porosity, both charge and discharge capacities are also improved.

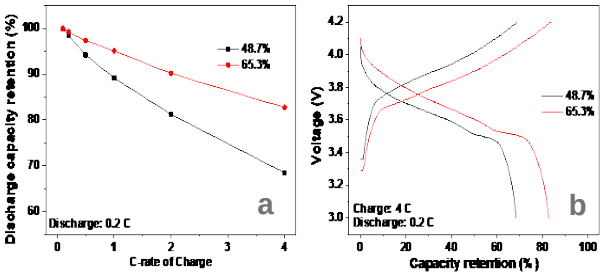

Electrochemical performances of Graphite/NMC full cells in which the porosities of graphite are different.
(a) Comparison of discharge capacity retention after being charged at different rates. (b) Voltage profiles of full cells. In both (a) and (b), the performances of untreated graphite electrodes with a porosity of 48.7% are compared with that of modified graphite electrodes (porosity of 65.3%).

Bulk Nanostructured Alloy Optimization: Designing for Processing and Thermal Stability

Aashish Rohatgi

PN16013/2790

This project will help develop the next generation of advanced materials for fuel-efficient transportation and high-efficiency power generation systems. These advanced materials possess a specially designed nanostructure to counter undesirable microstructural changes that otherwise limit the use of traditional metals and alloys at high temperatures.

Nano-sized microstructural features can produce significant improvement in structural and functional properties of materials. For example, nano-sized precipitates, present within a matrix of micron-scale grains, act as obstacles to dislocation motion and form a key basis of strengthening in a wide range of engineering materials, such as steels, super-alloys, aluminum (Al), and magnesium (Mg) alloys, etc. Even greater strengthening is predicted by the Hall-Petch relation, if the grain size itself is also reduced to within a certain nanometer (nm) size range.

In soft magnet materials, both theory and experiments show that a composite of soft iron (Fe) grains (approximately 10 nm) embedded in a ferromagnetic amorphous matrix with approximately 2 to 3 nm separation will give the best magnetic performance. Unfortunately, nanostructures are inherently unstable due to the high density of interfaces and, driven by the need to lower the interfacial energy (the driving force), coarsen rapidly even for temperatures moderately higher than room temperature.

Traditionally, coarsening is inhibited by a “kinetic” approach, where grain boundaries are pinned by nano-sized precipitates. However, this approach does not lower the interfacial free energy, but only lowers the grain growth rate and can be overcome at higher temperatures and/or at longer times. In order to reduce/eliminate the driving force, several research groups have proposed a “thermodynamic” approach, wherein segregation of solute atoms to the grain boundaries is used to lower the interfacial free energy, thereby preventing coarsening of the nanostructure and leading to a better thermal stability behavior.

In this project, the thermodynamic approach will be adopted, and existing analytical models will be used to identify thermally stable alloys. We will develop high-throughput experimental methodology to evaluate the thermal stability of these alloys and use atomistic modeling techniques for a fundamental understanding of how solute-atom and grain boundary interactions lead to enhanced thermal stability.

This research will follow an integrated experimental and modeling approach in order to achieve its objectives. We will use existing thermodynamic stabilization models to down-select a list of potential nanostructured alloy candidates that are predicted to be thermally stable based on criteria such as reduction in grain boundary energy, enthalpy of mixing, enthalpy of segregation, etc. Experimentally, we will use magnetron sputtering to create nanostructured thin films of model-predicted Mg-, Al-, and Fe-based compositions. Thermal stability of these nanostructured compositions will be evaluated by subjecting them to elevated temperatures and characterizing the resulting grain growth, solute distribution and diffusion, and precipitate formation. The experiments will be accomplished using analytical techniques such as transmission electron microscopy (TEM), atom probe tomography (APT), X-ray diffraction, etc. Finally, we will use atomistic and molecular dynamics simulations to understand interactions between solute atoms and grain boundaries.

In FY 2016, a lattice Metropolis Monte Carlo (MMC) method was used to evaluate thermal stability of nanostructured Al alloys, and it predicted an Al-Mg system to be a potential candidate. Accordingly, thin films of Al-Mg alloys were fabricated by magnetron sputtering and procedures developed to handle and anneal them and to analyze them by TEM and APT. Additionally, to evaluate the diffusivity of vacancy and silicon (Si) atom diffusion in α-Fe in the ferromagnetic state, *ab initio* calculated material properties of Fe and Fe-Si were used to derive pairwise-interaction energies between Fe-Fe, Si-Si, Si-Fe, Fe-vacancy, and Si-vacancy pairs.

In FY 2017, nanostructured Al-Mg thin films with different Mg content were evaluated in as-sputtered and annealed conditions using TEM and APT. The results showed that, while both pure Al and Al-Mg films underwent grain growth during annealing, Mg-containing films exhibited reduced grain growth (69%) compared to pure Al films (100%). Compositional analysis using APT and TEM cross-sectional observations suggested that the reduction of grain coarsening in Al-Mg alloys resulted from the retarding effect of both Mg solutes at grain boundaries (thermodynamic stabilization) and Mg-rich precipitates (kinetic stabilization), with the former playing a major role. Thus, these experimental results showing reduced grain growth in Al-Mg support the hypothesis of the effectiveness of Mg additions in increasing the thermal stability of nanostructured Al-Mg alloys and successfully validate the computational predictions of the MMC method from FY 2016.

Additionally, in FY 2017, we used a self-learning kinetic Monte Carlo method to determine the diffusivity of Si in the dilute-limit, and diffusivity of a vacancy at various Si concentrations, in the α-Fe matrix. Local atomic neighborhood dependent activation barriers for vacancy-atom exchanges were calculated on-the-fly using the pairwise interaction energies based on *ab initio* calculations. Results showed that in the dilute-limit and in the temperature range of 350 to 700 K, Si diffusivity is minimally affected by the magnetic order/disorder state of the α-Fe matrix. An increase in the magnetic disorder tends to increase the activation barrier (that lowers diffusivity), which is compensated by an increase in the diffusion pre-factor (that increases diffusivity). In the case of vacancy diffusion, its migration barrier remains more or less constant while the diffusion pre-factor decreases, thereby resulting in a decrease of its diffusivity with increasing Si concentration. Important vacancy-Fe/Si atom exchange processes were also identified. The results provide a further understanding of the diffusion of Si in α-Fe-Si and offer insight for Si-steel alloy design and processing.

In FY 2018, our goal was to evaluate the thermal stability of nanostructured Mg-based alloy films (e.g., Mg-Zinc [Zn]) in a manner analogous to the nanostructured Al-Mg films studied in FY 2016 to 2017. Nanostructured pure Mg and Mg-Zn thin films were fabricated by sputtering at room temperature followed by annealing at elevated temperatures. The as-sputtered and annealed films were analyzed for solute segregation and grain growth kinetics in order to evaluate the thermal stabilization potential of Zn solute.

Even though the annealing treatment was carried out in vacuum, Mg oxidation, rather than grain growth, was observed after annealing at a temperature of 200°C, as indicated by the presence of a diffuse ring (indexed as MgO [200]) in the diffraction pattern. When the annealing temperature was raised to 300°C, TEM diffraction pattern did not show the diffuse ring, and the micrograph image indicated possible reaction between Mg and silicon nitride coating on the TEM grid. Therefore, a baseline response of nanostructured Mg films to elevated temperature exposure could not be established conclusively, and further research is needed to develop improved test procedures that can anneal Mg-based films without any oxidation or deleterious reaction with the substrate.

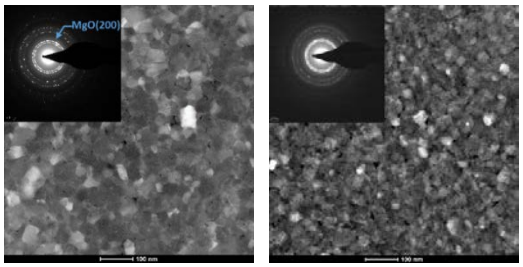

TEM bright-field image and diffraction pattern of nanostructured Mg films: After annealing at 200°C (left) with evidence of MgO diffraction ring, and after annealing at 300°C (right) with evidence of reaction with TEM grid. Scale bar in both the images is 100 nm.

In summary, this research program has useful implications for future alloy designs of high-strength light-weight materials and soft magnetic materials. We have developed an integrated experimental and modeling approach to identify and validate binary alloys that, when present as a nanostructure, are resistant to grain coarsening during exposure to elevated temperatures. Specifically, we were able to observe and understand the grain growth inhibition effect of Mg in the nanostructured Al-Mg system, corroborating our modeling results. Further work is needed to extend this approach to Mg-based alloys. Additionally, we have developed a self-learning kinetic Monte Carlo method to study the effect of Si concentration and magnetic order/disorder on the diffusion of Si and vacancies in the α-Fe matrix.

Carbon Rods with Unexpected Humidity-driven Water Expulsion

David J. Heldebrant
PN16020/2797

The goal of this project was to provide the scientific principles critical for understanding controlled nucleation and growth of carbon nanorods. Such knowledge will push the boundaries of scalable solution synthesis of nanocomposite particles with precise control over particle size, shape, and morphology.

This project focused on the Predictive Science of Synthesis, with the aim of understanding the structure and interaction of water at interfaces of nanomaterials to control the adsorption/ desorption and transport of water. Studies in FY 2018 were performed to learn how to perfect the synthesis via controlled nucleation and growth of the carbon rods. Synthetic efforts included testing variables such as time, temperature, heating rate that has significant impact on rod's geometry, and expulsion behavior. By careful tuning, we attempted to narrow down the controlling factors of the rod geometry that controls water adsorption behavior.

We continued our efforts to identify optimum conditions for the formation of rods. We investigated the effect of switchable ionic liquid (SWIL) purity and rate of heating effect on rod morphology and surface chemistry, which has impact on water expulsion behavior.

To begin with, we investigated the effect of SWIL purity and rate of heat on rod formation and water expulsion. We heated the reaction mixtures to 160°C with a heating rate of 1°C. In our first attempt, we observed the formation of rods and rods exhibited some (less than 1%) water expulsion at relative humidity (RH) 60. In an aim to repeat the experiment under the same experimental conditions (temperature and rate of heating) using freshly synthesized SWIL, we observed the formation of rods; although the rods did exhibit expulsion, the onset of expulsion was much different than what we observed previously.

We attempted to repeat the synthesis of carbon rods, and in every attempt, we observed formation of rods; however, the onset of water expulsion varied from batch to batch. It is not clear what other parameters are playing a role in onset of expulsion. As the carbon rods formed or a decomposed product obtained from SWIL, it was very important to fine tune the reactions conditions. With the results obtained, we are not able to conclude the exact reason for different onsets of expulsion.

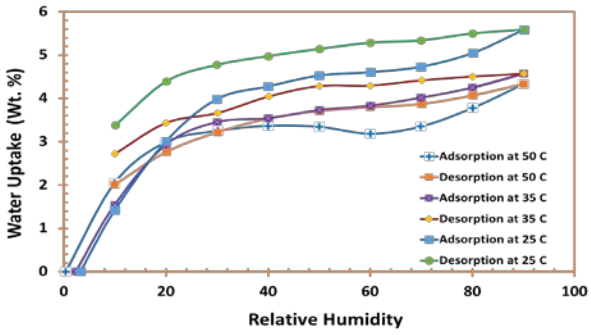

Water sorption isotherms of carbon-based materials at three different temperatures (25, 35, and 50°C).

To use the rods for evaporative cooling and water harvesting applications (i.e., multiple adsorption−desorption cycles a day), we performed water sorption isotherms at three different temperatures. It is interesting to note that the carbon rods exhibited water expulsion at 50°C, but the onset of expulsion is not the same at 35 and 25°C. The expulsion behavior appears to be tunable, with the capacity and humidity of expulsion different for each batch of rods that have been synthesized. Scanning electron microscopy and transmission electron microscopy imaging of these batches indicate different thickness, length, and morphologies of bundles. Unsurprisingly, each batch has different gravimetric capacity for water and different onsets of humidity of expulsion. Some batches reach peak uptake at 60%RH, while others achieve this at 90%RH or even 30%RH. Some batches adsorb 10 wt% water, while others reach saturation at 2 wt%. It is unclear what factors control the morphological structures of these rods.

We performed a preliminary assessment of these rods as either evaporative coolers or as water harvesting devices. We also modelled the performance of the carbon rods as a material that could act as an evaporative cooler, using the expulsion event to perform cooling with a humidity swing.

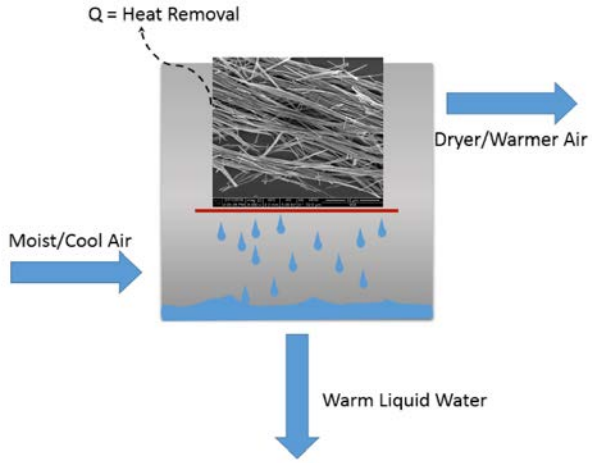

Proposed schematic of evaporative cooler.

The calculations of coefficient of performance (COP) suggest that, at current cycling capacity, the rods can achieve a COP of 0.24. The low number of the COP is solely due to the low cycle capacity of 2 wt% water.

We envision a prototype water harvesting device based on a feasible thermodynamic cycle. The adsorbed water capacity swing is currently small (about 1 to 2 wt%) relative to conventional desiccants, though the temperature at which adsorption and desorption occurs is expected to be nearly identical, allowing the shift in cycle to be accomplished through a shift in the inlet RH with uptake or release of heat at approximately ambient temperature. This enables the system to shift from adsorption to desorption without the delay and energy input typically required using conventional adsorbents. An advantage of this conceptual device is that it requires a cooling source only 5°C below ambient to collect water from the sorbent. Such a system consumes far less cooling than conventional condensers, which operate at 0.5°C to obtain liquid water. The 5°C cooling needed for this prototype could be achieved by simply burying the condenser 6 feet under the ground while leaving the collection unit above ground.

For the prototype, we anticipate the unit could be assembled using off-the-shelf components. The unit will be sized on 1 kg of sorbent split into two beds, where half of the sorbent adsorbs while the other is discharging. The unit is projected to be able to harvest 1L of water in 16.7 hours from ambient air in a demonstration.

Enhanced Value of Renewable Energy via High Temperature Electrolysis

Olga A. Marina
PN18079/3078

Relieving the grid of excess renewable electricity can be accomplished by powering a water electrolyzer to produce renewable hydrogen. This hydrogen can be temporarily stored and then used in filling stations, multiple industrial applications, or converted back to electricity when shortages occur. It can also be injected into the natural gas grid either directly or after methanation as "renewable fuel."

Solid oxide electrolysis cells (SOEC) offer the highest overall efficiency among other water splitting technologies to produce hydrogen, because the high operating temperature of SOEC significantly reduces the amount of required electrical energy. The biggest challenges for SOECs reported in literature are the rapid material degradation and the limited long-term stability due to their high operating temperatures. In principal, such cells can be used for both hydrogen production when operated in SOEC mode and for electricity production, if run as solid oxide fuel cells (SOFC). There is very little prior art on reversible solid oxide cells.

Recently, the Department of Energy's Office of Energy Efficiency & Renewable Energy has identified the following needs to make progress toward DOE H_2 cost goals: 1) performance and durability improvements for both stack and system and high-pressure operation, 2) materials development, 3) standardization of testing and interface specifications, 4) techno-economic analysis, and 5) megawatt-scale development program. This project focused on the materials development need.

This project has developed a unique SOEC/relative state-of-charge (RSOC) testing infrastructure and has evaluated standard SOEC materials to establish baseline cell performance and assess typical testing protocols.

Two test stands capable of simultaneous testing of eight SOEC/RSOC button cells in a single box furnace (16 cells in total) were designed, constructed, and operated in a ventilated space. This capability allows relatively quick screening of new SOEC materials, different operating conditions, and various cell designs.

The main distinctions of these test stands are 1) each cell (in a group of eight) has an independent gas delivery system allowing simultaneous testing at varied steam concentrations, 2) each cell can operate at either distinct or similar current/voltages allowing screening of operating conditions, 3) multiple "repeats" can be produced the same time, which accelerates the data collection process and aids in reliability of the obtained data, 4) data collection is done automatically. Steam is produced *in situ*, eliminating the need of difficult-to-control heated water lines.

Several SOEC cell sets were tested using previously fabricated in-house standard SOEC materials: yttria-stabilized zirconia (YSZ) electrolyte, Ni/YSZ negative electrode, and $(La,Sr)MnO_3$ (LSM)-YSZ or $(La,Sr)(Co,Fe)_3$ (LSCF) positive electrodes. Long-term electrochemical performance was recorded using a multichannel potentiostat over a range of operating conditions in both SOEC and SOFC modes to simulate operation of a reversible solid oxide cell. For each cell, losses associated with ohmic and electrodic processes were separated using electrochemical impedance spectrometry (EIS). Open-circuit voltage was periodically recorded in time to verify the quality of seals in a high steam environment, as well as the consistency in steam production. Following termination of electrochemical tests, LSM/YSZ surfaces and cross-sections of individual cells were analyzed using scanning electron microscopy (SEM) and energy dispersive spectroscopy (EDS). For comparison, as "controls," LSM/YSZ electrodes (both non-tested and tested in the SOFC mode) were characterized, as well.

Ohmic and polarization losses increased when switching from SOFC to SOEC mode. Electrode polarization losses were dominant, suggesting the need for a new, more active material set.

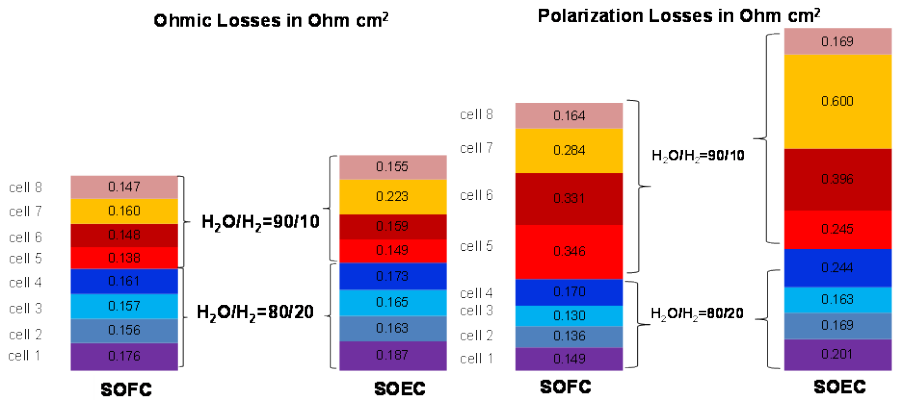

Twenty-four cells tested with LSM/YSZ positive electrodes at 800°C resulted in relatively low current densities at thermoneutral voltage, indicating low H_2 production rate. Cells degraded rapidly in less than 300 hours and tests were terminated. The SEM/EDS analysis revealed insignificant microstructural difference in the LSM/YSZ layer compared to "controls." However, all LSM/YSZ electrodes either completely or partially delaminated from the YSZ electrolyte that consecutively became brittle near the electrochemically active interface. This is consistent with the previous findings reported by other groups. The effect has been attributed to high currents responsible for the excessive oxygen pressure build up near the interface, leading to electrode delamination and YSZ deterioration. Our results indicate that cell failure can also occur at low current densities (low oxygen flux through the electrolyte). Cell fabrication methods and cell shelf life are important to minimize SOEC degradation.

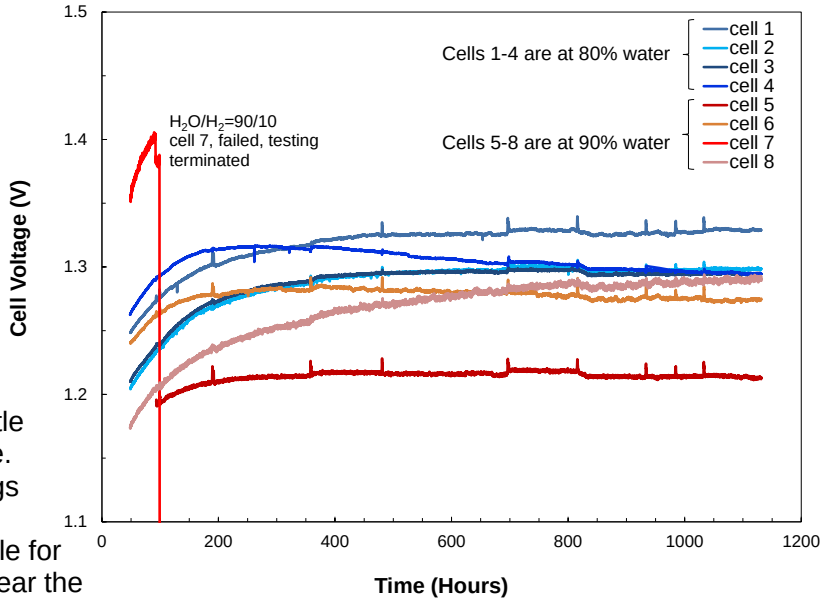

Long-term performance data indicate more rapid degradation at very early stages of testing. A different testing protocol needs to be developed to minimize the initial impact.

Eight cells with LSCF positive electrodes produced high current densities at thermoneutral voltage and, therefore, high H_2 production rate, indicating that LSCF is a more electrochemically active electrode material than LSM/YSZ. Cell performance somewhat decreased during the initial 200 hours because of an increase in both ohmic and polarization resistances. During the following 1,000 hours, a rather stable performance was observed with only a minimal increase in ohmic resistance (but not electrode polarization resistance). Several cells exhibited nearly no degradation, less than 0.4%/1,000 hours.

The multiple cell testing capability for SOEC/RSOC research was efficient in generation of baseline, long-term performance data. Redundancy of the cell tests allowed for the acquisition of useful data even if one or more of the cells exhibited anomalously poor performance.

Fundamental Investigations of Photoelectrochemical Water Splitting of Model Oxide Electrode Surfaces

Kelsey A. Stoerzinger
PN16105/2882

This project provides fundamental understanding necessary to rationally develop oxide-based heterostructures that effectively absorb the solar spectrum and efficiently utilize solar-generated carriers to create chemical fuels, such as hydrogen and oxygen gas, from water splitting.

Solar radiation represents an immense and renewable energy resource; however, storage of this intermittent source is critical in enabling grid integration and utilization in remote applications. One approach is utilizing the sun's energy to form chemical fuels through water splitting.

The efficiency in driving the hydrogen and oxygen evolution reactions is governed by that of electron-hole pair generation, propagation to the electrode surface (without recombination), and electrochemical conversion. Metal oxides constitute ideal aqueous interface layers because they are much more stable in solution than traditional semiconductors; however, fundamental understanding of the energetics and processes that occur at the surface is lacking.

Our goal is to fabricate well-defined oxide-terminated heterostructures using molecular beam epitaxy (MBE) that absorb well in the visible portion of the solar spectrum, have low defect densities (to minimize recombination and carrier trapping), and exhibit band bending and band alignments that facilitate carrier transport to and through the electrode surface to the aqueous medium. The outcome will be an important new set of design principles, along with useful materials, for photoelectrochemical water splitting.

Having established a photoelectrochemical (PEC) testing methodology of oxide thin films and heterostructures thereof in an inert atmosphere linked to materials growth and characterization facilities in the Environmental Molecular Sciences Laboratory, we have studied the influence of materials characteristics on PEC performance in FY 2018. We fabricated films of tunable band gap, band edge position, and carrier density with composition $La_{(1-x)}Sr_{(x)}FeO_3$ and studied their current-voltage characteristics as photoanodes in the oxidation of water to produce O_2 gas. A trade-off in the photovoltage and photocurrent results from the incorporation of charge carriers, linked to the changes in composition. The electrocatalytic activity for water oxidation has also been studied in a series of rare earth (*R*) nickelates ($RNiO_3$).

Mechanistic investigations of the water/oxide surface interaction have shed light on the functional groups that form on oxide surfaces *in situ*. Using ambient pressure X-ray photoelectron spectroscopy (AP-XPS) at the Advanced Light Source, we have probed the speciation resulting from interaction of oxides with water and electronic band bending at the surface. The absolute core-level binding energies measured with the surface saturated in water vapor yield valuable information of the effect that the aqueous environment and the associated adsorbates have on the presence and strength of built-in potentials in the near-surface region of the oxide. Likewise, the detailed line shapes, particular those for oxygen, reveal which species are present at the surface.

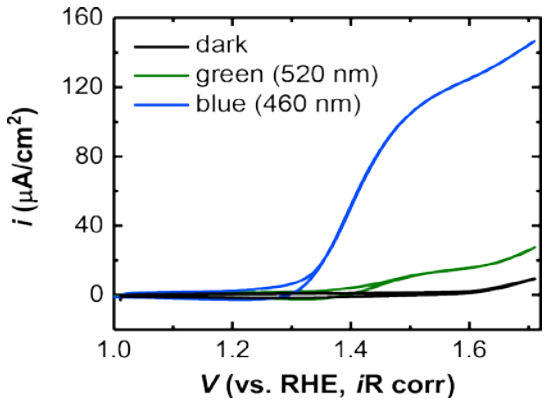

Cyclic voltammetry for a $La_{0.88}Sr_{0.12}FeO_3$ photoanode in the dark (black) compared to under wavelength-selected illumination. The decrease in onset voltage under illumination indicates photoabsorption and charge transfer to drive the oxygen evolution reaction during water oxidation.

Studies of the photoanode $La_{(1-x)}Sr_{(x)}FeO_3$ found notable differences in chemical reactivity with water, which originate from chemical substitution and the resultant changes in surface electronic structure. The dissociation of water on the surface and formation of hydroxyls is a key intermediate in water oxidation. Addition studies have considered the link between composition, electronic structure, and reduction/oxidation properties in the oxide interconnect and electrode $La_{(1-x)}Sr_{(x)}CrO_3$. The *operando* speciation of Pt surfaces in alkaline electrolytes was also studied to shed light on the reaction mechanism of water splitting.

Hierarchical Framework Materials by Advanced Materials Design

Miroslaw A. Derewinski
PN17046/2936

The goal of the study is to develop and provide access to both the micro- and mesoscopically organized porous materials with tailored chemical and structural properties for new challenging applications, such as catalytic processes in aqueous or biphasic polar/nonpolar liquid phase, while using PNNL's advanced capabilities to monitor the processes involved during synthesis.

Microporous materials, such as zeolites, characterized by very high pore volumes and having well-defined pore sizes, are prospective solid acid catalysts for tailored processes in dense/liquid phases. Confining their highly active sites inside micropores imposes, however, severe mass transport limitation on the catalytic processes. To expand the utilization of zeolite catalysts, new approaches to synthesize (hydro)thermally stable porous materials, which combine multiple levels of porosity, are highly desirable. Additional challenges, such as good hydrothermal stability in hot liquid water, which provides the basis for liquid phase transformation of biomass-derived feedstocks, require smart synthesis and material control to minimize hydrolytic degradation of the framework.

Hierarchical zeolites characterized by increased external and/or mesopore surface area are usually more active than their counterparts in diffusion-controlled reactions such as those involving the transformation of larger molecules or those undertaken in the liquid phase. Additionally, the interplay between different levels of porosity can offer exquisite control over tandem processes comprising a sequence of steps, with each requiring a different microenvironment.

To address these challenges, we synthesized robust MFI zeolites with hierarchical pore systems spanning multiple length scales by controlled solid-state crystallization of dry amorphous aluminosilicate nanogels without use of a meso-template. The applied procedure enables the preparation of robust and highly crystalline monolithic material (particles size 300 to 500 nm) built up with the interconnected nanocrystals (20 to 30 nm in size) and containing inter-particle mesopores.

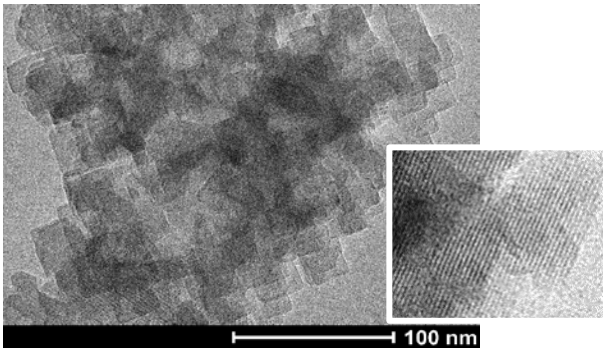

Scanning electron microscopy (SEM) of the hierarchical MFI zeolite prepared by solid-state crystallization of dry aluminosilicate nanogel.

In FY 2018, we also achieved more insight into the deactivation and disintegration of metastable zeolite framework in aqueous phase reactions (conversion of the biomass feedstock). To determine and deconvolute the role of structural defects and hydronium ions in BEA zeolite, we successfully synthesized highly crystalline and defect free zeolite BEA (across a wide range of Si/Al) via the fluoride route. The longer lifetime of this material is caused by a lower concentration of internal silanol defects (sites of the initial framework hydrolysis). Comparing BEA crystals of different size, we found a dependence on the nature of external surface. Durable and catalytically efficient Al-rich zeolites require hydrophobization with long chain alkyl groups. This modification led to a retarded diffusion of both liquid water into the pores (increasing of lifetime) and hydronium ions into the bulk solution (preventing loss of intrinsic activity).

Another thrust in FY 2018 was tackling the zeolite formation mechanism. *Ex situ* and *in situ* spectroscopy was used to follow the kinetic processes during formation of the large pore

faujasite (FAU) zeolite from hydrous gel. Solid state ^{27}Al and ^{23}Na magic angle spinning (MAS) nuclear magnetic resonance (NMR), and Al X-ray absorption near-edge structure were used to monitor transformation of amorphous gel into the crystalline material.

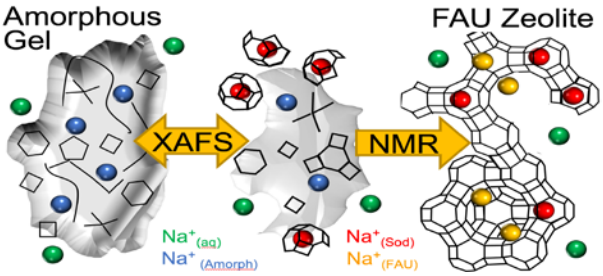

Stages of FAU zeolite formation observed using the combination of *in situ* spectroscopic techniques (e.g., X-ray absorption fine structure, ^{27}Al and ^{23}Na MAS NMR).

While the crystallization of zeolites can be described macroscopically by a layer-by-layer approach, we show that, on the atomic scale, the gradual conversion into regular FAU framework can be understood by an atom-by-atom growth model, where the structure-directing role of Na^+ cations is exploited to first form the sodalite-like subunits that are critical to the growth of the FAU structure.

In Situ Characterization of Corrosion in Magnesium (Mg) Alloys

Elizabeth V. Stephens
PN18040/3039

This project has developed and demonstrated a unique capability in corrosion evaluations via* in situ *transmission electron microscopy (TEM) and X-ray photoelectron spectroscopy (XPS) coupled with* ab initio *study to determine the in-process, local corrosion mechanisms occurring for Mg under corrosive environments. This fundamental and mechanistic understanding of electrochemical corrosion will drive us towards corrosion mitigating solutions.

Many materials, including Mg-based components, are usually coated with either organic or inorganic corrosion mitigation materials. However, these coatings are susceptible to failure when subjected to harsh atmospheres and are potentially lethal if they are more cathodic than the base material. More recently, alloying has been favored to decrease the corrosion rate by increasing corrosion potential of the base material.

Despite the extensive work being performed to aid in the deployment of materials, such as Mg alloys for structural applications, there is a lack of fundamental understanding of the real-time, local corrosion mechanisms occurring and very little has been done to understand the actual mechanism of corrosion in these systems at the atomic/nano scale. Using *in situ* techniques that describe the structural changes at an atomic scale will not only help in understanding the mechanism of corrosion, but it will also complement the classical, electrochemical measurements that allow opportunities for alloy and coatings development with improved corrosion properties.

In this research, we used customized, liquid/gaseous *in situ* XPS setup and TEM holders to directly observe the structural and chemical evolution of Mg under varied atmospheres and corroborated the results with molecular dynamics simulations.

By using *in situ*, environmental high-resolution TEM (HRTEM), the corrosion process of Mg in water vapor was thoroughly investigated. Upon leaking in water vapor (10^{-2} mbar), hydroxide crystals started to nucleate on the surface of MgO, showing a layer-structure and growing by the addition and expansion of (0 0 0 1) layers on the (0 0 0 1) surface of the crystal. This process was accompanied by pores formation in the Mg, presumably due to the Kirkendall effect. Additionally, we developed a novel method that generated fresh Mg (0 0 0 1) surface in TEM for the study of incipient oxidation process on Mg. The HRTEM results demonstrated that the oxidation of Mg was initiated by the formation of a metastable MgO phase, wherein the hexagonal close packed lattice of Mg remained intact, and oxygen atoms intercalated into the tetrahedral sites of the Mg lattice.

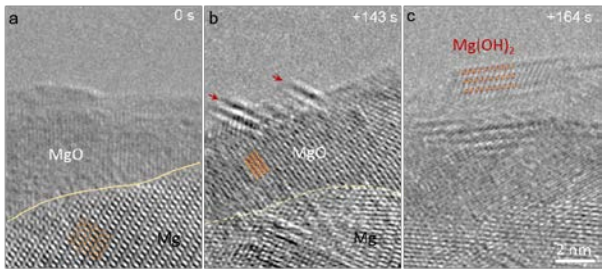

The progress of oxide scale on the Mg surface using *in situ* high-resolution scanning TEM.

Density functional theory simulations were conducted to study the interaction of the Mg (0 0 0 1) surface with water, both with and without solvated Cl^- ions. Our results indicate that H_2O molecules bind to the surface Mg atoms, forming Mg–O bonds if both O–H bonds are oriented away from the surface. The Mg atoms at the adsorption sites become partially oxidized and displace away from the surface by about 50 pm. We find that, in the electron rich limit (i.e., in the case of fresh non-oxidized Mg surface), the absorbed H_2O decomposes into negatively charged species H^- and OH^-, and that the latter can further decompose into O^{2-} and another H^-. The absorbed H^- ions are found to be transient species; they interact with H_2O and form H_2 and OH^- with the energy gain of

about 0.9 eV. The O^{2-} ions are found to preferentially occupy subsurface sites, either tetrahedral or octahedral. The latter configuration provides the local atomic structure that corresponds to the oxygen site in the bulk MgO. In contrast, OH^- ions remain at the Mg surface and occupy hollow sites where they are bound to three surface Mg each, forming structural motifs that correspond to $Mg(OH)_2$. Such configurations dominate in the electron-poor limit (i.e., in the case of partially oxidized Mg surface). These calculations suggest that MgO-like structural features will dominate at the interface with metallic Mg, while $Mg(OH)_2$-like features are prevalent at the interface with water.

Finally, our preliminary results indicate that interaction of solvated Cl^- with protons in the vicinity of the Mg surface lowers the activation energy of O–H dissociation and, thus, facilitates the corrosion process.

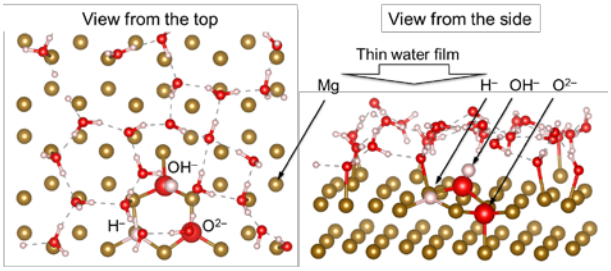

Density Functional Theory simulations predict energetics and preferential configurations of anions emerging as the surface oxidation proceeds.

These results were further corroborated with XPS studies. In this work, two sputter cleaned single crystal samples of Mg (0 0 0 1) were exposed to droplets of pure D_2O and 5 wt% NaCl in D_2O solutions in a controlled glove box environment for 60 minutes. After the reaction, both samples were cooled down to -120°C using a liquid nitrogen heat exchanger and transported to the XPS analysis chamber in their frozen states. The chemical speciation on the exposed surfaces were monitored as a function of temperature from -120°C to room temperature.

Furthermore, high-resolution helium ion microscopy imaging was employed to capture the reacted NaCl exposed surface, revealing the micro development of surface morphologies and cubic crystals. The observation was rationalized by the energetics based on simulations, and provided unprecedented direct evidence for the long-standing controversy involving the initial oxidation process of Mg.

Mastering the Macromolecular-materials Interface for Energy Science

Jim De Yoreo
PN17069/2959

The purpose of this project is to determine the mechanisms, pathways, and dynamics by which engineered, macromolecular building blocks, which are designed to interface with inorganic surfaces, interact and assemble into two-dimensional (2D) and 3D structures and, subsequently, direct nucleation of inorganic materials. This is achieved through molecular-level imaging and spectroscopy methods.

Living systems create macromolecular-inorganic interfaces to guide the formation of functional, hierarchical protein-scaffold-inorganic materials through biomineralization. Through this process, organisms create unique structures to realize complex biological functions. Previous studies have demonstrated that the assembly of protein scaffold is controlled by the sequence-dependent energy landscape, which is highly sensitive to the surrounding environment.

We have also found that the nucleation of crystals on protein scaffolds are impacted by a free energy barrier associated with the interfacial match between macromolecular matrices and the crystal lattice, as well as kinetic barriers associated with atomistic processes. However, still lacking is the knowledge and capabilities to design a hierarchical protein scaffold to control the formation of functional materials with complexity and specificity. Our goal is to combine a protein-engineering and *in situ* imaging approach to define the energetic and kinetic controls on assembly of 2D and 3D scaffolds and to control the nucleation of inorganic materials on those scaffolds.

In FY 2018, we used our new capability to carry out high-speed atomic force microscopy (AFM) during protein self-assembly to investigate the dynamics of assembly by the purpose-designed helical repeat protein DHR10-micaN (N=14 to 18), which is designed to bind epitaxially to the (001) face of muscovite mica. Our results show that, at low ionic strength, all proteins exhibit only small fluctuations, but those aligned along the preferred orientation on mica exclusively move by translating back and forth along their length, while those that are aligned along non-preferred directions exhibit repeated angular fluctuations until they find the preferred direction. At high ionic strength, which is the condition under which the proteins attain long-range order in the form to 2D nematic and smectic liquid crystal arrays, ordering comes about through large-scale fluctuations in in domain size and protein position. All proteins that are part of a domain exhibit a single orientation, and the average domain size scales exponentially with time until a threshold value is reached. Beyond this point, order percolates rapidly through the film leading to a single ordered domain. We are exploring the physics underlying observed time dependence and emergence of order through Monte Carlo methods via a User Project at the Molecular Foundry, an Office of Science Nanoscale Science Research Center at Lawrence Berkeley National Laboratory.

We also perfected the design of a mutant of DHR10-micaN-H (N=3 to 7) consisting of three of these proteins fused at a central point to form a three-fold symmetric building unit with three arms. This design self-assembles into perfectly ordered hexagonal lattices for which the lattice dimensions can be digitally controlled through the choice of N. Because the protein is designed to bind epitaxially to the underlying mica lattice, every domain is aligned to one another.

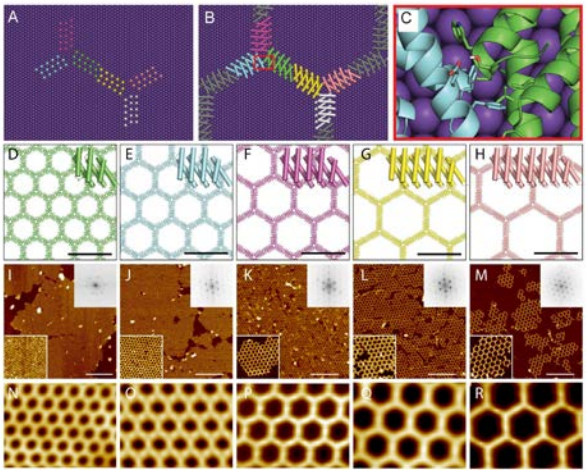

The *de novo* designed protein DHR-MicaN-H (N=3–7) self-assembles into hexagonal lattices on mica with lattice dimensions defined by the choice of N. (A–C) Hexagonal lattice design concept. (D–H) Computational models of DHR10-micaX-H hexagonal arrays for 3, 4, 5, 6, and 7 repeat units. Insets at right corners, one monomer with different repeat units. Alpha helices are shown as cylinders. The black scale bar is 20 nm. (I–M) AFM images of DHR10-micaX-H lattices with X=3, 4, 5, 6, and 7 repeat units. The white scale bar is 200 nm. Insets are higher magnification views (left-lower corner) and Fourier transforms (upper-right corner). (N–R) Averages of images in F–J. The field of view is 80 nm by 60 nm.

We are now in the process of modifying the basic design of DHR10-micaN to match the lattices of the semiconductor zinc oxide and the magnetic material magnetite. These protein arrays will then be grow hybrid materials where the protein lattice plays the role of an artificial scaffold that directs the nucleation of these materials in the way that natural protein scaffolds like collagen direct the formation of mineralized tissues like bone.

Modeling the Interfacial Effects, Partitioning, and Production Routes of Epsilon Particles in Uranium Oxide

Richard A. Clark
PN15100/2775

The goal of this work is to elucidate the physical and chemical mechanisms that govern the formation of noble metal inclusions in irradiated fuel to understand the radiological, physical, and chemical conditions leading to their formation and unique properties.

The chemical fractionation leading to the formation of five-metal "epsilon phases," composed primarily of the elements Mo, Tc, Ru, Rh, and Pd in a reduced state, from nuclear fuel under irradiation is a key knowledge gap in our understanding of nuclear fuels. The development of these phases within uranium oxide matrices over time under irradiation has been linked to many important phenomena over the life cycle of nuclear fuel, from in-reactor operations to long-term spent fuel disposition. It has been hypothesized that epsilon phase formation can affect fuel performance, control cladding erosion, and cause stress corrosion through both the physical disruption of the fuel matrix due to growth and the alteration of the fuel's electrochemical behavior resulting from the presence of a unique chemical species.

This effort aims to understand the formation mechanisms of the epsilon metal phase during nuclear fuel irradiation and to understand the solid-solid-gas interfacial equilibrium effects that lead to variations in the properties of this unique phase. Developing a fundamental understanding of the chemical, radiological, and material structure conditions that lead to precipitation of these phases will significantly improve our knowledge of nuclear fuel under irradiation conditions.

To understand the formation of epsilon particles, we utilized a varied analytical suite of techniques that combine experimental and modeling results to guide the research in a synergistic loop. Research was categorized into four key areas: Isotopic Analysis of Bulk Separated Particles, Advanced Microscopy of *In Situ Particles, Microscale Irradiations, and Modeling*.

Isotopic Analysis of Bulk Separated Particles. Previously separated noble metal epsilon particles from three commercial irradiated fuels were used for complete characterization. The separated particles were dissolved, and elements were separated for isotopic analysis. During the analysis, a sixth major metal (tellurium) was discovered as part of the epsilon phase. The separations and isotopic analysis were completed. The isotopic ratios for the epsilon particle metals yielded information about the genesis of the particles in the fuel, particularly indicating whether the included elements are produced by fission, activation, decay, or a combination.

The isotopic abundances of the noble metal phase components were compared to expected values of the full fuel inventory from ORIGEN-ARP calculations. This analysis revealed that the measured isotopic abundances of the six elements in the phase, with few exceptions, match well with the expected bulk fuel inventory. Exceptions include Pd-104 and -106, which appear to be enriched relative to predictions compared to the other Pd isotopes.

Analysis showed that the noble metal phase particles represent a sink for a significant portion of the total inventory of elements that make up this phase. This would suggest most of the inventory of semi-volatile fission products tellurium and technetium are bound up in this refractory phase and not likely to be released in the event of cladding failure during storage.

Advanced Microscopy of In Situ Particles. In previous years, a full cross-section of an irradiated UO_2 fuel pellet was prepared and removed from hot cells. In FY 2018, we continued to characterize this cross-section, with emphasis on the fuel-cladding interface region. We found that epsilon phase particles were present up to about 6 µm into the Zr cladding oxide region from the UO_2 fuel. The particle size

distribution varied with depth and correlated strongly with large Xe gas voids. The particles themselves were found to be a combination of multiple phases with Pd-Te rich regions.

Microscale Irradiations. Microscale samples (about 20 ng) of fresh UO_2 were irradiated in collaboration with the University of Missouri. In this work, noble metal precipitate formation was observed at very low burn-up equivalence. This work provides the first viability of microscale irradiations.

Modeling. Thermodynamic modeling was incorporated into this project in order to help determine the relative stability of different phases in the epsilon particle system. Early efforts used density functional theory (DFT) to simulate the free energy of formation of the Mo-Ru and Pd-Ru binary alloys. These calculations showed that the elemental composition observed in experimental studies is consistent with the most stable metal phase. More recent DFT work has included tellurium, which we have demonstrated can form a new, non-metallic phase that contains a high percentage of the total palladium and exists near the epsilon metal phase. In this way, local differences in elemental composition can be observed, even on a scale of just a few nanometers, thereby enhancing the known complexity of epsilon particles even further.

Noble metal inclusions are found as fission products in spent nuclear fuel, such as UO_2, and are thought to catalytically influence the rate of uranium oxidative dissolution. To examine the catalytic behavior of these noble metal inclusions, quantum-mechanical models were used to investigate the interaction between both oxidant and reductant adsorbates and surfaces. In addition, the catalytic effect of Te that is found in Pd-rich regions of the particles was also investigated by performing adsorption studies on palladium telluride.

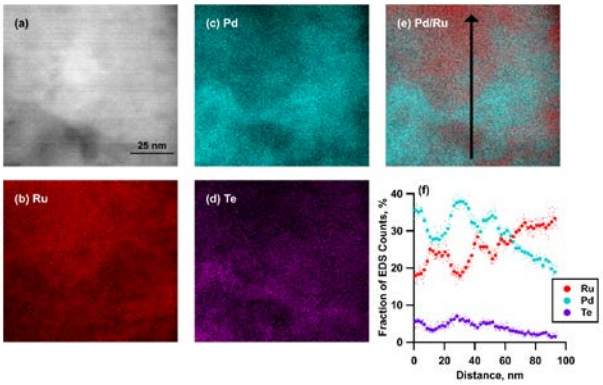

Ruthenium-rich and palladium-/tellurium-rich regions within noble metal particles.

Peptoid-based Biomimetic Materials with Tunable Structures and Functions

Chunlong Chen
PN17032/2922

We are developing sequence-defined peptoids as designable building blocks for assembly of biomimetic materials with hierarchical structures. We also use* in situ *imaging techniques and molecular simulations to track and understand peptoid assembly pathway and mechanisms.

The exquisite self-assembly of proteins and peptides into highly ordered and dynamic functional materials has inspired innovative approaches to biomimetic materials design and synthesis. Although synthetic approaches may yield highly stable polymers with intricate architectural morphologies, the introduction of peptide-like side-chain diversity has been a long-standing challenge for synthetic polymers. In 1992, Zuckerman et al. developed the solid-phase synthesis of peptoids (poly-N-substituted glycines) that combined synthetic opportunity for side-chain diversity with high molecular stability.

Subsequent research on peptoids focused primarily on mimicking structure and functionality of peptides for drug discovery and molecular recognition. More recently, it has been demonstrated that peptoid side-chain interactions can be exploited for assembly. Unlike peptides, peptoids do not form backbone hydrogen bonds; therefore, the assembly of peptoids into nanostructures will be less complex to understand and predict than that of peptides, while still having the capability of tuning assembly and function through side-chain structure and sequence. In addition, the peptoid architecture will yield stable materials for future functional applications.

In this work, peptoids will be used as designable building blocks by exploiting the reversibility of supramolecular interactions to assemble them into biomimetic materials and understand their assembly mechanisms. We will also address the challenge of predicting ensemble outcomes of assembly driven by the molecular details of sequence and the consequent interactions. Fusion of such experimental efforts with extensive computational simulations will enable the rational design of sequence-defined polymers for which self-assembly is programmable, and the resulting function is predictable.

In FY 2017, we designed and synthesized a large number (over 30) of peptoids that assembled into membrane-mimetic two-dimensional (2D) nanomaterials, nanotubes, and pore-forming networks. We determined the role of peptoid hydrophobic side chains in controlling assembly morphologies and pathways, as well as the mechanism by which peptoid assemble, by designing a series of amphiphilic peptoid oligomers (APOs), Nce6Nbpmn (n = 5, 6, 7) and their functionalized sequences, Nbpm = N-[(4-bromophenyl)methyl] glycines and [Nce = N-(2-carboxyethyl)glycine].

We demonstrated the assembly of APOs into a new family of highly designable, stiff, and dynamic single-walled peptoid nanotubes (SW-PNTs) through a unique “rolling-up and closure of nanosheet” mechanism. These SW-PNTs undergo a drastic contraction of approximately 46% in height upon solution pH decreases, and this pH-triggered response is reversible. We further demonstrated that SW-PNTs can be rationally engineered to tune their surface chemistry, wall thickness, PNT diameter, and mechanical properties. By precisely introducing β-cyclodextrins or arginylglycylaspartic acid peptides within SW-PNTs, we demonstrated the applications of functional PNTs in purifying azo-contaminated water and in enhancing cancer cell adhesion and uptake. This study offers the first route to assembly of stiff and dynamic nanotubes from sequence-defined synthetic molecules.

To increase the transmission electron microscopy (TEM) contrast and mechanical properties of peptoid assemblies, we synthesized over ten peptoid sequences that

contain polyhedral oligomeric silsesquioxane (POSS), a cage-like molecular structure that could be regarded as one of the smallest possible silica particles. In this design, POSS was introduced during the solid-phase peptoid synthesis as a side-chain. We demonstrate the assembly of POSS-containing peptoids into membrane-mimetic 2D nanomaterials and nanotubes. Atomic force microscopy (AFM) and TEM techniques were used to characterize these morphologies, and X-ray diffraction data show that POSS-containing peptoid membranes and nanotubes are crystalline. More importantly, as expected, these 2D nanomembranes and nanotubes can now be visualized under TEM without negative staining, which offers the potential of investigating the assembly pathways and kinetics of peptoid assembly using *in situ* TEM technique. We also demonstrate that dye molecules, such as dansyl and rhodamine can be introduced into these POSS-containing hybrid peptoid assemblies to generate biomimetic materials with ordered structures and tunable fluorescence properties.

Two-step nucleation pathways, in which disordered, amorphous, or dense liquid states precede appearance of crystalline phases, have been reported for a wide range of materials, but the dynamics of such pathways are poorly understood. Moreover, whether these pathways are general features of crystallizing systems or a consequence of system-specific structural details that select for direct versus two-step processes is unknown.

Using *in situ* AFM to directly observe crystallization of peptoids, we showed that crystallization pathways are sequence dependent. When a short hydrophobic region is added to the sequence that directly forms crystalline particles, crystallization follows a two-step pathway that begins with creation of disordered clusters of 10 to 20 molecules and is characterized by highly non-linear crystallization kinetics, in which clusters transform into ordered structures that then enter the growth phase. These results shed new light on non-classical crystallization mechanisms and have implications for design of self-assembling polymers.

The backbone parameterization of peptoids has been refined and is now consistent with high-level quantum simulations. Enhanced sampling methods showed the importance of peptoid sequence for the dimerization, highlighting the significant effect of hydrophobic residues on peptoid assembly process. We found that poly(sarcosine) showed a much larger conformational flexibility and stronger interactions with water than the peptide analogue poly(alanine) under bulk and interfacial solvation environments.

During FY 2018, we used both *in situ* AFM and TEM to investigate the assembly pathways and dynamics, as well as the formation of mechanisms of peptoid-based nanomaterials (e.g., nanotubes). We have introduced chromophore donors and acceptors into crystalline nanomembranes and nanotubes to build artificial light harvesting systems in the aqueous environment. We further used this systems for molecular sensing. We also investigated the influences of 1) the ordering of peptoid assemblies, 2) the density of D and A, and 3) the local environments of chromophores on the optical properties of functionalized peptoid assemblies. The simulation effort was focused on understanding the driven forces that lead to formation of nanosheets and nanotubes.

Probing Collective Phenomena at Solid-liquid Interfaces Under Reaction Conditions

Grant E. Johnson
PN17070/2960

This project aims to understand collective phenomena and atomic-level processes occurring at solid-liquid interfaces and how they influence electrochemical performance at dynamic reaction conditions. New experimental capabilities are being developed for synthesis and electrochemical imaging of supported cluster ensembles and* in situ *liquid X-ray photoelectron spectroscopy (XPS) that will have broad applications in energy storage and catalysis research.

Electrochemical processes that are critical to energy generation, storage, and catalysis take place at solid-liquid interfaces and may be promoted by supported clusters. Clusters have tunable properties that are not present in the bulk due to their large number of active surface sites, size-dependent redox reactivity, structural plasticity, and support-specific binding. While it has been demonstrated that certain intercluster interactions may improve the catalytic activity of clusters ensembles, it is not understood how collective cluster-support and cluster-cluster interactions change with coverage from isolated single clusters to dense assemblies and what effect this has on electrochemical performance.

Soft landing of mass-selected ions is ideally suited to preparing precisely defined ensembles of supported clusters with predetermined size and coverage for characterization by spatially resolved electrochemical techniques. These cutting-edge methods, when combined, will provide the insight required to design superior materials for energy generation, storage, and catalysis using predictive models that incorporate collective phenomena.

It also is well established that the solid-liquid interface determines rates of reactions and selectivity toward products. Consequently, it is important to determine geometric and electronic structure at solid-liquid interfaces at dynamic reaction conditions. Characterizing the atomic-level processes involved in the formation of solid electrolyte interphase (SEI) layers in rechargeable batteries remains an outstanding challenge due to the vacuum requirements of traditional surface analytical techniques. Limited understanding of the process of SEI formation, the structural and chemical properties of the SEI, and how it evolves during charge/discharge cycles limits the advancement of technology for rechargeable batteries. To address this challenge, an *in situ* XPS capability is being developed to gain insight into the electronic structure and chemistry of solid-liquid interfaces at reaction conditions.

In FY 2017, we used magnetron sputtering and gas aggregation to generate clusters and nanoparticles with controlled composition and morphology. We also explored how the presence of different functional groups in phosphine ligands influences the structures adopted by metal clusters that may subsequently be soft landed onto electrode surfaces. The electrochemical activity of these nanoparticles supported on glassy carbon surfaces was examined using spatially resolved scanning electrochemical cell microscopy (SECCM), which provides insight into how intercluster spacing and agglomeration influence the rate of catalytic O_2 reduction. It was found that clusters with higher surface coverage exhibited more zones with enhanced catalytic activity.

In FY 2018, we characterized different coverages of size-selected Pt_{13}^- clusters using scanning transmission electron microscopy and SECCM to better understand the influence of surface agglomeration on the efficiency of the oxygen reduction reaction. We also examined the structural evolution of differently sized gold nanoparticles supported on CeO_2 during exposure to controlled mixtures of reactant gases.

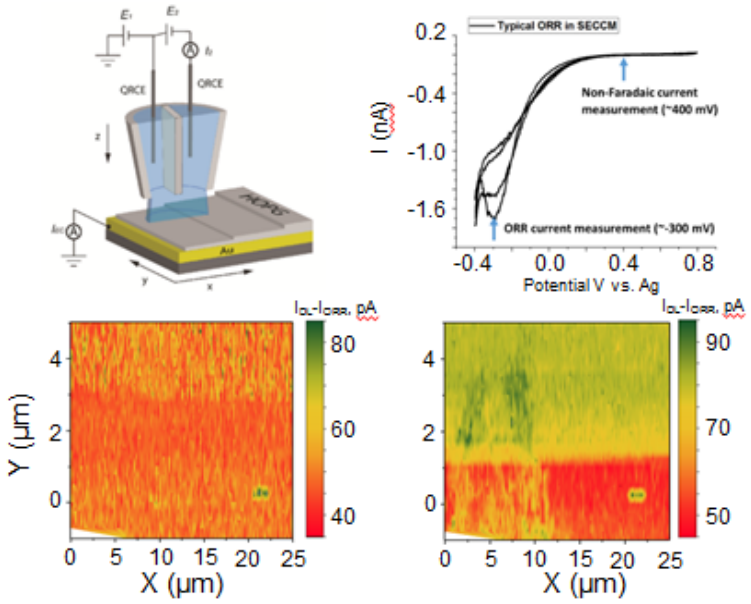

(Top left) Schematic diagram of the theta capillary used to form an electrochemical cell with the surface for imaging. (Top right) Cyclic voltammograms of Pt_{30}^- clusters soft landed on glassy carbon. (Bottom left) 2D SECCM image of 2 x 10^4 clusters/µm^2. (Bottom right) SECCM image of 5 x 10^4 clusters/µm^2.

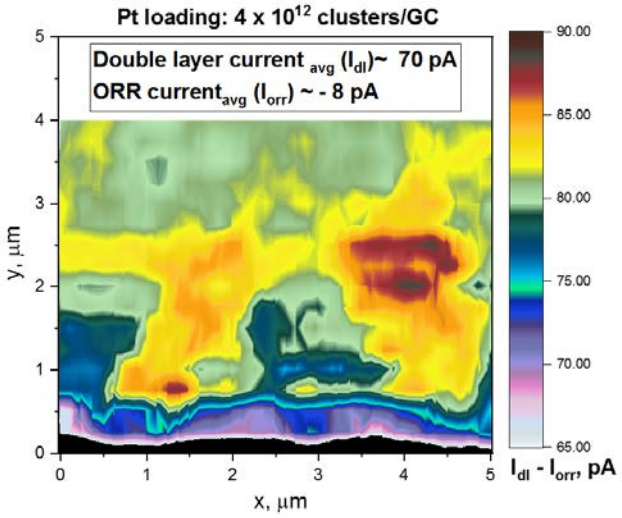

SECCM image of Pt_{13}^- clusters soft landed onto glassy carbon. Note the regions of enhanced current that are caused by cluster aggregation during the ORR measurement.

Fundamental insight into collective phenomena obtained from studying these well-defined model systems will revolutionize the design of materials for catalysis and energy storage by providing a new and potentially powerful route to tune electrode performance by controlling cluster size and coverage. Understanding the structure and dynamics of solid-liquid interfaces at reaction conditions is critical for designing future materials with improved interfacial transport and reactivity in electrochemical, ion-selective, and catalytic systems.

Quantum Defects in Synthesized Diamond Aerogel and Diamond Nanoparticles

Ilke Arslan
PN17080/2970

Quantum defects in materials are atomic-scale defects in crystalline solids that can act as quantum sensors in a variety of ways across physical and life sciences. Spin-dependent properties make diamond defects great for quantum computing or local sensing at the nanoscale, even within living cells. Diamond is chemically inert and has shown promise in drug delivery and promoting bone growth.

Diamond materials have received a substantial amount of both theoretical and experimental attention in recent years. In physical sciences, diamond has been investigated for use in catalytic nitrogen and oxygen reduction reactions, optically addressable qubits, optical magnetometry, stable electrochemical double-layer capacitors, seeding the growth of polycrystalline diamond thin films, and for monitoring the flux, position, and timing of intense X-ray beams from fourth-generation synchrotron light sources.

In biological sciences, diamond materials have been investigated for non-cytotoxic targeted-delivery of therapeutic molecules and for long-term visible and near-infrared *in vitro* cell labeling. However, to date, there are no well-established methods for synthesizing nanocrystalline diamond materials with well-defined point-defect microstructure. This fact stands in stark contrast with the immense knowledge base and literature for controlling both the size and composition of other semiconductor nanomaterials such as quantum dots and porous silicon. The central goal underlying the basic research in this project is to uncover new approaches for the synthesis and characterization of nanocrystalline diamond materials with well-defined point-defect microstructure.

The central aim of this project is two-fold: 1) demonstrate control over the concentration of nitrogen vacancy (NV) centers within a nanocrystalline diamond aerogel synthesized at high-pressure, high-temperature conditions using a laser-heated diamond anvil cell, and 2) to develop a protocol to map the distribution of nitrogen dopant atoms in the final material using high-resolution imaging and spectroscopy in the scanning transmission electron microscope (STEM) to advance understanding of quantum defects in diamond materials. STEM tomography will be used to illuminate the three-dimensional (3D) morphology of the diamond aerogel and complement the high-resolution spectroscopic mapping. This combination of synthesis and characterization will provide a feedback loop to work towards a controlled distribution of nitrogen dopant atoms.

A nanoscale STEM image of the morphology of the synthesized diamond. The porous nanostructure and ordered carbon layers are visible.

In the first six months, we synthesized diamond aerogel specimens. Due to the difficulty of the synthesis process at high-pressure and high-temperature conditions, only a small amount of material is synthesized during each experiment. The first set of challenges is mounting an appropriate amount of material on a grid that will be well-suited for electron tomography and microscopy. It must be in the center of a grid

square and one that is wide enough to reach high angles as the specimen is tilted to acquire many different images. The results of our first experiments working together showed that the diamond material they synthesized was high quality, but some of the small pieces fell off during shipment, and others were not suitable for tomography because of the similarities between the specimen and the grid. However, we were able to obtain good information on the outcome of the synthesis.

Separately, electron energy loss spectroscopy was performed on test specimens to determine the parameters for spectral imaging. It was determined that the material must be extremely thin to be able to observe any NV centers and as uniform as possible. The material should be below 50 nm in thickness, but closer to 20 or 30 nm would be better. Further, the density fluctuations of the carbon or thickness changes can affect the spectral results, so future spectral imaging to probe NV centers will likely need to be performed on specimens that have been put into a focused ion beam (FIB) and milled to an approximately 30-nm, uniform thickness across. Tomography will be performed on the materials in their native state, before the FIB sectioning, to ascertain their 3D morphology. Lastly, special care will be taken to place the small amounts of material on specific flat grids, and special shipping materials or hand delivering will be required to overcome any lost material in transition.

In the second year of the project, we began 3D tomographic reconstructions using a 200 kV Technai F20 electron microscope at the University of Washington's Molecular Analysis Facility. We worked to computationally process the multi-tilt reconstructions using the Radon transform implemented in MATLAB™ code. Substantial progress was made throughout the second year of the project, culminating in the successful 3D tomographic reconstruction of carbon aerogel precursor materials that serve as the starting samples for nanodiamond synthesis.

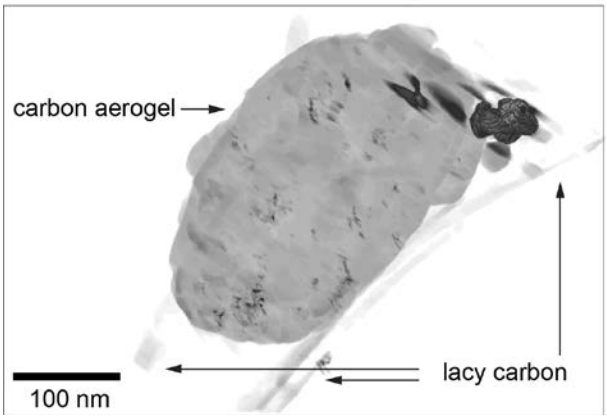

Three-dimensional Radon tomographic reconstruction of a carbon aerogel starting material used for nanodiamond synthesis. Seventy individual dark-field STEM images were collected at an angular tilt separation of 1 degree using a 200 kV Technai F20 microscope at UW. The images were reconstructed in MATLAB™ to map out the 3D volumetric reconstruction of the carbon aerogel.

Radiotracer Atmospheric Dynamics Chamber Feasibility and Design

David G. Abrecht
PN18059/3058

Understanding the atmospheric transport of radionuclides, particularly radionuclides that can undergo reactive chemical transformations, is critical to formulating an appropriate response following a nuclear accident. This one-year project focused on producing the engineering design for an atmospheric exposure chamber for radionuclide research studying fundamental reaction and phase transformation kinetics to feed atmospheric models. Construction of the chamber will be performed under a separate project

During a nuclear accident, atmospheric modeling of the radioactive plume is utilized to understand how best to establish accident response protocols, including evacuation zones and limited-time access zones. These zones can extend many miles and often involve displacing people from their homes and communities.

The atmospheric models used for these scenarios typically are of two different flavors: particle-tracking, where “tracer particles” are tracked as they move on the winds and are deposited in various areas by rain and general fallout, and gas models, where non-reactive gases are tracked as they mix with the winds and are transported long distances. These models are generally good, but do not easily account for *reactive gases*, which are able to either change chemical form or change phase (i.e., move from gas to particle/droplet and back).

Significant uncertainty still remains about the fundamental science behind how these species move in the environment, their kinetic rates of change between different species and phases, the effect of their isotopic identity on those rates, and their ultimate fate and deposition. This project was established to develop an experimental capability for measuring these transformation rates on real radioactive materials under realistic, controlled atmospheric conditions to better understand these fundamental rates—ultimately leading to improved uncertainties in models during nuclear accident scenarios.

The current one-year effort was focused on producing an engineering design for the experimental atmospheric chamber, to be built in subsequent projects. Specific challenges to designing a radioactive chamber are minimizing the volume and, thus, the required quantity of radioactive material and risk of contamination, while still maintaining an acceptable surface-to-volume ratio to minimize “wall effects” that are not representative of atmospheric processes during measurements. The expert team evaluated materials, flow rates, feed, mixing properties, ultraviolet light requirements, and most importantly, radioactive handling requirements, ultimately producing a working, costed chamber design from commercial off-the-shelf parts, which will be constructed in later projects.

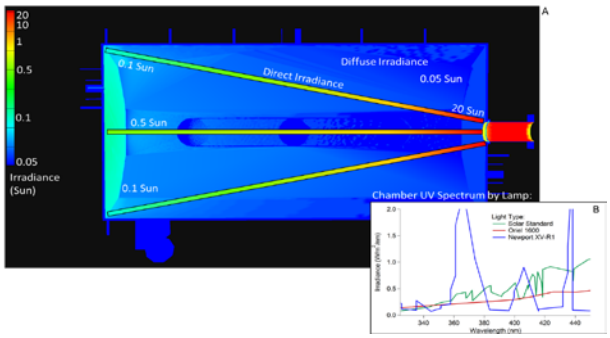

Optical modeling showing the expected wavelength-dependent ultraviolet irradiance in the chamber. These types of models are used to determine the brand of solar simulator to purchase for the chamber.

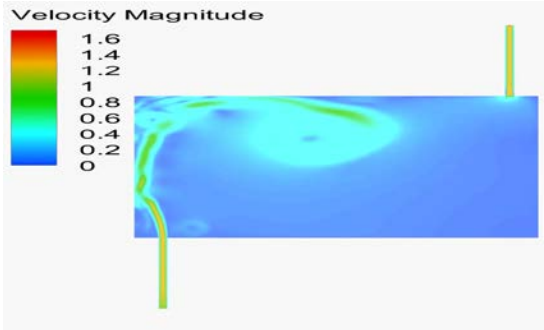

Computational fluid dynamics simulation of inlet stream and sampling outlet and the effect of stream placement on internal mixing. These types of simulations are used to minimize surface-to-volume ratio and mixing time in the design, as well as evaluate feed and sampling rates.

Statistical Microscopy Conjoined with Deep Learning – Revolutionary Insights Across Length Scales

Danny J. Edwards
PN18024/3023

Understanding and controlling radiation damage in materials requires the development of cutting-edge instrumentation and methods. This project has launched a new radiological scanning transmission electron microscope (STEM) and generated baseline data for future statistical analysis using machine learning techniques.

The unprecedented challenges associated with the safe use and disposal of nuclear materials requires a completely redesigned materials analysis platform. Electron microscopes currently used in radiological facilities across the Department of Energy (DOE) complex are limited by poor electron sources and inefficient older detectors. In addition, tedious manual analysis of images and samples greatly reduces productivity and hinders our ability to generate meaningful data quickly.

This project has launched a “GrandARM” aberration-corrected STEM, the only such instrument in the DOE complex. Equipped with a bright electron source and multiple high-speed X-ray detectors, this microscope has demonstrated the capability to rapidly examine the atomic-scale structure and chemistry of radiological samples. Furthermore, large volumes of data collected by this microscope represent an ideal input to advanced machine learning algorithms for future automated defect analysis across multiple length scales.

For this project, we have constructed a dedicated radiological microscopy suite shielded from electromagnetic interface, sound, and vibration, permitting excellent high-resolution imaging. The GrandARM instrument represents the cornerstone of this suite and draws on other co-located capabilities, including high-level radiological materials handling, surface imaging, and focused ion beam preparation.

Augmented with an advanced aberration-corrector, the GrandARM is capable of high-speed and high-resolution imaging of materials, and the system can achieve a 63 pm point-to-point resolution at 60 to 300 kV, enabling it to examine a wide range of alloys and ceramics. It is equipped with a dual X-ray detector setup that enables rapid compositional mapping of samples that can cut analysis times down from more than 2 hours to 5 minutes. We have demonstrated that this microscope can acquire atomic-resolution electron energy loss spectroscopy maps over 3x longer times (more than 14 minutes) versus the existing JEOL ARM (3 to 4 minutes), allowing mapping of large interfaces. Several large volume datasets have already been collected for future examination using “big data” machine learning methods.

This project has begun to transform our understanding of irradiated alloys, revealing previously undetected precipitates and phases. The instrumentation will spur innovation and new discoveries across multiple projects and sectors.

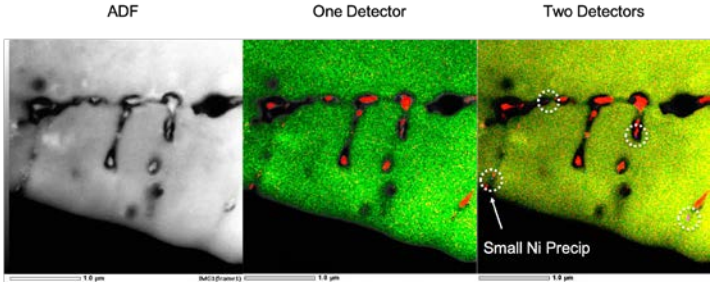

Enhanced composition mapping capability illustrated by a comparison between single (previously available) and multi-energy X-ray detector geometries. Fe = green; Cr = red; Ni = blue in a HT-09 alloy.

Surface Modifications of Laminar Graphene Oxide Water Separation Membranes

David W. Gotthold
PN17045/2935

Structured laminar membranes, consisting of hierarchically stacked two-dimensional (2D) graphene oxide with near perfect slip flow interfaces, are a fascinating material system with the potential for radically improved water separation through excellent selectivity and high permeability.

Laminar graphene oxide membranes have attracted a great deal of interest in the last few years as a potentially revolutionary method for separating water from other chemicals. In particular, the 2D systems have near-perfect slip boundary conditions that support orders of magnitude faster flow in nano-scale channels. However, early research has shown significant variation and instability in graphene oxide materials due to processing.

We have developed the fundamental test methodologies needed for understanding performance in liquid-liquid separation using graphene oxide membranes made by a new shear-force casting method to align micro grains. We also developed stable and repeatable methods for measuring transport of organic and aqueous liquids through the membranes. Importantly, with water/alcohol mixtures, the presence of alcohol rendered the membrane water selective, as demonstrated by the generation of osmotic pressure. This first-time observation (along with X-ray diffraction data) indicates the formation of water channels within graphene sheets, presumably due to a high degree of solvent ordering. Importantly, we observed a puzzling phenomenon of the near shutdown of fluxes and shrinking of inter-plane spacing in the presence of alcohols.

We continued to focus on understanding the effects of both surface structure and chemistry on membrane behavior and developing surface modifications that enhance stability and performance. We used diazonium dye, diazonium benzene sulfonate, and sulfuric acid treatments to increase polarity and measured the impact on alcohol selectivity. We determined that the alcohol-related transport shutdown is not affected by surface treatment. However, the flow reduction process is reversible and, through X-ray diffraction and Fourier transform infrared spectroscopy studies, discovered a new catalytic mechanism of chemical reduction of the graphene oxide by alcohol. Although adding complexity to flow separations (permeability values), this new phenomenon may be used for catalytic membrane reactors for alcohol oxidation products.

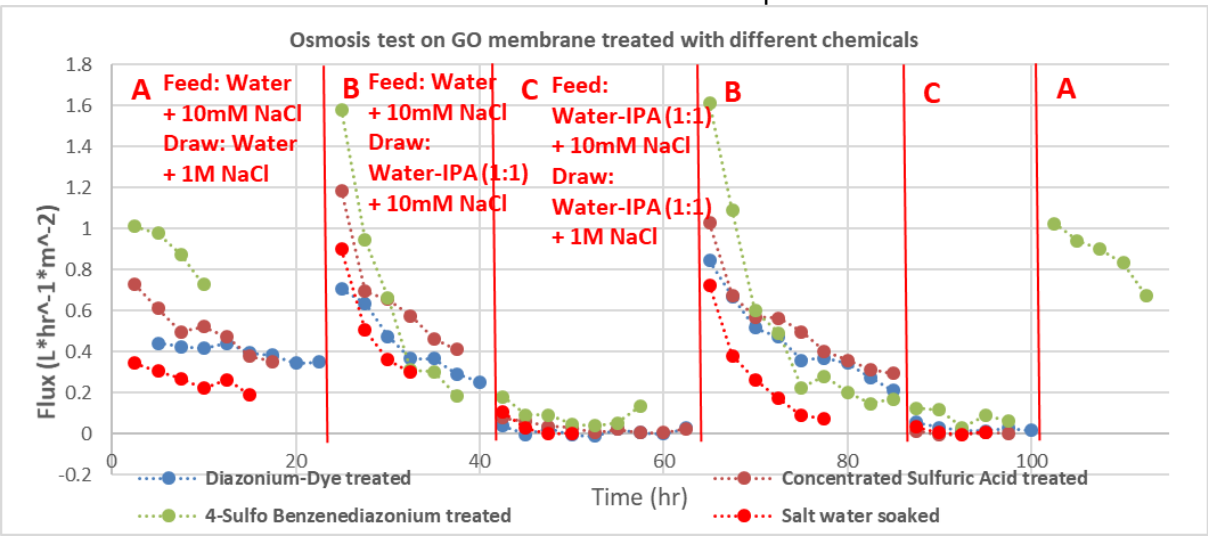

Osmosis test on graphene oxide membrane treated with different chemicals.

Towards a Better Understanding for Mineral Nanoparticle Assembly by Coupling Colloidal and Hydrodynamic Forces and Its Application to Superlattice Formation of Nanocrystals

Jaehun Chun
PN17031/2921

This project aims for a connection of different length-scale frameworks, combining fundamental studies in theories, simulations, and experiments for mineral nanoparticle assembly. The project will establish a self-consistency between theories and simulations, validated by experiments. Such self-consistent framework, combined with a correct description of the coupling between energetics and dynamics, will build a rigorous understanding of nanoparticle assembly.

Mineral nanoparticle self-assembly has been observed and studied; the self-assembly results from a combination of various short-/long-range forces between mineral nanoparticles, giving rise to superlattice formation, which would sometimes involve the alignment of lattices of the mineral particles to their crystallographic axes (i.e., oriented attachment). While the forces are beginning to be explored experimentally by using atomic force microscopy (AFM)-based dynamic force spectroscopy (DFS), a delicate balance/correlation between many existing forces that are influenced by detailed chemical physics at molecular scales is still unclear.

This project will develop a better understanding of the self-assembly (including the oriented attachment) through a connection between theories, simulations, and experiments, coupled with a correct description of dynamics of nanocrystals. A target system is mainly on ZnO($10\bar{1}0$). Through the superlattice formation of nanocrystals by using *in situ* transmission electron microscopy (TEM), the self-consistent framework can be generalized to understand the assembly of nanoparticles at large scales for various important applications such as energy storage.

We first prepared a stable the ZnO($10\bar{1}0$) tip by implementing a thin layer carbon (5 to 10 nm) as a coating layer; this thin layer protects tip dissolution and contamination, even after 8 hours of force measurements in $Zn(NO_3)_2$ solution with concentration from 0.2 to 2 mM. We then investigated the forces between two ZnO($10\bar{1}0$) nanocrystals. To explore an approach process until the jump-to-contact, our study employed a new scheme for the measurement; the tip was located at several nominal separations with a designated residence time at each separation while it gradually brings to the substrate. This can allow us to estimate reasonable separations between the tip and substrate, to be compared with potential of mean forces (PMF) obtained from simulations. We also performed the force measurements as a function of tip size and $Zn(NO_3)_2$ concentration, which can provide the effect of hydrodynamics and surface chemistry. We would further explore subsequent detailed analysis of the forces in a possible follow-up opportunity.

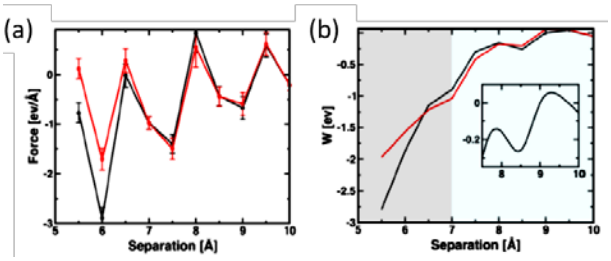

Total (in black) and hydration (in red) force curves between ZnO($10\bar{1}0$) surfaces by using ReaxFF and the corresponding PMFs, respectively, for both (a) forces and (b) potential. The inset in (b) shows the enlarged PMF curve at separations from 7.5 to 10 ångström. Note that the hydration force is, indeed, attractive in this case.

We investigated the impact of interfacial water structure on forces between ZnO($10\bar{1}0$) surfaces, specifically for hydration forces. We used the density functional molecular dynamics (DFT-MD) method to investigate the length scale and the oscillatory nature of the hydration force. Our findings demonstrated that hydration forces are only active within less than 1 nm separation and are not size dependent. Our study indicates

that the size-dependent nature of oriented attachment does not originate from the hydration force. More importantly, the hydration force is shown to be heavily dependent on the details of the surface chemistry; the surface chemistry even changes a sign of the hydration force (i.e., from repulsive to attractive). Therefore, our study clearly showed that the assembly of ZnO(10$\bar{1}$0) nanoparticles will be dictated by a balance between dispersion and hydration interactions.

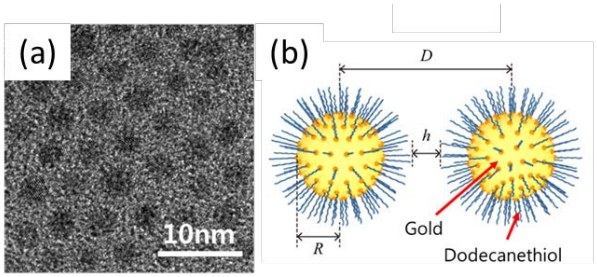

(a) Low magnification of TEM image for a hexagonal arrangement of Au nanoparticles and (b) a schematic diagram showing a basic configuration of the system: (D) a center-to-center distance, (R) particle radius, and (h) separation for Au-Au nanoparticles with polymer coating.

We planned to construct a scheme and associated code based on real-space multiple scattering theory combined with plane-wave DFT calculations of the microscopic dielectric properties to compute Green's functions for the full electromagnetic fields (including both vector and scalar potentials) of cluster models of crystalline ZnO(10$\bar{1}$0) surfaces. This quantity, a critical material property for dispersion forces, relates the total electrostatic potential in the material, including contributions from the electrons composing the material, to an externally applied potential of arbitrary shape in space and time. While the scheme itself could potentially work, it appears to have a limitation for "beyond" classical description.

Using synthesized monodisperse nanoparticles based on Pd, Ag, and Au, we investigated the growth kinetics and dynamics of nanoparticle superlattices by using *in situ* TEM equipped with direct detection camera and imaging capabilities, which enabled us to track the rapid motion of individual nanoparticles in real time. Focusing on Au nanoparticle systems, we coupled the experimental observations with detailed analysis of the particle forces to obtain mechanistic understanding of the process. Our study clearly demonstrated that a competition between various forces (i.e., Brownian, van der Waals, hydrodynamic, and steric hindrance forces) over various separations is critical for the kinetics of cluster growth, as well as the superlattice formation. Such methodology and analysis scheme can be applicable to other similar systems such as Pd nanorods/ nanospheres.

Towards Polarization-Switched Solid-State Molecular (POSSM) Pumps

Carlos A. Fernandez
PN17014/2904

The goal is to demonstrate proof-of-concept on a highly efficient molecular pumping approach that could render obsolete mechanical compressors used in many applications today. How? By simply switching "on" and "off" a capacitor. In the "on" position (presence of an electric field), polarizable molecules within the capacitor cavity can generate temporary dipoles, attracting and concentrating refrigerant molecules via hydrogen bonding. When the capacitor is switched off, the polarization disappears together with the H-bonding interaction, and the refrigerant molecules are set free. This simple concept provides a physical basis for non-mechanical pumping.

Although methods vary widely, the way fluids are pumped against pressure gradients is by means of mechanical compressors. These compressors all operate with the same basic underlying principles and achieve compression by changing the velocity, enclosed volume, and/or temperature of the gas flowing through the compressor.

We seek to introduce a fundamentally new compression approach that operates at the molecular level and involves zero moving parts. The main goal at the end of the project is to demonstrate proof-of-concept on polarization-switched solid-state molecular (POSSM) pumping.

POSSM will eliminate the related mechanical compressor inefficiencies due to energy conversions (combustion to mechanical rotation) and associated friction and dissipation (heat transfer). Instead, POSSM will operate by rapidly cycling the adsorption affinity of a thin layer of polarizable molecular sorbent arranged in a capacitor with similar volumetric pumping rates to traditional air conditioning and refrigeration/freezing systems, while consuming less than one-third the energy.

POSSM device comparison with benchmark system.

Parameters	Mechanical Compressor[1]	POSSM
Power In (kW)	0.88	0.23
Cooling Output (kW)	3	3.1
COP	3.4	13
Volume (L)	2.2	1.8
Weight (kg)	10.3	1.2
Manufacturing Cost	$250	$300

[1]Based on variable displacement compressor.

In this work, we have demonstrated, for the first time, the concept of electrical polarization-driven molecular pumping. This was performed by polarizing an organic chromophore deposited onto an electrode surface inside the capacitor via turning on and off the applied electric field. To this end, a gold-coated electrode was fabricated and functionalized with a chromophore, 4-acetamidothiophenol. The enthalpy change upon the sorption/desorption of HFC from a model electrode was determined to be 9 kcal/mol, which is sufficient to perform the pumping action.

To quantify the HFC exchange, a porous chromophore-functionalized electrode was used in a capacitor encased in a cell equipped with a gas flow capability. HFC exchange was demonstrated during absorption/desorption cycles upon switching the capacitor on and off.

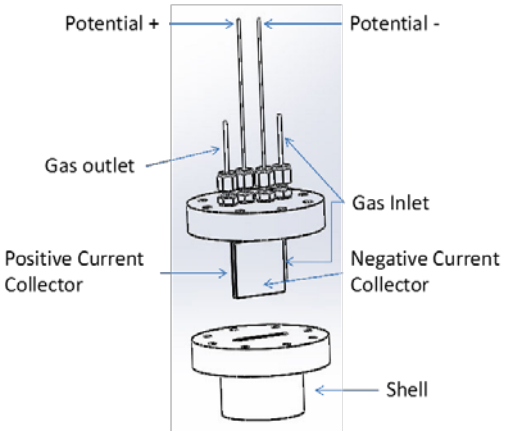

A schematic of the capacitor cell used in the electrically switched sorption/desorption experiments.

For a simple double-layer capacitor, the HFC exchange capacity was significant (0.11 mol HFC/L of chromophore). The work presented here addresses the need for new energy-efficient methods for the transport of gases against pressure gradients. The range of potential applications of this fundamentally new approach to use electrical energy to perform work is very broad and includes catalysis, refrigeration, gas separation, and sensing, among others.

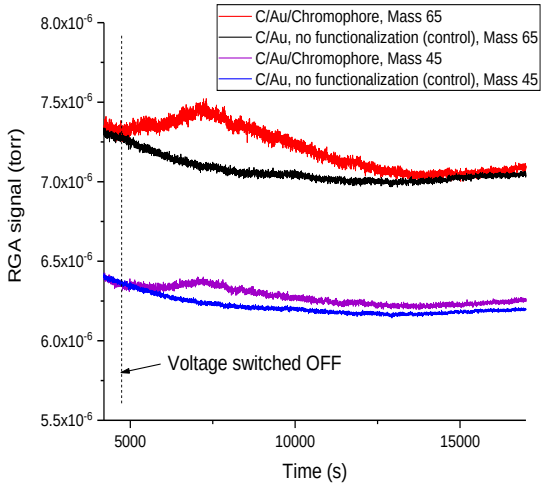

The response of the capacitor cell to switching off the capacitor voltage. Residual gas analyzer mass signals of the two characteristic fragments of the HFC, 45 and 65 a.m.u., are shown.

One challenge will be demonstrating the potential of solid-state molecular pumps as a replacement to mechanical compressors is the slow sorption-desorption process rate under allied bias. Towards this end, follow-on work will evaluate higher porosity substrates to increase HFC capacity and alternative chromophores for faster relaxation of dipole moment upon switching off the electric field.

Using *In Situ* Liquid Secondary Ion Mass Spectrometry and *In Situ* Transmission Electron Microscopy to Determine the Mechanism and Kinetics of Lithium Ion Mobility in Solid Electrolyte Interface Layers

Zihua Zhu
PN16009/2786

We are using the unique capabilities developed at PNNL, including* in situ *liquid secondary ion mass spectrometry (SIMS) and* in situ *transmission electron microscopy (TEM), to resolve critical questions regarding how Lithium-ion (Li^+) migrates through the solid-electrolyte interphase (SEI) under an electric field, as well as to provide a quantitative measurement of its mobility.

Li^+ batteries are now indispensably used as energy storage devices for portable electronics and electric vehicles and are starting to enter the market of the renewable energies. The rechargeable capacity and the battery life depend critically on the structural stability of the electrodes themselves, the electrolyte degradation rate, and the electrode-electrolyte interaction layer: the SEI. Processes that occur at the SEI in batteries are critical to battery lifetime and performance, but their details remain elusive because of the difficulty of examining the interface during battery operation. Although electron microscopy and magnetic resonance approaches have provided new insights, isotopic and time-resolved measurements using our novel *in situ* SIMS in combination with *in situ* TEM offer the potential to provide an unprecedented level of detailed information about mechanistic and dynamic processes.

For the SEI layer in rechargeable batteries, essentially, two critical questions need to be answered: 1) How do Li^+ ions migrate through SEI? Does a Li^+ ion need to pass through the SEI via some tunnels? Or is their migration similar to proton migration in water (i.e., the "Grotthus transport" model)? 2) What is Li^+ diffusivity and conductivity through SEI? Finding answers to these critical questions will enable further advancement of designing rechargeable Li^+ batteries for enhanced performance. To answer the two questions stated above, we need first to elucidate the formation mechanism of the SEI layer.

To date, many basic questions about SEI layer *in operando* are still not clear, despite many previous efforts. Critical questions include, but are not limited to: when does an SEI layer start to form? When does Li metal start to deposit on the anode surface? What is the thickness of the SEI layer at operational condition? What are major chemical components in the SEI layer?

During FY 2016, we focused on searching answers to these questions related to the formation mechanism of the SEI layer. The model system is composed of a Cu metal anode with lithium bis(fluorosulfonyl)imide in dimethoxyethane (LiFSI-DME) as an electrolyte, which is a very promising candidate of the next generation of Li^+ batteries.

Our results show that the SEI layer starts to form at about 1.5 V and almost fully forms at 2.0 V. At 3.0 V, a small amount of Li metal already deposits on the Cu electrode surface. Upon charging to 3.6 V, the Li metal layer continuously forms on the Cu electrode surface. After discharging, the Li metal is stripped from the electrode surface, but the SEI layer still stays on the Cu surface. A very interesting observation is that, after discharging, the components and thickness of SEI are very similar to those of the SEI layer upon charging to 2.0 V, indicating the SEI layer almost fully forms at 2.0 V.

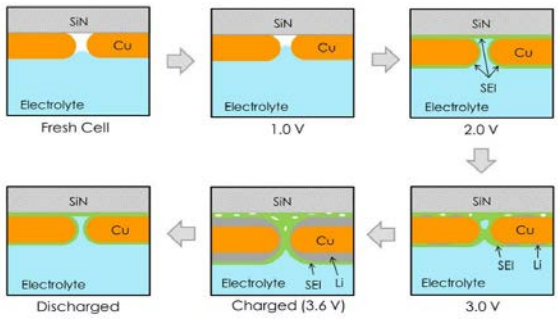

An illustration of the SEI formation mechanism based on our *in situ* liquid SIMS data.

In addition, the thickness of the SEI layer is about 10 to 15 nm *in operando*. More interestingly, lithium oxide and lithium hydroxide are found to be the major components in the SEI layer, but the concentration of lithium fluoride is unexpectedly low. Our computer simulation results show that the low concentration of fluorine in the SEI layer can be attributed to the formation of an electrical double layer at the electrode-electrolyte interface. The above findings provide key insights for designing the next generation of Li^+ batteries.

In FY 2017, for the first time, we successfully examined the Li^+ diffusion mechanism and determined the Li^+ diffusion coefficient in SEI. Our data show that 70 to 80% of Li^+ ions in SEI can be easily replaced, suggesting the “Grotthus transport” model may be more possible than the single Li^+ pass-through model. In addition, our data suggest that the Li^+ diffusion coefficient in the SEI layer is about $2^{-5}\times10^{-19}$ m^2/s at room temperature, which is much faster than Li^+ diffusion in glass (10^{-24}-10^{-25} m^2/s) and in lithium oxide (~10^{-22} m^2/s, extension from high temperature data). However, the Li^+ diffusion coefficient in liquid is about 10^{-9} m^2/s. Therefore, the property of SEI is more like a solid than a liquid.

In FY 2018, we successfully developed some exciting new capabilities. First, an innovative integration of the microfluidic cell in the *in situ* liquid SIMS to enable heating/cooling between -150 to +80°C. This innovation will be of great fundamental and practical interest. Also, *in situ* liquid SIMS was found to be softer than common electro-spray ionization, and it can be used to molecularly study ion-solvent interactions and initial nucleation of nanoparticle formation, which has been a great challenge for many years.

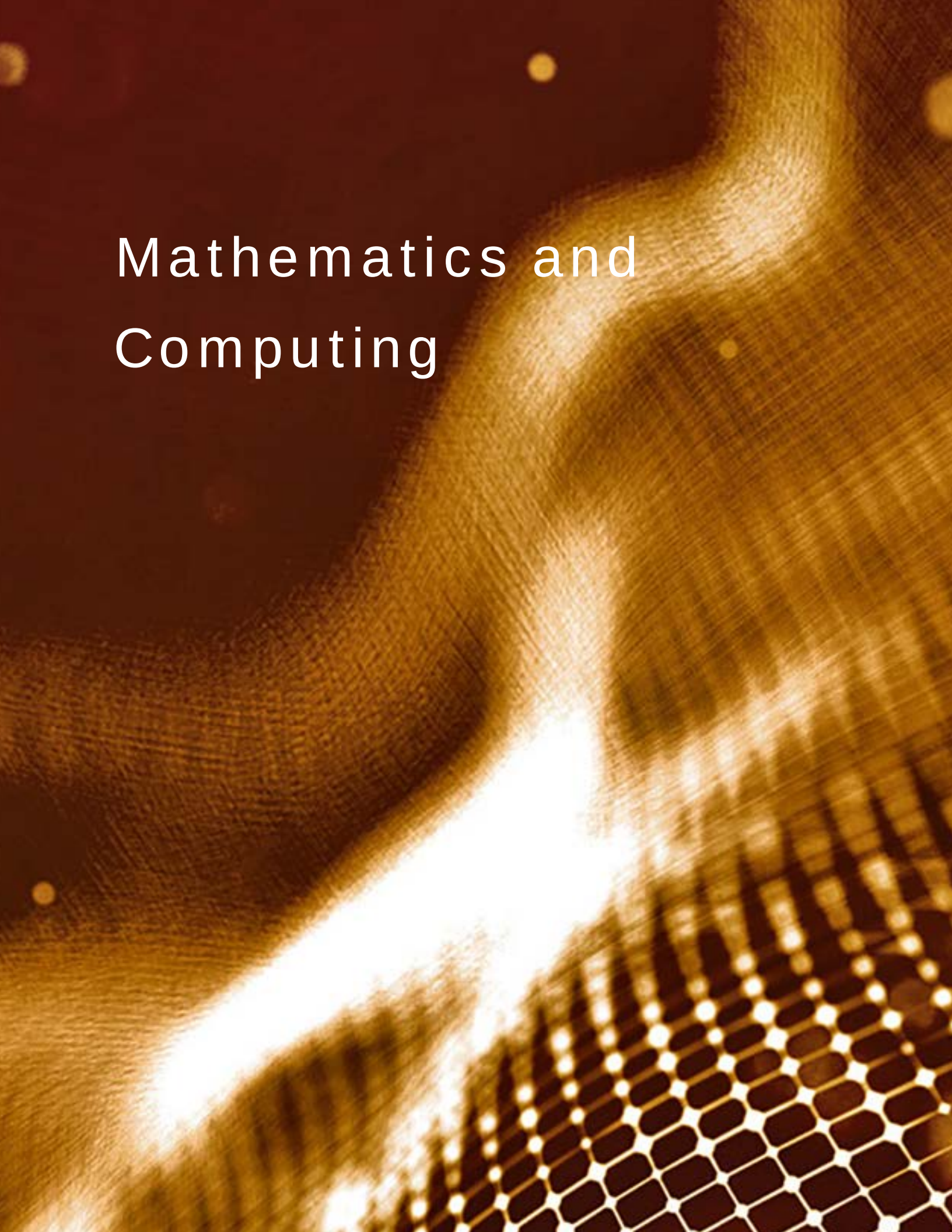
Mathematics and
Computing

BIFROST: Bounded Informational FRamework to Optimize Streaming sysTems

Luke J. Gosink
PN17065/2955

Game theory is the study of mathematical models of conflict and cooperation between intelligent, rational decision-makers. This work extends game theory to systems defined by both rational (machine) and irrational (human) decision-makers to form expectations on winning strategies, game equilibria, and characterize fairness of game rules.

Formally defining optimal performance for a streaming, complex system of systems is challenging. Operational components in these systems include a diverse array of roles, including human decision-makers and analysts tasked with maintaining situation awareness, machine learning methods that are critical for timely analysis tasks, and sensors that sample the environment based on different sensing and sampling modalities.

These components must complete their individual tasks under the constraints of shared, limited resources (e.g., compute resources, bandwidth, cache, available information, etc.). To ensure that such systems run optimally, control and decision frameworks must identify the best set of actions (from the space of all possible actions) for sharing resources and completing tasks.

This project will model the analysis processes and potential actions performed by such complex streaming systems as an Informational Theoretic (IT) problem. In this framework, each process is treated as an agent in a non-cooperative game. Bounded rational game theory asserts that each of these agents is fully "rational" and aware of the possible actions of every other agent, as well as the penalties and rewards of these actions. Based on each agents' assured rationality, this theory ensures the existence of an optimal, stable state for the system as a whole (i.e., the Nash equilibrium); any alternate state is guaranteed to result in degraded performance of the system.

BIFROST's framework benefits all domains and decision-makers tasked with ensuring optimal system performance, efficient resource management, and robust, adaptive contingency plans to address operational uncertainties.

BIFROST extends these notions to address the challenges posed by agents that may not act rationally (e.g., humans under stress). Specifically, this BIFROST addresses the theoretic difference between uncertainty and irrationality. In the first case, uncertainty about an agent's true goals, motivations, and strategies can make decisions appear irrational, when the error is actually in the way that the agent is modeled in the system. BIFROST is evaluating the hypothesis that machine learning methods can better account for these uncertainties and eliminate seemingly irrational behavior. If this hypothesis holds, many systems that cannot currently be modeled will be able to be evaluated in order to identify winning strategies and the set of optimal choices for system equilibria.

During FY 2018, BIFROST completed the mathematical formulation of its theoretic framework. This formulation is fully coded as a MATLAB™ library and is being used to evaluate a suite of test systems.

Distributed Deep Learning and System Identification for Community Detection and Classification

Enoch H. Yeung
PN17016/2906

Deep learning is computationally expensive, data intensive, and server centric. How do we create the next generation of learning algorithms that can operate in distributed computing environments and embedded systems? In short, how do we package deep learning for edge computing applications?

The modern graphics processing unit (GPU) is the workhorse for our current generation of learning algorithms. In addition to a plethora of high-performance computing solutions deployed on GPU systems, machine learning and deep learning, in particular, rely heavily on matrix and tensor operations that are naturally ported onto decades of graphics and image processing technology. The outcome is that GPU workstations, such as the NVIDIA DGX-1 or multi-GPU systems, are now the mainstay for challenging deep learning problems.

One of the reasons that deep learning is so effective is that deep neural networks efficiently search function space to discover nonlinear representations of feature spaces with complex geometry. Deep neural networks exploit the fact that a nonlinear relationship represented by data may require an exponential number of terms to capture with a certain basis, yet only a linear number of terms in another basis. During training, deep neural networks have a knack for finding efficient basis representations to solve classification and nonlinear regression problems.

In the first phase of this project, we explored integrating methods of deep learning and system identification. We developed a novel technique for data-driven discovery for governing equations of nonlinear systems using Koopman operator theory. Koopman operators provide linear representations of nonlinear dynamical systems via a change of coordinates. They enable formulation of time-series forecasting, stability analysis, and modal discovery of nonlinear processes as linear regression problems.

The outstanding challenge with Koopman operator learning is that learning a Koopman operator requires a transformation of coordinates from the underlying phase space of the nonlinear system to an often higher-dimensional phase space. In system identification problems or learning problems where the coordinates of the physical system, as well as the governing equations of the physical system, are unknown, identifying the coordinate transformation is a chicken-and-egg problem.

We developed a learning framework in Tensorflow (and Keras) that uses deep neural networks to simultaneously discover computationally efficient coordinate transformations and the corresponding Koopman operator. The power of this algorithm is its scalability; previous algorithms to discover Koopman basis functions and the Koopman operator required hard-coded basis functions incorporated by the scientist overseeing the learning problem (extended dynamic mode decomposition).

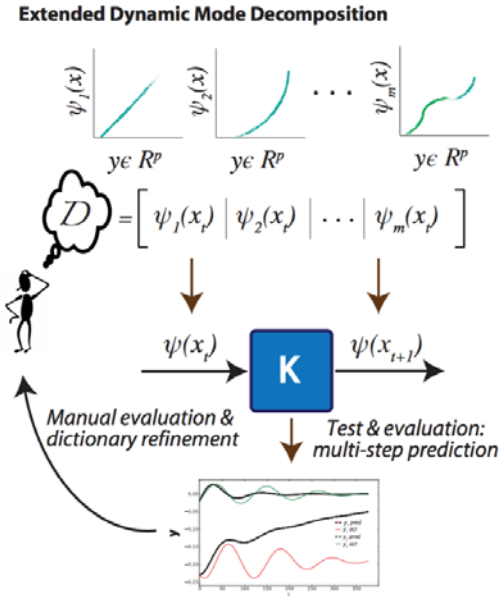

Model showing how extended dynamic mode decomposition works.

With deep Koopman learning, or deep dynamic mode decomposition, the basis functions are automatically discovered during the training process. Thousands of hypothetical bases (and combinatorial sets of basis functions) are tested in a single deep training instance. This allows deep dynamic mode decomposition to discover sparse but accurate basis sets that faithfully recapitulate the dynamics of the system.

One of our key innovations was the introduction of state-inclusive deep Koopman coordinate transformations. Since the Koopman basis functions define a nonlinear coordinate transformation, the recovery of the original state from a Koopman basis function is not guaranteed. Direct inclusion of the state in extended dynamic mode decomposition algorithms lead to explosion of the dimension of the dictionary or basis functions. We introduced a new class of state-inclusive deep Koopman coordinate transformations, inspired by the basis functions discovered in deep learning. In collaboration with researchers at IDeA Labs in Brigham Young University's Computer Science Department and the Chen research group at University of Colorado Boulder, we showed that these basis functions have mathematical properties of invariance to critical operations, which eliminate the dictionary explosion problem.

Deep Koopman operators enable discovery of the governing equations of nonlinear systems in nature and engineering. These systems can be represented by data or by models; either representation is amenable to deep Koopman operator learning. Moreover, discovery of deep Koopman operators enable spectral analysis to determine the dominant modes of a physical system and efficient basis representations of the underlying nonlinear relationships.

Our world is composed of complex, emergent nonlinear phenomena. Increasingly, many physical and engineered systems are presented in the form of data streams or signatures. We have shown that the integration of deep learning and system identification theory results in scalable learning algorithms for discovering the governing equations for such systems.

DYnamic Network Analysis via MOtifs (DYNAMO)

George Chin Jr.
PN17056/2946

The DYNAMO project is developing a graph, mining-based approach and framework that will allow humans to discover and detect graph patterns in data streams through the analysis of local patterns of interactions and behaviors of actors, entities, and/or features. We refer to these local graph patterns, which are small, directed attributed subgraphs, as network motifs.

Dynamic network motif analysis represents a graph-theoretic approach to conduct "pattern-of-life" analysis of agents or entities. Conceptually, this approach equates to identifying small, local subgraphs in a massive virtual dynamic network (generated from data streams) that have specific meaning and relevance to the user and are indicators of an activity or event. Detecting motifs in streaming data amounts to more than looking for the occurrence of specific entities or features in particular states, but also their relationships, interactions, and collaborative behaviors.

Dynamic network motif analysis allows an analyst or scientist to:

- expose relationships and interactions of an agent with other various articles or entities such as other people, computing resources, places or locations, and subject areas
- learn normal relationship and interaction patterns of different classes of agents from monitored activities
- detect when anomalous patterns occur and offer potential explanations
- facilitate encoding of hypothetical behavioral patterns or indicators for an agent to use in future detection
- provide framework for evaluating and confirming multiple indicators
- analyze temporal evolution of interactions and behaviors of an agent
- support all the above analytics in the presence of streaming data.

The two key development efforts in this project were to create algorithms to detect approximate motif patterns in a data stream and to construct an interactive framework for defining motifs for querying and monitoring. Network motif mining falls into the class of non-deterministic polynomial-time (NP)-hard graph algorithms known as subgraph isomorphism or subgraph pattern matching. A variety of subgraph isomorphism algorithms have been published over the last several decades. Graph mining through the prism of small graph structures has also been studied for decades but has experienced a recent renaissance of research interests in areas and problem spaces such as triadic analysis, triangle counting, and biological network analysis. Subgraph and motif mining in the presence of streaming data adds yet another level of complexity and uniqueness to the subgraph isomorphism problem. The project explored existing research and development in this area and implemented new algorithms to enable dynamic motif analysis.

The dynamic network analysis algorithms and framework were applied to an insider cyber threat use case. One may characterize the type of an insider agent, computer user, or organizational role by examining the modes and frequencies of its local interactions or network motifs within the cloud. For example, a cloud interaction graph may be generated from cloud telemetry data that shows a user's particular interactions with or access to specific tenants, data stores, and applications. In examining such a graph, one can look closely for small, local graph patterns or network motifs that are indicative of an insider cyber threat. Additional motif analysis of proximity card access data may identify changes in actors' work patterns (time and place) and the people with whom they interact. Motif analysis of email and phone communications records may additionally

identify an actor's interactions with other people and their associated statuses and roles.

To support a more explorative motif analysis approach, the project developed advanced capabilities to identify and capture normal motif behaviors of specific agents or entities. The idea is to automatically capture a behavioral census of motif patterns that show how an agent is interacting with other agents, machines, data repositories, devices, and other resources. Once that behavioral census is captured, one can monitor the streaming data behavior of that agent and flag when that behavior becomes anomalous or strongly deviates from its behavioral census.

The project also explored the use of random forests, neural networks, and deep belief networks to see if it could predict future motif patterns based on past motif patterns. Our initial testing was conducted with Carnegie Mellon University (CMU) Computer Emergency Response Team (CERT) insider threat data, and the deep belief networks were found to be the most accurate technique. The CMU CERT data, however, involved only a very small set of motifs, so being able to distinguish and predict across these motifs was not particularly challenging or insightful. The project continued to exercise and evolve the deep belief network approach to support motif prediction with more complex data and signals such as those emanating through the normative behavioral motif patterns described above. The project integrated this predictive analysis capability into the motif analysis framework to connect to the data streams, motif-mining algorithms, and user interface/visualizations.

The concepts of the network motif and the motif census have some very compelling characteristics for threat, event, or feature detection. They provide a simple and intuitive representation for users to encode critical patterns. They provide a structure for assessing multiple indicators. They enable a mechanism for throttling the accuracy of findings and limiting false positives by adjusting the threshold associated with the computed similarity distance measure (e.g., lower threshold equals higher accuracy and less false positives). Indicators in a motif census may be active or inactive depending on whether data is available to assess the indicator. In the case where active indicators may be alerting a potential insider or critical event, the inactive indicators identify additional data to gather and assess to further confirm or reject the alert. This enables an approach for directing humans or systems to specific areas to look for additional information or data.

EvoGraph: Highly Efficient Large-scale Graph Processing on Accelerator-based Supercomputers

Leon Song
PN17067/2957

Efficient large-scale graph processing is an essential and challenging problem, covering many areas of interest that span social network traffic analysis and power grid development to biological/ environmental research and physics simulation. In this work, we are developing an accelerator-based graph processing framework to address this issue.

High-performance machines are increasingly using graphics processing units (GPUs) to leverage their scalability and low dollar to floating point operations per second, or FLOPS, ratios. As a result, GPUs have become the main compute engines for today's high-performance computing supercomputers. This trend continues with the move toward exascale machines that are expected to be composed of millions of accelerators and general purpose cores, whether packaged as "thin" or "fat" nodes. Another recent trend is the gain in popularity of GPU processing in many domains such as social networks, e-commerce, advertising, and genomics. This has motivated the growing interest in large-scale, real-world graph processing for both scientific and commercial applications, as well as the recent efforts in accelerator-based graph processing frameworks.

An important aspect of real-world graphs, like Facebook friend lists or Twitter follower graphs, is that they are massive and evolving. Thus, there is a huge need to quickly analyze this high-velocity stream of graph data. However, state-of-the-art graph analytics for dynamic graphs follow a store-and-static-compute model that involves batching these updates into discrete time intervals, applying all of the updates to the total graph, and then rerunning the static analysis. There is considerable redundancy and inefficiency in this approach to analyzing this evolving graph sequence.

Static graph analytics on a single version of the evolving graph, even when leveraging a massive amount of parallelism offered by thousands of cores in a GPU, can be very slow due to the large scale of many real-world graphs. Additionally, data movement of the entire input graph repeatedly between the host and the GPU over the slow peripheral component interconnect express link can result in substantial overhead, which in turn can overshadow the benefits from the massive parallelism offered by a GPU. To tackle these challenges, we are developing an accelerator-based incremental graph processing framework named EvoGraph. This work includes 1) completing the design of the framework and its attached optimization strategies, 2) understanding graph algorithm's merge pattern (stateful, partially stateless, or fully stateless) for efficient targeted processing, and 3) exploring deep learning strategies for predicting future graph properties to enable effective, current computation management strategies.

An extensive evaluation of three general classes of graph algorithms (i.e., stateful, partially stateless, and fully stateless) on real-world and synthetic graph datasets demonstrates that EvoGraph can significantly outperform the existing static recomputation approaches. Compared to competitive frameworks like STINGER, EvoGraph achieves a speedup of up to 232x and overall throughput of 429 million updates/sec.

The core advancement of this year is that we utilize the framework to conduct significant research for graph property prediction. We use partial static graph, along with deep learning method, to predict what the changes are going to be for future updates. This has significance and can be applied to many domains.

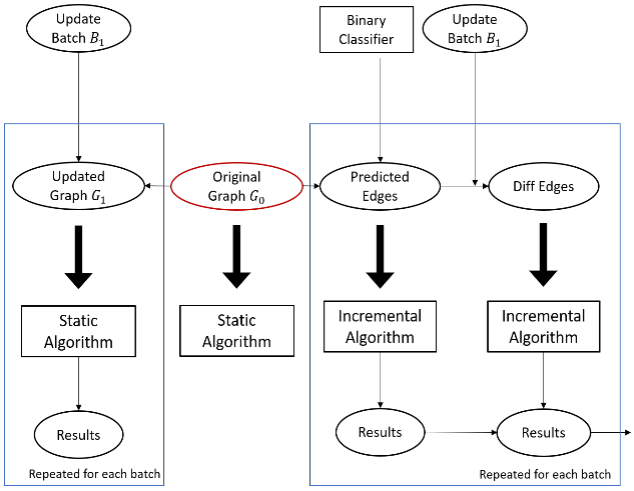

General prediction framework using partial static graph, along with deep learning method, to predict what the changes are going to be for future updates.

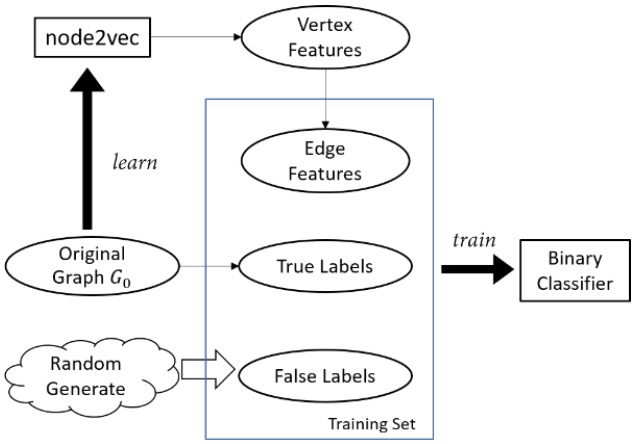

The training binary classifier.

Explanatory Question-answering on Knowledge Graphs

Sutanay Choudhury
PN18034/3033

Question-answering (QA) is one of the major challenges in Artificial Intelligence. Over recent years, the field of QA research has seen major progress in accomplishing tasks such as factoid question-answering and reading comprehension. One area that notably remains difficult is explanatory QA, where we need to answer "why" or "how" questions to explain complex events or relationships observed in the data.

We had analyzed a dataset from U.S. Customs in earlier projects. We discovered an anomaly with Ford Motors importing unusually high quantities of palladium. Whenever an analyst detects an anomaly or such an event, the next logical step is to look for an explanation accompanied by a confidence score. We can come up with multiple explanations for the observed event such as:

- Ford is a Car Manufacturer, Car Manufacturers make Cars, Cars contain Catalytic Convertors, Catalytic Convertors use Palladium.
- Ford is a Manufacturer, Manufacturers make Products, Products use Rare Earth Mineral, Palladium is a Rare Earth Mineral.
- Ford has headquarters in USA, USA was involved in cold war with Russia, Russia is major supplier of Palladium.

Selection of the best answer is not just governed by correctness; it depends on the query context and human preferences involved in interpreting the answer. Integrating deep learning with knowledge graphs for reasoning and studying human preferences for QA are the key novelties of the proposed research.

We solved a constrained version of the above problem with the following: given a pair of entities (such as Ford and palladium), return a meaningful path in a knowledge graph explaining their relationship. knowledge graphs are a critical representation that allows knowledge extracted from multiple (potentially multi-modal) data sources to be integrated into a unified structure.

Source-Destination Pairs	Binary Class	Multi-Class	Data
Tom Cruise: Bruce Lee	Acceptable	Good	Tom Cruise actedIn Legend (film). Cork Hubbert actedIn Legend (film). Cork Hubbert is type of actor. Bruce Lee is type of actor.
		Okay	Tom Cruise hasGender male. Bruce Lee hasGender male.
	Not Acceptable	Bad	Tom Cruise isMarriedTo Katie Holmes. Katie Holmes actedIn The Singing Detective (film). Dennis Potter created The Singing Detective (film). Dennis Potter hasGender male. Bruce Lee hasGender male.
Pete Carroll: Joe Paterno	Acceptable	Good	Pete Carroll is type of football coach. Joe Paterno is type of football coach.
		Okay	Pete Carroll is type of football coach. Homer Woodson Hargiss is type of football coach. Homer Woodson Hargiss is type of football player. Joe Paterno is type of football player.
	Not Acceptable	Bad	Pete Carroll is type of football coach. Chuck Collins (American football) is type of football coach. Chuck Collins (American football) is type of People from Oak Park Illinois. People from Oak Park Illinois is type of person. Joe Paterno is type of person.

Example of user feedback on QA pairs.

We developed a memory-network-based algorithm for explanatory QA. Memory networks are extensions of recurrent neural networks, where the output state of the neural network is governed by both input questions as well as an external memory, which is the knowledge graph for this case. We used the Wikispeedia dataset and YAGO knowledge base for evaluation. Wikispeedia was collected to study “human pathfinding” between divergent entities or topics.

We also performed analysis on user feedback data on questions and answers generated from the YAGO database.

In addition to the algorithm, a major contribution of this work was to develop metrics to quantify the goodness of both questions and answers in terms of their information theoretic properties, as well as human preferences.

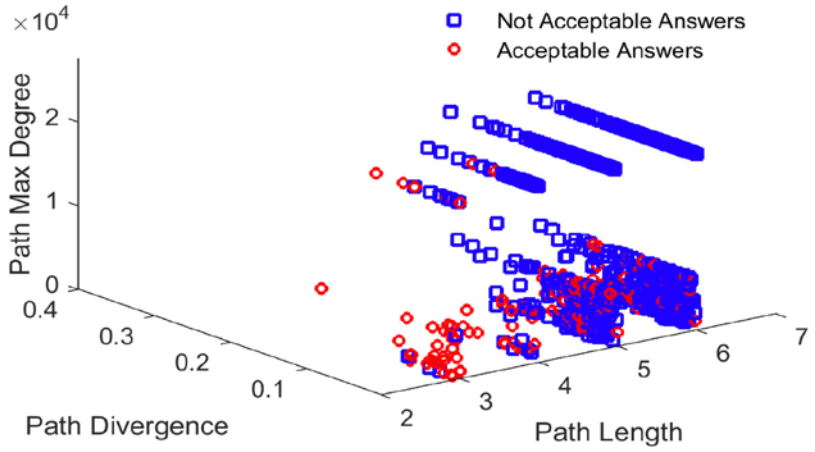

Visualization of answer quality metrics.

High-throughput Genome-to-Metabolome Computational Methods for Microbiome Metabolomics and Modeling

Ryan S. Renslow
PN16018/2795

How can we identify metabolites if standards do not exist or, critically, if molecular structures are not even known? This project's goal is to develop a high-throughput metabolite-identification approach based on a quantum chemistry, super-computer-driven software engine for application in complex microbiome metabolomics.

Metabolomic tools are limited by the ability to build libraries of compounds, which are required to identify and quantify metabolites. The premier nuclear magnetic resonance (NMR) metabolomics tool, Chenomx, has a library of approximately 900 compounds with about 11 new compounds added per year and one of the largest open-access databases, the Biological Magnetic Resonance Data Bank, has data for approximately 1,200 compounds. In both of these libraries, most compounds are derived from urine and human health-related samples.

Currently, there is no robust environmental- and microbial community-focused NMR metabolomics library, and well over 90% of the known metabolites in BioCyc are not found in an accessible library. To achieve the Department of Energy's goal of understanding, predicting, and controlling complex microbial communities, and to understand specific microbiomes undergoing transition, the capability to comprehensively identify and quantify metabolites is necessary.

Quantum chemical calculations have been used to predict NMR chemical shifts and ion mobility spectrometry-mass spectrometry (IMS-MS) collision cross-sections (CCSs) of metabolites; however, to date, these calculations have been limited to small sets of molecules. Datasets are typically arbitrarily chosen, particularly in the case of NMR, and most simulations do not emphasize compounds common in environmental sources or microbial communities. Furthermore, most simulations and current databases for metabolomics do not consider molecular conformers or custom solvent conditions.

Our novel computational research will expand the current sets of simulated molecules by one to two orders of magnitude and provide a streamlined process for generating relevant metabolite libraries from microbial genomes (or community metagenomes). Currently, there is not a unified method for generating reaction/pathway lists with corresponding metabolites to build a library for identification and quantification.

This past year, we developed a supercomputer-driven pipeline to predict NMR chemical shifts and IMS-MS CCS values for any metabolite automatically, rooted in quantum chemical calculations. Solvation effects are accounted for via computationally efficient implicit models for a reasonable description of the solvent behavior. The performance of the software has been tested successfully on a set of metabolites via a benchmark study for quantum chemical theories.

To the best of our knowledge, our metabolite set is the largest studied so far in the literature. The outperforming method gives 3.93 ppm and 0.33 ppm of error compared to experimental results for ^{13}C and ^{1}H NMR chemical shifts, respectively. The level of confidence in the computed NMR chemical shifts is currently being studied to understand the accuracy required for small molecule identification in complex mixtures.

Additionally, computationally efficient explicit solvent models are being developed for the water-solvated compounds common in environmental microbial communities to account for the behavior of water-solvated condensed phases with more accurate predictions and improved understanding of the physical processes. Another program to handle conformers automatically is being developed by our team, which is intended to be a part of our

NMR and IMS-MS metabolite prediction pipeline.

Furthermore, we investigated the minimum level of accuracy required to identify the metabolites using the set of 11,716 small molecules found in the Human Metabolome Database (HMDB). Our automated program provided calculation of NMR chemical shifts of the molecule set for the unified method, which was determined via the benchmark study. As a result, 90% of these molecules in a pure sample can be successfully identified when errors of ^{13}C and ^{1}H chemical shifts reach 3.4 ppm and 0.38 ppm, respectively. Unsurprisingly, in complex mixtures, as the complexity of the mixture increased, greater and greater accuracy of the calculated chemical shifts was required.

During FY 2018, molecular conformers were also considered, and solvation effects were taken explicitly into account, in order to decrease the error of our calculations compared to experimental results. Ultimately, our research is expected to identify currently unknown metabolites and, overall, to build a metabolome library specifically for microbiomes and environmental samples.

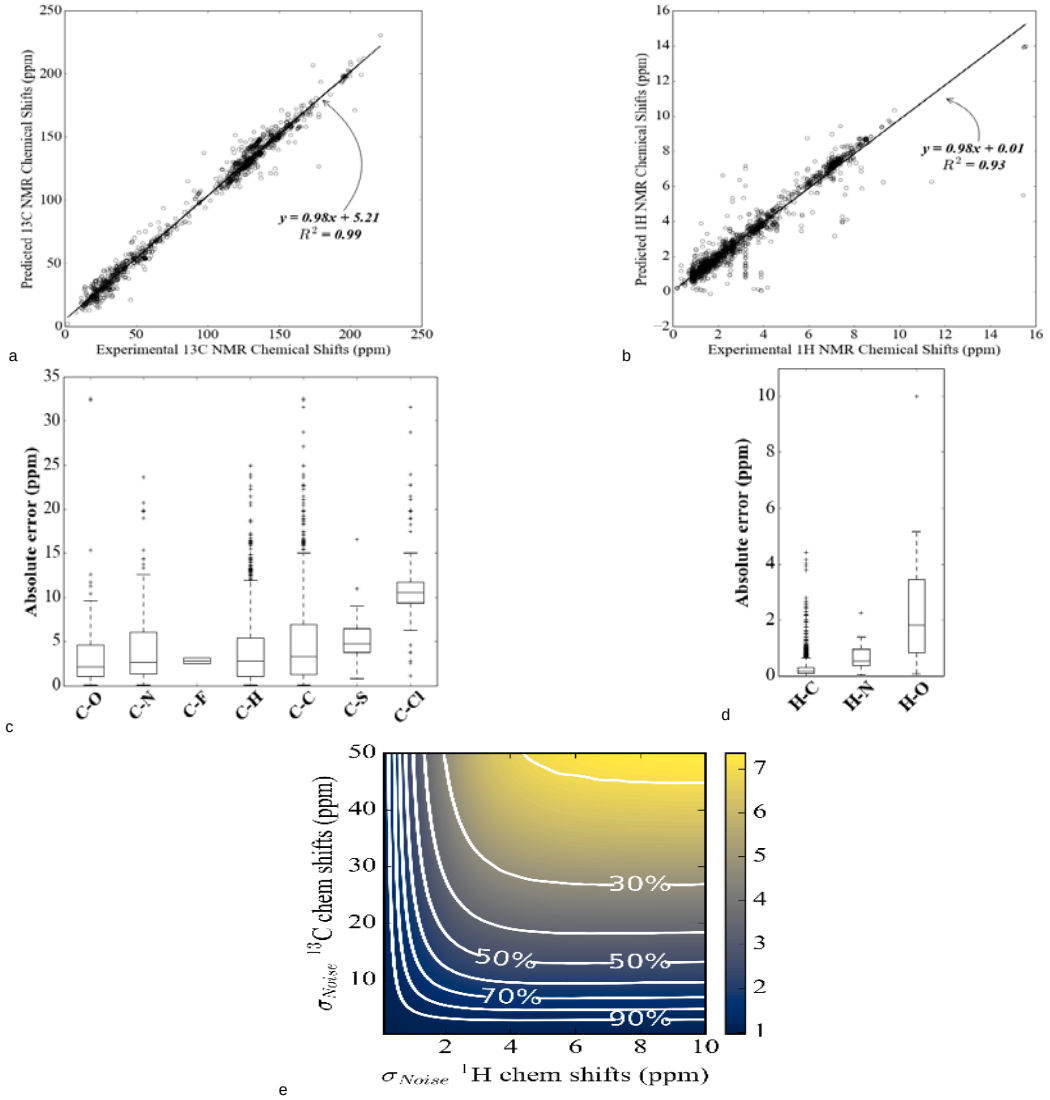

Performance of the quantum chemical calculation pipeline: a & b) plots of calculated ^{13}C NMR chemical shifts versus experimental ^{13}C and ^{1}H NMR chemical shifts, respectively (these figures illustrate how the calculated chemical shifts are close to experimental data); c & d) plots of absolute errors found in different functional groups bonded to ^{13}C and ^{1}H NMR chemical shifts, respectively; e) plot showing the minimum level of error for various levels of identification with respect to ^{13}C and ^{1}H NMR chemical shifts' errors.

Modeling Continuous Human Information Processing

Leslie M. Blaha
PN16096/2873

This project seeks to identify models and related metrics for dynamic decision-making to support the development and evaluation of adaptive interfaces for interactive streaming analytics.

Analyst behavior in a streaming visualization environment demands online, continuous decision-making. Modeling human decision-making, in general, requires formal mechanisms to characterize information accumulation, choice biases, and trust or reliance on the machine intelligence supporting the analytic activities. Models of decision-making, particularly from the human information processing perspective, can tease apart the mechanisms involved in the decision-making process based on non-invasive behavioral data, namely response choice and response time. Existing models capture discrete decision events in static environments.

To capture continuous decision-making, we seek to extend information processing models of decision-making to capture both the discrete decision events and the cognitive dynamics for waiting and monitoring in between explicit decision events. This requires theoretical extension of response time modeling approaches, incorporating exploration of the correlations between sequential decisions.

Additionally, we want to test novel measures of performance based on both total response time and motor dynamic of executing the response. The full dynamic profiles provide insights about the decision-making as the process unfolds. We will develop appropriate metrics to enable use of these dynamics to inform and evaluate the design of analytics interfaces. We further seek to integrate assessment of workload and trust, to understand how the decision-making behaviors are influenced by the characteristics of the interactive environments people are leveraging to complete complex tasks.

The first step of the research was to evaluate models of decision preparation dynamics as candidates for modeling the cognitive behaviors between specific decision-making events. We identified a successful candidate model of decision anticipation, which predicts the likelihood that an event requiring a decision and response will occur at different points in the foreperiod (the time prior to the onset of the stimulus or event cue). The model captures probabilities of cuing events occurring as a function of the time since a response or an alerting event indicating the start of a decision-making trial. Model simulations show that the model predicts a series of important response time effects, including the foreperiod effect, in which the duration of waiting time affects the speed of responding. Preliminary model fits have been conducted against the average data values from a continuous detection task requiring sustained attention, the psychomotor vigilance task.

We have made additional, parallel strides in the use of Gaussian process models for functional analysis of hand and eye movement behaviors. A new, functional version of Fitts' Law is the result of modeling hand movement data, which we have demonstrated on touchscreen interaction data for two-dimensional movements. We developed a data-driven approach to classifying eye movements according to the movement dynamics. This approach extracts estimates of gaze position, velocity, and acceleration and uses a beta-process vector auto-regressive hidden Markov model to group those dynamics into unique classes of gaze behavior. We can map those to known movement types, like saccades, fixations, and smooth pursuits, in a way that adapts to variability in the data characteristics.

To support the study of dynamic time series of data simulated or captured by these models, we collaborated with the User-Centered Hypothesis Design program to develop a storyline visualization technique for eye movement data. This technique leveraged dynamic time warping for aligning data from multiple human observers viewing movie clips. We found patterns of similar behavior, which likely reflect people who have similar task strategies.

We have made strides in establishing foundational methods for assessing strategies and workload efficiency in continuous multitasking. We have established that the capacity coefficient of response times can be used for a more nuanced analysis of workload efficiency, instead of or in addition to standard dual task assessment measures. As a testbed for this work, we developed the Modifiable Multitasking Environment (ModME) software to support flexible, dynamic multitasking.

To advance our modeling of decision-making when more autonomy or machine intelligence is integrated to aid the analyst, we developed the Cognitive Behavioral Analytics Testbed (COBALT). This environment simulates operation of multiple unmanned air vehicles (UAVs) that must be used to complete an object search task. It provides automated aids and representations of information with variable reliability. We can demonstrate leveraging this complex environment for modeling decision-making, workload, and the user's trust and reliance on the aids in the system, using the models discussed above. We can advance this capability to examine various concepts of operations for people working in similarly complex environments and will seek to integrate the models into the system to test concepts of real-time adaptivity support for human decision-making tasks.

Collectively, we are advancing fundamental capabilities needed to achieve human-machine teaming in dynamic environments. The results of this work provide a new set of models, metrics, and visualizations that can be used to characterize user performance in interactive streaming analytics tasks. We also advanced the science of usability evaluation, while enabling the study of the cognitive mechanisms behind interactive streaming analytics decision-making.

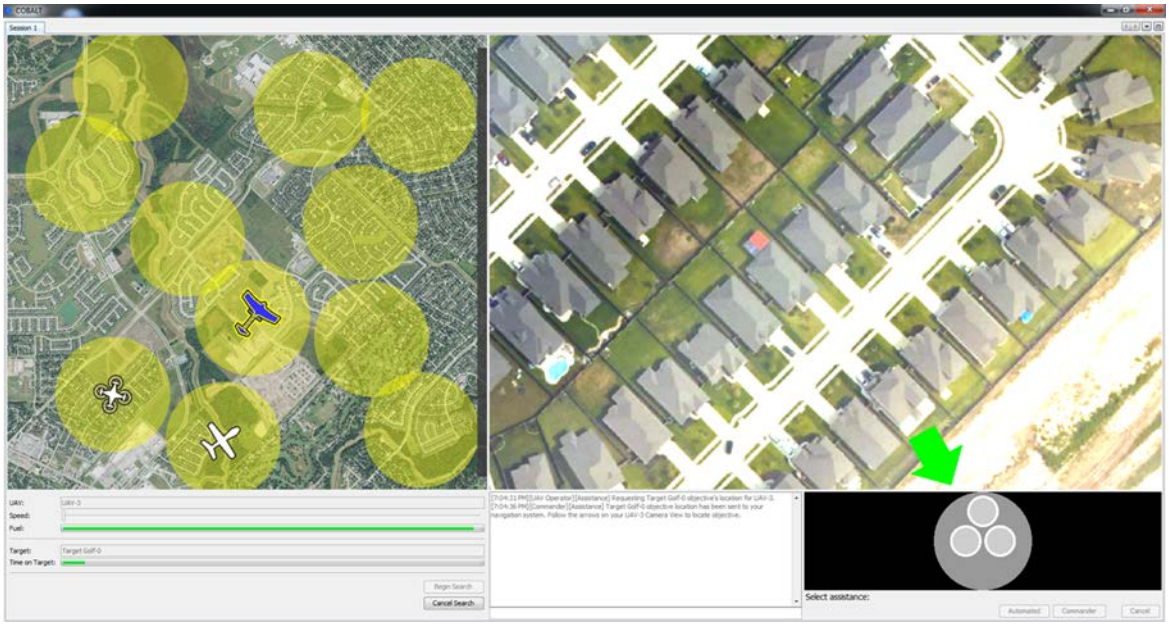

COBALT, designed as an experimental platform for jointly assessing dynamic decision-making and trust/reliance on automated machine aids. The overall task is based on multi-UAV control, where an operator must use UAVs to help find objectives in overhead imagery. Automated aids are available to help but vary in their reliability. The interface allows multiple ways of representing information about the sensors to help analysts decide to rely on them or not. COBALT enables evaluation of concepts of operation, leveraging machine intelligence with varying reliability and transparency, on decision-making efficiency, workload, and trust. COBALT will be made available through open-source release.

Predicting the Predictions: A Visual Analytic Workflow for Data-driven Reasoning about Climate Model Predictions

Aritra Dasgupta
PN17013/2903

A current major challenge in climate science is the establishment of appropriate methods and tools to assess the ability of climate models to faithfully simulate observed past and present climate. Novel data analysis tools have the potential to dramatically speed up the calibration of scientific models and lead to improved understanding of, and new scientific insights into, complex model behaviors and the physical processes they represent. To this end, we are developing and evaluating a visual analytic workflow for supporting and distilling expert understanding of the agreement of model predictions with observations (commonly termed model "fidelity") and exposing their dependencies on complex combinations of model parameters.

Climate model fidelity is measured by the degree of consistency between models and observations for specific model output variables or features. Scientists frequently summarize aspects of the model's fidelity, using statistical metrics such as (but not limited to) the root-mean-square error, correlation, and relative variance of the model output variables compared to observations of the same variable.

Because a credible climate simulation requires reasonable simulations of many different physical processes and state variables, it is typically not sufficient to evaluate models on a single metric; instead, models must be compared across a suite of such metrics, leading to a more complex analysis situation. In addition, identifying models that exhibit similar or dissimilar patterns of performance across a suite of metrics may lead to important insights into model behaviors.

However, for such multi-model, multi-variable, and multi-metric analysis, two key problems exist. First, there is a lack of analytical solutions that let climate scientists compare across hundreds of combinations of models, variables, and metrics for developing alternative hypotheses about good or bad model behavior. Second, there is a lack of consensus in the climate science community about the relative importance of different variables and metrics in classifying model performance as "good" or "bad."

To address these problems, we are developing and evaluating visualization techniques and statistical methods that will better enable climate scientists to elicit their expert judgment in the analysis process. We hypothesize that these analytical techniques will lead to a much more reliable and efficient climate modeling workflow, as compared to the current state of the art.

Some of this project's accomplishments include developing novel model fidelity visualization techniques that are more preferred by experts and, in some cases, more accurate than existing techniques; conducting a broad survey for eliciting expert judgment about relative importance of model outputs; and developing an interactive visual analytic tool allowing experts to simultaneously compare hundreds of models and incorporate expert knowledge in ranking models based on their performance.

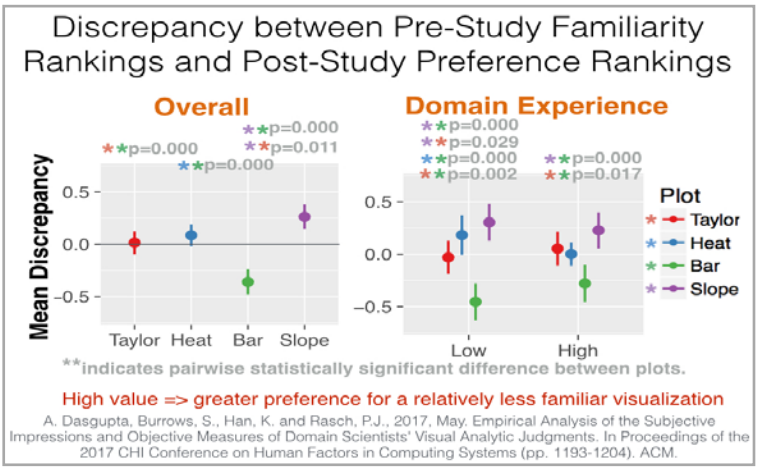

Novel visualizations for climate model fidelity analysis were objectively more accurate and preferable by most climate scientists.

Robust Statistical Data Exploration and Analysis for Microbiome Metabolomics

Lisa M. Bramer
PN16017/2794

As capabilities to detect and quantify abundances of small molecules grow, the need for integrative and robust statistical methods for exploratory data analysis, data normalization and quality control, and biomarker discovery are needed for impactful and interpretable biological research. This project aims to improve analysis methodologies, develop a robust and reproducible biomarker discovery process, and improve the quality and reduce the time to reach meaningful results integrating multiple heterogeneous data types.

The microbiome response to perturbation is first observed as changes in the metabolome, followed by changes in the metatranscriptome and metaproteome and, ultimately, to the metagenome in the case of a chronic perturbation. However, the analysis of metabolic data from complex microbiome communities poses several challenges: multiple analytic platforms are available, each with unique capabilities and differences in run-time variability and, therefore, varying data analysis requirements.

The ability to perform exploratory data analysis (EDA) is the critical first step in analyzing such data. EDA is of paramount importance for the purposes of assessing data quality, determining relationships among explanatory variables, assessing relationships between explanatory and outcome variables, and making a preliminary selection of appropriate models. Metabolomics data from a microbiome has unique challenges for the EDA process. The biochemical relationships between variables (metabolites) are often complex and, in the presence of other confounding variables, such as censored or missing data, traditional statistical metrics (e.g., correlation) are insufficient, and data quality procedures become extremely difficult, sometimes resulting in large amounts of data going unused or being underused.

This project aims to modify existing methodologies and develop new ones for EDA, data quality control, and normalization to identify important biological relationships based on multiple sources of ’omics data. These methods and algorithms developed will be deployed in an interactive framework, allowing researchers to actively investigate data in a manner flexible to multiple data types. Finally, this project aims to be scalable to large amounts of data that are produced in biological experiments. It will do so by using a divide and recombine paradigm that allows for high-performance statistical computing and integration into high-powered visualization tools, which can be combined with statistical metrics.

In FY 2018, we further developed a streamlined framework for data management that is generalizable across data types. This structure was developed in the form of an R package, “pmartR,” providing the framework for reproducible research and automated reporting and tracking of data filtering, normalization, etc. We developed functionality for analyzing and visually exploring data generated by PNNL’s Fourier transform ion cyclotron resonance (FTICR) instrument, which is utilized across many biological experiments. These functions were implemented in an R package that deploys the data in an interactive environment, allowing the researcher to effectively explore and interact with large amounts of data.

We further extended this to a user interface for researchers to use without requiring knowledge of statistical programming. This FTICR R Exploratory Data Analysis (FREDA) tool was deployed and is publicly available. These packages and tools were used in collaboration with several biological experiments and are now deployed on FTICR data generated for any Environmental and Molecular Sciences Laboratory user proposal.

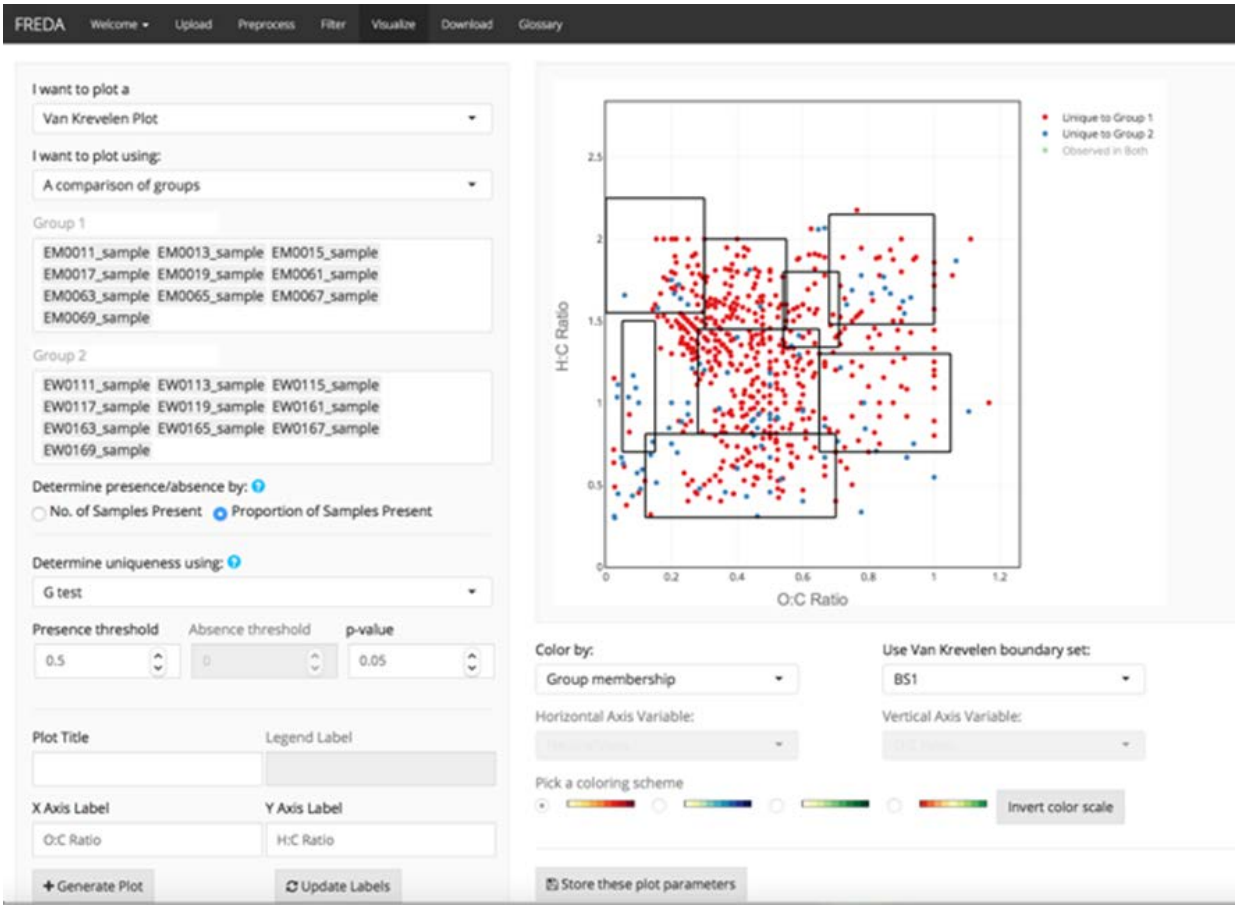

Screenshot of FREDA's visualization page.

SQUINT: Streaming Query User Interface

Dustin L. Arendt
PN17054/2944

This project addressed an often-overlooked challenge with building effective machine learning models—acquiring labeled data necessary to train supervised learning models. We developed an architecture, CHISSL, that allows an analyst to rapidly explore and annotate large datasets and then deploy predictive machine learning models.

Better models, more powerful hardware, and higher-quality training data has led to significant advancements in supervised machine learning over the past decade. While state-of-the art deep learning models are available as open source, and graphics processing unit (GPU)-accelerated deep learning hardware is relatively inexpensive, high-quality training data is only available for a few general applications. Building models for specialized applications is challenging because of the scarcity of domain experts—crowdsourcing annotations is not always possible. Visual interactive labeling (VIL), an alternative to Active Learning (AL), may better address the challenges of acquiring labels from a few domain experts, but technical and design challenges prevent its widespread adoption.

To address these challenges, we developed CHISSL, a scalable, semi-supervised machine learning technique, appropriate for either AL or VIL, that allows a user to obtain immediate model predictions and recommendations after every interaction. This technique was designed to address threats to scalability posed from both computational and visual (i.e., human) standpoints. Our solution is a scalable, approximately 1-NN classification algorithm with $O(n)$ time and space complexity. The algorithm is "representation free," allowing user feedback to be incorporated without consulting the original feature matrix. This makes the algorithm both memory- and central processing unit (CPU)-efficient and suitable for exploring and annotating large datasets in lightweight web clients with many simultaneous users.

The responsiveness and simple design of our system encourages rapid iteration and hypothesis testing—an analyst can build and deploy a classifier without any initially labeled data within minutes.

CHISSL fits into the bigger picture for a streaming data analytics workflow. An analyst first defines a simple query to sample streaming data, which generates a raw, unlabeled data set. The raw data is transformed into a matrix representation that is usable by machine learning algorithms. This representation is clustered to reveal broad/hierarchical trends and fed into CHISSL's user interface. This allows an analyst to rapidly explore and annotate the clustered data. The interface is fast and intuitive—the analyst drags and drops examples of the original raw data to form customizable groups, allowing for the analyst to discover "unknown unknowns" during the exploration and annotation phase. The analyst can send intermediate annotations back to the representation learning phase where the subsequent clustering can be improved by user feedback. Then, the analyst can combine the recommended labels from our algorithm with the original data to train a supervised machine learning classifier. This allows new downstream data to be binned into the user-created groups, enabling, for example, more semantically meaningful alerts or a user-tailored streaming dashboard.

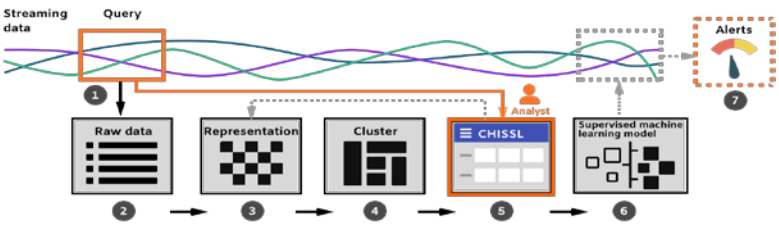

CHISSL supporting a streaming data analytics workflow by allowing a model to be rapidly built from a query and deployed back on the stream to provide situation awareness or alerting, for example.

A thorough computational evaluation showed that our approach is competitive with several off-the-shelf supervised and semi-supervised classification algorithms when using very small amounts of labeled data. We conducted a user study revealing that participants were more accurate using our interface design compared to a traditional AL design. Our system has been applied to a multitude of standard benchmark application domains including image, text, and structured data analysis, as well as specialized use cases in pattern-of-life analysis for insider threat detection and cloud telemetry analysis. In these use cases, we found our technique allowed the analyst to easily discover “unknown unknowns,” making it superior to AL approaches, where the analyst must begin with a clear concept of the class structure in the data.

CHISSL applied to PNNL cloud ceilometer data. Each card is a visualization of one virtual machine’s resource utilization (i.e., memory, CPU, disk IO, network IO) in a one-hour time block. The user is able to organize data by dragging and dropping examples.

Stream Adaptive Foraging for Evidence (SAFE): Human-computer Co-assisted Signature Discovery and Evidence Generation for Streaming Data with Deep Learning

Nicole M. Nichols
PN16044/2821

Some of the most pressing machine learning applications, such as cyber security and multi-sensor data monitoring, lack sufficient ground-truth data to build a supervised classifier. We solve this problem by using unsupervised deep learning techniques to determine when data were anomalous from a baseline norm and provide interpretable event identification to the system's user.

Traditional modeling methods require either expert-derived features to construct models or large volumes of prior example data. Cutting-edge, deep learning approaches are now been used to characterize complex events, but they have generally not been applied to the streaming environment. However, these techniques require a great deal of data, which is typical of large-scale streaming data applications.

We demonstrated the use of an autoencoder and relevant featurization techniques to both learn a feature space and then identify anomalous portions without the aid of labeled data or domain knowledge. We have additionally developed capability to work directly from raw data streams of arbitrary format. In this way, we demonstrate the detection of anomalous features without domain knowledge or tagged examples and delivered these features to users.

In FY 2016, the SAFE project developed initial autoencoders and other deep learning techniques for finding the most relevant data from a stream. Models were dynamically trained on numeric or event-based data streams and generated estimates for reconstruction of these same streams. The difference between the input and reconstructed data at every point was compared to determine where rare or unexpected behavior happened in the data set. This method was applied to find real and synthesized heart conditions. Using an aggregate featurization technique and initial Computer Emergency Response Team cyber data, we showed the capability of these methods to both enhance the likelihood of detecting these events in real time and to deliver likely reasons the identified behavior was anomalous.

In FY 2017, we applied the extremely positive results of these methods to several additional data sets, including Los Alamos National Laboratory (LANL) cyber security data and VOLTTRON™ building efficiency sensor data.

We also extended this capability by introducing a new processing method that works directly from raw system logs. This eliminates the cumbersome step of generating aggregate features that can unnecessarily restrict the expression of input data, as well as extending time to deployment. This new capability uses a two-tiered model, where the first tier learns to encode sequences of characters or tokens, and the second tier provides the temporal context across the history of raw logline data. In a standardized comparison, processing the raw loglines showed better performance than the aggregated feature methodology.

Several approaches to visualization were created to demonstrate presentation of detected anomalies to a user and provide supporting information.

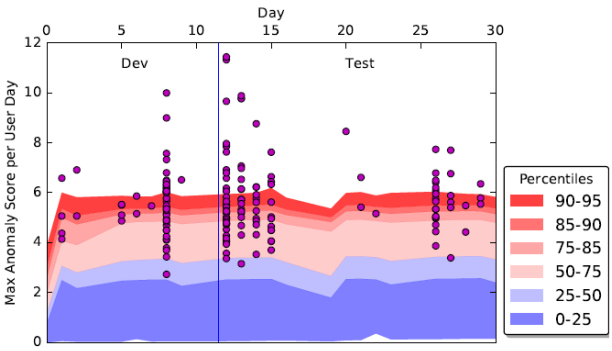

Example of anomaly detection using SAFE Technique for LANL cyber security data.

In FY 2018, we extended the work on interpretability and investigated semi-supervised techniques. We implemented an attention mechanism for the long short-term memory model. This introduces shortcuts in the flow of information on the computational graph, which can yield insight to the model's decision process. By plotting the relative weights on the sequence tokens, we can identify which had the highest impact on the output prediction.

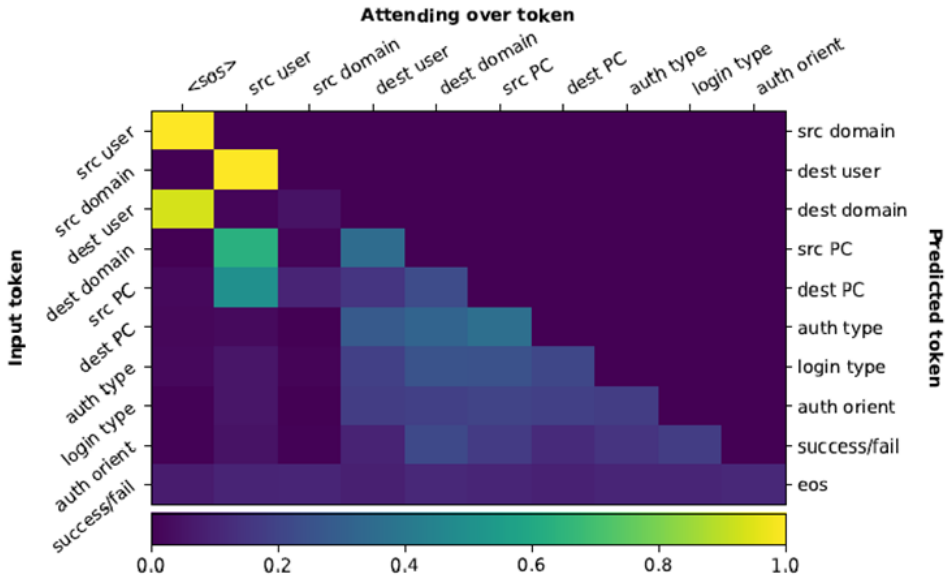

Average syntax attention weights and example of importance patterns that emerge.

Temporal Modeling in Streaming Analytics

Bryan A. Stanfill
PN16039/2816

As data recording capabilities continue to grow, research on classification and predictive modeling on data in near real time plays an important role in modern data analysis. This project aims to improve current streaming analysis methods—making model output more useful and timelier to decision-makers—by leveraging the temporal nature of streaming data.

Machine learning algorithms can easily be implemented on streaming data. In traditional machine learning settings, both supervised and unsupervised learning algorithms operate under the assumption that the data is stationary (i.e., the mean and covariance structure are the same for all parts of the dataset), and observations are independent of one another. Analytic methods for streaming data must differ from standard machine learning practices, because in the streaming context, there is a continuous flow of data rather than a static set of data, the data distribution is expected to evolve over time, and observations are seen over time in sequential order and likely are not independent.

This project aims to broaden the understanding of the role that temporal dependence has on the performance of state-of-the-art algorithms for streaming data. This will be accomplished by leveraging the temporal nature of streaming data sources to improve prediction and classification analytics capabilities by incorporating temporal information into algorithms and models for streaming data. These new methods will be computationally scalable to operate within a streaming environment.

Additionally, we will strive to provide insight into quantifying the benefit of incorporating temporal information into predictive models over a variety of conditions.

Finally, we aim to develop methods for integrating multiple data sources that may be observed at different and/or irregular time scales, which generate reliable predictions at user-specified time steps.

In FY 2018, we refined several models and algorithms initially created in previous fiscal years, which incorporated temporal dependence, and applied these algorithms to three unique domains: electron microscopy, remote sensing, and social media—with data collected in a streaming context.

Aerial radiological survey data downloaded from Lawrence Berkeley National Laboratory's data cloud. The green lines indicate the areas of the flight path that were classified as background. An artificial source was inserted and successfully detected in the upper-right corner, indicated by the bright area in the flight path.

For the electron microscopy (EM) use case, we refined and extended the methods developed in previous fiscal years for sparsely sampled images from a microscope. The method previously developed to quantify features in EM experiments was made faster and more automated to deal with arbitrary experiment conditions and to give near-real-time results. We successfully applied the event quantification algorithm to several new types of *in situ* experiments, including sophisticated nucleation experiments where events are differentiated based on both grayscale value and event

shapes, which vary based on the nucleation site relative to the field of view.

The methods developed in the EM use case were adapted to identify anomalies in remotely sensed data in the form of gamma ray spectra collected during aerial radiological surveys. To illustrate this capability, we analyzed a publicly available gamma ray spectra dataset made available by Lawrence Berkley National Laboratory's Gamma-Rap Data Cloud. To quantify the accuracy of our method, we inserted an artificial signal in the data. Our methods were able to correctly classify most of the flight path as background but still identify the artificial source.

The social media work started in FY 2017 and continued in FY 2018 has provided many success stories. The multivariate anomaly detection algorithm has been used in social media data streams for many sponsors with successful anomaly detection reported almost every time. The algorithm uses a non-parametric approach that accounts for temporal and multivariate dependence.

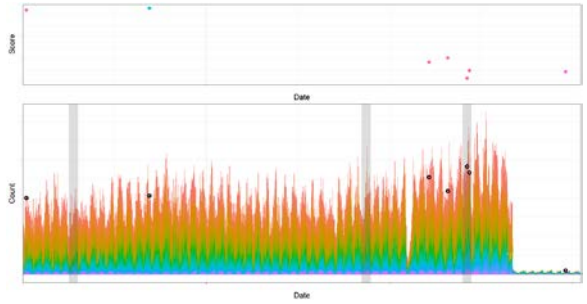

(Lower) Normalized social media volumes for multiple streams (denoted by color), with events detected by multivariate algorithm denoted by points and known anomalous dates denoted by gray bars. (Upper) Streams contributing to anomalous event score with magnitude of anomaly shown.

Despite the success, the multivariate anomaly detection algorithm is limited to detecting outliers. Often in social media, a trending alert is also necessary. To address this limitation, the mean drift algorithm was developed. It detects trending topics and can report flags during either an increase or decrease in volume. It uses both univariate and multivariate non-parametric slope estimation to detect trends.

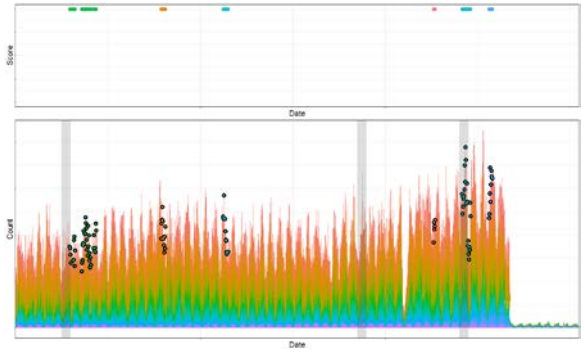

(Lower) Normalized social media volumes for multiple streams (denoted by color), with events detected by mean drift algorithm denoted by points and known anomalous dates denoted by gray bars. (Upper) Streams contributing to anomalous event score with magnitude of anomaly shown.

Test Bed Federation Tools for Control of Complex Systems Research

David O. Manz

PN16004/2781

We are enabling high-fidelity experiments on complex systems by designing and implementing tools for federating geographically dispersed test beds to support the sharing of cyber and physical resources for collaborative experiments on control of complex systems such as the electric power grid.

The highest form of research evidence is gained through experimentation with real systems. However, when attempting to research systems like buildings and their interaction with the power grid, it is impossible for one research organization to fund and support enough equipment to model at realistic scale and complexity. The most reasonable solution is to collaborate among the research community to achieve the desired scale and complexity to fully explore new control architectures, paradigms, and algorithms for operational use. This project focuses on developing the tools necessary to enable federation among individual test beds that are geographically dispersed.

A goal of this work is to facilitate formation of a coalition of facilities owned and operated by multiple participating organizations. The tools needed for enabling this collaboration include secure tunnels across the internet, access controls, experiment model sharing, and information and control transmission. Specific needs for tools will be defined in a parallel effort of all participating organizations.

This project supports identification of the needs for tools, design of a system necessary to fulfill requirements, and implementation and testing of the tools. To foster collaboration and speed progress, the tools developed will be packaged so they are easy to distribute to partners for operation within their test bed environments. This packaging can include the creation of an operating system image, a virtual machine (VM), or even a prebuilt and preconfigured piece of hardware. We have identified the following three options: 1) a VM, 2) a bare-metal installation, and 3) a portable, deploying hardware solution to bring the resources to the collaborators. As every organization has their own policies and acceptable risk levels, the tools are being developed with as much flexibility as possible. This flexibility can extend through every layer of federation, including multiple types of tunnels with varied security protocols, multiple field protocols, and multiple methods of integrating equipment.

As the goal of the test bed is to study new control methods, the federation tools also must enable the distribution, management, and operation of control logic. In support of this goal, the federation tools team is investigating the use of the VOLTTRON™ platform, developed at PNNL, as one of the tools to enable the distribution of control agents into collaborator test bed environments.

In FY 2016, the initial design of the federation tools was created. This design includes the packaging of the tools within a VM that can be shared with collaborators. The VOLTTRON platform provides a translation interface that allows communication with devices on collaborator sites, from operational protocols like Modbus to a routable protocol like the VOLTTRON Interconnect Protocol. Initial implementations of this design were created to start discussions with collaboration partners.

In FY 2017, the design was improved based on collaborator feedback. The VM approach was augmented with a bare-metal installation for collaborators who are unable or unwilling to run virtual machine images that PNNL produces. In addition to this approach, initial designs have been made on a hardware-in-a-box solution that can bring limited collaboration resources to the partner sites, if needed. Additionally, trial federation has been conducted with one collaborator, and multiple collaboration sessions walked them through the federation connection process. The pilot ended in a full end-to-end connection being established.

In FY 2018, we shifted from design into more substantial piloting and testing. The focus for the

initial pilots directly addressed more deliberate and integrated collaboration among multiple sites. Currently, all parties were more focused on pairwise federation instead of multiple-party federations. We were, however, able to accomplish this by parallelizing pairwise federation. Either way, the collaboration among parties enabled live distributed experimentation, and the study of control methods applied to complex systems was pursued not only for performance and reliability, but also for distributed control.

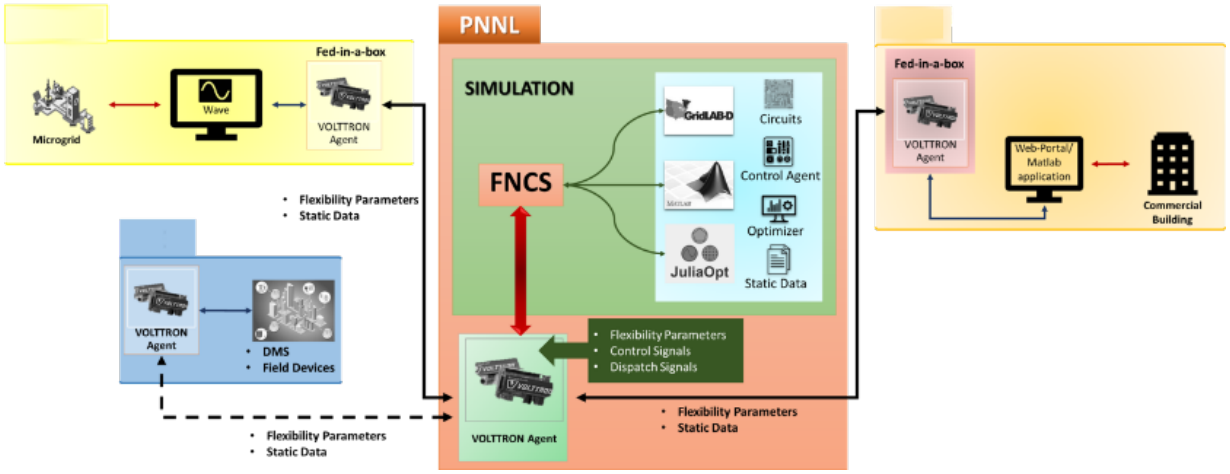

Example federation diagram.

Towards an Understanding of the Role of Hydration and Hydrodynamic Forces in Modeling Synthesis

Huan Lei
PN17034/2924

Our research aims to develop an accurate and computational framework for modeling nanoscale multiphase fluid in presence of non-local interfacial energy and thermal fluctuation, potentially leading to deep understanding of the fundamental mechanisms and control of the formation of hierarchical structures composed of simply shaped rods, bricks, and sheets interacting in aqueous solution.

During the past few decades, theoretical modeling of the self-assembly of hierarchical structures has been dominated by focusing solely on the role of repulsive forces under the conditions of packing that give rise to the formation of complex structure. Herein, we focus on additional solution-mediated forces for a more traditional approach to nanoscale synthesis. These forces have their origin in the theory of hydrophobicity. Moreover, the dynamical response of a fluid that gives rise to a non-trivial hydrodynamic interaction may be an important ingredient in understanding the kinetics of synthesis at the nanoscale.

Currently, there is no such well-established framework for the aforementioned problem. Our aim is to establish quantitative understanding of the interplay and propagation of the molecular-based fluid-mediated interactions and their effect on assembly of hierarchical structures at the macroscopic scale. In particular, we will focus on the role of hydrodynamic and hydration forces on the process of assembly. The forces will likely depend on the molecular details that modify the solid-liquid boundary and the ultimate pathway to synthesis.

We develop computational methods for the study of fluid-structure interactions subject to thermal fluctuations when confined within channels with slit-like geometry. The methods take into account hydrodynamic coupling and diffusivity of microstructures when influenced by their proximity to no-slip walls. We developed stochastic numerical methods subject to no-slip boundary conditions using a staggered finite volume discretization. We introduced techniques for discretizing stochastic systems in a manner that ensures results consistent with statistical mechanics. We showed how an exact fluctuation-dissipation condition can be used for this purpose to discretize the stochastic driving fields and combine with an exact projection method to enforce incompressibility. We demonstrated our computational methods by investigating how the proximity of ellipsoidal colloids to the channel wall affects their active hydrodynamic responses and passive diffusivity. We also studied, for many interacting particles, collective drift-diffusion dynamics and associated correlation functions.

We expect the introduced stochastic computational methods to be broadly applicable to applications in which confinement effects play an important role in the dynamics of microstructures subject to hydrodynamic coupling and thermal fluctuations.

At nanoscale, lubrication theory shows limitation to model the hydrodynamic interaction between solid particles due to the breakdown of the solvent incompressibility. In particular, the local compressibility shows pronounced effects on the dynamics of the solid particle. To quantify this effect, we have conducted numerical studies based on the smoothed dissipative particle dynamics to model the hydrodynamic interactions between spherical particles.

Our previous study showed that this model can successfully characterize the coupling of the local compressibility and the thermal fluctuations, which yields nanoscale non-local interfacial energy (surface tension). In this study, we computed friction tensor between two spherical particles of different radius. While the friction tensor is consistent with the lubrication theory for the large-size particle, the friction tensor shows smaller values than lubrication theory for nanoscale particles (less than 100 nm). This result is also consistent with the

molecular dynamics (MD) simulation results reported earlier.

This study indicates that the continuum theory based on lubrication theory (or Stokes's dynamics) may show the limitations to characterizing dynamics of nanoscale colloid particles in aqueous environments. We need to develop a more sophisticated computational framework, which will enable us to accurately impose the nonlocal hydrodynamic interaction and interfacial energy.

The studies presented above indicate that it is a challenging task to accurately model dynamics of nanoscale colloid particle suspension in presence of non-local hydrodynamic interactions, interfacial energy, and thermal fluctuations. One possible computational framework was developed in our earlier work, where the solvent is explicitly modeled by Lagrangian particle method. However, for large-scale systems, such framework could be computationally expensive.

This motivates us to develop a new computational framework with implicit modeling of the solvent. Unlike the lubrication theory and Stokes's dynamics, the hydrodynamic interaction is modeled as the non-local memory term in the dynamics of colloid particles. While directly solving this non-local memory term is computationally intractable (theoretically, we can solve it by Mori-Zwanzig projection), we employ a data-driven parametrization procedure to learn the memory term directly from the data set collected from explicit-solvent simulations. The thermal fluctuations are imposed as the stochastic term following the fluctuation-dissipation theorem.

Towards Automated Vulnerability and Mitigation of Critical Infrastructure

Arif Khan
PN18062/3061

At present, in the cyber domain, less than 5% of common vulnerabilities have been mapped to Common Weakness Enumeration (CWE™), and less than 35% of those have been mapped to Common Attack Pattern and Enumeration Classifications (CAPEC™); thus, the utility for automated processing of Common Vulnerabilities and Exposures (CVEs®) is a critical necessity for optimal mitigation of known vulnerabilities and threats. We propose to develop computational tools for automated categorization of CVEs and for mapping of CVEs to CWEs, as well as mapping CWEs to CAPECs.

CVE is a list of common identifiers for publicly known cybersecurity vulnerabilities. CVEs provide classification and categorization of vulnerabilities, attacks, faults, and reference points for data exchange so that cybersecurity products and services become standardized and interoperable and enable information collection and sharing.

CWE is a community-developed, formal list of common software weaknesses, such as Buffer Overflows, Structure and Validity Problems, Handler Errors, and Authentication Errors. CWE provides a common language to describe software security weaknesses, a metric for assessing software security tools addressing the vulnerabilities, and a baseline standard for weakness identification, mitigation, and prevention efforts.

CAPEC is a list of common attack patterns classified in an intuitive manner, including a comprehensive schema for describing related attacks and sharing information about them. An attack pattern represents knowledge about how specific parts of an attack are designed and executed.

We propose to extend these concepts to other critical infrastructure networks, such as the power grid and natural gas system. Mapping of CVEs to higher abstractions, such as CWEs and CAPECs, enables a better understanding of threat action and mitigation. We will address the following questions in this research: 1) given an arbitrary unclassified (or new) CVE, can a mathematical framework map this CVE to the corresponding CWE and known CVEs (classified or labeled) with acceptable accuracy; and 2) can CVEs with high correlation (or similarity) exhibit similar threat actions and be mitigated with similar mitigation actions?

The goal is to build a scalable pipeline, where input is the unstructured data (e.g., CVEs), to a structured output (e.g., a graph) on which we can apply data analytics tools. The pipeline consists of three main parts, as follows:
1) Natural Language Processing, including N-grams, cosine similarity, and stemming;
2) Linear Algebra, including singular value decomposition, nonnegative matrix factorization, and pointwise mutual information; and 3) Graph Algorithms, including k-nearest neighbor graph, as well as clustering, centralities, and inf. max.

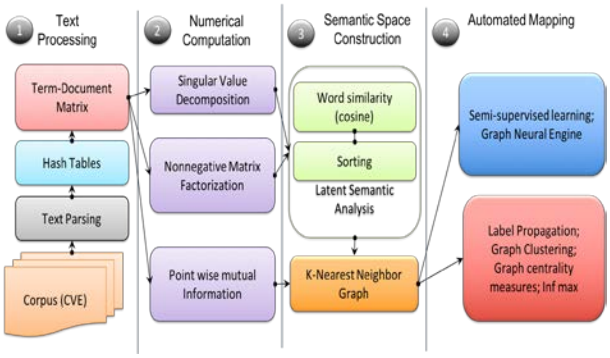

A breakdown of the parts included in the scalable pipeline this project aims to build. We have developed scalable code base for each of the components mentioned.

Communities of similar cyberattacks identified with Louvain algorithm on the generated graph of 500 CVE.

Transpire: Transparent Model-driven Discovery of Streaming Patterns

Aritra Dasgupta
PN16038/2815

In streaming data environments, the only thing that is constant is change. To the human observer or analyst, changes are often too fast to notice, too many to remember, and too complex to understand or make predictions. To help analysts discover and reason about changes, we will be developing a transparency-based, explanatory visual analytics framework for integrating streaming data visualization techniques with automated methods that increase confidence and utility of human judgment for streaming data analysis.

Most existing visual analytics techniques are based on assumptions about how human-stream feedback should work and are not supported by concrete empirical evidence. In our work, we fill these gaps through three main contributions.

First, we tested how varying levels of model transparency can best leverage the high bandwidth of human perception systems for communicating key insights. By conducting qualitative studies through surveys and interviews of analysts from diverse domains, we developed a characterization of model transparency and its impact on analysts' perception of streaming patterns.

Second, we used this transparency characterization for developing visual analytics methods and techniques for context-aware human reasoning about streaming data. We study how differences in model transparency affect efficiency, effectiveness, and the trustworthiness of human insights.

Finally, we aim to demonstrate the efficacy of our methods through case studies and quantitative user studies that demonstrate how these visual analytics methods can significantly improve human interpretability of machine-detected streaming patterns.

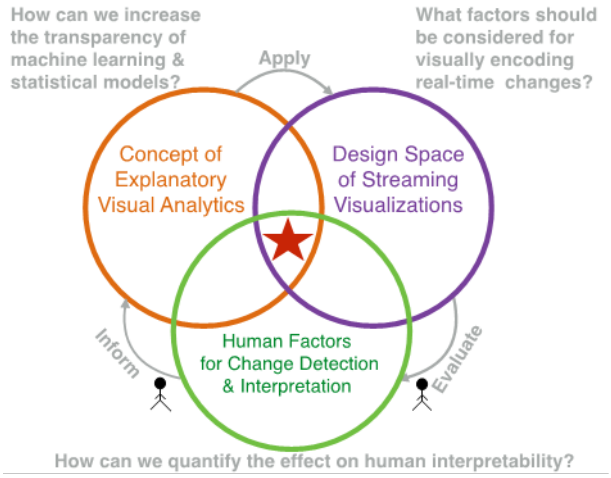

Illustrating the three-fold objectives of Transpire.

We established a streaming data visualization design framework for analyzing trade-offs related to change perception. We developed a visual analytic tool for instance-level explanations of binary classifiers. Finally, we developed a visualization technique for comparing baseline patterns in a stream of many data objects (e.g., users in a network, items in a transaction database, etc.).

Following the success of our visual explanation techniques, we engaged experts from the medical and cyber domains for expanding the scope of machine learning model explanations.

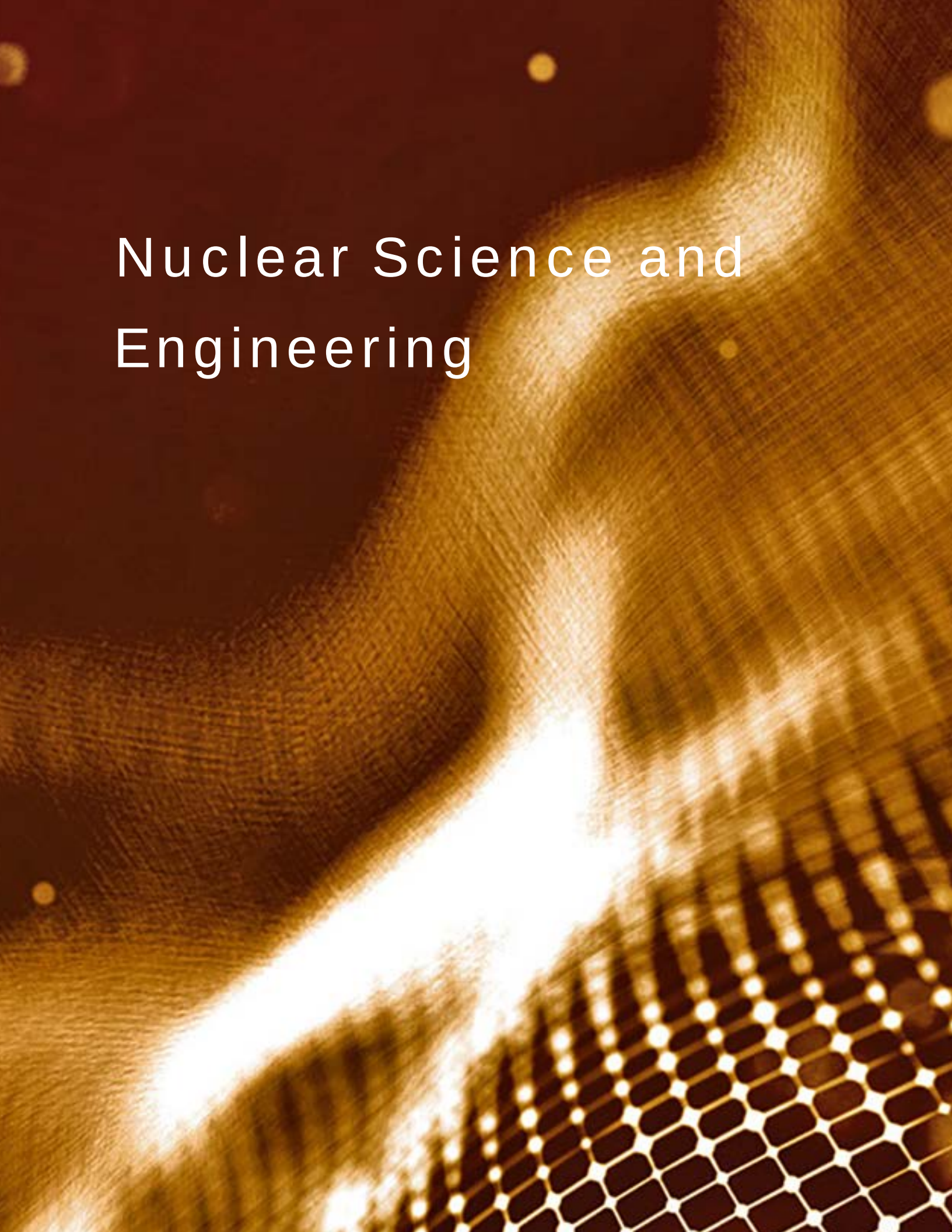
Nuclear Science and
Engineering

Affordable and Rapid Radionuclide Production

Samuel S. Morrison
PN18038/3037

This project was performed to investigate implementation of a novel fissile target design for rapid and affordable production of fission products.

This project was initiated based on results from an innovation computational modeling assessment of fission product recoil ejection out of uranium targets and into various recoil capture layers. Conceptually, the intention of this project is to confirm our previous computational modeling, which suggested fission products could be ejected out of sub-micron fissile targets and captured in a layer separate from the fissile material.

Our major result this year was that we demonstrated, at a laboratory scale, fission product recoil ejection and capture in a select recoil capture layer. In the recoil capture layer, we recovered 49±7% of the fission product isotopes that were detectable, and we recovered less than 0.01% of the ^{235}U target material in the recoil capture layer.

We prepared and irradiated an array of fissile targets. After irradiation and decoupling of the target, we quantified the fission product recovery in each layer by gamma spectroscopy and the uranium recovery by inductively coupled plasma mass spectrometry analysis.

Our most optimal target preparation method involved vapor deposition using nitrogen triflouride to coat a nickel rod with of a micron ^{235}U layer; the uranium-coated rod was then housed in a vanadium capsule (prepared by electrical discharge machining of vanadium wire).

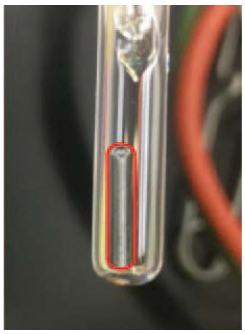

Displayed is the final target that was prepared for offsite irradiation. This target was three-layered, with the inner layer Ni, the middle layer ^{235}U, and an outer V capsule. After irradiation, we quantified fission products in Ni layer and the V capsule with no detectable ^{235}U present.

Uranium-235 layering by electrodeposition onto a graphite rod was examined for target preparation. This method did result in successful recoil ejection; however, the consistency in ^{235}U thickness across the surface area of the rod was non-ideal and may have resulted in increased suppression of fission product ejection.

Outer polymer layers were prepared, and we determined that our ideal polymers could not withstand the sample preparation process prior to offsite irradiation. Microsphere ^{235}U dispersion in a polymer wafer was investigated and did not result in adequate dispersion of the microspheres.

Fission product and ^{235}U recovery for target type and individual layers.

Design (inner/middle/ outer)	Inner %FP % ^{235}U	Middle %FP % ^{235}U	Outer %FP % ^{235}U
Nickel-^{235}U-Vanadium (n=6, ±1σ)	52±8% FP >0.01% ^{235}U	2±2% FP 98±3% ^{235}U	49±7% FP >0.01% ^{235}U
Graphite-^{235}U-Vanadium (n=3, ±1σ)	40±7% FP, >0.01% ^{235}U	23±8% FP 97 ±2 % ^{235}U	35±8% FP >0.01% ^{235}U
Graphite-^{235}U-polymer	Incompatible with Ampoule Sealing		
Sonic Dispersion ^{235}U microspheres in polymer	Inconsistent Dispersion & Clustering of Microspheres (not a valid target preparation method)		

An *In Situ* Investigation of Boehmite (gamma-AlOOH) Dissolution Under High pH (potential of hydrogen) Conditions

Edgar C. Buck
PN15090/2765

Boehmite found in the Hanford waste tanks is an intractable problem, as the concentration of Al(aq) in the tank waste does not fully account for the documented drastic decrease in boehmite dissolution rate and extent. By probing dissolution processes relevant to Hanford waste processing and spent fuel dissolution at the nanoscale with modern electron microscopy techniques, the role of both intrinsic and extrinsic factors on the variability of mineral reactivity can be tested.

The Waste Treatment Plant (WTP) under construction on the Hanford Site will be designed to separate the waste into two fractions for immobilization. After the high-level waste (HLW) is separated from the low-activity waste liquid stream by ultrafiltration in the Pretreatment Facility, the concentrated HLW will undergo caustic and oxidative leaching processes to dissolve and wash out materials (aluminum, chromium, phosphates, and sulfates) that would otherwise limit HLW loading in the glass waste form.

Reactions at solid or particle surfaces include dissolution, precipitation, and sorption. Heterogeneities of the mineral surface that include defects and dislocations, as well as expression of different crystallographic faces, represent “intrinsic” factors that cause variability in reactivity. “Extrinsic” factors that may affect reactivity include sorbed molecules and colloids, tenacious nano-scale surface coatings, and, particularly relevant to nuclear system, nano-bubbles from radiolytic processes.

This research has been focused on direct observation of the dissolution processes relevant to Hanford waste processing at the nanoscale with modern *in situ* electron microscopy techniques.

The dissolution and precipitation of gibbsite (α-Al[OH]$_3$) and boehmite (γ-AlOOH) is of prime importance to the final disposition of HLW stored at the Hanford Site. Gibbsite and sodium aluminate, which are common in the tanks, are easily dissolved by heating under caustic conditions; however, boehmite is more stable and requires more aggressive conditions.

In this final year of investigations, we have examined the role of specific dopants on controlling the dissolution of boehmite with specific dopants added to the material. We published the results of the effect of chromium on boehmite dissolution and showed how chromium was not incorporated into the boehmite structure. We found tentative evidence for the role of manganese and iron in boehmite dissolution, which agreed with some of the findings of previous researchers for the role of titanium during boehmite dissolution.

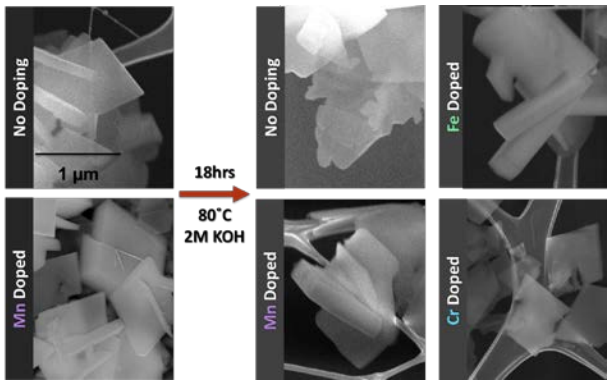

Transmission electron microscopy analysis of boehmite platy crystals showing the effect of dopants on dissolution.

We further examined the dissolution behavior of boehmite with *in situ* transmission electron microscopy and cryo-electron microscopy. The strong link between boehmite dissolution and delamination found by other researchers hinted at an important role for hydrogen bonding between the structural units in the dissolution process. An apparently large stabilization effect with doping boehmite with iron also suggested

that a detailed theoretical effort is warranted to help untangle the possibilities. These efforts are now on-going elsewhere.

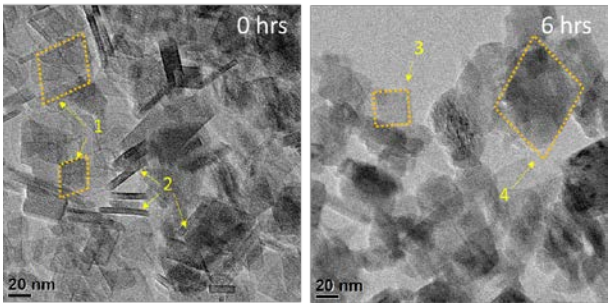

Comparison of boehmite dissolution in 2M KOH for (left) 0 and (right) 6 hours. At 0 hours, the boehmite crystals exhibit the characteristic shape (1) and show extensive stacking (2); however, following caustic dissolution, the boehmite rhombohedral plates no longer exhibit these characteristic angles (3) and have rounded corners (4).

We had previously confirmed that dissolution under the electron beam *in situ* was significantly lowered with iron-doped boehmite. However, these later experiments under WTP-relevant dissolution conditions confirm the role that iron plays in the dissolution of boehmite. These *in situ* liquid cell, cryoEM, and advanced high-resolution electron microscopy methods have enabled great insight into the corrosion mechanisms of boehmite under WTP-relevant conditions.

The results clearly confirm the microscopy evidence that iron-doped boehmite dissolves much slower than undoped boehmite.

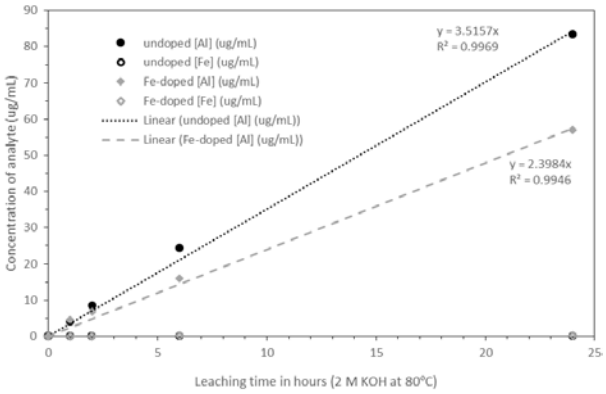

Dissolved component showing the reduction in dissolution rate with the iron-doped boehmite.

Correlation of Colloidal Interactions and Macroscopic Rheology in Concentrated Electrolyte Solutions

Jaehun Chun
PN15091/2766

This project will develop a "science-based," fundamental understanding of macroscopic rheology (flow properties) of slurry under conditions relevant to storage in harsh conditions and nuclear waste treatment process. In particular, we will connect phenomena at different length scales (i.e., particle interactions, aggregate structures, and bulk rheology). The project will build a scientific framework to accomplish safe and efficient nuclear waste treatment processing, in addition to proper design and operation of waste disposition processes (e.g., pretreatment facility in the Hanford Waste Treatment and Immobilization Plant).

Hanford tank wastes are radiological mixtures of insoluble and soluble solids in highly concentrated salt solutions, leading to complex non-Newtonian waste rheology. While understanding such rheological nature is quite challenging, it must be considered during design and optimization of Hanford wastes disposition processes. The rheology of colloidal dispersion is governed by long-range ordering of individual particles or particle aggregates that result from particle interactions correlated with interfacial phenomena at molecular and colloid scales.

Particle forces in simple colloidal suspensions have been studied and are well understood; colloidal forces have been modeled using the Deryaguin-Landau-Verwey-Overbeek (DLVO) theory. Resultant rheology has been reasonably understood via the DLVO theory. However, this cannot be simply applied to Hanford waste slurry due to its unique nature such as high salt concentrations and particle size distributions (PSDs). Furthermore, owing to surface roughness of various minerals in the dispersed phase, rheology can be influenced by friction forces, and solvent structuring can fundamentally influence particle interactions.

This project considered these unique particle forces and interactions to understand how they arise, in terms of the chemical physics at solid-liquid interface and, especially, to determine how these interactions are correlated to long-range ordering of colloidal waste particles and bulk rheology in tank-waste-relevant-systems.

During the project period, we have developed a customized atomic force microscopy (AFM)-dynamic force spectroscopy (DFS) capability and investigated interactions between boehmite particles at high salt concentrations. We have developed a simulation framework for predictive capability of bulk suspension rheology and studied rheological behavior of dense suspensions as a function of various physicochemical parameters relevant to conditions for Hanford tank wastes. Furthermore, we developed an *in situ* capability based on system for analysis at the liquid vacuum interface (SALVI) implementing scanning electron microscopy (SEM) for particle aggregation/identification and studied aggregation behavior of boehmite particles at high salts and pH conditions.

Using the developed the AFM-DFS capability, along with natural boehmite crystals from the Smithsonian museum, we studied interactions between boehmite surfaces as a function of pH and $NaNO_3$ concentrations. Our data showed that the force becomes more attractive as a function of pH (from 6 to 10), as expected, because the point of zero charges would be at pH of about 9 to 10. Further measurements indicated that the force becomes more attractive with increasing $NaNO_3$ concentrations (which is consistent with dynamic light scattering measurements that show rapid aggregation). However, the force becomes sparingly less attractive at a high salt concentration (about 0.1 to 0.5M of $NaNO_3$). We would further study this unique nature in a possible follow-up opportunity.

While the natural boehmite crystals can be used for the AFM-DFS, the availability of large boehmite single crystals is preferred. We used pulsed laser deposition to prepare achieve large-scale single crystals of boehmite (010). We studied parameters influencing nucleation and growth of the thin film of boehmite such as substrate surface temperature, substrate surface, and background pressure. Our results indicated that AlOOH (010) thin film can be prepared over a TiO_2 (001) anatase buffer layer on top of $LaAlO_3$ (001) substrate; the specified system showed about 2.4% along one direction and about 24% along orthogonal but domain-matching epitaxy, which corresponds to 0.9% (i.e., 3-unit cells anatase corresponding to 4-unit cells boehmite). However, the instability of AlOOH has been identified as an issue to prepare the large-scale single crystal.

Using the developed *in situ* capability, we studied morphology of particles and aggregates as a function of pH and salt ($NaNO_3$) concentrations. Both secondary electron (SE) and backscattered electron modes were good indicators to show different particle morphology from pH of 3 to 10 (more single separate particles at low pH, more cluster-like particles at higher pH). Furthermore, the SE mode at pH 7 and 12 identified the degree of aggregation. Using a particle distance as an indicator for aggregation, our study shows that, as pH increases, the distance increases, implying that more and faster aggregation behavior occurs at the higher pH.

Based on Lubricated Flow-Discrete Element Method (LF-DEM), we obtained quantitative understanding of the effects of PSD on rheological responses. We also established a new scheme to study poly-disperse suspensions via a statistical equivalence between bi-dispersity and poly-dispersity. Our study showed that bi-disperse and poly-disperse suspensions always show lower viscosities and weaker normal stress response, compared to monodisperse suspensions, which provides practical implications on nuclear waste treatment process at Hanford. Furthermore, the study clearly illustrated that universal behavior for suspension viscosity can be obtained by scaling the particle volume fraction with a corresponding maximum packing fraction.

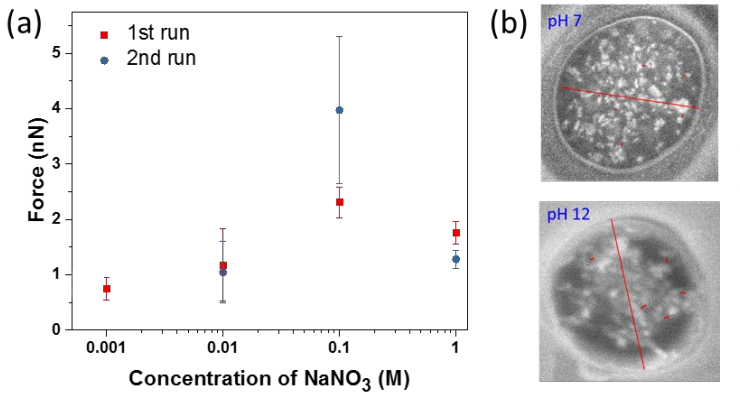

Experimental results from the AFM-DFS and *in situ* liquid SEM imaging capabilities: (a) forces between boehmite surfaces as a function of $NaNO_3$ concentrations and (b) the SE mode at pH 7 and 12 for studying aggregation.

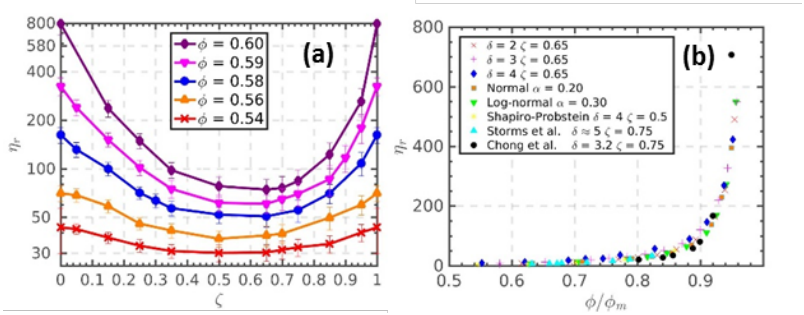

LF-DEM simulations on effects of PSD on rheology: (a) the reduction of slurry viscosity in bi-disperse suspensions and (b) a universal scaling curve for slurry viscosity over various bi- and poly-disperse suspensions from simulations and experiments.

Interfacial Diffusion and Crud Formation at the Liquid-liquid Interface of Solvent Extraction Processes

Amanda J. Casella
PN16090/2867

The radiation present during reprocessing of used nuclear fuel breaks down the extractant that isolates uranium and plutonium from fission products. Rather than separating into the organic phase, uranium and plutonium can complex with the degradation products and form crud (solids) at the liquid-liquid interface. This project seeks to gain a stronger fundamental understanding of these complexes in order to enhance processing operations, thus enabling innovative solutions for challenges in the expansion of the current U.S. nuclear fuel cycle.

This work targets a fundamental understanding of how crud (solids) forms at the liquid-liquid interface during solvent extraction processes. By using *in situ* measurement techniques coupled with molecular dynamic modeling, the phenomena and drivers leading to crud formation can be captured, providing a more holistic understanding than was previously achievable. The impacts from this study will lead to a stronger understanding of the fundamental mechanisms controlling the transfer of the butyl phosphate extractants across the interface, how the rates affect the chemical fractionation of the extractants and the mechanisms of nucleation leading to the formation of the interfacial solids.

The first year of this project focused on an in-depth review of historical Hanford records, along with other open-literature published work to provide the framework and prioritization for experimental investigations in years two and three.

The focus in year two was on establishing and validating the macro-scale testing along with implementation of the complementary microfluidic studies. Both systems use *in situ* monitoring by Raman spectroscopy, which enables capture of rapid transients, along with detailed kinetics, prior-to, during, and after extraction. The macro-scale tests are performed in a Lewis cell, a long-standing/validated method for kinetic analysis.

In addition to experimental work, computational approaches are being used to gain further molecular insights regarding liquid-liquid interfacial processes. Examination of the relationship between adopted configurations of the solute, orientation of the solvent, and the ability of the solute to enhance microsolvation provide clues regarding molecular organization of precursors to solid phase nucleation and formation of interfacial solids. These computational results are being integrated with experimental results in order to gain molecular insight.

Computational fluid dynamic modeling, also developed on the project in years two and three, was used to determine the necessary additional fluid transport insight to enable extrapolation of kinetic measurements within the microfluidic chip. The microfluidic studies greatly enhance the number of conditions and parameters that can be studied as they offer more efficient change in parameters along with approximately a six order of magnitude reduction in solution volume.

This year expanded conditions/parameters beyond those used for benchmark validation developed in year two. Systems involving mixtures of degradation products with the typical extraction components were studied to determine the complexation and effects. Crud formation was studied within the microfluidic device to give a better understanding of fundamental rates of transfer, drivers, nucleation, and complexation at the liquid-liquid interface.

Monitoring Diffusion of Actinide Daughters and Granddaughters in Metals for Chronometer Applications

Dallas D. Reilly
PN15095/2770

This project seeks to understand trace element fractionation during the production, casting, or melting of uranium (U) metal or other actinide metals. These metallurgical processes are important to the nuclear forensics community for the application of radiochronometers to investigations involving nuclear material. They are also important from a worker health and safety point of view for producing metallic nuclear fuels.

Past studies have observed trace elements like thorium (Th), the daughter product of U decay, fractionate quantitatively during the casting of U. However, the mechanisms controlling this phenomenon are not understood. The goal of this project is to elucidate these mechanisms by combining high-temperature controlled experiments, molecular-scale observations, and theoretical modeling. If successful, determining the fractionation mechanisms of Th during U metal casting will not only confirm the use of U/Th parent/daughter radiochronometers as an endogenic nuclear forensic signature of U casting process age, but also lay the groundwork for interpreting the next generation of chemical process signatures within actinide metals.

One experiment conducted within this project showed, for the first time, quantitative fractionation of Th during the production of U metal (in a conversion to uranium tetrafluoride to the metallic phase in a process known as bomb reduction). In that study, Th moved from the tetrafluoride to the crucible and slag during the reduction. Modeling experiments have also been conducted with a focus on carbon in the U metal system, since the resulting U carbides (UC) could potentially scavenge trace elements like Th during these reactions. Those studies have resulted in two publications, and a novel way of seeding crystals in phase field models (a type of model that is growing in popularity due to its simplicity and ability to model phase precipitation and dissolution at the micron scale).

Finally, in an attempt to monitor the fractionation of plutonium (Pu) daughter products during a similar bomb reduction experiment as the U, atom probe tomography (APT) was performed on a bomb-reduced Pu metal. Although this method wasn't adequate to measure dilute quantities of Pu daughter products, it was the first ever Pu APT performed and resulted in valuable information on the bomb reduction process and corrosion mechanisms.

Plutonium APT sample.

Particle-filter Surface Interactions and Dynamics in the Presence of Cross-flow

Richard C. Daniel
PN16058/2835

This project aims to provide a fuller understanding of the fouling processes that hinder efficient and sustainable filtration of industrial slurries through a combination of studying the rate of flux decline in prototype dead-end and cross-flow filter elements and through detailed characterization of the physical properties of solids that accumulate on those elements. This effort will facilitate a deep understanding of the mechanisms governing foulant transport to and interaction with the filter membrane that will enable improved industrial operating strategies and chemical treatments that optimize filtration throughput and efficiency.

Treatment and disposal of the 55 million gallons of highly radioactive tank waste stored at the Hanford Site in the state of Washington will take 40 years and cost at least $110 billion. Hanford waste treatment costs are driven by process bottlenecks that limit waste throughput. One such potential bottleneck is separation of radioactive waste solids from liquids and non-radioactive components by filtration. Indeed, bench- and engineering-scale evaluation of filters used in Hanford waste treatment have identified waste separations are subject to an unexpected loss in filter performance that results from a slow but persistent fouling of the filter by waste solids. This fouling will necessitate frequent, time-intensive chemical cleaning operations to restore filter performance.

Modification and optimization of the filter process to avoid or minimize such fouling by improving performance, even by a modest 5%, could result in billions in saved operational costs and years in reduced mission lifecycle. The goal of the current project is to develop filtration optimizations through improved understanding of waste solid/filter interactions that lead to lost filter performance.

Recent studies of Hanford waste filtration have focused primarily on operational feasibility of waste filtration to prove cross-flow filtration as a viable separation technology for Hanford wastes. These studies have allowed the maturation of cross-flow filtration operations for Hanford waste treatment but have been unable to aide in the development of physical-realistic fouling mechanisms that could form the basis of optimization strategies.

In addition, waste immobilization will also frequently employ dead-end filtration to limit transport of solids into downstream storage vessels or unit operations (like ion exchange). To date, few studies have evaluated the efficiency of dead-end filter operations when processing Hanford relevant waste streams. Recent dead-end tests conducted in 2018 with actual Hanford tank AP-105 and AP-107 wastes have found significant fouling, even in nominally solids-free waste, that may challenge waste throughput targets.

The FY 2018 activities conducted under this project study dead-end and cross-flow filtration using Hanford-specific waste simulants to provide a highly controlled set of filter fouling experiments. The results of these experiments will be used to develop a convective-diffusion-based filter fouling model that is extensible to both dead-end and cross-flow filtration and that provides a more complete mechanistic picture of filter fouling by Hanford wastes that existing models, which are highly empirical and do not allow extension of predictive results to different waste concentrations and filter operating conditions, do not address. These studies not only improve understanding of the filter fouling behavior observed for mineral oxide slurries undergoing cross-flow filtration but will aid in process optimization to reduce the impact fouling has on waste immobilization costs and schedule.

FY 2018 research efforts on this project focused on testing of industrial relevant slurries in both

cross-flow and dead-end filter configurations to help illuminate the mechanisms that govern the rate and extent of filter flux decline.

Efforts to evaluate the filtration of industrially relevant waste materials led to the development and filter performance evaluation of a Hanford tank AP-105 chemical simulant. Testing of this simulant is both timely and relevant, as tank AP-105 is a candidate for early-start waste processing through the Direct-Feed Low-Activity Nuclear Waste program.

AP-105 simulant filtration was first validated against AP-105 actual waste filtration results, showing that the simulation formulation resulted not only in matching chemistry, but in matching filtration performance, as well. This key step provides confidence that insights gained by simulant testing will translate to real-world engineering.

Extended dead-end and cross-flow testing of the AP-105 simulant confirmed lower than expected performance of dead-end filtration, showing rates three orders of magnitude lower than that expected for entirely solids-free liquids. Fouling of the filters appear to be primarily impacted by colloidal iron, which was observed to pass through the filter upon start-up of dead-end filtration and subsequently accumulate on the filter, leading to a rapid and extensive reduction in filter performance.

Evaluation of the flux decline and transients associated with step changes in filtration pressure found the accumulation dynamics are consistent with cake filtration and that colloidal diffusion (or a diffusive-like mechanism) plays an important role in governing the fouling dynamics during start-up and changing operational conditions. A convective-diffusion dead-end fouling model was developed and successfully applied to describe the time-rate of change in filter performance observed in the AP-105 simulant.

Historical modeling of Hanford waste cross-flow filtration has not found a model that accurately captures the rate and extent of observed waste and waste simulant fouling behavior over the full range of relevant process times (from start-up to continued filtration over several hundred hours).

Additionally, while existing models provide good fits of measured data, they do not readily allow extension of those fits to other operating conditions. A review of historical cross-flow test and modeling efforts, in conjunction with convective-diffusive-based modeling of dead-end filtration, led to the development of a convective-diffusive-based model for cross-flow filtration. This work highlights the role of gel-polarization and convective and diffusive infiltration of solids into the membrane on filter flux. This model is theoretical, allowing predictive extension to different foulant concentrations, cross-flow velocities, and operating pressures.

As part of the project effort, PNNL hosted an intern who evaluated the role of temperature on cross-flow filtration using viscosity-matched Hanford waste simulants. The study highlighted the role of the simulant suspending phase chemistry on cross-flow filtration performance.

The project also continued a collaborative partnership with the Department of Civil and Environmental Engineering and Howard University by supporting development of the companion cross-flow visualization cell at Howard University.

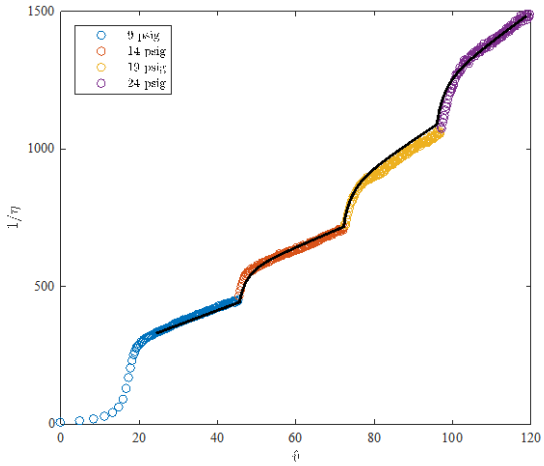

Scaled dead-end filter resistance ($1/\eta$) as a function of scaled permeate volume produced ($\hat{v}$) for an AP-105 chemical simulant for four sequential pressure-set points. Solid line represents a fit of the data to the convective-diffusive model.

Phase Field Modeling of Microstructure Development in Plutonium (IV) Oxalate Precipitation

David G. Abrecht
PN17043/2933

In order to aid forensic analysis of interdicted nuclear materials for law enforcement, this project focuses on developing modeling techniques to describe the microstructural evolution of precipitating solid materials. The focus material for the project is plutonium (IV) oxalate, which forms a variety of shapes and structures based on the conditions under which it is grown. The phase field models being developed under this project are aimed at capturing the correlation between the precipitating conditions and final structures, to develop a predictive understanding of the final observable crystal shapes and structures.

The microstructure of materials, including their grain size and orientation and defect concentration, is responsible for many of the physical properties of materials. As such, crystal growth and grain structure evolution modeling has long been a goal of material scientists attempting to control material properties. However, simulating the moving interface of a material undergoing phase changes has been computationally difficult until recently. Advances in computing power and modeling techniques, such as phase field modeling, where the interface is treated as a continuous mathematical field, have allowed these dynamic simulations to become more accessible.

This effort aims to apply phase field modeling techniques to a highly different problem—the chemical precipitation of actinide materials—in order to establish a relationship between crystal shapes observed by microscopy and the conditions of the chemical system, including temperature, concentration of reagents, and reaction time.

Year one efforts focused on establishing the physical constants for the plutonium oxalate system (i.e., plutonium diffusion rates, thermal conductivity, surface tension, solubility, etc.) needed to describe the crystallization behavior in phase field models and on establishing the thermodynamic properties of the highly acidic, highly saline solutions from which plutonium oxalate is normally precipitated.

Early efforts in year two focused on construction of electronic structure models to acquire information not readily available in the literature, including the energy associated with creating new solid-liquid interface area and the energy of capturing water molecules within the plutonium oxalate crystal structure. These values were established successfully and were incorporated into phase field models under development.

Numerical representation of the thermodynamic relationships between solid and liquid phases that were compatible with phase field models were created, including the effect of ionic strength on the free energy of the solution, and schemes were developed for incorporating the ionic strength condition, as well as variable conditions of temperature and concentration of individual analytes, into the developing models. In addition, new code is being developed for three-dimensional crystal structure evolution in the MOOSE code used for phase field modeling. As this project ends, these changes will be incorporated into future funded efforts.

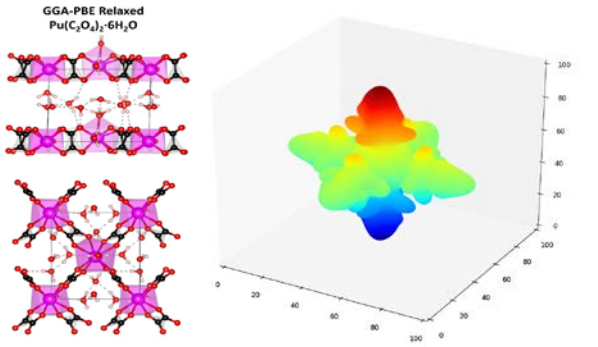

Aspects of the modeling effort. (Left) Electronic structure theory model of plutonium (IV) oxalate with six waters of hydration, showing the alterations in the layer uniformity due to water presence. This alteration affects the energy required to form the bulk phase. (Right) Development of three-dimensional phase field modeling techniques using the evolution of a toy system model, Kobayashi's dendrite, intended to be incorporated with thermodynamics of the plutonium (IV) oxalate system for complete phase field models.

Provenance and Pathways Investigations of Uranium Oxide Particles Using Oxygen Isotope Ratios

Dallas D. Reilly
PN16034/2811

This project seeks to discover ways in which nuclear forensics scientists can use natural variations in oxygen isotope ratios to provide information during their investigations. When successful, this research will allow end users to understand questions about nuclear material such as: Where was this material produced? Where was it stored? When was it chemically altered?

This project was initiated because there has been a significant amount of groundwork laid by the geochemistry and climatology communities on oxygen isotope fractionation to study the history of our planet, and there is a potential for using similar studies on materials of interest to the national security community. Oxygen is made of three stable isotopes, with mass numbers 16 (99.76%), 17 (0.04%), and 18 (0.20%). Due to the small difference in mass when oxygen is present in water, they can vary based on several factors (e.g., altitude, precipitation cycles, temperature, etc.). There is a very good understanding of the oxygen isotope ratio in water vapor across the planet; if a material like a uranium oxide is diverted from a known location and is interdicted at another known location, the water vapor absorbed by that material may indicate which route it took between those points. That information may help nuclear forensics scientists answer important questions relating to their investigation. By the end of this project, we hope to be able to apply oxygen isotope measurements to compounds like uranium oxides to provide qualitative information on its origin.

This project has developed the capability to analyze oxygen isotope ratios on nuclear materials on individual particles via large geometry secondary ion mass spectrometry (LG-SIMS). It is a difficult task to do so, and there is more work that would be required to bring this analysis to real-world nuclear forensics investigations, but we have successfully analyzed uranium dioxide produced from two geographic locations.

In addition, this project set up a fluorination system that separates oxygen from nuclear materials, allowing for highly precise isotopic analysis of bulk nuclear materials. This system has now been used on various uranium compounds. Unfortunately, one of the main findings of that work was that, during the production of a common fuel cycle product (U_3O_8), the oxygen isotope signature present in the uranium precursor dissipates rather quickly (about 2 hours), meaning that oxygen isotope analysis of this compound is not useful unless it has absorbed a significant amount of water prior to interdiction by law enforcement.

However, there is still promise in various precipitates that are common in the fuel cycle. One such precipitate, uranyl peroxide, was fluorinated and showed unique behavior with this system, forming unexpected compounds and opening some new possibilities for uranium halide chemistry.

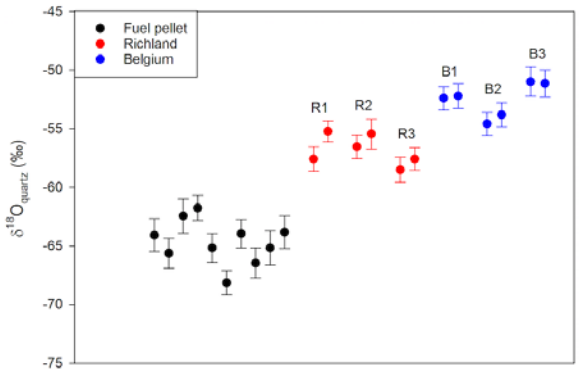

Oxygen isotope ratios obtained from LG-SIMS on a bulk uranium dioxide fuel pellet (black), particles from a fuel pellet produced in Richland, Washington (red), and particles from a fuel pellet produced in Belgium (blue).

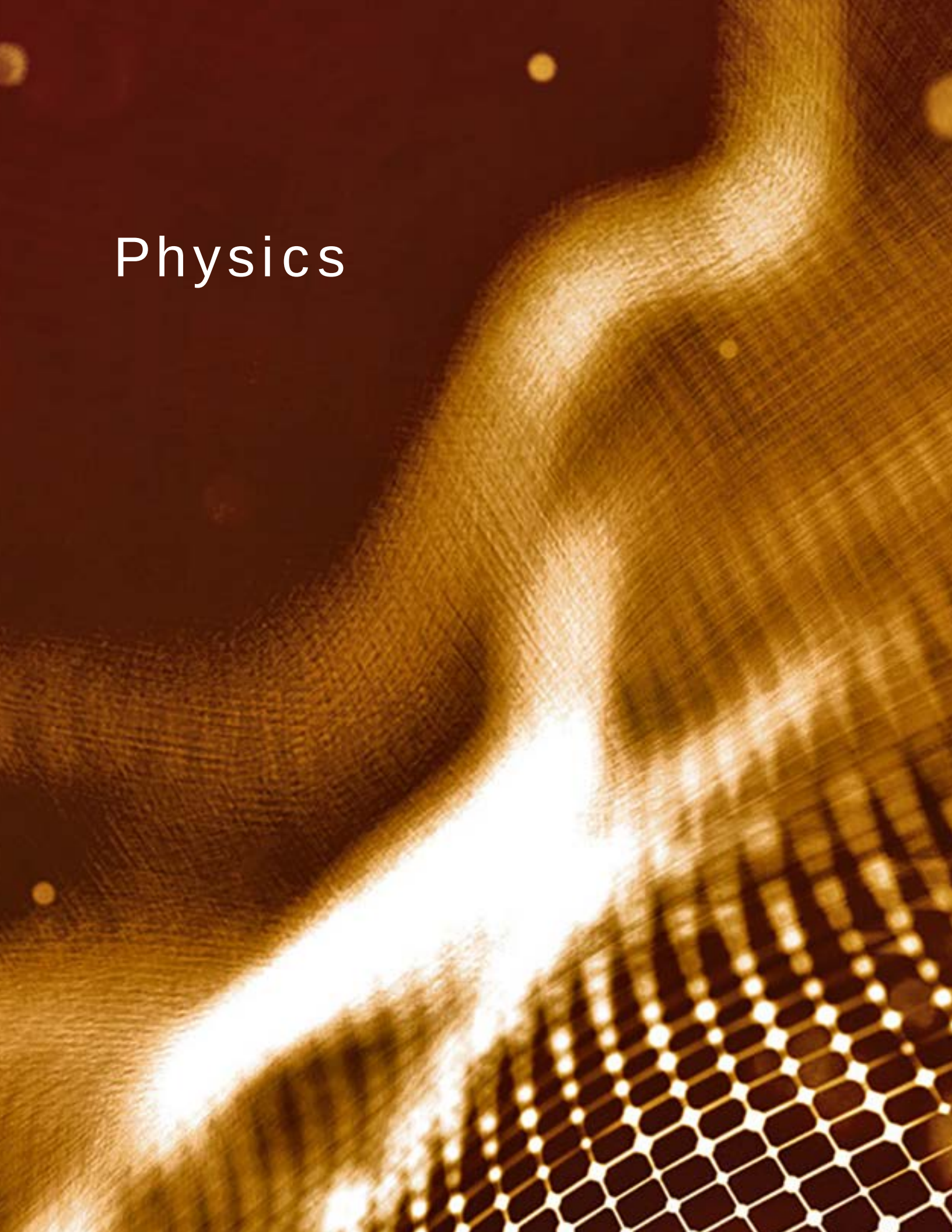
Physics

CLEAN Detection of Dark Matter and Low Energy Neutrinos

Christopher M. Jackson
PN16097/2874

Monolithic detectors using noble liquid targets hold promise to significantly extend the sensitivity and potential discovery of particle dark matter and new physics in the neutrino sector well beyond the state of the art anticipated for the Generation-1 (G1) and G2 experiments. The efficacy of the so-called "single-phase" approach for the detection of dark matter and neutrinos will be examined with the MiniCLEAN and DEAP-3600 experiments operating deep underground at SNOLAB, and the "dual-phase" approach will be examined with DarkSide-20k at Gran Sasso.

The astronomical and cosmological observations of dark matter in the universe are well established and are one of the very few places where there is direct experimental evidence for physics beyond the standard model. Primordial nucleosynthesis argues that the dark matter is non-baryonic; observations of structure formation indicate only a small contribution from neutrinos. Therefore, dark matter is exotic, and Weakly Interacting Massive Particles (WIMPs) are a compelling candidate that provide a cold, dark relic of the Big Bang and could be directly detected as they scatter from massive, ultra-pure detector targets operating deep beneath the earth's surface.

The challenge to realizing sensitive dark matter detectors is in separating backgrounds from the nuclear-recoil events characteristic of the WIMP signature. Future progress hinges on improving sensitivity by several orders of magnitude beyond existing or planned experiments before the background floor imposed by the coherent scattering of neutrinos from the atmosphere and from the sun will limit sensitivity to WIMPs. Detectors based on the noble liquids are particularly well suited to achieving the target masses (approximately 300 tonnes) necessary to pursue this challenge.

CLEAN (Cryogenic Low-Energy Astrophysics with Noble) liquids exploits a single-phase approach where only scintillation light is measured. Simplicity of design affords the construction of a very large detector at low cost, while pushing the major sources of background outside of the region of interest for a sensitive WIMP search. MiniCLEAN serves as a technical demonstration of the principles of a single-phase detector, using 500 kg of liquid argon (LAr) as the target material and including three-dimensional event reconstruction. The MiniCLEAN detector is deployed in the Cube Hall, 6,800 feet underground, at SNOLAB.

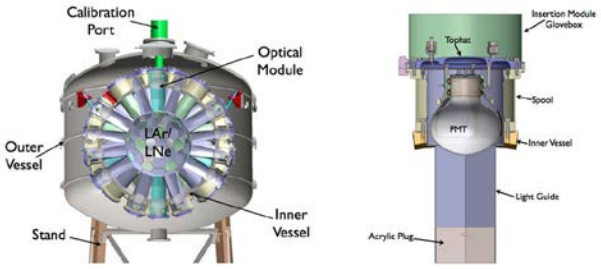

(Left) Model of the MiniCLEAN central detector with its 4π target viewed by 92 optical cassettes. (Right) The optical cassettes are 30-cm long and consist of a 10-cm-thick acrylic plug, the front surface of which is coated with a wavelength-shifting fluor (tetraphenyl butadiene [TPB]) and 30-cm light guide leading to the photomultiplier tubes. The inner target, defined by the TPB surface, contains 500 kg of LAr within a nominal radius of 44 cm.

This year, the MiniCLEAN gas operations phase completed with excellent results. The full detector analysis and readout was demonstrated and a triplet lifetime (a measure of the late light that is vital to distinguish the dark-matter-like events from background electron recoils) was measured to be 3.48 +/- 0.01 µs, the longest ever measured lifetime in argon gas. This demonstrates the exceptional purity achievable with this technology. Detailed measurements of triplet lifetime and light yield as function of impurity level were performed, which will allow purity requirements of future detectors to be benchmarked.

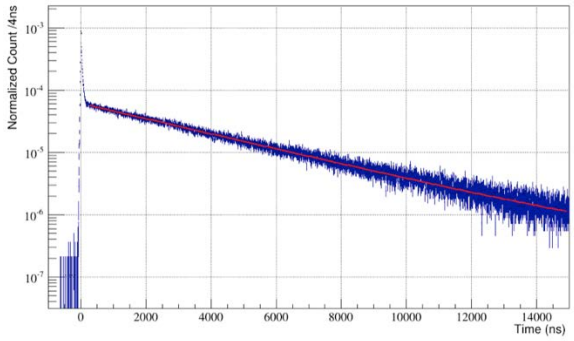

Pulse time distribution of argon-39 events in gas data, showing the long-lived triplet light.

MiniCLEAN significantly filled with LAr during the year, and the technical demonstration analysis is ongoing in the collaboration. PNNL contributions to MiniCLEAN operations including leading onsite shifts, production simulation, and data processing. Staff members also led the analysis group, performing background modelling and physics analysis.

A test bench to assay the argon-39 content of a sample for use as a calibration source was designed and deployed. This source showed enrichment to 0.02%, with a total activity of about 0.5 MBq. This source is now available to calibrate future argon dark matter detectors and for study of the argon-39 decay, the main background in these experiments.

PNNL continued its role in the next-generation LAr dark matter detector, DarkSide-20k, focusing on developing general tools necessary to determine radioactivity limits required for detector construction materials. This included a framework that consists of an assay organization and recording tool, drawing together capabilities across the entire collaboration and allowing efficient sharing of expertise. Additionally, in order to determine the required assay level, a tool to estimate the level of uranium and thorium permitted in materials due to neutron production in (a,n) reactions was created. These tools were completed and handed on to the DarkSide-20k collaboration for deployment.

In summary, the CLEAN Detection of Dark Matter and Low Energy Neutrinos has demonstrated the exceptional purity of the MiniCLEAN cold single-phase approach, supporting the technical demonstration for a 300-tonne-scale detector. Several analysis, calibration, and background tools have been developed that will support future argon dark matter detectors as they move ever lower in sensitivity.

Deep Learning Applied to Accelerator Neutrino Physics in Liquid Argon Time Proportional Chambers

Eric D. Church
PN17064/2954

For this project, we will measure properties of neutrinos arriving from accelerators at Fermilab to detectors such as MicroBooNE (micro Booster Neutrino Experiment). PNNL will contribute computationally sophisticated deep learning (DL) techniques to lead these measurements.

Since beginning in February 2017, we have produced simulated and real data in the hdf5 file format to store MicroBooNE experimental datasets to which all scientists have been applying DL techniques. With these data, we have produced DL networks that are competitive with previous work from the MicroBooNE experiment. Further, we have established roles for PNNL researchers within the MicroBooNE and Deep Underground Neutrino Experiment (DUNE) collaborations. This ensures continued access to new data, engages us in understanding the data quality, gives us a role in detector development, and gives us leadership in the scientific output of the experiments.

Within this project, we are conducting research on the following three fronts: 1) developing networks that optimize use of the full, correlated information from the three planes of the MicroBooNE detector; 2) working with the keras/tensor-flow infrastructure and hdf5 files to allow for quicker scientific exploration and effective collaboration; and 3) bringing these techniques to nucleon decay search strategy development and cross-section measurements within the MicroBooNE and DUNE experiments.

We have begun work recently on a semantic segmentation network for MicroBooNE, in which each pixel in the image is labeled by the particle species that produced its charge deposition. This is novel for high energy physics and nucleon decay search, and it will allow even more precise identification of a neutrino or nucleon decay signature. Previous MicroBooNE work showed a 1:2 signal to background result in neutrino event identification using DL, which we have confidence, using our new analysis techniques and incorporating the cosmic ray detector data, will improve by 50%. Further, our innovative work maintains the full detector image fidelity, which will bring large background reduction. The impact here to suppress MicroBooNE's most pernicious background—that from irreducible cosmic rays—could not be overstated, if achieved.

The nucleon decay search with DL, which shows an early indication of increasing DUNE's sensitivity for this paradigm-changing discovery by an estimated 40%, would immediately make PNNL the leader in this exciting physics on DUNE. Analyses will be enabled and informed by the MicroBooNE DL work we have done already and will demonstrate an increase in signal efficiency and an increase in background rejection.

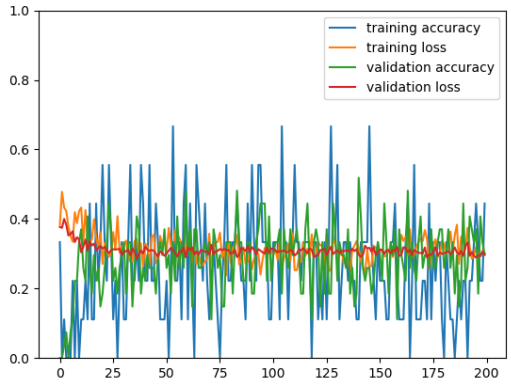

A typical loss and accuracy plot versus epoch. For us, an epoch is one batch, which is 10 events. Each 10 events are a new set, not seen in another epoch. This plot is typical of the current state of the research, in that after early training, the loss and accuracy stall, despite varying learning rate and other parameters.

Currently, we are seeing an approximately 2x-random classification accuracy for five particles of about 35% but with a large, not-understood volatility from batch-to-batch. We expect to achieve a mid-80% accuracy. We believe a full examination of the underlying data integrity must occur next.

Low-mass Dark Matter Backgrounds Research and Development

Raymond A. Bunker III
PN16086/2863

The nature of dark matter (DM) is a fundamental question in modern physics. This project focused on understanding backgrounds that limit searches for low-mass dark matter and on the development of background-reduction strategies to enable future, more sensitive experiments.

Dark matter is 85% of matter in the universe, but its nature is unknown. Current DM searches have phenomenal sensitivity and are beginning to push into the "low mass" regime, in which ultra-sensitive detectors search for DM particles with masses less than 10x the mass of the proton. However, background-radiation requirements are extraordinary and progress in the field is directly tied to the backgrounds achieved. Although the next generation of experiments will explore a broad range of new parameter space, trace levels of radioactivity in the detectors are expected to limit their sensitivities.

The goals of this project were two-fold:
1) characterize backgrounds expected to limit the sensitivity of low-mass DM searches and
2) develop strategies for the reduction of such backgrounds. Research and development (R&D) focused on methods for measuring and mitigating detector backgrounds—leveraging PNNL's expertise in radiopure materials and high-sensitivity radioassay—as well as development of generalized background modeling tools for evaluating the impacts of residual backgrounds on experimental sensitivity.

In FY 2016, two dominant categories of backgrounds were identified: 1) cosmogenic radioisotopes in detector materials—in particular, tritium and ^{32}Si—and
2) radiocontamination in copper (the primary structural material used to house low-mass DM detectors). Results from this project have significantly improved our understanding of these backgrounds and how to mitigate them in future experiments.

At present, there is no direct measurement of the rate at which tritium is "activated" by cosmic-ray neutrons in silicon-based detectors. In FY 2018, a new method was developed to measure this rate for the first time, using the Los Alamos Neutron Science Center neutron beam and silicon charge-coupled devices (CCDs). Heat treatments—to facilitate diffusion—were explored as a potential tritium mitigation strategy. Initial results suggest further R&D to explore "baking" as a possible general method for the mitigation of radiocontaminants in solid materials.

In FY 2016 to 2017, a thorough study was performed to understand ^{32}Si sources and identify vectors by which it can enter commercial silicon products, including investigation of high-sensitivity ^{32}Si-assay methods and mitigation strategies. Results concluded that isotopically pure ^{28}Si is the most promising strategy for creating future ^{32}Si-mitigated detectors.

A primary focus throughout this project has been new applications of PNNL's electroforming capability, to mitigate backgrounds associated with trace concentrations of primordial radioisotopes (e.g., ^{238}U and ^{232}Th) in structural materials. Electroforming of Cu-Cr alloys was demonstrated, for potential use in detectors requiring a material with higher strength and purity than available from commercially sourced metals.

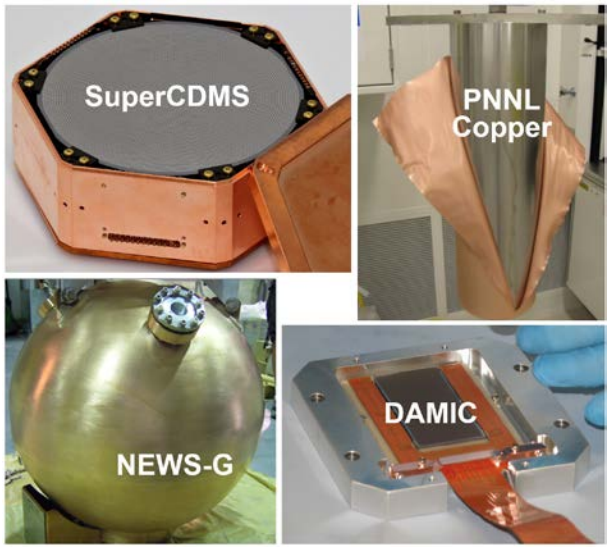

(Counterclockwise from top-left) Detectors from the Super Cryogenic Dark Matter Search (SuperCDMS), New Experiments with Spheres-Gas (NEWS-G), and Dark Matter in CCDs (DAMIC) experiments; (top-right) copper is essential for all three—PNNL copper is the purest in the world and is crucial to the success of future low-mass dark matter experiments.

Copper was electroformed to explore how best to package CCDs for DM searches. Also, new methods were developed to electroform copper onto previously fabricated detector components, thus adding a high-purity layer of copper to shield detectors from radioactivity in those components. Collectively, these new methods represent a toolkit that will extend the discovery potential of future low-mass DM experiments.

Finally, this project developed a general framework for modeling of backgrounds in DM experiments, with a web-based interface—the Background Explorer—that facilitates evaluation of detector designs in order to understand the recipe of background mitigations required to achieve a specific overall background performance (and thus experimental reach). This approach and the associated software will be made available to the community and is expected to help shape the future direction of low-mass DM searches.

Mitigating Challenges Toward an Enduring Supply of Low-radioactivity Argon for Ongoing Pacific Northwest National Laboratory National Security and Basic Science Programs

Henning O. Back

PN16036/2813

This project aimed to understand and mitigate the challenges that were faced in the production of the first 200 kg of low-radioactivity underground argon for the DarkSide-50 dark matter search experiment and to identify the source or sources of the residual ^{39}Ar and ^{85}Kr. This will ensure the successful establishment of an enduring supply of low-radioactivity argon with the lowest ^{39}Ar levels, without the need for isotopic separation.

Argon that is derived from the atmosphere contains a small fraction of the radioactive isotope ^{39}Ar and is the limiting background in all very-low-level radiation detectors that use argon, particularly argon-based dark matter detectors. The future successes of these programs depend on the establishment of an enduring source of low radioactivity argon that is free, or nearly free, of ^{39}Ar.

Argon from active CO_2 wells in southwestern Colorado has been found to contain very low levels of ^{39}Ar, with an upper limit of 0.07% atmospheric concentrations. The first production of low-radioactivity underground argon (UAr) was hampered by poisoning of sorbents and contaminate freeze-out in cryogenic systems. We successfully identified the contamination in the original adsorption and cryogenic systems, and through collaboration with the University of Houston, the contamination concentrations in the CO_2 feed were measured.

Examples of contaminants found in UAr extraction and purification plants.

C_3H_8	$C_5H_{10}O$	$C_6H_{13}I$	C_7H_{16}	$C_6H_{10}O_2$
$C_5H_{10}O$	C_6H_{14}	C_7H_{16}	$C_6H_{12}O$	C_8H_{18}
C_5H_{12}	$C_6H_{12}O$	$C_6H_{12}O$	$C_5H_8O_2$	C_9H_{20}
C_6H_{14}	C_6H_{12}	C_7H_{16}	C_8H_{16}	
C_5H_{10}	C_7H_{14}	C_6H_6	C_8H_{18}	

These results are being used in the design of the next generation of UAr production plant to produce 50 tons of UAr for the DarkSide-20k dark matter search experiment, Urania. Urania is a collaborative effort between Princeton University, the University of Houston, the University of Naples in Italy, Queen's and Carleton Universities in Canada, Fort Lewis College in Colorado, and PNNL.

In addition to the minor contamination identification, a goal of the project was to determine the origin of the ^{39}Ar and ^{85}Kr in the original UAr production. We explored the following three possibilities for their origin: 1) they are intrinsic to the UAr, 2) they are contaminations from an air infiltration, and/or 3) the ^{39}Ar is produced by cosmic rays.

As a part of this project, we found strong circumstantial evidence that the ^{39}Ar and ^{85}Kr in the first production of UAr for DarkSide-50 was from an air infiltration. In order to explore this hypothesis, we built a long-term gas analyzer (LOGAN) to monitor several gas streams at the remote location of the CO_2 wells. It was, indeed, determined that there is a minor air infiltration that can account for the amount of ^{39}Ar and ^{85}Kr in the original production of UAr. This air infiltration is also an issue for the commercial owners of the CO_2 operations (Kinder-Morgan). We helped to identify mitigation techniques that will benefit their operations and will be mitigated for the Urania plant.

In exploring the production of ^{39}Ar in the UAr by cosmic ray neutrons, we found that the cross-sections for the relevant reactions are only estimates and vary by an order of magnitude. These production rates are critical to understanding the transportation and storage of UAr on the earth's surface. By using the known history of the previous UAr production, we estimated that up to 20% the ^{39}Ar in DarkSide-50 could have come from cosmogenic production.

Knowing the production rate of ^{39}Ar due to cosmic rays is critical to understanding the proper handling of the UAr once it has reached Earth's surface and will determine the limits to the science reach of an argon-based dark matter experiment. It can also be used to estimate the concentration of ^{39}Ar in the atmosphere and to compare to the known atmospheric value.

In FY 2018, a small volume of UAr was irradiated at the Los Alamos Neutron Science Center accelerator at Los Alamos National Laboratory, and the ^{39}Ar was counter at PNNL. We discovered a production rate greater than what is generally accepted and is consistent with the highest calculated cross-sections.

A highlight of the original UAr production is Rep. Jerry McNerney's presentation to Congress on June 16, 2016, about UAr as it relates to helium production in the United States.

The results of this project have greatly influenced the next generation of UAr production. The UAr enables not only dark matter physics, but also is being explored for an argon shield for the LEGEND neutrinoless double-beta decay experiment, as a target for coherent neutrino-nuclear scattering, and as potential for the DUNE experiment.

Search for Lepton Number Violation

John L. Orrell
PN16079/2856

This project will assist development of a ton-scale neutrinoless double-beta ($0\nu\beta\beta$) decay experiment employing ^{136}Xe operated as a liquid xenon (LXe) time projection chamber (TPC) by working with the nEXO Collaboration. The focus of this project is on background estimation, material radio-impurity assay, low background materials development, and isotopic enrichment of xenon, which are areas of PNNL expertise.

PNNL is investing in the development of the next generation of neutrinoless double-beta decay research, an experimental program recommended by the scientific community in the 2015 *Nuclear Physics Long-Range Plan* to search for explicit lepton number violation and the nature of the neutrino. Lepton number—the quantum number identifying electrons, muons, taus, and their respective neutrinos—is conserved in all observed Standard Model particle interactions. However, due to their electrically neutral nature, neutrinos and their antimatter counterpart, anti-neutrinos, may be unique among the Standard Model particles, in that they are actually the same identical particle, proving lepton number cannot be a conserved quantity.

Neutrinoless double-beta decay—the double-beta decay of an unstable nucleus without the emission of the otherwise requisite two anti-neutrinos—is potentially an experimental means to identify the matter-antimatter uniqueness of neutrinos. The discovery of lepton number violation through $0\nu\beta\beta$ decay would open the door to a possible explanation of the matter-antimatter asymmetry of the universe: the fact that matter predominates, and antimatter has only a fleeting existence in our world. The scale of future $0\nu\beta\beta$ decay experiments is driven by the need to observe a large number of candidate nuclei, given the anticipated half-life is on the order of 10^{28} years expected for this ultra-rare nuclear decay process.

The nEXO Collaboration is an international organization of research institutions developing a ton-scale, next-generation $0\nu\beta\beta$ decay experiment employing a target mass enriched in ^{136}Xe and operated as an LXe TPC. PNNL expertise in background estimation, material radio-impurity assay, low background materials development, and isotopic enrichment are significant contributions to the research and development program to demonstrate the feasibility of the nEXO experimental design.

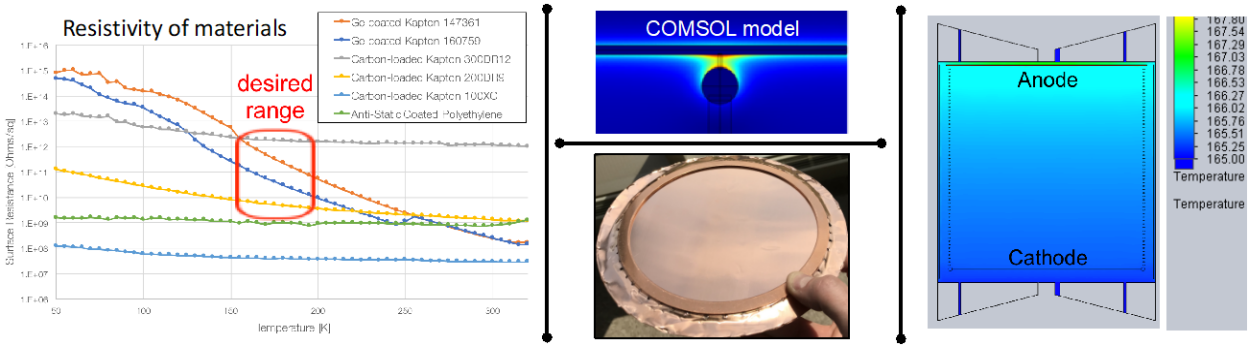

Left panel shows material resistivity as a function of temperature measured at PNNL. Upper-middle panel shows the PNNL COMSOL model of electric field strength in the SLAC spark-discharge test setup. Lower-middle panel shows a small-scale test production of an all-copper, conductive cathode design. Right panel shows modeled temperature profile in the LXe TPC.

In FY 2018, the PNNL team has focused significant attention to feasibility issues for the large and complex nEXO detector. PNNL chemists have continued to use inductively coupled plasma mass spectrometry to survey potential experimental construction materials for their trace levels of uranium, thorium, and potassium. These material assay measurements are crucial to understanding if nEXO can achieve the needed low background levels to search for neutrinoless double-beta decay. Work is ongoing to evaluate resistive material selection as a method for mitigating the risk associated with spark discharges in the high-voltage TPC of the nEXO experiment. A portion of this work was performed in conjunction with the Stanford Linear Accelerator Center (SLAC) to understand controlled spark discharge tests, using COMSOL® to model the SLAC test set-up.

The PNNL group has also advanced the construction feasibility of an all-copper, conductive cathode design. Graduate student research in computational fluid dynamics has evaluated the impact of thermal heat loads within the nEXO LXe volume, showing there are significant constraints on the internal electronics if boiling is to be avoided. In addition to these design feasibility evaluations, PNNL physicists led authorship of the scientific motivating section of the *nEXO Pre-Conceptual Design Report* and performed a study on the scientific impact of material assay upper limits (i.e., when instrument sensitivity isn't sufficient) on the projected scientific reach of low background experiments such as nEXO.

Ultrasensitive Nanoscale Chemical Imaging with Controllably Tailored Electromagnetic Waves

Patrick Z. El-Khoury
PN17084/2974

Through this project, we will design, fabricate, and test the performance of novel constructs that can be used to controllably guide light on the nanoscale. We will then use the nascent nanoscale electromagnetic fields to identify and image molecules on the same length scale through Raman and ultraviolet-visible (UV-Vis) nano-spectroscopy, with joint sub-5-cm^{-1} spectral and sub-5-nm spatial resolution that has not been previously demonstrated. Imaging at these length scales would benefit many applications, including cellular studies, chemical detection, photovoltaics, and many others.

Metallic nanostructures can support confined and enhanced electromagnetic fields, which may be used to chemically identify and image molecules (e.g., through surface-enhanced Raman scattering [SERS] and tip-enhanced Raman scattering [TERS]). However, the attainable spatial resolution and sensitivity in near-field optical microscopy and spectroscopy come at a price; the recorded molecular signatures are obfuscated by the complex interplay between molecules and ill-defined plasmonic metal nanostructures. Slight nanometric variations in the composition and structures of the plasmonic nanostructures are difficult to control and may completely alter the plasmonic response and structure of the local electric fields interacting with nearby molecules.

This is particularly the case in emerging techniques, such as TERS, which hold great promise for nanoscale chemical and biological imaging applications. In this regard, the commonly adopted practice of correlating structural/topographic images of plasmonic nanostructures with near-field optical spectra is often insufficient; there is a need for novel approaches that can be used to controllably tailor electromagnetic fields on a few-nanometer-length scale.

Attaining high spatio-spectral resolution using conventionally macro-microscopic techniques necessitates the use of plasmonic antennae. To controllably couple, interfere, guide, and focus microscopic light sources onto the nanoscopic apex of a probe, we will employ helium ion lithography to etch nanostructures onto the metallic probes. The performance of these tips will then be tested using a state-of-the-art combined atomic force microscopy-optical microscopy platform, which will be used to perform both nano-Raman and nano-UV-Vis imaging measurements.

In FY 2017, we established a protocol that can be used to simulate the optical properties of lithographically patterned metal-coated probes.

In the simulations, the “contrast” obtained by adding the lithographic pattern design to the metallic tip was evident. Under both incident laser polarizations, we observed a 5x enhancement in the electric field magnitude for the patterned design when compared to the reference construct. Although a modest increase in signal magnitude is observed in this case, this result clearly demonstrates how a simple lithographic pattern may be used to enhance the optical signals from (bio)molecules coaxed into plasmonic tip-surface nanojunctions.

Modifying the lithographic pattern design and repeating the simulations resulted in a much higher contrast. In this case, a 15x enhancement in the electric field magnitude was observed.

Our next step was to test this premise in the laboratory. In FY 2017, we produced several such probes using helium ion lithography (HIL). We were successful in lithographically etching trenches of various widths. Based on our simulations, we anticipated at least one of the tips to yield a 15x enhancement in the

electric field magnitude and, hence, 50,000x enhancement in Raman scattering cross-sections in nanoscopy mode.

The optical properties of our tip of choice for this report were measured using hyperspectral optical absorption microscopy. A UV-vis absorption image (hyperspectral image slice) of the tip illustrates the intensity distribution at any wavelength. Similarly, each pixel contains the full spectral response of the tip in the near-UV-near-infrared spectral region. Sharp resonances at approximately 420 nm were observed from our tips, commensurate with the expected plasmonic response.

In FY 2018, we repeated some of the HIL experiments to tailor contaminant-free tips and substrates. This allowed us to test the performance of our novel tip designs in nanoscopy mode. To date, we have identified several different promising tip designs through finite-difference time-domain simulations.

Pacific Northwest National Laboratory

902 Battelle Boulevard
P.O. Box 999
Richland, WA 99354
1-888-375-PNNL (7665)

www.pnnl.gov